ENZYMES FROM EXTREME ENVIRONMENTS

EDITED BY: Noha M. Mesbah and Felipe Sarmiento

PUBLISHED IN: Frontiers in Bioengineering and Biotechnology

frontiers Research Topics

frontiers

ISSN 1664-8714
ISBN 978-2-88919-830-6
DOI 10.3389/978-2-88919-830-6

About Frontiers

Frontiers is more than just an open-access publisher of scholarly articles: it is a pioneering approach to the world of academia, radically improving the way scholarly research is managed. The grand vision of Frontiers is a world where all people have an equal opportunity to seek, share and generate knowledge. Frontiers provides immediate and permanent online open access to all its publications, but this alone is not enough to realize our grand goals.

Frontiers Journal Series

The Frontiers Journal Series is a multi-tier and interdisciplinary set of open-access, online journals, promising a paradigm shift from the current review, selection and dissemination processes in academic publishing. All Frontiers journals are driven by researchers for researchers; therefore, they constitute a service to the scholarly community. At the same time, the Frontiers Journal Series operates on a revolutionary invention, the tiered publishing system, initially addressing specific communities of scholars, and gradually climbing up to broader public understanding, thus serving the interests of the lay society, too.

Dedication to quality

Each Frontiers article is a landmark of the highest quality, thanks to genuinely collaborative interactions between authors and review editors, who include some of the world's best academicians. Research must be certified by peers before entering a stream of knowledge that may eventually reach the public - and shape society; therefore, Frontiers only applies the most rigorous and unbiased reviews.
Frontiers revolutionizes research publishing by freely delivering the most outstanding research, evaluated with no bias from both the academic and social point of view.
By applying the most advanced information technologies, Frontiers is catapulting scholarly publishing into a new generation.

What are Frontiers Research Topics?

Frontiers Research Topics are very popular trademarks of the Frontiers Journals Series: they are collections of at least ten articles, all centered on a particular subject. With their unique mix of varied contributions from Original Research to Review Articles, Frontiers Research Topics unify the most influential researchers, the latest key findings and historical advances in a hot research area! Find out more on how to host your own Frontiers Research Topic or contribute to one as an author by contacting the Frontiers Editorial Office: **researchtopics@frontiersin.org**

ENZYMES FROM EXTREME ENVIRONMENTS

Topic Editors:
Noha M. Mesbah, Faculty of Pharmacy Suez Canal University
Felipe Sarmiento, Swissaustral USA LLC

Barnes springs complex at The Cedars. The Cedars is an area in northern California noted for the presence of abundant ultrabasic, highly alkaline springs (pH 11-12).

Image taken form Preiss L, Hicks DB, Suzuki S, Meier T and Krulwich TA (2015) Alkaliphilic bacteria with impact on industrial applications, concepts of early life forms, and bioenergetics of ATP synthesis. Front. Bioeng. Biotechnol. 3:75. doi: 10.3389/fbioe.2015.00075

Enzymes are nature's biocatalysts empowered with high catalytic power and remarkable substrate specificity. Enzymes perform a wide range of functions throughout nature, and guide the biochemistry of life with great precision. The majority of enzymes perform under conditions considered normal for mesophilic, neutrophilic, terrestrial microorganisms. However, the Earth's biosphere contains several regions that are extreme in comparison, such as hypersaline lakes and pools, hydrothermal vents, cold oceans, dry deserts and areas exposed to intensive radiation. These areas are inhabited by a large number of extremophilic microorganisms which produce enzymes capable of functioning in unusual conditions.

There is an increasing biotechnological and industrial demand for enzymes stable and functioning in harsh conditions, and over the past decade screening for, isolation and production of enzymes with unique and extreme properties has become one of the foremost areas of biotechnology research. The development of advanced molecular biology tools has facilitated the quest for production of enzymes with optimized and extreme features. These tools include large-scale screening for potential genes using metagenomics, engineering of enzymes using computational techniques and site-directed mutagenesis and molecular evolution techniques.

The goal of this Research Topic is to present reports on latest advances in enzymes from all types of extreme environments. Contributions dealing with isolation of enzymes from extremophilic microorganisms or directly from natural environments, screening for and expression of enzymes with extreme properties using metagenomic approaches are welcome. In addition, contributions dealing with all forms of biocatalyst production and improvement are welcome, such as fermentation technology, protein engineering, directed evolution, rational design, and immobilization techniques.

Citation: Mesbah, N. M., Sarmiento, F., eds. (2016). Enzymes from Extreme Environments. Lausanne: Frontiers Media. doi: 10.3389/978-2-88919-830-6

Table of Contents

05 ***Editorial: Enzymes from Extreme Environments***

Noha M. Mesbah and Felipe Sarmiento

07 ***Cold and hot extremozymes: industrial relevance and current trends***

Felipe Sarmiento, Rocío Peralta and Jenny M. Blamey

22 ***Enzymes from extreme environments and their industrial applications***

Jennifer A. Littlechild

31 ***Biochemical and structural properties of a thermostable mercuric ion reductase from Metallosphaera sedula***

Jacob H. Artz, Spencer N. White, Oleg A. Zadvornyy, Corey J. Fugate, Danny Hicks, George H. Gauss, Matthew C. Posewitz, Eric S. Boyd and John W. Peters

39 ***Highly thermostable xylanase production from a thermophilic Geobacillus sp. strain WSUCF1 utilizing lignocellulosic biomass***

Aditya Bhalla, Kenneth M. Bischoff and Rajesh Kumar Sani

47 ***First glycoside hydrolase family 2 enzymes from Thermus antranikianii and Thermus brockianus with β-glucosidase activity***

Carola Schröder, Saskia Blank and Garabed Antranikian

57 ***A New Thermophilic Nitrilase from an Antarctic Hyperthermophilic Microorganism***

Geraldine V. Dennett and Jenny M. Blamey

66 ***Biochemical and structural characterization of enolase from Chloroflexus aurantiacus: evidence for a thermophilic origin***

Oleg A. Zadvornyy, Eric S. Boyd, Matthew C. Posewitz, Nikolay A. Zorin and John W. Peters

78 ***Functional screening of hydrolytic activities reveals an extremely thermostable cellulase from a deep-sea archaeon***

Benedikt Leis, Simon Heinze, Angel Angelov, Vu Thuy Trang Pham, Andrea Thürmer, Mohamed Jebbar, Peter N. Golyshin, Wolfgang R. Streit, Rolf Daniel and Wolfgang Liebl

88 ***Alkaliphilic bacteria with impact on industrial applications, concepts of early life forms, and bioenergetics of ATP synthesis***

Laura Preiss, David B. Hicks, Shino Suzuki, Thomas Meier and Terry Ann Krulwich

frontiers in Bioengineering and Biotechnology

EDITORIAL
published: 07 March 2016
doi: 10.3389/fbioe.2016.00024

Editorial: Enzymes from Extreme Environments

Noha M. Mesbah[1] and Felipe Sarmiento[2]*

[1] Faculty of Pharmacy, Suez Canal University, Ismailia, Egypt, [2] Swissaustral USA LLC, Athens, GA, USA

Keywords: extremozymes, enzymes and coenzymes, biotechnology, extremophiles, biocatalysis

The Editorial on the Research Topic

Enzymes from Extreme Environments

Enzymes are nature's biocatalysts and are equipped with high catalytic activity and remarkable substrate specificity. Enzymes catalyze the metabolic reactions necessary for all of life's processes and are able to catalyze reactions at much higher rates than would be possible without their action. The majority of enzymes are optimized to perform under physiological conditions or conditions considered normal for mesophilic, neutrophilic microorganisms (de Carvalho, 2011). However, a particular set of enzymes called "extremozymes" are adapted to perform the same enzymatic functions as their non-extreme counterparts, but with greater versatility and adaptability to harsh conditions. These enzymes are found in extremophiles, organisms that thrive in extreme physical and/or chemical conditions. Extremophiles are found in some of the most severe environments on Earth, including hydrothermal vents, hypersaline lakes and pools, alkaline soda lakes, dry deserts, cold oceans, and volcanic areas.

Many industries are making efforts to move away from the use of harmful chemical processes. As a result, there is increasing biotechnological demand for enzymes that are stable and active under extreme conditions, such as those found in industrial processing. Over the past decade, screening, isolating, and optimizing the production of extremozymes has become one of the major areas of biotechnology research. The development of advanced, high-throughput screening and molecular biology techniques has facilitated the production of enzymes with extreme and optimized features. Despite these advances, however, the current enzyme toolbox is unable to meet industrial demands for processes requiring extreme conditions, such as high temperature, alkaline pH, low water activity, and resistance to metal ions. This Research Topic features some the latest progress in extremozyme research, with a focus on stability under extreme conditions and applicability to industrial processes.

Beginning with the first use of an enzymatic preparation for a commercial application, Sarmiento et al. review the history of enzyme discovery and the development of the market need for robust extremozymes. The authors then focus on the characteristics of psychrophilic, thermophilic, and hyperthermophilic enzymes and discuss their current applications in research and industrial areas, the challenges of working with extremozymes, and highlight future trends in the discovery and production of extremozymes.

Extremophilic enzymes play key roles in catalyzing commercially valuable chemical conversions without the production of toxic waste, which is the hallmark of traditional industrial chemical processes. These enzymes can be cloned and over-expressed, allowing for production of sufficient quantities for detailed biochemical and structural characterization and large-scale production for industrial processes. Littlechild describes several extremozymes with applications in biocatalysis, which have been developed for industrial processes, such as γ-lactamase, L-aminoacylase, and carboxypeptidase.

Among the different classes of extremozymes, thermophilic and thermostable enzymes are the most extensively sought after for industrial processes owing to their stability and activity at high temperatures. Thermophilic enzymes are also more resistant than their mesophilic counterparts to

OPEN ACCESS

Edited by:
Maizirwan Mel, International Islamic University Malaysia, Malaysia

Reviewed by:
Rafael Luque, Universidad de Cordoba, Spain

****Correspondence:***
Noha M. Mesbah
noha_mesbah@pharm.suez.edu.eg

Specialty section:
This article was submitted to Process and Industrial Biotechnology, a section of the journal Frontiers in Bioengineering and Biotechnology

Received: *01 February 2016*
Accepted: *22 February 2016*
Published: *07 March 2016*

Citation:
Mesbah NM and Sarmiento F (2016) Editorial: Enzymes from Extreme Environments. Front. Bioeng. Biotechnol. 4:24. doi: 10.3389/fbioe.2016.00024

organic solvents, metal cations, and chemical denaturants. Artz et al. describe the biochemical and structural characterization of a thermostable mercuric ion reductase that remains active after prolonged incubation at temperatures greater than 90°C and potentially has a unique method of coordinating mercury ions. Bhalla et al. describe the purification and characterization of an extremely thermophilic xylanase with a half-life of 12 days at 70°C that exhibits activity on untreated lignocellulose, giving it great potential for application in biofuels production. Schröder et al. describe two unique, highly thermostable glycosyl hydrolases with β-glucosidase activity. Dennett and Blamey describe the production and purification of a thermophilic nitrilase that retains activity after prolonged incubation at 85°C. Finally, Zadvornyy et al. present the characterization of a thermophilic enolase from the green, non-sulfur bacterium *Chloroflexus aurantiacus* with maximal activity at 80°C and exhibiting structural properties that indicate it is thermally adapted.

Advances in metagenomics have contributed greatly to the production of novel extremozymes since these techniques can help overcome the limitations of culture-based approaches. Following the screening of a large-insert mixed genomic DNA library of pooled isolates of hyperthermophilic archaea from deep sea vents, Leis et al. isolated an extremely thermophilic endo-1,4-β-glucanase that showed maximal activity at 92°C and was active toward various substrates.

Alkaliphilic enzymes have increased resistance to alkali and other denaturing chemicals. The majority of alkaliphilic enzymes characterized to date are produced by extremely alkaliphilic *Bacillus* strains. Preiss et al. reviewed alkaliphilic bacteria and the bioenergetics aspects of survival in a dearth of protons. The review focuses on the bioenergetic challenges faced by alkaliphiles that carry-out proton-coupled oxidative phosphorylation and provides a detailed discussion of adaptations of alkaliphile F_1F_o-ATP synthases that support function at a low proton motive force.

The works highlighted in this Research Topic illustrate the continuing advancements in the field of extremozymes research, as well as the applicability of these enzymes to several industries. However, the potential of extremozymes is far from being fully understood and continued research efforts are still needed. The development of novel culture methods, suitable molecular tools, more efficient production processes, and improvements in novel technologies, such as functional metagenomic screenings, genome mining, and protein engineering, are key factors to fully unlocking the power of extremozymes. Advancing in this direction will greatly improve the yield and variety of extremozymes produced and their potential industrial applications.

AUTHOR CONTRIBUTIONS

Both authors have read and revised the manuscript.

REFERENCE

de Carvalho, C. C. C. R. (2011). Enzymatic and whole cell catalysis: finding new strategies for old processes. *Biotechnol. Adv.* 29, 75–83. doi:10.1016/j.biotechadv.2010.09.001

Conflict of Interest Statement: The authors declare that the research was conducted in the absence of any commercial or financial relationships that could be construed as a potential conflict of interest.

frontiers in Bioengineering and Biotechnology

REVIEW
published: 20 October 2015
doi: 10.3389/fbioe.2015.00148

Cold and hot extremozymes: industrial relevance and current trends

Felipe Sarmiento[1], *Rocío Peralta*[2] *and Jenny M. Blamey*[1,2]*

[1] Swissaustral USA, Athens, GA, USA, [2] Fundación Científica y Cultural Biociencia, Santiago, Chile

The development of enzymes for industrial applications relies heavily on the use of microorganisms. The intrinsic properties of microbial enzymes, e.g., consistency, reproducibility, and high yields along with many others, have pushed their introduction into a wide range of products and industrial processes. Extremophilic microorganisms represent an underutilized and innovative source of novel enzymes. These microorganisms have developed unique mechanisms and molecular means to cope with extreme temperatures, acidic and basic pH, high salinity, high radiation, low water activity, and high metal concentrations among other environmental conditions. Extremophile-derived enzymes, or extremozymes, are able to catalyze chemical reactions under harsh conditions, like those found in industrial processes, which were previously not thought to be conducive for enzymatic activity. Due to their optimal activity and stability under extreme conditions, extremozymes offer new catalytic alternatives for current industrial applications. These extremozymes also represent the cornerstone for the development of environmentally friendly, efficient, and sustainable industrial technologies. Many advances in industrial biocatalysis have been achieved in recent years; however, the potential of biocatalysis through the use of extremozymes is far from being fully realized. In this article, the adaptations and significance of psychrophilic, thermophilic, and hyperthermophilic enzymes, and their applications in selected industrial markets will be reviewed. Also, the current challenges in the development and mass production of extremozymes as well as future prospects and trends for their biotechnological application will be discussed.

Keywords: extremophiles, extremozymes, cold-adapted enzymes, psychrophiles, thermophiles, hyperthermophiles

OPEN ACCESS

Edited by:
Maizirwan Mel, International Islamic University Malaysia, Malaysia

Reviewed by:
Jose M. Bruno-Barcena, North Carolina State University, USA
Azlin Suhaida Azmi, International Islamic University Malaysia, Malaysia

***Correspondence:**
Jenny M. Blamey, Swissaustral USA, 111 Riverbend Road, Office 271, Athens, GA 30602, USA
jblamey@swissaustral.ch

Specialty section:
This article was submitted to Process and Industrial Biotechnology, a section of the journal Frontiers in Bioengineering and Biotechnology

Received: *20 April 2015*
Accepted: *14 September 2015*
Published: *20 October 2015*

Citation:
Sarmiento F, Peralta R and Blamey JM (2015) Cold and hot extremozymes: industrial relevance and current trends. Front. Bioeng. Biotechnol. 3:148. doi: 10.3389/fbioe.2015.00148

Historical Background and Commercial Prospects of Enzymes

Enzymes are nature's own catalysts. They are proteins which accelerate the rate and specificity of chemical reactions by reducing the required activation energy. Unknowingly, enzymes have been used as biotechnological tools since ancient times for the production of food and alcoholic beverages, but only recently have significant knowledge and understanding of enzymes been cultivated. Early ideas about enzymes and bio-catalytic processes started to take form during the seventeenth and eighteenth centuries; however, the first major breakthroughs were not achieved until the nineteenth century. In 1833, the first enzyme was discovered, diastase (Payen and Persoz, 1833), now known as amylase. The term enzyme was not adopted until 44 years later in 1877 by the German scientist Kühne (1877).

Nearly 40 years later, the first enzymatic preparation for a commercial application was developed by Otto Rohm in 1914. He isolated trypsin from animal pancreases and added it to washing detergents to degrade proteins. It was not until the 1960s that enzymatic biocatalysis became a viable industrial option with the mass production of microbial proteases for use in washing powders. Industrial enzymes have since evolved into a multibillion dollar global market. The global market for industrial enzymes is expected to reach $7 billion by 2018 with a compound annual growth rate (CAGR) of 8.2% from 2013 to 2018 (Dewan, 2014). In addition, the global specialty enzymes market is forecasted to reach about $4 billion by 2018[1]. This market will likely continue to grow for the foreseeable future as a result of advancements in the biotechnology industry, the continued need for cost-efficient manufacturing process, and calls for greener technologies.

The enzyme market is becoming increasingly dynamic. Recent enzyme discoveries and developments in genetics and protein engineering have increased the reach of enzymes in industry. Indeed, industrial catalysis is increasingly dependent on enzymes. Enzymes have become important tools for diverse industrial markets, such as food and beverage, animal feed, detergents, and technical enzymes, including biofuels, leather, pulp and paper, and textile markets. Specialty enzyme use is also growing in markets, such as diagnostics, pharmaceuticals, and research and development.

From Enzymes to Extremozymes

Due to the intrinsic characteristics of enzymes, they have influenced almost every industrial market and their demand has constantly increased over the years. These natural catalysts are fast, efficient, and selective, in addition to producing low amounts of by-products. They are also fully biodegradable molecules, resulting in a low environmental impact (Rozzell, 1999) and a greener solution to many industrial challenges.

Since the first steps toward commercial scale enzyme production in the 1960s, when Novozymes (Bagsvaerd, Denmark) began marketing and mass producing proteases from *Bacillus* for use in detergents, microorganisms have played a pivotal role in the discovery and development of novel enzymes for industrial applications. The diversity, and unique properties of microbial enzymes, e.g., consistency, reproducibility, high yields, and economic feasibility among others, have elevated their biotechnological interest and application to different industrial areas (Gurung et al., 2013). However, the vast majority of current industrial processes are performed under harsh conditions, including extremely high and low temperatures, acidic or basic pHs, and elevated salinity. Standard enzymes have specific requirements for maximal function, performing optimally in narrow ranges of physical and chemical conditions. These requirements are quite different from industrial processing settings, where standard enzymes are easily denatured. In many cases, traditional chemical solutions are still the only viable option under such harsh conditions. There is a clear need for more sustainable and environmentally friendly methods to replace the current potentially harmful chemical processes. The identification of more novel enzymes with properties that can cope with industrial processing conditions is the key to the future of biocatalysis.

Extremophiles are organisms, mainly microorganisms, which belong to the domains *Archaea* and *Bacteria*. They thrive in environmental conditions considered by human standards to be extreme. Extremophiles grow and reproduce under high temperatures in hot springs or thermal vents, low temperatures in glaciers or the deep sea, acidic and basic pHs in industrial or mine wastewater effluents, high concentration of salts in salt lakes, and high levels of radiation and extreme desiccation in deserts among other physical or chemical extreme conditions in various ecological niches. For additional information about extremophiles and their specific characteristics and habitats, please visit the following reviews (Madigan and Marrs, 1997; Rothschild and Mancinelli, 2001; Canganella and Wiegel, 2011).

The following question then arises: how can these organisms survive, let alone thrive under such harsh conditions? The answer sounds simple at first: extremophiles evolved and adapted to their environments by developing unique mechanisms to keep their cellular components stable and active. However, these mechanisms are quite complex. For example, to cope with high concentrations of salt, extremophiles produce increased amounts of compatible solutes inside the cells or use ion pumps to keep an osmotic equilibrium; in the presence of low pH, they use proton pumps to keep an adequate pH inside the cell; and in the presence of low or high temperatures, they can modify the composition of their cytoplasmic membrane.

In many cases, enzymes from extremophiles have adapted to withstand extreme conditions on their own. These adaptations correspond to key changes in the amino acid sequence, which are translated into variations in the structure, flexibility, charge, and/or hydrophobicity of the enzymes. These changes do not follow a pattern or a specific trend. Extremophilic proteins display substantial variability in adaptations for similar extreme physical or chemical conditions (Reed et al., 2013).

These diverse adaptations allow extremozymes to expand the ranges of optimal enzyme performance enabling enzymatic biocatalysis under the enzymatically unfavorable conditions found in industrial processes. Through actively bioprospecting extreme environments and/or using genetic engineering, it is possible now to discover and develop extremozymes that can accommodate existing industrial processes or products. Extreme biocatalysis offers exciting opportunities to improve current enzyme technologies and represents a highly attractive, sustainable, cost-effective, and environmentally friendly option compared to chemical catalysis.

The present review focuses on the diverse adaptations and characteristics of psychrophilic, thermophilic, and hyperthermophilic enzymes and some of their current applications in select industrial and research areas.

Cold Extremozymes: Industrial Relevance and Current Trends

Psychrophilic Microorganisms

More than three-quarters of our planet is comprised of environments which experience extremely low temperatures ($\leq$15°C). It is

[1]http://www.marketsandmarkets.com/PressReleases/specialty-enzymes.asp

not surprising, therefore, that the majority of Earth's biomass is generated at temperatures below 5°C (Siddiqui and Cavicchioli, 2006). These habitats sustain a wide diversity of microorganisms, which naturally thrive in cold environments, known as psychrophilic microorganisms. They are adapted to grow, reproduce, and maintain their vital metabolic rates under such extreme conditions.

Psychrophiles are present in all three domains of life (*Archaea*, *Bacteria*, and *Eukarya*) and use a wide variety of metabolic pathways, including photosynthetic, chemoautotrophic, and heterotrophic pathways. By definition, psychrophiles are able to sustain growth in cold temperatures ranging from −20°C to +10°C. They are able to maintain an active metabolism at low temperatures, and many grow well at temperatures around the freezing point of water. The bacteria *Planococcus halocryophilus* Or1, isolated from high Arctic permafrost, grows and reproduces at −15°C, the lowest temperature demonstrated to date (Mykytczuk et al., 2013). Metabolically active bacteria have been reported at temperatures as low as −32°C (Bakermans and Skidmore, 2011), pushing the limits of life even further.

Psychrophiles face diverse challenges inherent to living in cold environments: low enzyme activity and low enzymatic rates, altered transport systems, decreased membrane fluidity, and protein cold-denaturation among others (D'Amico et al., 2006). To overcome these challenges, they have developed remarkable adaptations. For example, psychrophiles produce higher amounts of unsaturated and methyl-branched fatty acids and shorter acyl-chain fatty acids to increase membrane fluidity (Russell, 1997; Chintalapati et al., 2004). They also produce cold-shock proteins to aid in different cellular processes, such as protein folding or membrane fluidity (Phadtare, 2004), and antifreeze proteins that inhibit ice crystal growth. In addition, all components of their cells must be suitably adapted to cold temperatures, including cold-adapted enzymes that are extremely flexible and maintain high specific activities at low temperatures.

Structural Features and Action Mechanism of Cold-Adapted Extremozymes

At low temperatures, the mean kinetic energy available for reactions is low and insufficient to overcome the energy barrier of activation for catalysis. This translates into reduced enzymatic activity. Proteins also tend to denature as temperatures drop because of a decrease in the availability of water molecules as the molecules become more ordered and less associated with proteins (Karan et al., 2012). Cold-adapted (or psychrophilic) enzymes have a combination of specific adaptations in their structural features that give them more flexible structures than mesophilic and thermophilic enzymes. This trait allows for high catalytic activity at low temperatures (Siddiqui and Cavicchioli, 2006), and thermolability. These adaptations correspond to specific genetic changes, which are a consequence of long-term selection. In recent reviews on psychrophilic enzymes, the following features were mentioned as important adaptations for keeping high flexibility and high activity at low temperatures: (a) decreased core hydrophobicity, but increased surface hydrophobicity, (b) changes in amino acid compositions, such as lower arginine/lysine ratio, more glycine residues for better conformational mobility, fewer proline residues in loops, but more in α-helices, and more non-polar residues on the protein surface, (c) weaker protein interactions, such as inter-domain and inter-subunit interactions, less disulfide bridges, fewer hydrogen bonds and other electrostatic interactions, and less/weaker metal-binding sites, (d) decreased secondary structures and oligomerization, but an increase in the number and size of loops, and (e) an increase in conformational entropy of the unfolded protein state (Feller, 2010; Cavicchioli et al., 2011). As a consequence of these special features, the reaction rate of psychrophilic enzymes tends to decrease more slowly compared to similar enzymes from mesophilic or thermophilic microorganisms when the temperature decreases (Feller, 2013). Collins and collaborators compared cold-adapted and mesophilic xylanases and demonstrated that cold-adapted enzymes are more active at low temperatures, but more thermolabile when the temperature increases (Collins et al., 2002).

Biotechnological Applications of Cold Extremozymes

In recent years, scientific and industrial efforts to discover and develop novel cold-adapted enzymes have increased substantially. The intrinsic characteristics of cold-adapted enzymes, high activity at low temperatures and thermolability, are extremely valuable for different biotechnological applications in a wide variety of industries from molecular biology, to detergency to food and beverage preparation (Marx et al., 2007; Cavicchioli et al., 2011; Feller, 2013). As a consequence, psychrophilic enzymes are replacing mesophilic enzymes in many different industrial processes.

There are several benefits to the application of cold-adapted enzymes in industry. Due to their high activity, the desired result from a biochemical reaction can be reached using smaller amounts of a psychrophilic enzyme compared to its mesophilic or thermophilic homologs under optimal conditions. This faster activity translates into savings in time, energy, and money for a particular reaction. In addition, due to their thermolability, cold-adapted enzymes can be selectively inactivated in a complex mixture by increasing the temperature of the reaction. This represents a distinct advantage when an enzyme is needed only for a certain period of time in a particular reaction, e.g., meat tenderizing by proteases, or to avoid an undesirable byproduct of that particular enzymatic reaction that is produced at higher temperatures. This characteristic allows for improved control and a higher effectiveness of the overall reaction and represents a clear advantage for the use of enzymes in various processes, including those used in molecular biology. Since psychrophilic enzymes function optimally at moderate and low temperatures, they can catalyze reactions at ambient temperatures eliminating the need for heat input into a system. This translates into the development of more cost-efficient processes. This particular trait is of the utmost importance to the detergent industry. It allows for the development of detergents effective at ambient temperatures that are necessary not only to reduce the environmental and economic impact of reducing washing temperatures but also to

TABLE 1 | Examples of commercially available cold-active enzymes.

Market	Enzyme	Commercially available	Uses
Molecular Biology	Alkaline phosphatases	Antarctic phosphatase (New England Biolabs Inc.)	Dephosphorylation of 5′ end of a linearized fragment of DNA
	Uracil-DNA N-glycosylases (UNGs)	Uracil-DNA *N*-glycosylase (UNG) (ArcticZymes), Antarctic Thermolabile UDG (New England Biolabs Inc.)	Release of free uracil from uracil-containing DNA
	Nucleases	Cryonase (Takara-Clontech)	Digestion of all types of DNA and RNA
Detergent	Lipases	Lipoclean®, Lipex®, Lipolase® Ultra, Kannase, Liquanase®, Polarzyme®, (Novozymes)	Breaking down of lipid stains
	Proteases	Purafect® Prima, Properase®, Excellase (Genencor)	Breaking down of protein stains
	Amylases	Stainzyme® Plus (Novozymes), Preferenz™ S100 (DuPont), Purafect® OxAm (Genencor)	Breakdown starch-based stains
	Cellulases	Rocksoft™ Antarctic, Antarctic LTC (Dyadic), UTA-88 and UTA-90 (Hunan Youtell Biochemical), Retrocell Recop and Retrocell ZircoN (EpyGen Biotech), Celluzyme®, Celluclean® (Novozymes)	Wash of cotton fabrics
	Mannanases	Mannaway® (Novozymes), Effectenz™ (DuPont)	Degradation of mannan or gum
	Pectate lyases	XPect® (Novozymes)	Pectin-stain removal activity
Textile	Amylases	Optisize® COOL and Optisize NEXT (Genencor/DuPont)	Desizing of woven fabrics
	Cellulases	Primafast® GOLD HSL IndiAge® NeutraFlex, PrimaGreen® EcoLight 1 and PrimaGreen® EcoFade LT100 (Genencor/DuPont)	Bio-finishing combined with dyeing of cellulosic fabrics
Food and beverages	Pectinases	Novoshape® (Novozymes), Pectinase 62L (Biocatalysts), Lallzyme® (Lallemand)	Fermentation of beer and wine, breadmaking, and fruit juice processing
Other	Catalase	Catalase (CAT), (Swissaustral)	Textile, research, and cosmetic applications

supply working products to people with limited access to warm water. Lastly, psychrophiles have adapted to extremely cold environments, with varying substrate availability, ecology, and other characteristics not found in mesophilic and thermophilic environments. Psychrophiles represent an interesting source of novel enzymes that may use different substrates or co-factors, and/or perform innovative reactions applicable to industry. Described below are the applications in selected industrial markets and some examples of in-development and commercially available cold-adapted enzymes (**Table 1**).

Cold Extremozymes Applied in Molecular Biology

The heat lability associated with cold-adapted enzymes is an essential feature for sequential enzymatic applications in a variety of processes, including many techniques used in molecular biology. One of the most commonly used enzymes in molecular biology is alkaline phosphatase (AP). This enzyme is used to dephosphorylate the 5′ end of a linearized fragment of DNA to prevent re-circularization when performing cloning techniques and also in many other applications. For many years, the only APs in the market were from *Escherichia coli* or calf intestine. Since these enzymes are heat-stable, it is necessary to carefully inactivate them using detergents; these detergents, however, can interfere with subsequent steps of this particular technique. In contrast, psychrophilic heat-labile AP can be easily inactivated in the same tube by a moderate heat treatment (~65°C). The first heat-labile AP was purified in 1984 from a bacterium isolated from Antarctica (Kobori et al., 1984). A recombinant AP isolated originally from another Antarctic bacterium (Rina et al., 2000), and further improved through directed evolution (Koutsioulis et al., 2008) is commercially available as Antarctic phosphatase by New England Biolabs (Ipswich, MA, USA). The first commercially available cold-adapted AP was developed from the arctic shrimp *Pandalus borealis* by ArcticZymes (Tromsø, Norway) in 1993. ArcticZymes launched a recombinant version of this AP in 2010. A novel psychrophilic AP was recently isolated from a metagenomic library constructed using ocean-tidal flat sediments from the west coast of Korea (Lee et al., 2015). This enzyme exhibits similar characteristics and comparable efficiency to other commercially available APs.

There are other examples of cold-adapted enzymes used in molecular biology: (a) Uracil-DNA N-glycosylase (UNG) catalyzes the release of free uracil from uracil-containing DNA. UNG is used to control carry-over contamination in PCR and RT-PCR, in site-directed mutagenesis and in SNP genotyping among other applications. ArcticZymes produces a commercially available cold-adapted UNG enzyme that is completely and irreversibly inactivated by heat treatment (55°C). This enzyme is derived from Atlantic cod (*Gadus morhua*) and its recombinant version produced in *E. coli* is available commercially (Lanes et al., 2002). A novel heat-labile UNG was discovered by mining the genome of the bacterium *Psychrobacter* sp. HJ147. This enzyme was cloned and expressed in *E. coli*. It functions with an optimal temperature of 20–25°C and a half-life of 2 min at 40°C (Lee et al., 2009). Additionally, New England Biolabs offers Antarctic Thermolabile UDG, a recombinant UNG enzyme produced in *E. coli* from a psychrophilic marine bacterium with an inactivation temperature above 50°C. (b) Double strand-specific DNase allows for the

digestion of double-stranded DNA without any effect on single-stranded DNA molecules, such as primers or probes. This enzyme is used to decontaminate PCR mixes or to remove genomic DNA from RNA preparations. A heat-labile version of this enzyme (inactivated at 55°C) isolated from shrimp (*P. borealis*) and further genetically engineered is offered from ArcticZymes. A recombinant version produced in *Pichia pastoris* is offered by Affymetrix USB (Santa Clara, CA, USA) and is inactivated after exposure to 70°C for 25–30 min. (c) Cryonase, a recombinant cold-active nuclease offered by Takara-Clontech (Mountain View, CA, USA), is derived from a psychrophilic strain of *Shewanella* sp. It is produced in *E. coli* and can digest all types of DNA and RNA (single-stranded, double-stranded, linear, or circularized). This enzyme is active even when samples are left on ice and can only be completely inactivated after a 30 min incubation at 70°C (Awazu et al., 2011).

The introduction of new cold-adapted enzymes to the molecular biology market would greatly benefit this field and would be an ideal application for psychrophiles. For example, cold-active recombinases are part of the new recombinase polymerase amplification (RPA) PCR kits being developed by TwistDx (Cambridge, UK). RPA is an isothermal amplification method that utilizes a recombinase to facilitate the insertion of oligonucleotide primers onto their complement in a double-stranded DNA molecule. The use of opposing primers allows for the exponential amplification of a defined region of DNA in a manner similar to PCR. This technology has been successfully applied in the detection of HIV and protozoan parasite like *Plasmodium falciparum*, the causal agent of malaria.

DNA ligases are commonly utilized tools in molecular biology for catalyzing the formation of phosphodiester bonds in nicked double-stranded DNA molecules. Currently, the market of DNA ligases is dominated by recombinant versions of bacteriophage-derived DNA ligases, such as the T4 and T7 ligases, and *E. coli* DNA ligases. All of these function at temperatures above 15°C. At these elevated temperatures, residual nucleases may interfere with the ligation process. The introduction of cold-adapted DNA ligases from psychrophiles may offer a novel advantage by maintaining a high specific activity at temperatures low enough that nucleases are no longer active. A novel DNA ligase from the psychrophile *Pseudoalteromonas haloplanktis* has been cloned, overexpress and characterized. This DNA ligase displays activity at temperatures as low as 4°C (Georlette et al., 2000). Proteinase k is another cold-adapted enzyme with potential applicability to molecular biology. This enzyme, which belongs to the serine proteases family, is normally used to degrade unwanted enzymes from crude extracts or enzymes used in previous steps of an experimental protocol. Current commercially available proteinase k needs to be inactivated by chemical removal (phenol-chloroform extraction/ethanol precipitation) which can lead to sample loss and contamination, or heat inactivation at high temperatures (95°C) which can denature the target product. A cold-adapted thermolabile proteinase k-like serine protease would be highly active at low temperatures and could be inactivated with mild heat (45–60°C), increasing the overall efficiency of the experiments and reducing contamination risk. There is currently no cold-adapted DNA ligase or proteinase k is commercially available.

Cold Extremozymes Applied in Detergent Market

For many years, enzymes have been common components of detergent formulations in developed countries. The global market for detergent enzymes in 2013 was valued at approximately $1 billion and is expected to reach $1.8 billion by 2018 with a CAGR from 2013 to 2018 of 11.3% (Dewan, 2014). Detergent enzymes will represent 25–30% of the global market of enzymes for industrial applications. The current trend in the detergent market is cold-water detergents that can work as efficiently as common detergents but at lower temperatures. The application of cold-water detergents would allow for reduced energy consumption and carbon dioxide emissions as well as improved fabric protection. Despite the appeal of this idea, it has taken time to become a widely spread option. Hot water remains the preferred standard method for cleaning clothes. However, recent efforts to discover and develop novel enzymes that can work efficiently at cold temperatures are helping to change the cleaning industries awareness and creating an excellent opportunity for the application of cold-wash detergents. The percentage of global cold-water washing machine loads increased from 38 to 53% from 2010 and 2014. Additionally, one of the main goals of Proctor & Gamble and Unilever, the largest producers of detergent technologies, for 2020 is to have 70% of all machine washer loads done in cold water, reducing the energy impact and greenhouse gas emissions of laundry activities[2,3].

Several different cold-adapted enzymes are of interest for improving the efficacy of cold-water household and industrial laundry and dishwasher detergents, some of the most important are described below.

Lipases catalyze the hydrolysis of fats (lipids) and remove fatty stains (butter, oil, and sauces) from fabrics. Novozymes, one of the worldwide largest producers of enzymes, has developed Lipoclean®, a cold-adapted lipase that targets stains from triglycerides. Lipoclean® is active at low temperatures (~20°C) and is very stable in multienzyme solutions. In addition, Novozymes has developed two other alternative lipases: Lipex® and Lipolase® Ultra, which perform optimally in low–moderate temperatures. Research for the discovery and development of novel cold-adapted lipases from psychrophilic microorganisms is booming because of the useful application of lipases in detergents and the trend toward cold-washing detergency (Park et al., 2009; Xuezheng et al., 2010; Cheng et al., 2011; Litantra et al., 2013; Jiewei et al., 2014; Ji et al., 2015). A high-performance lipase from *Pseudomonas stutzeri* PS59 was recently identified for use in detergent formulations. This lipase has optimal activity at 20°C, pH 8.5 and in the presence of different surfactants and oxidizing agents (Li et al., 2014).

Proteases are enzymes that catalyze the hydrolysis of peptide bonds that link amino acids together, digesting proteins into shorter fragments. They fulfill an important role in the detergency industry by breaking down protein stains, such as blood, egg, grass, cocoa, and human sweat (Joshi and Satyanarayana, 2013). Bacterial proteases were first used in laundry detergents in

[2]http://www.unilever.com/sustainable-living-2014/reducing-environmental-impact/greenhouse-gases/reducing-ghg-in-consumer-use/index.aspx
[3]http://www.pg.com/en_US/downloads/sustainability/reports/PG_2014_Sustainability_Report.pdf

1959 for the development of the detergent Bio 40 from Gebruder Schnyder-Biel. Novozymes has developed several cold-adapted proteases for different detergency applications. Kannase® (or Liquanase®), released in 1998, was one of the first proteases for washing laundry at cold temperatures, between 10 and 20°C. It corresponds to a non-specific protease that belongs to the serine proteases group. Novozymes also released, Polarzyme®, another variation of a serine protease for use when hand washing laundry using cold water. Polarzyme® maintains high activity in a broad range of temperatures from 5 to 60°C. The enzyme production company Genencor (Palo Alto, CA, USA), a division of DuPont (Wilmington, DE, USA), developed two cold-adapted proteases for laundry detergents, Purafect® Prime and Properase®, with optimal activity for soil stains removal at temperatures between 20 and 40°C. Genencor also developed Excellase for dishwashing at low or moderate temperatures. Recent research has focused in discovering novel cold-adapted proteases in psychrophilic microorganisms derived from Arctic and Antarctic ecosystems. A recent study screened and identified 68 protease-producing bacterial strains from the Arctic (Chen et al., 2013a). A novel serine protease was isolated from *Glaciozyma antarctica* strain PI12, cloned and expressed in *P. pastoris*, and displays high activity at 20°C (Alias et al., 2014). These new proteases represent an interesting alternative to currently utilized cold-adapted proteases. In recent years, two patents for cold-adapted bacterial proteases have been filed (Zhang et al., 2013; Asenjo et al., 2014b).

Amylases are widely used enzymes in detergent formulations. They breakdown starch-based stains from different foods, such as cereals, fruits, BBQ sauce, gravy, pasta, and potatoes. The most commonly used amylase class in detergency is α-amylase, which hydrolyzes the 1,4-α-glucosidic bond found in starch and decomposes it into water-soluble dextrins and oligosaccharides (Hmidet et al., 2009). Currently, there are few cold-active amylases on the market, but their applications have increased over time. In 2004, Novozymes released Stainzyme® an amylase that is effective at temperatures between 30 and 70°C. Even though this enzyme is not classified as a psychrophilic enzyme because of the temperature range for its activity, it was the first recognized amylase for moderate/low-temperature washing. In 2007, Novozymes released an improved version of this enzyme, Stainzyme® Plus, which displays an in-wash bleach tolerance and works efficiently at even lower temperatures (~20°C). DuPont Industrial Biosciences developed Preferenz™ S100, an amylase enzyme that enables high-performance laundry at 16°C. Consistent effort is being made to develop a new generation of cold-active amylases from psychrophilic/psychrotolerant microorganisms. For instance, in 2013 a novel cold-active, detergent-stable α-amylase from *Bacillus cereus* GA6 was characterized (Roohi et al., 2013). This extracellular enzyme is stable and active at low temperatures (4–37°C, with optimal activity at 22°C) and in alkaline pH (pH 7–11) and demonstrates good compatibility with commercial laundry detergents. Another amylase with potential applicability in detergency was isolated from the marine bacterium *Zunongwangia profunda* in 2014 (Qin et al., 2014). The recombinant *E. coli* form is active in a wide range of temperatures, from 0 to 35°C, maintaining 39 and 46% of activity at 0 and 5°C, respectively.

Cellulases are hydrolytic enzymes that breakdown cellulose into monosaccharides or "simple sugars" by catalyzing the degradation of β-1,4-glycosidic bonds. They are used in detergents for color and brightness care as they reduce the build-up of fuzz and pills in knitted garments. Normal use and repeated washing of cotton fabrics breaks down the cotton fibers (made of cellulose), causing them to trap dirt and soil. Cellulases digest the broken cellulose fibers removing the captured dirt particles. Additionally, cellulase removes β-glucan stains from oat products, such as cookies, cereals and snack bars. Currently, there are several available cellulases that are marketed for cold-washing, but these cellulases are not typically classified as a psychrophilic or even psychrotolerant enzyme. They display optimal activity between 30 and 60°C, but are active at lower temperatures as well. Examples of these enzymes includes: Rocksoft™ Antarctic and Antarctic LTC from Dyadic International (Jupiter, FL, USA), UTA-88 and UTA-90 from Hunan Youtell Biochemical (Shangai, China), and Retrocell Recop and Retrocell ZircoN from EpyGen Biotech (Dubai, UAE) (Kasana and Gulati, 2011). Truly cold-adapted cellulases were developed by Novozymes: Celluzyme®, which is derived from the fungus *Humicola insolens* and is active at low temperatures (~15°C), and Celluclean® a mix of cellulases for low-temperature washing.

In addition to these common detergent enzymes, the laundry and dishwashing industry is actively looking for other cold-active enzymes, such as mannanases and pectinases. Mannanase are used to degrade mannan or gum, a carbohydrate used extensively in food and personal care products. This enzyme hydrolyzes the β-1,4 bonds in mannose polymers, breaking them down into smaller more soluble carbohydrates. Few cold-active mannanases are currently commercially available: Mannaway® (Novozymes) can be used at temperatures as low as 20°C and Effectenz™ (DuPont) has optimal activity at 30°C. Pectinases are a group of enzymes that hydrolyzes pectin, a polysaccharide found in a variety of fruits, fruit juices, marmalades, and tomato sauces. This group of enzymes provides pectin-stain removal activity for detergent formulations. Cold-active pectinases are a current target for the detergent industry. XPect® (Novozymes) was released into the European market in 2010. XPect® is a cold-active pectate lyase that cleaves the α-1,4 glycosidic bonds of polygalacturonic acid into water-soluble "simpler sugars" optimally at 20°C.

Despite the several advances made in the development of cold-active enzymes for the detergent industry in recent years, there is a clear need for still more psychrophilic/psychrotolerant enzymes that can perform optimally under the current cold-washing practices. Enzymes that can work optimally at low temperatures (15–25°C), but maintain a high activity through a wide range of temperatures (between 5 and 60°C), and stay active in the presence of surfactants and alkaline pH are the future for this industry.

Cold Extremozymes Applied in the Food and Beverages Market

For hundreds of years, enzymes have been used in foods and beverages. In the dairy industry, enzymes are used for cheese production and in the preparation of dairy products; in the baking industry, enzymes improve the quality of bread; and in the beverage industry, enzymes are used to maintain wine color and

clarity, and to reduce the sulfur content. Some industrial enzymes can also be used to enhance filterability and improve the flavor of final products. Food and beverage enzymes make up one of the biggest markets for industrial enzyme applications. In 2011, this market was worth $1.2 billion and is expected to grow at a CAGR of 5.1% from 2013 to 2018, reaching a worldwide value of $1.7 billion by 2018 (Dewan, 2014). Europe is predicted to be the most active region.

Food enzymes can be divided into categories depending on their preferred use: food additives, food ingredients, and processing aids. In general, enzymes functioning as food additives are used to preserve flavor or enhance taste and appearance. For example, invertase and lysozyme are used as stabilizers and preservatives, respectively. Both enzymes are authorized by the European Commission (EC) as food additives. Enzymes used as food ingredients are added to increase nutritional value. Enzymes functioning as processing aids are added to food preparations for technical reasons; however, they do not have a function in the final food product. Lactase from *Kluyveromyces lactis*, for instance, is used to hydrolyze the lactose in milk for the manufacture of lactose-free products (Mateo et al., 2004). Other enzymes, such as α-amylases, peptide hydrolases, lipases, and catalases are some examples of enzymes that are added during food processing to confer specific characteristics to the food. These enzymes are inactivated in the final product.

The current food and beverage industry trend is to replace high-temperature processes with low-temperature processes. Low-temperature processing provides economic and environmental advantages. Some of the benefits of low-temperatures processing are energy savings, prevention of contamination and spoilage, retention of labile and volatile flavor compounds, minimization of undesirable chemical reactions that may occur at higher temperatures, and a higher degree of control over cold-active enzymes since they can be inactivated at high temperatures (Horikoshi, 1999; Pulicherla et al., 2011). As a consequence, a myriad of cold-adapted enzymes have been discovered and developed for use in the food and beverages market. A few examples are discussed below.

As in the detergent industry, amylases have applications in several food and beverage industry processes including, fermentation of beer and wine, bread making and fruit juice processing. All these applications are based on the degradation of starch into less complex sugars. The vast majority of amylases currently in use in the food and beverages industry are thermophilic, but this is changing because of the benefits of using cold-active enzymes. The first cold-adapted α-amylase studied was isolated from an Antarctic bacterium, *Alteromonas haloplanktis*, and has been successfully expressed in the mesophilic host *E. coli* (Feller et al., 1998). This enzyme and other cold-active α-amylases, such as the extracellular α-amylase from the bacterium *Microbacterium foliorum GA2* isolated from the Gangotri glacier (Kuddus, 2012) or the cold-active α-amylase from marine bacterium *Z. profunda* (Qin et al., 2014), represent good candidates for application in this particular industry. A patent relating to a variant of the parent α-amylase from *Bacillus licheniformis* displaying increased specific activity at temperatures from 10 to 60°C was granted to Novozymes in 2004 (Borchert et al., 2004).

Among enzymes in the food industry, β-galactosidases or lactases are highly valuable to the food industry. Lactases, as mention above, hydrolyze lactose into galactose and glucose, allowing for the production of lactose-free foodstuffs. The development of cold-active β-galactosidases is an intriguing idea for many companies because of the potential applications cold-active β-galactosidases would allow lactose degradation milk and other dairy products during refrigeration, cheese whey bioremediation, and sweetener production. Several companies, such as Biocatalysts (Wales, UK), DSM/Valley Research (South Bend, IN, USA), DuPont/Danisco (Wilmington, DE, USA), and Enzyme Development Corporation (New York, NY, USA), offer β-galactosidases or lactases which are not psychrophilic enzymes but show certain activities at low temperatures. A recent report compared several commercially available food-grade β-galactosidases, and demonstrated that those enzymes are sufficiently active in milk at refrigeration temperatures to enable the lactose hydrolysis process (Horner et al., 2011). However, novel cold-active β-galactosidases could simplify and reduce the cost of manufacturing lactose-free products. A cold-active β-galactosidase isolated from a marine psychrophilic bacterium was recently characterized. This β-galactosidases hydrolyzed around 80% of the lactose in raw milk at 20°C and pH 6.5 (Ghosh et al., 2012; Pulicherla et al., 2013). In 2012, a patent was granted to Stougaard and Schmidt (2010) for a cold-active β-galactosidase with stable enzymatic activity at temperatures <8°C. A company called Damhert Nutrition (Heusden-Zolder, Belgium) is currently using β-galactosidase as the first step for tagatose production, a novel sweetener that is obtained from lactose. In this process, lactose is broken down into galactose and glucose by β-galactosidase, subsequently, galactose is enzymatically transformed into tagatose. A recent publication demonstrated the benefits of using a cold-active β-galactosidase from the Antarctic marine bacterium *P. haloplanktis* for lactose hydrolysis at low temperatures (refrigeration conditions) from whey permeate and its potential applicability in tagatose production (Van de Voorde et al., 2014).

Pectinases are an integral part of the food industry. These enzymes catalyze the degradation of the plant carbohydrate pectin and are used in several food-related applications, like fruit juice processing for clarification and viscosity reductions and vinification and extraction of natural oils (Adapa et al., 2014). Today, most commercially available pectinases are derived from mesophilic organisms, but the current trend toward processing foods under low-temperature conditions is opening doors for the development of new cold-adapted pectinases. Several pectinases for use in the food and beverages industry are commercially available, but none are classified as psychrophilic enzymes. However, there are a couple of pectinase products that show activity at low temperatures. These include, Novoshape® (Novozymes), a pectin-methylesterase produced by a genetically modified strain of the fungus *Aspergillus oryzae*, and Pectinase 62L (Biocatalysts Ltd.), which is composed of a mix of polygalacturonase and pectin lyase derived from *Aspergillus sp.* Novoshape® and Pectinase 62L exhibit a temperature range for activity between 10 and 60°C. Lallemand (QC, Canada) produces Lallzyme® a set of pectinase mixes (polygalacturonase, pectin esterase and pectin lyase) from the fungus *Aspergillus niger*. These mixes possess activity between

5 and 20°C and are used for the clarification of juices, musts, and wines. Additional information about the current state of cold-active pectinase research for the food industry and advances in this field can be found in a recent review by Adapa et al., 2014.

In bread making, xylanases convert the insoluble hemicellulose of dough into soluble sugars before baking, producing a fluffy but strong dough and voluminous loaves of bread with soft and elastic properties. Since these properties are obtained at low temperatures, before baking the bread, cold-active xylanases may provide a significant benefit. Despite their potential applicability, cold-active xylanases have been poorly studied and many of the xylanases used in industry today appear to be mesophilic or thermophilic (Collins et al., 2005). A recent report demonstrated that three psychrophilic xylanases from *P. haloplanktis* TAH3A, *Flavobacterium* sp. MSY-2 and one from an unknown bacterial origin effectively improved dough properties and final bread volume (up to 28%) when compared to mesophilic xylanases from *Bacillus subtilis* and *Aspergillus aculeatus* (Dornez et al., 2011). Several novel cold-adapted xylanases from different organisms have been reported in the last years (Wang et al., 2012; Chen et al., 2013b; Del-Cid et al., 2014), including one patented by Asenjo et al. (2014a).

Other Cold-Adapted Enzymes

Many other cold-active enzymes have further applications within the textile industry. Optisize® COOL amylase (Genencor-DuPont) allows for the desizing of woven fabrics at low temperatures, Primafast® GOLD HSL cellulase (Genencor-DuPont) can be applied during the bio-finishing of cellulosic fabrics, and IndiAge® NeutraFlex cellulase allows low-temperature enzymatic stonewashing at a neutral pH.

Recently, the gene that codes for the psychrotolerant enzyme catalase (CAT) from a psychrotolerant microorganism belonging to the *Serratia* genus was successfully cloned and expressed in *E. coli*. CAT is a very active and extremely efficient antioxidant enzyme even at low temperatures. This enzyme is involved in trapping reactive oxygen species generated by oxidative stress. Psychrotolerant catalase was expressed as a recombinant enzyme and showed excellent catalytic properties and stability. This enzyme kept 50% of its activity after 7 h of 50°C exposure and is active in a wide range of temperatures from 20 to 70°C. Due to these unique characteristics, it can be applied in the textile, research, cement, and cosmetic industries. This enzyme is now commercially available through Swissaustral Company[4] (Athens, GA, USA).

Hot Extremozymes: Industrial Relevance and Current Trends

Thermophilic and Hyperthermophilic Microorganisms

Thermophiles and hyperthermophiles are defined as organisms that not only survive but thrive at high temperatures. Thermophiles can be found in environments with temperatures over 50°C, and hyperthermophiles in environments over 80°C. To date, the highest temperatures known to sustain thermophilic microbial life are 113°C for the chemolithoautotrophic archaea *Pyrolobus fumarii* (Blochl et al., 1997; Cowen, 2004) and 122°C for the methanogenic hyperthermophile *Methanopyrus kandleri* (Takai et al., 2008). Thermophiles and hyperthermophiles are found in environments like hot springs and deep sea vents where temperatures easily surpass 100°C. Other habitats include geysers and highly geothermal volcanic areas.

Numerous thermophilic prokaryotes have been identified and thoroughly studied. The majority of thermophilic prokaryotes are from the domain Archaea, but some representatives from the domain Bacteria have also been identified (Huber and Stetter, 1998; Klenk et al., 2004). It has been suggested that hyperthermophiles are the most deeply branching organisms on the phylogenetic tree, making them among the most ancient known organisms (Di Giulio, 2005).

Sulfate-dependent organisms are some of the most common thermophiles and hyperthermophiles. Sulfate reduction, as found in the hyperthermophilic archaea *Archaeoglobus fulgidus* (Beeder et al., 1994; Klenk et al., 1997), is thought to be one of the most ancient energetic pathways (Wagner et al., 1998; Roychoudhury, 2004). Many of these organisms are from the archaeal phylum *Crenarchaeota* (Achenbach-Richter et al., 1987; Friedrich, 1998). Other anaerobic metabolic pathways used by (hyper)thermophiles include the production of methane from hydrogen and carbon dioxide, such as in the case of *Methanocaldococcus jannaschii* (Bult et al., 1996).

Sulfate oxidation also occurs in organisms that thrive in these extreme conditions. Examples of sulfate and, in some cases, elemental sulfur-oxidizing organisms are found within the *Sulfolobus* family (Brock et al., 1972; Kletzin et al., 2004). The oxidation of organic compounds and metals has also been reported and can be associated with low pH conditions as well (Larsson et al., 1990).

Structural Features and Action Mechanism of Hot Extremozymes

A great deal of attention has been focused on proteins from (hyper)thermophiles as thermostable enzymes have gained importance in biotechnological processes. Comparative studies on mesophilic and thermophilic enzymes and other proteins have shown that in most cases, amino acid sequences are highly conserved, although certain changes in composition have been observed. Studies of the glutamate dehydrogenase from *Pyrococcus furiosus*, which grows at 105°C, compared with mesophilic versions of the enzyme have shown a higher content of hydrophobic amino acids and a decrease in the content of polar and charged amino acids. A drop in the number of glycine residues was also observed (Maras et al., 1994). These results are not surprising when considering how thermodynamic factors influence protein stability.

Highly dense packing structures with tight hydrophobic cores minimize solvent interaction with this core and therefore, have a stabilizing effect. Since protein stability is dependent on small non-covalent forces, a high degree of cooperation among these hydrophobic interactions is expected. Another factor of increased thermostability is a decrease in the protein surface area in proportion to protein size. This has been observed in proteins from *P. furiosus*. Enzymes from *P. furiosus* have highly packed

[4]http://www.swissaustral.com

hydrophobic cores with many ionic pairs and buried atoms to help diminish unfavorable solvent interactions (Rice et al., 1996; Kumar and Nussinov, 2001).

When comparing 3D structures of (hyper)thermophilic proteins to their mesophilic counterparts, a highly conserved structure has been observed. This suggests the conserved residues have some functional significance. The majority of differences can be observed in the region of the protein that interacts with solvent: differences in the sizes of helices, beta sheets and ionic modifications in terminal portions (Ladenstein and Antranikian, 1998; Kumar and Nussinov, 2001). Again, tight packaging is observed, but this does not alter the final conformation.

Biotechnological Applications of Hot Extremozymes

From an industrial viewpoint, (hyper)thermophilic enzymes possess certain advantages over their mesophilic counterparts. These enzymes are active and efficient under high temperatures, extreme pH values, high substrate concentrations and high pressure. They are also highly resistant to denaturing agents and organic solvents. In addition, hot extremozymes perform faster reactions and are easier to separate from other heat-labile proteins during purification steps.

Due to their overall activity and stability at high temperatures, (hyper)thermophilic enzymes are attractive for several important industrial activities. It is difficult, however, to obtain pure enzymes from source microorganisms and yields are typically low when cultivated on a large scale for industrial applications. Efforts to overcome these problems have focused on cloning and expressing (hyper)thermophilic enzymes in mesophilic hosts. Ideally, this can be done without losing their activity and thermostability. Thermostable enzymes expressed in mesophilic hosts can typically be purified easily and the degree of purity obtained is suitable for industrial applications. The availability of an increasing number of hot extremozymes has opened new possibilities for industrial processes. There is a high availability of hot extremozymes with applications in several markets. This section of the review will focus on two established, but growing markets for their application, food and beverages and pulp and paper. Other markets, such as feed and biofuels, will not be covered here due to the large number of enzymes available and the complexity of these markets. Select examples of in-development and commercially available hot extremozymes are listed below (**Table 2**).

Hot Extremozymes Applied in the Food and Beverage Market

Since 1973, the starch-processing industry has grown into one of the largest markets for enzymes. Enzymatic starch hydrolysis is used to form syrups through liquefaction, saccharification, and isomerization processes. Products of starch hydrolysis, such as glucose, maltose, and oligosaccharides, can be used for the production of a variety of non-food products including alcohols, polyols, ascorbic acid, lysine, etc. In the manufacture of syrups, liquefaction and saccharification processes are run at high temperatures, easily over 60–70°C (Bentley and Williams, 1996). α-amylases are used during the liquefaction step to form maltodextrins and mash viscosity prior to saccharification and fermentation with yeast. Novozymes Avantec®, Termamyl® SC

TABLE 2 | Examples of commercially available thermostable enzymes.

Market	Enzyme	Commercially available	Uses
Food and beverages	Amylases	Avantec®, Termamyl® SC, Liquozyme®, Novamyl®, Fungamyl® (Novozymes), Fuelzyme® (Verenium), AlphaStar PLUS (Dyadic)	Enzymatic starch hydrolysis to form syrups. Applied in processes, such as baking, brewing, preparation of digestive aids, production of cakes and fruit juices
	Glucoamylases	Spirizyme® (Novozymes)	Used on liquefied starch-containing substrates
	Glucose (xylose) isomerases	Sweetzyme® (Novozymes)	Isomerization equilibrium of glucose into fructose
	Proteases	Protease PLUS	Applied in brewing to hydrolyze most proteins
	Amyloglucosidases	GlucoStar PLUS (Dyadic)	Used in processing aids
	Xylanases, cellulases, pectinases, mannanases, β-xylosidases, α-l-arabinofuranosidases, amylases, protease, other	CeluStar XL, BrewZyme LP, Dyadic Beta Glucanase BP CONC, Dyadic xylanase PLUS, Xylanase 2XP CONC, AlphaStar CONC and Protease AP CONC. (Dyadic), Panzea BG, Panzea 10X BG, Panzea Dual (Novozymes), Cellulase 13P (Biocatalysts)	Hydrolyis of hemicellulose and cellulose to lower molecular weight polymers in brewing
	Lipases and xylanases	Lipopan® and Pentopan® (Novozymes)	Obtaining of stronger dough in bakery
	Glucose oxidases	Gluzym® (Novozymes)	Used to obtain stronger gluten in bakery
Pulp and paper	Xylanases	Luminase® PB-100 and PB-200 (Verenium), Xylacid® (Varuna Biocell), Xyn 10A (Megazyme)	Bio-bleaching
	Laccases	Laccase (Novozyme)	Bio-bleaching
	Lipases and esterases	Lipase B Lipozyme® CALB L, Lipase A NovoCor®AD L, Resinase™ HT and Resinase A2X (Novozymes), Optimyze® (Buckman Laboratories)	Pitch control
	Cellulases/hemicellulases preparations	FibreZyme® G5000, FibreZyme® LBL CONC, FibreZyme™ LDI and FibreZyme™ G4 (Dyadic)	Modify cellulose and hemicellulose components of virgin and recycled pulps
	Amylase	Dexamyl-HTP (Varuna Biocell)	Modification of starch of coated paper

and Liquozyme® products liquefy and prepare the starch source for optimal fermentation, resulting in higher yields and reduced operating costs. During the saccharification step, pullunases and glucoamylases like Spirizyme® from Novozymes, are used on liquefied starch-containing substrates to produce sugars for the fermentation at 70°C. These hot extremozymes allow for maximum starch conversion and consistent fermentation across variable mash and plant conditions. Pullunases and glucoamylases are used for producing glucose syrups, and pullunase and β-amylase for producing maltose syrups. The thermophilic α-amylase Fuelzyme®, developed and marketed by Verenium Corporation (San Diego, CA, USA), a division of BASF (Mannheim, Germany), is used for obtaining superior reduction in mash viscosity when starch liquefaction is performed at low pH. Fuelzyme® performs at a temperature of 88–91°C and is also used to increase fuel ethanol yields as a result of improved starch conversion.

Commonly, enzymes isolated from hyperthermophiles work optimally between 80 and 110°C and at pH levels from 4.0 to 7.5. These conditions correlate with the optimal conditions for starch liquefaction (100°C and pH 4.0–5.0) (Niehaus et al., 1999). Thus, characterization and development of novel hyperthermophilic enzymes is essential for these industrial processes. The expression of a mutant thermostable α-amylase from *B. licheniformis*, with optimum activity at high temperature and lower pH, in *E. coli* and *P. pastoris,* was recently achieved (Du et al., 2006). Because of their high-temperature activity profiles, β-amylases from *Thermoanaerobacterium thermosulfurigenes* and *Clostridium thermocellum* SS8 are also good candidates for saccharification processes (Kitamoto et al., 1988; Swamy et al., 1994). However, further research into new β-amylases is still needed.

In recent years, amylopullulanases have emerged as useful starch-processing enzymes for the production of maltose and maltotriose syrups. Amylopullulanases are sparking a new trend of replacing α-amylases and β-amylases in the conventional starch liquefaction process, because of their bi-functionality for catalyzing debranching and liquefying reactions, and because of their calcium independence. In addition to their applications in industrial starch conversion, the previously mentioned amylopullulanases features make them useful as detergent additives. Several thermophilic amylopullulanases have been discovered and cloned into microorganisms like *E. coli* and *B. subtilis* for increased expression (Nisha and Satyanarayana, 2013). A starch saccharification process using only amylolytic enzymes (α-amylase, amylopullulanase, and glucoamylase) from thermophiles was described in 2004 (Satyanarayana et al., 2004).

Glucose (xylose) isomerases catalyze the isomerization of glucose into fructose for the preparation of fructose-based syrups. The conversion rate of glucose-fructose is altered at high temperatures between 60 and 90°C. Sweetzyme® from Novozymes is an immobilized glucose isomerase from *Streptomyces murinus* that is able to perform at temperatures from 55 to 60°C. Other xylose isomerases have been characterized from *Thermotoga neapolitana*, *Thermotoga maritima*, *Thermus aquaticus*, and *Thermus thermophilus* (Vieille et al., 1995) among other microorganisms. These are not yet commercially available. Recent reports have described thermophilic glucose isomerases isolated from *Fervidobacterium gondwanense* and *Bacillus sp.* isolated from agricultural soil, with optimal temperatures for activity of 70°C, making both enzymes good candidates for industrial applications (Kluskens et al., 2010; Sukumar et al., 2013).

Amylases are also applied in processes, such as baking, brewing, the preparation of digestive aids, and in the production of cakes and fruit juices. Currently, Novamyl® (Novozymes) a thermostable maltogenic amylase of *Bacillus stearothermophilus* is used commercially in the bakery industry for improved freshness and other bread qualities. AlphaStar PLUS is a food grade, bacterial α-amylase from *B. subtilis* used in brewing applications. These enzymes are endoamylases, capable of randomly hydrolyzing the predominating *a*-D-(1 → 4) glucosidic linkages of starch to rapidly reduce the viscosity of gelatinous starch. It is stable up to 90°C. GlucoStar PLUS (Dyadic International) is an industrial amyloglucosidase liquid product used in processing aids which is derived from a non-genetically modified strain of *A. niger*. The enzyme α-amylase is used to break down both components of starch, amylose and amylopectin, as well as the resultant products of their dextrinization. CeluStar XL (Dyadic International) is an enriched preparation that contains xylanase, cellulase, β-glucanase, pectinase, mannanase, xyloglucanase, laminarase, β-glucosidase, β-xylosidase, α-L-arabinofuranosidase, amylase, and protease to hydrolyze hemicellulose and cellulose to lower molecular weight polymers under the proper processing conditions. This product is used in brewing, typically within a broad range of pH (3.5–7.5) and temperature 35 and 60°C. Other thermophilic enzymes developed by Dyadic International, mainly applied in the brewing industry, are BrewZyme LP, Dyadic Beta Glucanase BP CONC, Dyadic xylanase PLUS, Xylanase 2XP CONC, AlphaStar CONC, Protease AP CONC, and Protease PLUS.

Panzea BG and Panzea 10X BG of Novozymes, are both pure xylanases from *B. licheniformis* used in the bakery industry. These products aid in the large-scale manufacture of dough with the desired texture and appearance. Other hot extremozymes from Novozymes with applications in the food industry are Fungamyl® (α-amylase), which is used to improve the color and volume of bread, Lipopan® (lipase) and Pentopan® (xylanase) which are used to obtain stronger dough and Gluzym® (glucose oxidase) which is used to obtain stronger gluten.

Hot Extremozymes Applied in Pulp and Paper

Pulp is a cellulosic fibrous material made from wood, fiber crops, and waste paper. Commonly, pulp is made by chemical and mechanical procedures that separate cellulose fibers from the rest of the components of wood (hemicellulose and lignin). These methods include applying harsh conditions like extremely high temperatures (in many cases over 80°C), alkaline pHs and the use of strong chemicals (sodium sulfide, sodium hydroxide, and chlorine). In efforts to complement the current pulping procedures, enzymatic bio-pulping is becoming an attention-grabbing approach as it offers an eco-friendly, safer, and profitable solution for the pulp and paper industry. The utilization of stable hyperthermophilic/alkaline enzymes represents a valuable addition to the current pulping processes by increasing the efficiency and reducing the use of dangerous chemicals. Despite the fact that currently the market for enzymes in the pulping and paper industry is small, it is expected to reach a size of $261.7 million in 2018,

with a CAGR of 7% (2013–2018). Europe is positioned as the main geographical market (Dewan, 2014).

Among the enzymes related to bio-pulping, xylanases are considered of the highest impact. They can break down the hemicellulose from plant cell walls by degrading the linear polysaccharide β-1,4-xylan into xylose. In this manner, xylanases facilitate the release of lignin, in a process called bio-bleaching. Hyperthermophilic xylanases have been isolated from a number of different microorganisms, such as *T. maritima*, *Streptomyces sp.*, *Thermotoga thermarum*, and *Thermoascus aurantiacus*. Some of these enzymes have already been tested in bio-bleaching processes (Chen et al., 1997; Beg et al., 2000; Milagres et al., 2004; Jiang et al., 2006; Shi et al., 2013). However, few xylanases are currently available in the market for pulp and paper applications. Luminase® PB-100 and PB-200, for example, are highly thermostable xylanases supplied by Verenium Company. Luminase® PB-100 acts between 40 and 70°C, while Luminase® PB-200 can be used between 60 and 90°C. Megazyme (Bray, Ireland) offers Xyn 10A, a recombinant endo-1,4-β-D-xylanase from *T. maritime*, which has an optimal temperature of 80°C but displays temperature stability up to 90°C, and a pH stability up to pH 9.

Laccases are also applied in the bio-bleaching of pulp. By directly degrading lignin, the substance that gives a dark color to pulp, laccases increase the brightness of the final product. In addition, laccases have been observed to play a role in the removal of lipophilic extractives which are part of the problem of pitch deposition (Virk et al., 2012). Several laccases have been described for use in bio-bleaching, particularly from fungal origin since bacterial laccases are not well characterized (Baldrian, 2004; Virk et al., 2012). Novozymes commercialize a recombinant thermostable laccase from the fungus *Myceliophthora thermophila* which has been cloned in *A. oryzae* and is active up to 70°C (Xu et al., 1996; Berka et al., 1997) In 2006, AB Vista (Wiltshire, UK) was granted a patent for a thermostable laccase enzyme which is effective at temperatures between 30 and 80°C (Paloheimo et al., 2006). Even though there are certain commercial options, it is necessary to discover and develop novel laccases that can perform optimally under the harsh conditions of the pulping process. A recent report described the bio-bleaching of wheat straw pulp using a recombinant laccase from the hyperthermophilic bacterium *Thermus thermophiles*, which performs optimally at 85°C (Zheng et al., 2012).

Hyperthermophilic lipases are applied for pitch control in the paper production process. Pitch generates sticky deposits which affect mill operations and the quality of the final product. Lipases degrade the triglycerides of pitch reducing its deposition. Novozymes offers Resinase® HT, a lipase with temperature stability up to 90°C and pH stability between pH 5 to 9. This enzyme was developed by directed evolution of an older Resinase® variant and is one of the most used enzymes for pitch control in the pulp and paper industry in North America, China, Japan, and other countries (Gutierrez et al., 2009). In addition to lipases, novel hyperthermophilic esterases have been suggested to improve pitch control, by degrading other sticky compounds, such as adhesive and coatings which contain significant amounts of esters (Calero-Rueda et al., 2004). Optimyze®, developed by Buckman Laboratories (Memphis, TN, USA) is an enzyme-mix which contains an esterase that breaks up ester bonds of polyvinyl acetate with activity up to a temperature of 60°C. Novel hyperthermophilic lipases and esterases with higher optimal temperatures and more alkaline pHs are needed to solve the pitch problems of the pulp and paper industry.

Other hyperthermophilic enzymes that find application in the pulp and paper industry are cellulases. These enzymes increase the brightness and strength properties of paper sheets and the overall efficiency of the refining process (Kuhad et al., 2011). In 2012, Dyadic International launched FibreZyme® G500, a cellulase with a wide temperature and pH range for activity, from 35 to 75°C and pH 4.5 to 9. This is an adaptable product for most pulping procedures. In addition, a recent report described a novel recombinant archaeal cellulase with an optimal activity at 109°C, a half-life of 5 h at 100°C, and it is highly resistant to strong detergents, high-salt concentrations, and ionic liquids (Graham et al., 2011).

Even though many advances have been made toward developing novel enzymes for the pulp and paper industry, additional efforts are needed to discover and develop high-performance enzymes that are better adapted to the current conditions of the pulping industry. In addition to xylanases, lipases, esterases and cellulases, hyperthermophilic pectinases (improve retention in mechanical pulps), and amylases (finishing and coating of paper) will further aid in the implementation of environmentally friendly and more efficient procedures for the pulp and paper industry (Reid and Ricard, 2000; de Souza and de Oliveira Magalhaes, 2010).

Challenges and Conclusion

Despite the inherent advantages of extremozymes, the actual number of available extremophilic bio-catalytic tools is very limited. Working with extremophiles and/or extremozymes requires the adaptation and creation of new methodologies, assays, and techniques that operate under non-standard conditions. Many of the tools that are currently used in classical microbiology and biochemistry experimentation cannot be applied toward extremophilic research because they do not possess the chemical and/or mechanical properties to withstand extreme conditions. Similarly, techniques for researching common microorganisms need to be further adjusted to fit the requirements of extremophiles. A classic example is the plating of hyperthermophiles on a solid surface. Conventional streaking on agar-based media is impracticable because agar melts and water evaporates quickly at such high temperatures. Alternative solidifying agents are used to grow thermophiles and hyperthermophiles, such as silica gel, starch, and Gelrite, a low-acetyl gellan gum made from *Pseudomonas*. Additionally, the large technical gap between producing an enzyme under laboratory conditions and obtaining a final commercializable product is still a problem for the development of novel biocatalysts. Several scientific challenges need to be solved before it will be possible to fully realize the potential of extremozymes.

Nature provides a vast source of biocatalysts. However, the probability of finding the right enzymatic activity for a particular application depends on the available technical capabilities to

efficiently assess this large biodiversity. This capability is mainly mediated by technologies, such as metagenomic screenings, genome mining, and direct enzymatic exploration (Leis et al., 2013; Adrio and Demain, 2014; Bachmann et al., 2014).

Metagenomic screenings and genome mining are commonly based on the presence of DNA/RNA sequences coding for determined enzymes. These methods require that the search for a novel enzyme is based on genetic sequence homology to already described enzymes. This creates a bias and hinders the discovery of truly new enzymes. The discovery of new enzymes based on genetic sequences also does not always give accurate information, especially for less studied organisms like extremophiles. To get industry-quality results for new enzymes, these approaches require further processing through directed evolution and protein engineering. Also, in the case of functional metagenomic screenings, there are several technical challenges that need to be addressed. For instances, the isolation of high-quality DNA from environmental samples, which often is contaminated with humic acids, the difficulties to lyse extremophilic microorganisms, the cell recovery biases, and the need of appropriate hosts for heterologous expression of recovered genes from metagenomics data.

An alternative method is presented in the direct exploration of extremophilic enzymes based on functional screenings of enzymatic activities in large collections of microorganisms. The functional detection of an enzymatic activity determines the existence of the target biocatalyst in the sample, and its behavior under previously determined conditions. It is important to note that confirming the presence and the functionality of a biocatalyst, under the actual conditions of a particular industrial process, is an important step toward further developing an industrial product. There are also drawbacks to this approach. To test the presence of an enzyme in the crude extract of a microorganism, extremely robust enzymatic assays needs to be developed and implemented. These then have to be adapted to the required conditions for enzyme activity. Also, in order to make functional detection more appealing for industry purposes, it is absolutely required that this approach is further developed to handle hundreds of samples simultaneously under small-scale and automated conditions to allow for high-throughput discovery of efficient biocatalysts for a specific application. Developing automated systems for working with extremophiles and extremozymes is not only a scientific challenge, but a technological and engineering one as well. The task is not only related to media composition or assay development, it also involves developing tools and instruments that can withstand and function optimally under extreme conditions. Currently, High-Throughput Screening (HTS) technologies are being implemented by pharmaceutical companies for identifying new drugs and chemicals (Zhu et al., 2010). The application of these technologies toward the search for novel biocatalysts may be the solution to some of these problems (Donadio et al., 2009; King et al., 2010; Glaser and Venus, 2014). Additionally, the application of novel culture techniques for uncultured bacteria, such as the recently reported iChip (Ling et al., 2015) will further aid in the identification and development of novel industrial enzymes.

Technical limitations are not only found at the moment of discovering novel biocatalysts, but also when the biocatalysts are fine-tuned for industrial applications. Using extremophiles directly as the producing microorganism for extremozymes is an ideal situation, but it presents several difficulties. Operating bioreactors under extreme conditions, such as high and low pHs, high temperatures or high concentration of salts, shortens the lifetime of sensors and seals in the bioreactors. Also, in many cases, extremophiles do not grow optimally in bioreactors. In the case of (hyper)thermophiles this problem has been attributed to the accumulation of toxic compounds as a result of Maillard reactions (a series of complex reactions between reducing sugars and amino acids, occurring at high temperatures), as described in the cultivation of *Aeropyrum pernix* (Kim and Lee, 2003). One of the alternatives to overcome the low biomass yields is to appropriately design the culture medium. Although there are examples where a defined synthetic medium is used for the cultivation of extremophiles (Biller et al., 2002), complex culture medium containing yeast extract and peptone is, by far, the most commonly employed for cultivation of extremophiles (Dominguez et al., 2004; Fucinos et al., 2005a,b).

Due to the limitations of growing extremophiles for producing extremozymes, the current strategy used is to clone and express the genes encoding the desired product in mesophilic hosts prior to the operation in a bioreactor (Karlsson et al., 1999). Many thermophilic genes have been cloned and expressed in mesophilic hosts, yielding highly active and temperature stable enzymes, such as the thermoalkalophilic lipase from *Bacillus thermocatenulatus* (Rua et al., 1998). However, recombinant expression of (hyper)thermophilic enzymes in *E. coli* and other bacterial hosts is still problematic. Expressing genes from archaea, for example, in these mesophilic host organisms can lead to misreading genes. This is not the case with bacterial genes, making them better candidates for cloning into bacterial hosts (Kristjansson, 1989). There is a clear need for new hosts able to properly express hyperthermophilic archaeal enzymes, such as the recent efforts reported for the expression of hyperthermophilic cellulases of the archaea *Pyrococcus sp* in the fungus *Talaromyces cellulolyticus* (Kishishita et al., 2015). The development of novel culture and molecular tools, more efficient mass production processes, and novel technologies for genetic and protein engineering will further advance the application of extremozymes in different industries.

References

Achenbach-Richter, L., Stetter, K. O., and Woese, C. R. (1987). A possible biochemical missing link among archaebacteria. *Nature* 327, 348–349. doi:10.1038/327348a0

Adapa, V., Ramya, L. N., Pulicherla, K. K., and Rao, K. R. (2014). Cold active pectinases: advancing the food industry to the next generation. *Appl. Biochem. Biotechnol.* 172, 2324–2337. doi:10.1007/s12010-013-0685-1

Adrio, J. L., and Demain, A. L. (2014). Microbial enzymes: tools for biotechnological processes. *Biomolecules* 4, 117–139. doi:10.3390/biom4010117

Alias, N., Ahmad Mazian, M., Salleh, A. B., Basri, M., and Rahman, R. N. (2014). Molecular cloning and optimization for high level expression of cold-adapted serine protease from antarctic yeast *Glaciozyma antarctica* PI12. *Enzyme Res.* 2014, 197938. doi:10.1155/2014/197938

Asenjo, J. A., Andrews, B. A., Acevedo, J. P., Parra, L., and Burzio, L. O. (2014a). *Protein and DNA Sequence Encoding a Cold Adapted Xylanase*. US Patent No 8679814 B2. United States Patent and Trademark Office.

Asenjo, J. A., Andrews, B. A., Acevedo, J. P., Reyes, F., and Burzio, L. O. (2014b). *Protein and DNA Sequence Encoding a Cold Adapted Subtilisin-Like Activity*. US Patent No 8759065 B2. United States Patent and Trademark Office.

Awazu, N., Shodai, T., Takakura, H., Kitagawa, M., Mukai, H., and Kato, I. (2011). *Microorganism-Derived Psychrophilic Endonuclease*. US Patent No 8034597 B2. United States Patent and Trademark Office.

Bachmann, B. O., Van Lanen, S. G., and Baltz, R. H. (2014). Microbial genome mining for accelerated natural products discovery: is a renaissance in the making? *J. Ind. Microbiol. Biotechnol.* 41, 175–184. doi:10.1007/s10295-013-1389-9

Bakermans, C., and Skidmore, M. L. (2011). Microbial metabolism in ice and brine at -5 degrees C. *Environ. Microbiol.* 13, 2269–2278. doi:10.1111/j.1462-2920.2011.02485.x

Baldrian, P. (2004). Purification and characterization of laccase from the white-rot fungus *Daedalea quercina* and decolorization of synthetic dyes by the enzyme. *Appl. Microbiol. Biotechnol.* 63, 560–563. doi:10.1007/s00253-003-1434-0

Beeder, J., Nilsen, R. K., Rosnes, J. T., Torsvik, T., and Lien, T. (1994). *Archaeoglobus fulgidus* isolated from hot North Sea oil field waters. *Appl. Environ. Microbiol.* 60, 1227–1231.

Beg, Q. K., Bhushan, B., Kapoor, M., and Hoondal, G. S. (2000). Enhanced production of a thermostable xylanase from *Streptomyces* sp. QG-11-3 and its application in biobleaching of *Eucalyptus* kraft pulp. *Enzyme Microb. Technol.* 27, 459–466. doi:10.1016/S0141-0229(00)00231-3

Bentley, I. S., and Williams, E. C. (1996). "Starch conversion," in *Industrial Enzymology*, ed. W. S. Godfrey (New York, NY: Stockton Press), 341–357.

Berka, R. M., Schneider, P., Golightly, E. J., Brown, S. H., Madden, M., Brown, K. M., et al. (1997). Characterization of the gene encoding an extracellular laccase of *Myceliophthora thermophila* and analysis of the recombinant enzyme expressed in *Aspergillus oryzae*. *Appl. Environ. Microbiol.* 63, 3151–3157.

Biller, K. F., Kato, I., and Markl, H. (2002). Effect of glucose, maltose, soluble starch, and CO2 on the growth of the hyperthermophilic archaeon *Pyrococcus furiosus*. *Extremophiles* 6, 161–166. doi:10.1007/s007920100244

Blochl, E., Rachel, R., Burggraf, S., Hafenbradl, D., Jannasch, H. W., and Stetter, K. O. (1997). *Pyrolobus fumarii*, gen. and sp. nov., represents a novel group of archaea, extending the upper temperature limit for life to 113 degrees C. *Extremophiles* 1, 14–21. doi:10.1007/s007920050010

Borchert, T. V., Svendsen, A., Andersen, C., Nielsen, B., Nissem, T. L., and Kjærulff, S. (2004). *Exhibit Alterations in at Least One of the Following Properties Relative to Parent Alpha-Amylase: Improved pH Stability at pH 8-10.5, Improved Calcium Ion Stability at pH 8-10.5, Increased Specific Activity at 10-60 Degrees C*. US Patent No 6673589 B2. United States Patent and Trademark Office.

Brock, T. D., Brock, K. M., Belly, R. T., and Weiss, R. L. (1972). Sulfolobus: a new genus of sulfur-oxidizing bacteria living at low pH and high temperature. *Arch. Mikrobiol.* 84, 54–68. doi:10.1007/BF00408082

Bult, C. J., White, O., Olsen, G. J., Zhou, L., Fleischmann, R. D., Sutton, G. G., et al. (1996). Complete genome sequence of the methanogenic archaeon, *Methanococcus jannaschii*. *Science* 273, 1058–1073. doi:10.1126/science.273.5278.1058

Calero-Rueda, O., Gutierrez, A., Del Rio, J. C., Prieto, A., Plou, F., Ballesteros, A., et al. (2004). Hydrolysis of sterol esters by an esterase from *Ophiostoma* piceae: application to pitch control in pulping of *Eucalyptus globulus* wood. *Int. J. Biotechnol.* 6, 367–375. doi:10.1504/IJBT.2004.005519

Canganella, F., and Wiegel, J. (2011). Extremophiles: from abyssal to terrestrial ecosystems and possibly beyond. *Naturwissenschaften* 98, 253–279. doi:10.1007/s00114-011-0775-2

Cavicchioli, R., Charlton, T., Ertan, H., Mohd Omar, S., Siddiqui, K. S., and Williams, T. J. (2011). Biotechnological uses of enzymes from psychrophiles. *Microb. Biotechnol.* 4, 449–460. doi:10.1111/j.1751-7915.2011.00258.x

Chen, C., Adolphson, R., Dean, J. F. D., Eriksson, K. L., Adams, M. W. W., and Westpheling, J. (1997). Release of lignin from kraft pulp by a hyperthermophilic xylanase from *Thermatoga maritima*. *Enzyme Microb. Technol.* 20, 39–45. doi:10.1016/S0141-0229(97)82192-8

Chen, M., Li, H., Chen, W., Diao, W., Liu, C., Yuan, M., et al. (2013a). [Isolation, identification and characterization of 68 protease-producing bacterial strains from the Arctic]. *Wei Sheng Wu Xue Bao* 53, 702–709.

Chen, S., Kaufman, M. G., Miazgowicz, K. L., Bagdasarian, M., and Walker, E. D. (2013b). Molecular characterization of a cold-active recombinant xylanase from *Flavobacterium* johnsoniae and its applicability in xylan hydrolysis. *Bioresour. Technol.* 128, 145–155. doi:10.1016/j.biortech.2012.10.087

Cheng, Y. Y., Qian, Y. K., Li, Z. F., Wu, Z. H., Liu, H., and Li, Y. Z. (2011). A novel cold-adapted lipase from *Sorangium cellulosum* strain So0157-2: gene cloning, expression, and enzymatic characterization. *Int. J. Mol. Sci.* 12, 6765–6780. doi:10.3390/ijms12106765

Chintalapati, S., Kiran, M. D., and Shivaji, S. (2004). Role of membrane lipid fatty acids in cold adaptation. *Cell Mol. Biol. (Noisy-le-grand)* 50, 631–642. doi:10.1170/T553

Collins, T., Gerday, C., and Feller, G. (2005). Xylanases, xylanase families and extremophilic xylanases. *FEMS Microbiol. Rev.* 29, 3–23. doi:10.1016/j.femsre.2004.06.005

Collins, T., Meuwis, M. A., Stals, I., Claeyssens, M., Feller, G., and Gerday, C. (2002). A novel family 8 xylanase, functional and physicochemical characterization. *J. Biol. Chem.* 277, 35133–35139. doi:10.1074/jbc.M204517200

Cowen, D. A. (2004). The upper temperature of life – where do we draw the line? *Trends Microbiol.* 12, 58–60. doi:10.1016/j.tim.2003.12.002

D'Amico, S., Collins, T., Marx, J. C., Feller, G., and Gerday, C. (2006). Psychrophilic microorganisms: challenges for life. *EMBO Rep.* 7, 385–389. doi:10.1038/sj.embor.7400662

de Souza, P. M., and de Oliveira Magalhaes, P. (2010). Application of microbial alpha-amylase in industry – a review. *Braz. J. Microbiol.* 41, 850–861. doi:10.1590/S1517-83822010000400004

Del-Cid, A., Ubilla, P., Ravanal, M. C., Medina, E., Vaca, I., Levican, G., et al. (2014). Cold-active xylanase produced by fungi associated with Antarctic marine sponges. *Appl. Biochem. Biotechnol.* 172, 524–532. doi:10.1007/s12010-013-0551-1

Dewan, S. S. (2014). *Global Markets for Enzymes in Industrial Applications*. Wellesley, MA: BCC Research.

Di Giulio, M. (2005). A comparison of proteins from *Pyrococcus furiosus* and *Pyrococcus abyssi*: barophily in the physicochemical properties of amino acids and in the genetic code. *Gene* 346, 1–6. doi:10.1016/j.gene.2004.10.008

Dominguez, A., Sanroman, A., Fucinos, P., Rua, M. L., Pastrana, L., and Longo, M. A. (2004). Quantification of intra- and extra-cellular thermophilic lipase/esterase production by *Thermus* sp. *Biotechnol. Lett.* 26, 705–708. doi:10.1023/B:BILE.0000024092.27943.75

Donadio, S., Monciardini, P., and Sosio, M. (2009). Chapter 1. Approaches to discovering novel antibacterial and antifungal agents. *Methods Enzymol.* 458, 3–28. doi:10.1016/S0076-6879(09)04801-0

Dornez, E., Verjans, P., Arnaut, F., Delcour, J. A., and Courtin, C. M. (2011). Use of psychrophilic xylanases provides insight into the xylanase functionality in bread making. *J. Agric. Food Chem.* 59, 9553–9562. doi:10.1021/jf201752g

Du, B. B., Hao, S., Li, Y. M., Yue, L. L., and Jiao, Q. H. (2006). [Expression of a thermostable a-amylase mutant into *Escherichia coli* and *Pichia pastoris*]. *Wei Sheng Wu Xue Bao* 46, 827–830.

Feller, G. (2010). Protein stability and enzyme activity at extreme biological temperatures. *J. Phys. Condens. Matter* 22, 323101. doi:10.1088/0953-8984/22/32/323101

Feller, G. (2013). Psychrophilic enzymes: from folding to function and biotechnology. *Scientifica (Cairo)* 2013, 512840. doi:10.1155/2013/512840

Feller, G., Le Bussy, O., and Gerday, C. (1998). Expression of psychrophilic genes in mesophilic hosts: assessment of the folding state of a recombinant α-amylase. *Appl. Environ. Microbiol.* 64, 1163–1165.

Friedrich, C. G. (1998). Physiology and genetics of sulfur-oxidizing bacteria. *Adv. Microb. Physiol.* 39, 235–289. doi:10.1016/S0065-2911(08)60018-1

Fucinos, P., Abadin, C. M., Sanroman, A., Longo, M. A., Pastrana, L., and Rua, M. L. (2005a). Identification of extracellular lipases/esterases produced by *Thermus thermophilus* HB27: partial purification and preliminary biochemical characterisation. *J. Biotechnol.* 117, 233–241. doi:10.1016/j.jbiotec.2005.01.019

Fucinos, P., Dominguez, A., Sanroman, M. A., Longo, M. A., Rua, M. L., and Pastrana, L. (2005b). Production of thermostable lipolytic activity by thermus species. *Biotechnol. Prog.* 21, 1198–1205. doi:10.1021/bp050080g

Georlette, D., Jonsson, Z. O., Van Petegem, F., Chessa, J., Van Beeumen, J., Hubscher, U., et al. (2000). A DNA ligase from the psychrophile *Pseudoalteromonas haloplanktis* gives insights into the adaptation of proteins to low temperatures. *Eur. J. Biochem.* 267, 3502–3512. doi:10.1046/j.1432-1327.2000.01377.x

Ghosh, M., Pulicherla, K. K., Rekha, V. P., Raja, P. K., and Sambasiva Rao, K. R. (2012). Cold active beta-galactosidase from Thalassospira sp. 3SC-21 to use in milk lactose hydrolysis: a novel source from deep waters of Bay-of-Bengal. *World J. Microbiol. Biotechnol.* 28, 2859–2869. doi:10.1007/s11274-012-1097-z

Glaser, R., and Venus, J. (2014). Screening of *Bacillus coagulans* strains in lignin supplemented minimal medium with high throughput turbidity measurements. *Biotechnol. Rep.* 4, 60–65. doi:10.1016/j.btre.2014.08.001

Graham, J. E., Clark, M. E., Nadler, D. C., Huffer, S., Chokhawala, H. A., Rowland, S. E., et al. (2011). Identification and characterization of a multidomain hyperthermophilic cellulase from an archaeal enrichment. *Nat. Commun.* 2, 375. doi:10.1038/ncomms1373

Gurung, N., Ray, S., Bose, S., and Rai, V. (2013). A broader view: microbial enzymes and their relevance in industries, medicine, and beyond. *Biomed Res. Int.* 2013, 329121. doi:10.1155/2013/329121

Gutierrez, A., del Rio, J. C., and Martinez, A. T. (2009). Microbial and enzymatic control of pitch in the pulp and paper industry. *Appl. Microbiol. Biotechnol.* 82, 1005–1018. doi:10.1007/s00253-009-1905-z

Hmidet, N., Ali, N. E. H., Haddar, A., Kanoun, S., Alya, S. K., and Nasri, M. (2009). Alkaline proteases and thermostable α-amylase co-produced by *Bacillus licheniformis* NH1: characterization and potential application as detergent additive. *Biochem. Eng. J.* 47, 71–79. doi:10.1016/j.bej.2009.07.005

Horikoshi, K. (1999). Alkaliphiles: some applications of their products for biotechnology. *Microbiol. Mol. Biol. Rev.* 63, 735–750.

Horner, T. W., Dunn, M. L., Eggett, D. L., and Ogden, L. V. (2011). beta-galactosidase activity of commercial lactase samples in raw and pasteurized milk at refrigerated temperatures. *J. Dairy Sci.* 94, 3242–3249. doi:10.3168/jds.2010-3742

Huber, H., and Stetter, K. O. (1998). Hyperthermophiles and their possible potential in biotechnology. *J. Biotechnol.* 64, 39–52. doi:10.1016/S0168-1656(98)00102-3

Ji, X., Chen, G., Zhang, Q., Lin, L., and Wei, Y. (2015). Purification and characterization of an extracellular cold-adapted alkaline lipase produced by psychrotrophic bacterium *Yersinia enterocolitica* strain KM1. *J. Basic Microbiol.* 55, 718–728. doi:10.1002/jobm.201400730

Jiang, Z. Q., Li, X. T., Yang, S. Q., Li, L. T., Li, Y., and Feng, W. Y. (2006). Biobleach boosting effect of recombinant xylanase B from the hyperthermophilic *Thermotoga maritima* on wheat straw pulp. *Appl. Microbiol. Biotechnol.* 70, 65–71. doi:10.1007/s00253-005-0036-4

Jiewei, T., Zuchao, L., Peng, Q., Lei, W., and Yongqiang, T. (2014). Purification and characterization of a cold-adapted lipase from oceanobacillus strain PT-11. *PLoS ONE* 9:e101343. doi:10.1371/journal.pone.0101343

Joshi, S., and Satyanarayana, T. (2013). Biotechnology of cold-active proteases. *Biology (Basel)* 2, 755–783. doi:10.3390/biology2020755

Karan, R., Capes, M. D., and Dassarma, S. (2012). Function and biotechnology of extremophilic enzymes in low water activity. *Aquat. Biosyst.* 8, 4. doi:10.1186/2046-9063-8-4

Karlsson, E. N., Holst, O., and Tocaj, A. (1999). Efficient production of truncated thermostable xylanases from *Rhodothermus marinus* in *Escherichia coli* fed-batch cultures. *J. Biosci. Bioeng.* 87, 598–606. doi:10.1016/S1389-1723(99)80121-2

Kasana, R. C., and Gulati, A. (2011). Cellulases from psychrophilic microorganisms: a review. *J. Basic Microbiol.* 51, 572–579. doi:10.1002/jobm.201000385

Kim, K. W., and Lee, S. B. (2003). Inhibitory effect of Maillard reaction products on growth of the aerobic marine hyperthermophilic archaeon *Aeropyrum* pernix. *Appl. Environ. Microbiol.* 69, 4325–4328. doi:10.1128/AEM.69.7.4325-4328.2003

King, O. N., Li, X. S., Sakurai, M., Kawamura, A., Rose, N. R., Ng, S. S., et al. (2010). Quantitative high-throughput screening identifies 8-hydroxyquinolines as cell-active histone demethylase inhibitors. *PLoS ONE* 5:e15535. doi:10.1371/journal.pone.0015535

Kishishita, S., Fujii, T., and Ishikawa, K. (2015). Heterologous expression of hyperthermophilic cellulases of archaea *Pyrococcus* sp. by fungus *Talaromyces* cellulolyticus. *J. Ind. Microbiol. Biotechnol.* 42, 137–141. doi:10.1007/s10295-014-1532-2

Kitamoto, N., Yamagata, H., Kato, T., Tsukagoshi, N., and Udaka, S. (1988). Cloning and sequencing of the gene encoding thermophilic beta-amylase of *Clostridium* thermosulfurogenes. *J. Bacteriol.* 170, 5848–5854.

Klenk, H. P., Clayton, R. A., Tomb, J. F., White, O., Nelson, K. E., Ketchum, K. A., et al. (1997). The complete genome sequence of the hyperthermophilic, sulphate-reducing archaeon *Archaeoglobus fulgidus*. *Nature* 390, 364–370. doi:10.1038/37052

Klenk, H. P., Spitzer, M., Ochsenreiter, T., and Fuellen, G. (2004). Phylogenomics of hyperthermophilic archaea and bacteria. *Biochem. Soc. Trans.* 32(Pt 2), 175–178. doi:10.1042/bst0320175

Kletzin, A., Urich, T., Muller, F., Bandeiras, T. M., and Gomes, C. M. (2004). Dissimilatory oxidation and reduction of elemental sulfur in thermophilic archaea. *J. Bioenerg. Biomembr.* 36, 77–91. doi:10.1023/B:JOBB.0000019600.36757.8c

Kluskens, L. D., Zeilstra, J., Geerling, A. C., de Vos, W. M., and van der Oost, J. (2010). Molecular characterization of the glucose isomerase from the thermophilic bacterium *Fervidobacterium gondwanense*. *Environ. Technol.* 31, 1083–1090. doi:10.1080/09593330903486673

Kobori, H., Sullivan, C. W., and Shizuya, H. (1984). Heat-labile alkaline phosphatase from Antarctic bacteria: Rapid 5' end-labeling of nucleic acids. *Proc. Natl. Acad. Sci. U.S.A.* 81, 6691–6695. doi:10.1073/pnas.81.21.6691

Koutsioulis, D., Wang, E., Tzanodaskalaki, M., Nikiforaki, D., Deli, A., Feller, G., et al. (2008). Directed evolution on the cold adapted properties of TAB5 alkaline phosphatase. *Protein Eng. Des. Sel.* 21, 319–327. doi:10.1093/protein/gzn009

Kristjansson, J. K. (1989). Thermophilic organisms as sources of thermostable enzymes. *Trends Biotechnol.* 7, 395–401. doi:10.1016/0167-7799(89)90035-8

Kuddus, M., Roohi, Saima, and Ahmad, I. Z. (2012). Cold-active extracellular α-amylase production from novel bacteria *Microbacterium foliorum* GA2 and *Bacillus cereus* GA6 isolated from Gangotri glacier, Western Himalaya. *J. Genet. Eng. Biotechnol.* 10, 151–159. doi:10.1016/j.jgeb.2012.03.002

Kuhad, R. C., Gupta, R., and Singh, A. (2011). Microbial cellulases and their industrial applications. *Enzyme Res.* 2011, 280696. doi:10.4061/2011/280696

Kühne, W. (1877). Über das Verhalten verschiedener organisirter und sog. ungeformter Fermente. *Verhandlungen des naturhistorisch-medicinischen Vereins zu Heidelberg* 1, 190–193.

Kumar, S., and Nussinov, R. (2001). How do thermophilic proteins deal with heat? *Cell. Mol. Life Sci.* 58, 1216–1233. doi:10.1007/PL00000935

Ladenstein, R., and Antranikian, G. (1998). Proteins from hyperthermophiles: stability and enzymatic catalysis close to the boiling point of water. *Adv. Biochem. Eng. Biotechnol.* 61, 37–85.

Lanes, O., Leiros, I., Smalas, A. O., and Willassen, N. P. (2002). Identification, cloning, and expression of uracil-DNA glycosylase from Atlantic cod (*Gadus morhua*): characterization and homology modeling of the cold-active catalytic domain. *Extremophiles* 6, 73–86. doi:10.1007/s007920100225

Larsson, L., Olsson, G., Holst, O., and Karlsson, H. T. (1990). Pyrite oxidation by thermophilic archaebacteria. *Appl. Environ. Microbiol.* 56, 697–701.

Lee, D. H., Choi, S. L., Rha, E., Kim, S., Yeom, S. J., Moon, J. H., et al. (2015). A novel psychrophilic alkaline phosphatase from the metagenome of tidal flat sediments. *BMC Biotechnol.* 15:1. doi:10.1186/s12896-015-0115-2

Lee, M. S., Kim, G. A., Seo, M. S., Lee, J. H., and Kwon, S. T. (2009). Characterization of heat-labile uracil-DNA glycosylase from *Psychrobacter* sp. HJ147 and its application to the polymerase chain reaction. *Biotechnol. Appl. Biochem.* 52(Pt 2), 167–175. doi:10.1042/BA20080028

Leis, B., Angelov, A., and Liebl, W. (2013). Screening and expression of genes from metagenomes. *Adv. Appl. Microbiol.* 83, 1–68. doi:10.1016/B978-0-12-407678-5.00001-5

Li, X. L., Zhang, W. H., Wang, Y. D., Dai, Y. J., Zhang, H. T., Wang, Y., et al. (2014). A high-detergent-performance, cold-adapted lipase from *Pseudomonas stutzeri* PS59 suitable for detergent formulation. *J. Mol. Catal. B. Enzym.* 102, 16–24. doi:10.1016/j.molcatb.2014.01.006

Ling, L. L., Schneider, T., Peoples, A. J., Spoering, A. L., Engels, I., Conlon, B. P., et al. (2015). A new antibiotic kills pathogens without detectable resistance. *Nature* 517, 455–459. doi:10.1038/nature14098

Litantra, R., Lobionda, S., Yim, J. H., and Kim, H. K. (2013). Expression and biochemical characterization of cold-adapted lipases from Antarctic *Bacillus pumilus* strains. *J. Microbiol. Biotechnol.* 23, 1221–1228. doi:10.4014/jmb.1305.05006

Madigan, M. T., and Marrs, B. L. (1997). Extremophiles. *Sci. Am.* 276, 82–87. doi:10.1038/scientificamerican0497-82

Maras, B., Valiante, S., Chiaraluce, R., Consalvi, V., Politi, L., De Rosa, M., et al. (1994). The amino acid sequence of glutamate dehydrogenase from *Pyrococcus furiosus*, a hyperthermophilic archaebacterium. *J. Protein Chem.* 13, 253–259. doi:10.1007/BF01891983

Marx, J. C., Collins, T., D'Amico, S., Feller, G., and Gerday, C. (2007). Cold-adapted enzymes from marine Antarctic microorganisms. *Mar. Biotechnol.* 9, 293–304. doi:10.1007/s10126-006-6103-8

Mateo, C., Monti, R., Pessela, B. C., Fuentes, M., Torres, R., Guisan, J. M., et al. (2004). Immobilization of lactase from *Kluyveromyces lactis* greatly reduces the inhibition promoted by glucose. Full hydrolysis of lactose in milk. *Biotechnol. Prog.* 20, 1259–1262. doi:10.1021/bp049957m

Milagres, A. M. F., Santos, E., Piovan, T., and Roberto, I. C. (2004). Production of xylanase by *Thermoascus aurantiacus* from sugar cane bagasse in an aerated growth fermentor. *Process Biochem.* 39, 1387–1391. doi:10.1016/S0032-9592(03)00272-3

Mykytczuk, N. C., Foote, S. J., Omelon, C. R., Southam, G., Greer, C. W., and Whyte, L. G. (2013). Bacterial growth at -15 degrees C; molecular insights from the permafrost bacterium planococcus halocryophilus Or1. *ISME J.* 7, 1211–1226. doi:10.1038/ismej.2013.8

Niehaus, F., Bertoldo, C., Kahler, M., and Antranikian, G. (1999). Extremophiles as a source of novel enzymes for industrial application. *Appl. Microbiol. Biotechnol.* 51, 711–729. doi:10.1007/s002530051456

Nisha, M., and Satyanarayana, T. (2013). Recombinant bacterial amylopullulanases: developments and perspectives. *Bioengineered* 4, 388–400. doi:10.4161/bioe.24629

Paloheimo, M., Puranen, T., Valtakari, L., Kruus, K., Kallio, J., Maentylae, A., et al. (2006). *Novel Laccase Enzymes and Their Uses*. US Patent No 77321784 B2. United States Patent and Trademark Office.

Park, I. H., Kim, S. H., Lee, Y. S., Lee, S. C., Zhou, Y., Kim, C. M., et al. (2009). Gene cloning, purification, and characterization of a cold-adapted lipase produced by *Acinetobacter baumannii* BD5. *J. Microbiol. Biotechnol.* 19, 128–135. doi:10.4014/jmb.0802.130

Payen, A., and Persoz, J. F. (1833). Memoir on diastase, the principal products of its reactions, and their applications to the industrial arts. *Ann. Chim. Phys.* 53, 73–92.

Phadtare, S. (2004). Recent developments in bacterial cold-shock response. *Curr. Issues Mol. Biol.* 6, 125–136.

Pulicherla, K. K., Kumar, P. S., Manideep, K., Rekha, V. P., Ghosh, M., and Sambasiva Rao, K. R. (2013). Statistical approach for the enhanced production of cold-active beta-galactosidase from *Thalassospira frigidphilosprofundus*: a novel marine psychrophile from deep waters of Bay of Bengal. *Prep. Biochem. Biotechnol.* 43, 766–780. doi:10.1080/10826068.2013.773341

Pulicherla, K. K., Mrinmoy, G., Kumar, S., and Sambasiva Rao, K. R. (2011). Psychrozymes – the next generation industrial enzymes. *J. Mar. Sci. Res. Dev.* 1, 102. doi:10.4172/2155-9910.1000102

Qin, Y., Huang, Z., and Liu, Z. (2014). A novel cold-active and salt-tolerant alpha-amylase from marine bacterium *Zunongwangia profunda*: molecular cloning, heterologous expression and biochemical characterization. *Extremophiles* 18, 271–281. doi:10.1007/s00792-013-0614-9

Reed, C. J., Lewis, H., Trejo, E., Winston, V., and Evilia, C. (2013). Protein adaptations in archaeal extremophiles. *Archaea* 2013, 373275. doi:10.1155/2013/373275

Reid, I. I., and Ricard, M. (2000). Pectinase in papermaking: solving retention problems in mechanical pulps bleached with hydrogen peroxide. *Enzyme Microb. Technol.* 26, 115–123. doi:10.1016/S0141-0229(99)00131-3

Rice, D. W., Yip, K. S., Stillman, T. J., Britton, K. L., Fuentes, A., Connerton, I., et al. (1996). Insights into the molecular basis of thermal stability from the structure determination of *Pyrococcus furiosus* glutamate dehydrogenase. *FEMS Microbiol. Rev.* 18, 105–117. doi:10.1111/j.1574-6976.1996.tb00230.x

Rina, M., Pozidis, C., Mavromatis, K., Tzanodaskalaki, M., Kokkinidis, M., and Bouriotis, V. (2000). Alkaline phosphatase from the Antarctic strain TAB5. Properties and psychrophilic adaptations. *Eur. J. Biochem.* 267, 1230–1238. doi:10.1046/j.1432-1327.2000.01127.x

Roohi, R., Kuddus, M., and Saima, S. (2013). Cold-active detergent-stable extracellular α-amylase from *Bacillus cereus* GA6: biochemical characteristics and its perspectives in laundry detergent formulation. *J. Biochem. Technol.* 4, 636–644.

Rothschild, L. J., and Mancinelli, R. L. (2001). Life in extreme environments. *Nature* 409, 1092–1101. doi:10.1038/35059215

Roychoudhury, A. N. (2004). Sulphate metabolism among thermophiles and hyperthermophiles in natural aquatic systems. *Biochem. Soc. Trans.* 32(Pt 2), 172–174. doi:10.1042/bst0320172

Rozzell, J. D. (1999). Commercial scale biocatalysis: myths and realities. *Bioorg. Med. Chem.* 7, 2253–2261. doi:10.1016/S0968-0896(99)00159-5

Rua, M. L., Atomi, H., Schmidt-Dannert, C., and Schmid, R. D. (1998). High-level expression of the thermoalkalophilic lipase from *Bacillus* thermocatenulatus in *Escherichia coli*. *Appl. Microbiol. Biotechnol.* 49, 405–410. doi:10.1007/s002530051190

Russell, N. J. (1997). Psychrophilic bacteria – molecular adaptations of membrane lipids. *Comp. Biochem. Physiol. A Physiol.* 118, 489–493. doi:10.1016/S0300-9629(97)87354-9

Satyanarayana, T., Noorwez, S. M., Kumar, S., Rao, J. L., Ezhilvannan, M., and Kaur, P. (2004). Development of an ideal starch saccharification process using amylolytic enzymes from thermophiles. *Biochem. Soc. Trans.* 32(Pt 2), 276–278. doi:10.1042/bst0320276

Shi, H., Zhang, Y., Li, X., Huang, Y., Wang, L., Wang, Y., et al. (2013). A novel highly thermostable xylanase stimulated by Ca2+ from *Thermotoga thermarum*: cloning, expression and characterization. *Biotechnol. Biofuels* 6, 26. doi:10.1186/1754-6834-6-26

Siddiqui, K. S., and Cavicchioli, R. (2006). Cold-adapted enzymes. *Annu. Rev. Biochem.* 75, 403–433. doi:10.1146/annurev.biochem.75.103004.142723

Stougaard, P., and Schmidt, M. (2010). *Cold-Active Beta-Galactosidase, a Method of Producing Same and Use of Such Enzyme*. Canadian Patent No 2751957 A1. Canadian Intellectual Property Office.

Sukumar, M. S., Jeyaseelan, A., Sivasankaran, T., Mohanraj, P., Mani, P., Sudhakar, G., et al. (2013). Production and partial characterization of extracellular glucose isomerase using thermophilic *Bacillus* sp. isolated from agricultural land. *Biocatal. Agric. Biotechnol.* 2, 45–49. doi:10.1016/j.bcab.2012.10.003

Swamy, M. V., Sai Ram, M., and Seenayya, G. (1994). β-amylase from *Clostridium thermocellum* SS8 – a thermophilic, anaerobic, cellulolytic bacterium. *Lett. Appl. Microbiol.* 18, 301–304. doi:10.1111/j.1472-765X.1994.tb00875.x

Takai, K., Nakamura, K., Toki, T., Tsunogai, U., Miyazaki, M., Miyazaki, J., et al. (2008). Cell proliferation at 122 degrees C and isotopically heavy CH4 production by a hyperthermophilic methanogen under high-pressure cultivation. *Proc. Natl. Acad. Sci. U.S.A.* 105, 10949–10954. doi:10.1073/pnas.0712334105

Van de Voorde, I., Goiris, K., Syryn, E., Van den Bussche, C., and Aerts, G. (2014). Evaluation of the cold-active *Pseudoalteromonas haloplanktis* β-galactosidase enzyme for lactose hydrolysis in whey permeate as primary step of d-tagatose production. *Process Biochem.* 49, 2134–2140. doi:10.1016/j.procbio.2014.09.010

Vieille, C., Hess, J. M., Kelly, R. M., and Zeikus, J. G. (1995). xylA cloning and sequencing and biochemical characterization of xylose isomerase from *Thermotoga neapolitana*. *Appl. Environ. Microbiol.* 61, 1867–1875.

Virk, A. P., Sharma, P., and Capalash, N. (2012). Use of laccase in pulp and paper industry. *Biotechnol. Prog.* 28, 21–32. doi:10.1002/btpr.727

Wagner, M., Roger, A. J., Flax, J. L., Brusseau, G. A., and Stahl, D. A. (1998). Phylogeny of dissimilatory sulfite reductases supports an early origin of sulfate respiration. *J. Bacteriol.* 180, 2975–2982.

Wang, S. Y., Hu, W., Lin, X. Y., Wu, Z. H., and Li, Y. Z. (2012). A novel cold-active xylanase from the cellulolytic myxobacterium *Sorangium cellulosum* So9733-1: gene cloning, expression, and enzymatic characterization. *Appl. Microbiol. Biotechnol.* 93, 1503–1512. doi:10.1007/s00253-011-3480-3

Xu, F., Shin, W., Brown, S. H., Wahleithner, J. A., Sundaram, U. M., and Solomon, E. I. (1996). A study of a series of recombinant fungal laccases and bilirubin oxidase that exhibit significant differences in redox potential, substrate specificity, and stability. *Biochim. Biophys. Acta.* 1292, 303–311. doi:10.1016/0167-4838(95)00210-3

Xuezheng, L., Shuoshuo, C., Guoying, X., Shuai, W., and Ning, D. J. (2010). Cloning and heterologous expression of two cold-active lipases from the Antarctic bacterium psychrobacter sp. G. *Polar Res.* 29, 421–429. doi:10.1111/j.1751-8369.2010.00189.x

Zhang, S., Yang, J., Li, J., Mai, Z., Tian, X., and Yin, H. (2013). *Marine Bacteria Cold-Adapted Protease and Encoded Gene and Application Thereof*. International Patent No WO2013177834 A1.

Zheng, Z., Li, H., Li, L., and Shao, W. (2012). Biobleaching of wheat straw pulp with recombinant laccase from the hyperthermophilic *Thermus thermophilus*. *Biotechnol. Lett.* 34, 541–547. doi:10.1007/s10529-011-0796-0

Zhu, Y., Zhang, Z., Zhang, M., Mais, D. E., and Wang, M. W. (2010). High-throughput screening for bioactive components from traditional Chinese medicine. *Comb. Chem. High Throughput Screen.* 13, 837–848. doi:10.2174/138620710793360257

Conflict of Interest Statement: The authors declare that the research was conducted in the absence of any commercial or financial relationships that could be construed as a potential conflict of interest.

frontiers in Bioengineering and Biotechnology

REVIEW
published: 13 October 2015
doi: 10.3389/fbioe.2015.00161

Enzymes from extreme environments and their industrial applications

*Jennifer A. Littlechild**

Exeter Biocatalysis Centre, Biosciences, College of Life and Environmental Sciences, University of Exeter, Exeter, UK

This article will discuss the importance of specific extremophilic enzymes for applications in industrial biotechnology. It will specifically address those enzymes that have applications in the area of biocatalysis. Such enzymes now play an important role in catalyzing a variety of chemical conversions that were previously carried out by traditional chemistry. The biocatalytic process is carried out under mild conditions and with greater specificity. The enzyme process does not result in the toxic waste that is usually produced in a chemical process that would require careful disposal. In this sense, the biocatalytic process is referred to as carrying out "green chemistry" which is considered to be environmentally friendly. Some of the extremophilic enzymes to be discussed have already been developed for industrial processes such as an L-aminoacylase and a γ-lactamase. The industrial applications of other extremophilic enzymes, including transaminases, carbonic anhydrases, dehalogenases, specific esterases, and epoxide hydrolases, are currently being assessed. Specific examples of these industrially important enzymes that have been studied in the authors group will be presented in this review.

Keywords: γ-lactamase, L-aminoacylase, transaminase, carbonic anhydrase, epoxide hydrolase, esterase, dehalogenase

OPEN ACCESS

Edited by:
Noha M. Mesbah, Suez Canal University, Egypt

Reviewed by:
Robert Kourist, Ruhr-University Bochum, Germany
Skander Elleuche, Hamburg University of Technology, Germany

***Correspondence:**
Jennifer A. Littlechild
j.a.littlechild@exeter.ac.uk

Specialty section:
This article was submitted to Process and Industrial Biotechnology, a section of the journal Frontiers in Bioengineering and Biotechnology

Received: *18 August 2015*
Accepted: *28 September 2015*
Published: *13 October 2015*

Citation:
Littlechild JA (2015) Enzymes from extreme environments and their industrial applications. Front. Bioeng. Biotechnol. 3:161. doi: 10.3389/fbioe.2015.00161

INTRODUCTION

A problem with using enzymes for industrial biotransformation reactions is often their inherent stability to the conditions employed. During industrial processes, the enzymes are often exposed to a different environment to their natural conditions within the cell such as non-natural substrates, high substrate concentrations, non-aqueous conditions, and extremes of pH. When using non-natural substrates, enzymes from different classes can be found to accept the same substrate such as the case with racemic γ-lactam described below. Enzymes can also carry out "side reactions" when used at a different pH than that found inside the cell.

The availability of new genome sequences makes the search for new industrial enzymes a relatively easy process. Also the isolation of metagenomes from extremophilic sources provides DNA from potentially uncultivatable organisms. However, the identification of specific enzymes from this resource is only as good as the current bioinformatic analyses and many novel or unknown activities can be missed. It is therefore important to also screen genomic libraries against substrates of commercial interest for specific biocatalytic activities especially if turnover of a non-natural substrate is required.

The diversity which "nature" provides for extremophilic environments of temperature, pH, acidity, alkalinity, pressure, and salinity can be exploited to discover new novel and potentially robust enzymes that are better suited for use in industrial applications. The increased number

of extremophilic genomes and metagenomes that can now be sequenced by next-generation sequencing technologies provides an ever expanding resource for identification of new enzymes.

The mechanism of protein stabilization under extreme conditions varies depending on the microbial species and level of adaption required for survival in the host organism. For the acidophiles and alkalophiles, it is only the proteins exported from the cell that have to be stable under the extreme pHs of the growth environment, since the proteins inside the cell do not have to withstand these extreme conditions as the intracellular pH is maintained around pH 5.0–6.0. Some general features of enzyme stability have been observed from the analysis of the three-dimensional structures of enzymes isolated from extreme environments of high temperatures have been reviewed by Littlechild et al. (2013).

Many archaeal and bacterial enzymes isolated from extremophiles have general applications in molecular biology such as the hyperthermophilic *Pyrococcus* polymerase enzyme which has improved fidelity in PCR reactions when compared to thermophilic bacterial polymerase enzymes. Other thermophilic enzymes are of great importance to the breakdown of biomass and other materials such as waste plastics in order to contribute to a circular economy where nothing is wasted.

This review will concentrate on several specific examples of interest to the author where extremophilic enzymes are currently playing an important role as biocatalysts for the pharmaceutical and fine chemical industries.

SPECIFIC EXAMPLES

The *Sulfolobus solfataricus* γ-Lactamase Enzyme

An enzyme from the thermophilic archaeon *Sulfolobus solfataricus* MT4 can use the bicyclic synthon (rac)-γ-lactam (2-azabicyclo[2.2.1]hept-5-en-3-one) as a substrate to obtain a single enantiomer of the γ-bicyclic lactam product which is an important building block for the anti-HIV compound, Abacavir (Taylor et al., 1993). This (+)-γ-lactamase was identified in the *Sulfolobus* strain by screening colonies from an expression library for their ability to produce the amino acid product when supplied with the racemic γ-lactam. Screening was carried out using genomic libraries using a filter paper overlay. The colonies on the plate that were active showed a brown coloration of the filter paper when the amino acid was produced which had been soaked in ninhydrin stain. Another non-thermophilic bacterial (+)-γ-lactamase that can also carry out this reaction has been identified within the bacterial *Delftia* species (PDB code 2WKN, Gonsalvez et al., 2001). This enzyme is of a different class, structure, and mechanism from the archaeal enzyme but both can use the non-natural γ-lactam as a substrate. It is related to the bi-zinc containing metalloprotease formamidase by analysis using the SCOP2 database (Andreeva et al., 2014). A third (−)-γ-lactamase of opposite stereoselectivity is related to a α/β hydrolase fold esterase enzyme which can also carry out the side reaction of bromination at pH 4.0 and was referred to as a non-cofactor containing bromoperoxidase (Line et al., 2004).

The *Sulfolobus* (+)-γ-lactamase has been cloned and overexpressed in *Escherichia coli* and purified to homogeneity (Toogood et al., 2004). The molecular mass of the monomer was estimated to be 55 kDa by SDS-PAGE, which is consistent with the calculated molecular mass of 55.7 kDa. The native molecular weight was 110 kDa as determined by gel filtration chromatography, indicating that the enzyme exists as a dimer in solution. The purified enzyme has been crystallized with a view to determining its three-dimensional structure.

This thermostable archaeal (+)-γ-lactamase has a high sequence homology to the signature amidase family of enzymes. It shows similar inhibition to the amidase enzymes with benzonitrile, phenylmethylsulfonyl fluoride, and heavy metals such as mercury, and it is activated by thiol reagents. Alignment of the amino acid sequences of the (+)-γ-lactamase from *S. solfataricus* with four amidases from *Pseudomonas chlororaphis* B23, *Rhodococcus* sp. N-771, *Rhodococcus erythropolis* N-774, and *Rhodococcus rhodochrous* J shows it has a 41–44% sequence identity to these enzymes. The amidases belong to the signature amidase family as they all contain the consensus sequence GGSS(S/G)GS. The amino acid sequence of the γ-lactamase contains the highly conserved putative catalytic residues aspartic acid and serine but not the highly conserved cysteine residue (Kobayashi et al., 1997).

The purified (+)-γ-lactamase enzyme has been immobilized as a cross-linked, polymerized enzyme preparation and packed into microreactors (Hickey et al., 2009). The thermophilic (+)-γ-lactamase retained 100% of its initial activity at the assay temperature, 80°C, for 6 h and retained 52% activity after 10 h, indicating the advantage of the immobilization. The free enzyme began to display a reduction in activity after 1 h at 80°C. The higher stability of the immobilized enzyme provided the advantage that it could be used to screen many compounds in a microreactor system without denaturation.

L-Aminoacylase and Pyroglutamyl Carboxyl Peptidase from the Thermophilic Archaeon *Thermococcus litoralis*

Many pharmaceutically active compounds contain nitrogen and can be derived from amino acids (Drauz, 1997). These compounds need to be optically pure, which can be achieved by the use of specific L or D aminoacylase enzymes. There is a large growth in the use of unnatural amino acids, for example, L-*tert*-leucine is a precursor to many pharmaceutically active compounds such as the antitumor compounds (Bommarius et al., 1998). A thermophilic archaeal L-aminoacylase has been cloned and overexpressed from the archaeon *Thermococcus litoralis* (Toogood et al., 2002a). The enzyme was identified from a *Thermococcus* DNA expression library which gave a positive hit for esterase activity. This esterase gene was later found to code for a pyroglutamyl carboxyl peptidase, which is a novel cysteine protease that cleaves the pyroglutamyl group from the N-terminus of biologically important peptides. The enzyme has been characterized both biochemically and structurally and demonstrated to be a new class of cysteine protease (Singleton et al., 1999). The commercial use of this enzyme is to cleave the

pyroglutamyl group from "blocked" peptides allowing them to be N-terminally sequenced. The *Thermococcus* protease forms a tetrameric structure held together by disulfide bonds between the dimer subunit interface and is stabilized by an unusual hydrophobic core at the center of the tetrameric structure. This unusual feature is formed from four two-stranded antiparallel β-sheets, one from each subunit. The sheets are built from the hydrophobic amino acid residues Phe–Phe–Leu–Leu (**Figure 1**). This hydrophobic insertion is unique to the *T. litoralis* enzyme, with no equivalent structure seen in other bacterial or archaeal pyroglutamyl carboxyl peptidase enzymes (Singleton et al., 1999).

The *Thermococcus* L-aminoacylase enzyme which was identified next to the novel cysteine protease and has an 82% sequence identity to an L-aminoacylase from *Pyrococcus furiosus* (Tanimoto et al., 2008) and 45% sequence identity to a carboxypeptidase from another thermophilic archaeon *S. solfataricus*. The *Thermococcus* enzyme is not inhibited by conventional aminoacylase inhibitors such as mono-*tert*-butyl malonate so appears to be novel. It is thermostable, with a half-life of 25 h at 70°C and has an optimal activity at 85°C in Tris-HCl, pH 8.0. This *T. litoralis* L-aminoacylase has a broad substrate specificity preferring the amino acids: Phe ≫ Met > Cys > Ala ≃ Val > Tyr > Propargylglycine > Trp > Pro > Arg. A column bioreactor containing the recombinant *Thermococcus* enzyme has been constructed by immobilization onto Sepharose beads. This bioreactor showed no loss of activity towards the substrate *N*-acetyl-DL-Trp after 5 days and 32% of the activity remained after 40 days at 60°C (Toogood et al., 2002b). The enzyme has more recently been immobilized by covalent attachment to an epoxy resin formed in channels of a microreactor allowing a "flow-through" procedure to be used (Ngamsom et al., 2010). This can be used for rapid substrate screening of the L-aminoacylase and eliminates potential substrate and product inhibition. It has been shown in pilot-scale biotransformation reactions using the substrate *N*-acetyl-DL-propargylglycine that this enzyme does show substrate inhibition (Toogood et al., 2002a).

The *Thermococcus* L-aminoacylase enzyme is now being used for multiton commercial production of L-amino acids and their analogs by Chirotech/Dow Pharma and more recently by Chirotech/Dr Reddys (Holt, 2004). A racemase enzyme has been developed in order to convert the isomer not used by the enzyme to the form that is used which can enable a more efficient process resulting in a 100% conversion of the racemic substrate (Baxter et al., 2012).

There are differences in substrate specificity between the *Thermococcus* L-aminoacylase and another thermophilic archaeal enzyme from *Pyrococcus* species. The substrate *N*-acetyl-L-phenylalanine is the most favorable substrate for the *Thermococcus* enzyme; however, this substrate is not used by the *Pyrococcus* L-aminoacylase (Tanimoto et al., 2008).

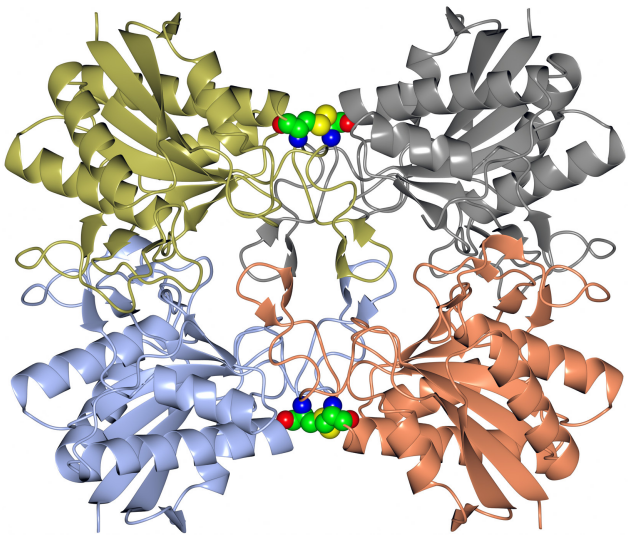

FIGURE 1 | A diagram showing the tetrameric structure of the *Thermococcus* pyroglutamyl carboxyl peptidase. The secondary structural elements are shown in a different color for each subunit. The hydrophobic core structure is shown in the center of the molecule and the disulfide bonds at the subunit interfaces in sphere mode (Singleton et al., 1999, PDB code 1A2Z).

Carboxyl Esterase from a Thermophilic Bacterium *Thermogutta terrifontis*

Esterases are a class of commonly used enzymes in industrial applications. This is partially due to their inherent stability in organic solvents and the ability to freely reverse the enzyme reaction from hydrolysis to synthesis by the elimination of the water that is used during the hydrolysis mechanism. The carboxyl esterases catalyze the hydrolysis of the ester bond of relatively small water-soluble substrates. A new carboxyl esterase (TtEst) has been identified in a recently identified thermophilic bacterium *Thermogutta terrifontis* from the phylum *Planctomycetes*. This enzyme has been cloned and overexpressed in *E. coli* (Sayer et al., 2015). The enzyme has been characterized biochemically and shown to have activity towards small *p*-nitrophenyl (*p*NP) carboxylic esters with optimal activity for *p*NP-propionate. The TtEst enzyme is very thermostable and retained 95% of its activity after incubation for 1 h at 80°C. The enzyme has been crystallized and its structure determined without ligands bound in the active site and in complex with a substrate analog D-malate and the product acetate. The bound ligands in the structure have allowed the identification of the carboxyl and alcohol binding pockets in the enzyme active site (**Figure 2**). It has also allowed a detailed comparison with structurally related enzymes that has given insight into how differences in the catalytic activity can be rationalized based on the properties of the amino acid residues in different active site pockets. An overall comparison of the alcohol binding pocket in TtEst with the equivalent pocket in the 3-oxoadipate-enol lactonase from *Burkholderia xenovorans* (PcaD) with 29% sequence identity (PDB code 2XUA) (Bains et al., 2011) and *Aureobacterium* species (−) γ-lactamase (Agl) with 30% sequence identity (PDB code 1HKH) (Line et al., 2004) has been carried out. The catalytic triad residues and the position of the oxyanion hole are conserved between these enzymes. The PcaD and Agl show that the TtEst pocket has a much more polar and charged environment in the active site, which allows the binding of organic acids such as D-malate where the distant carboxyl is coordinated by Arg139 and Tyr105. The PcaD and Agl

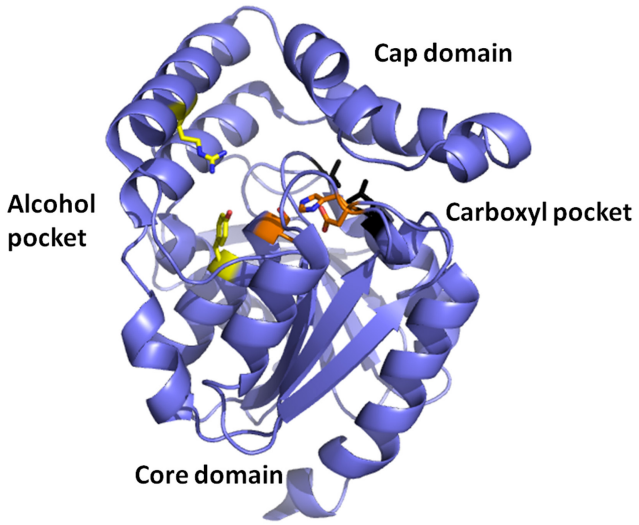

FIGURE 2 | A cartoon representation of the *Thermogutta* carboxyl esterase structure showing the active site residues in stick mode between the cap and the core domain. The binding pockets for the carboxyl group and the alcohol groups of the para nitrophenol ester substrate are also highlighted (Sayer et al., 2015, PDB code 4UHC).

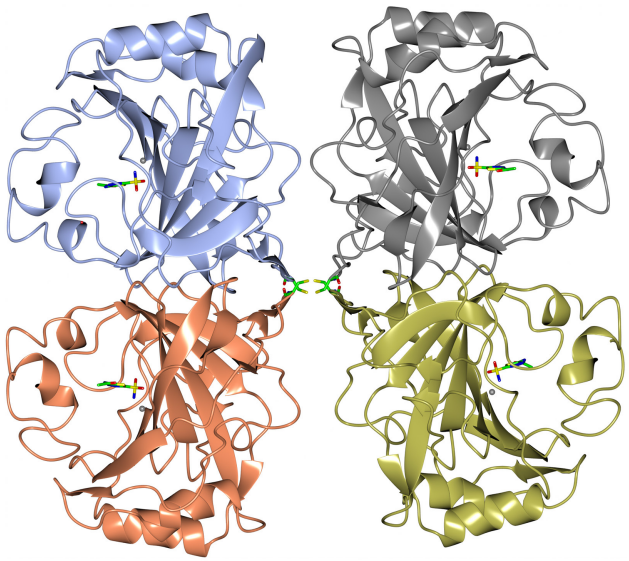

FIGURE 3 | A diagram of the thermophilic carbonic anhydrase from *Thermovibrio* showing the tetrameric structure held together by disulfide bonds in the center of the molecule (James et al., 2014 PDB code 4UOV).

enzymes have more hydrophobic substrate binding pockets, with the residues Arg139 and Tyr105 in TtEst replaced by Trp135 and Ile129 in PcaD and Trp204 and Leu125 in Agl. In both PcaD and Agl, the active site is better suited for the binding of structures such as lactone and γ-lactam rings. Similarly, the *Pseudomonas fluorescens* esterase with 30% sequence identity (PDB code 3HEA) (Yin et al., 2010) has an alcohol pocket where the structure is lined with several hydrophobic phenylalanine side chains that should have affinity for the lactone ring. This would explain its lactonase activity towards caprolactone (Cheeseman et al., 2004) in addition to the esterase activity.

Mutant enzymes have been constructed to extend the substrate range of *T. terrifontis* esterase to accept the larger butyrate and valerate *p*NP esters. These mutant enzymes have also shown a significant increase in activity towards acetate and propionate *p*NP esters. A crystal structure of the Leu37Ala mutant has been determined with the butyrate product bound in the carboxyl pocket of the active site. The mutant structure shows an expansion of the pocket that binds the substrate carboxyl group, which is consistent with the observed increase in activity towards *p*NP-butyrate.

A α-Carbonic Anhydrase from the Thermophilic Bacterium *Thermovibrio ammonificans*

Carbonic anhydrase enzymes catalyze the reversible hydration of carbon dioxide to bicarbonate. A stable robust α-carbonic anhydrase has been identified in the thermophilic bacterium *Thermovibrio ammonificans*. The enzyme has been cloned and overexpressed in *E. coli*. This protein has been characterized both biochemically and structurally (James et al., 2014). The crystal structure of this enzyme has been determined in its native form and in two complexes with bound inhibitors. It is unusual since it forms a tetrameric structure rather than the dimer reported for some previously studied related enzymes. The *Thermovibrio* enzyme is stabilized by a unique core in the center of the molecule formed by two intersubunit disulfide bonds and a single lysine residue from each monomer (**Figures 3** and **4**). The structure of this central core region protects the intersubunit disulfide bonds from reduction. The enzyme is located in the endoplasmic reticulum of *Thermovibrio* as evidenced by the presence of an N-terminal signal peptide. When the recombinant protein is oxidized to mimic the natural environment of the periplasmic space, it shows an increase in thermostability and retains 90% of its activity after incubation at 70°C for 1 h. These properties make it a good candidate for commercial carbon dioxide capture. Another thermophilic bacterial α-carbonic anhydrase has been described from *Sulfurihydrogenibium yellowstonense*. This carbonic anhydrase is also thermostable and is a dimer stabilized by ionic networks (Di Fiore et al., 2013).

The thermophilic bacteria appear to contain the high-activity α-carbonic anhydrase enzymes that have a similar structure to the well-studied bovine carbonic anhydrase enzyme, whereas the archaea have carbonic anhydrases that have different structures and mechanisms. There are six distinct families of CAs (α, β, γ, δ, ζ, and η) (Smith et al., 1999; Guler et al., 2015). The amino acid sequences are conserved between each family; however, there is no sequence or structural similarity between the different families. The carbonic anhydrase activity requires the presence of a catalytic zinc ion which is coordinated to either histidine or cysteine amino acids depending on the class of the enzyme (Silverman and Lindskog, 1988).

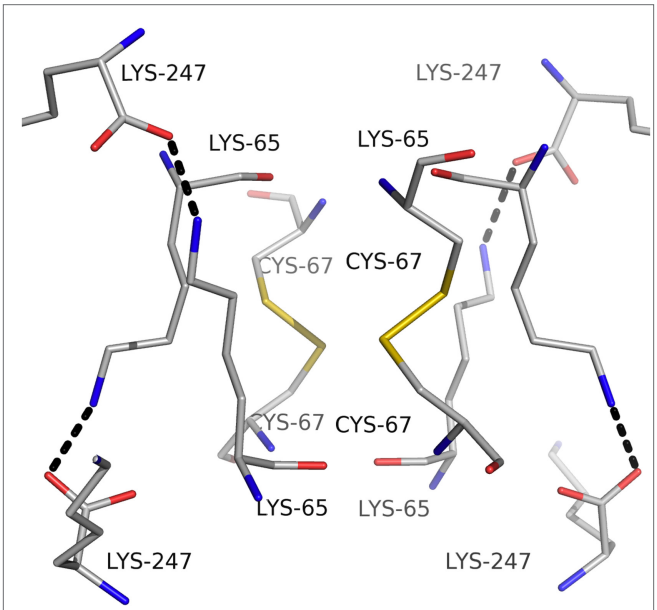

FIGURE 4 | A diagram showing the unusual structural feature of disulfide bonds in the center of the *Thermovibrio* carbonic anhydrase which are shielded by lysine amino acid residues (James et al., 2014, PDB code 4UOV).

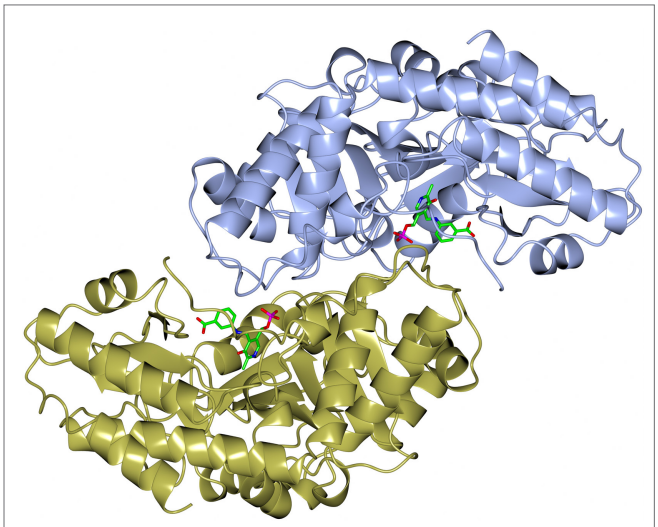

FIGURE 5 | A diagram of the structure of the *Sulfolobus* transaminase dimer showing the cofactor pyridoxal phosphate (PLP) forming an irreversible complex with the inhibitor gabaculine, shown in stick mode in the two active sites (Sayer et al., 2012, PDB code 3ZRP).

A Thermophilic Transaminase Enzyme from *Sulfolobus solfataricus*

The transaminase enzymes are important biocatalysts for the pharmaceutical industries since they produce chiral amines which are components of a range of different drug molecules. The archaeon *S. solfataricus* has been found to be an interesting source of a thermostable transaminase enzyme of the group IV Pfam group (Sayer et al., 2012). This pyridoxal phosphate (PLP)-containing enzyme is involved in the non-phosphorylated pathway for serine synthesis which is not found in bacteria but is found in animals and plants. The *Sulfolobus* transaminase carries out the conversion of L-serine and pyruvate to 3-hydroxypyruvate and alanine. It also has activity towards methionine, asparagine, glutamine, phenylalanine, histidine, and tryptophan and can be used in a cascade reaction with a C–C bond making enzyme, transketolase, for the synthesis of optically pure drug intermediates (Chen et al., 2006).

The dimeric thermophilic archaeal transaminase enzyme structure has been solved in the holo form of the enzyme and in complex with an inhibitor gabaculine and in a substrate complex with phenolpyruvate, the keto product of phenylalanine (Sayer et al., 2012). **Figure 5** shows a cartoon diagram of the dimeric *S. solfataricus* transaminase with an inhibitor bound to the cofactor PLP in the two active sites. The structural studies of this enzyme have given some insight into the conformational changes around the active site occurring during catalysis and have helped to understand the enzyme's substrate specificity (Sayer et al., 2012). How different members of the PLP enzyme family are able to accept a variety of substrates is vitally important to understand for the use of these enzymes in commercial applications.

The *Sulfolobus* transaminase is relatively thermostable for 10 min at 70°C and at pH 6.5. Features of the archaeal enzyme that relate to its increased stability when compared with a mesophilic related yeast enzyme show that the *Sulfolobus* enzyme has 21 salt bridges compared to 10 in the mesophilic enzyme including several three to four amino acid networks which offer increased stability. There is a C-terminal extension in the *Sulfolobus* enzyme and shorter surface loops which are all general features that are found in thermophilic enzymes. The *Sulfolobus* transaminase dimer interface is unusual being hydrophobic in nature with few ionic interactions which are generally associated with more thermophilic archaeal enzymes. This *Sulfolobus* serine transaminase is the first example of a thermophilic archaeal serine transaminase to be studied structurally and is shown to have properties that meet the requirements for the commercial application of the enzyme in biocatalysis.

New Epoxide Hydrolases from Extremophilic Metagenomes

An important enzyme activity of interest to the pharmaceutical industry is the ability to catalyze the hydrolysis of an oxirane (epoxide) ring by addition of a molecule of water to form a vicinal diol as a product (Widersten et al., 2010; Kotik et al., 2012). The enzymes that can carry out this reaction are ubiquitously expressed in all living organisms and they play an important physiological role in the detoxification of reactive xenobiotics or endogenous metabolites and in the formation of biologically active mediators. The epoxide hydrolases are already used for the production of optically pure epoxides and diols which are important synthons for the preparation of fine chemicals and drugs, for example, the chiral precursors of β-blockers (Kong et al., 2014; Nestl et al., 2014). The epoxide hydrolase enzymes fall into two classes with completely different 3D structures, the α/β hydrolase

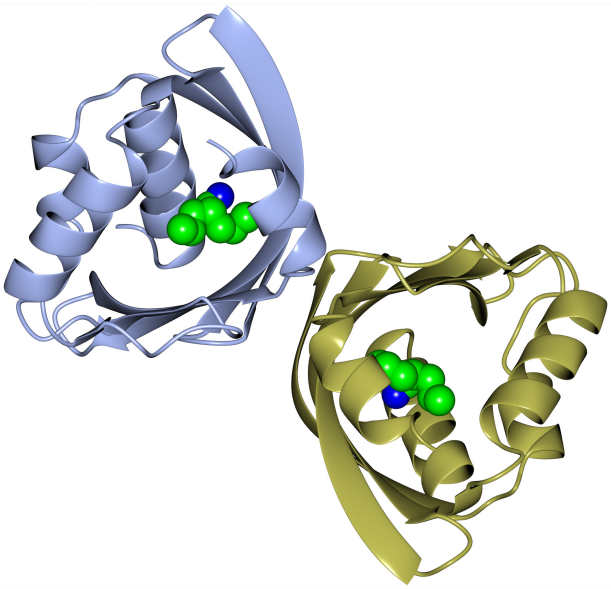

FIGURE 6 | A diagram showing the thermophilic limonene epoxide hydrolase isolated from the metagenomic sample collected from hot springs in Russia. The inhibitor, valpromide, is bound into the active site and is shown in sphere mode (Ferrandi et al., 2015a, PDB code 5AIH).

fold class and the limonene class (LEH) of which only few have been fully characterized. The LEH enzyme active site contains three residues (Asp, Arg, and Asp) that have been proposed to act in a concerted fashion to activate a water molecule which is able to open the epoxide ring without the formation of a covalently bound alkyl-enzyme intermediate (Arand et al., 2003; Hopmann et al., 2005).

Recently, as part of a thermophilic metagenomic project, two new thermostable epoxide hydrolases of the limonene class have been discovered. The metagenomes were isolated in Russia and China from hot terrestrial environments growing at 46°C and 55°C and at neutral pH. A bioinformatic approach was used to identify the genes coding for these industrially important enzymes which have been cloned and overexpressed in *E. coli*. The resultant proteins have been fully characterized as far as their biochemical properties, specificity, stereoselectivity, and crystal structure (Ferrandi et al., 2015a). The structure of the LEH from the Russian metagenome is shown in **Figure 6**. The new LEH enzymes have also been further evaluated and used in pilot-scale biotransformations for industrial applications (Ferrandi et al., 2015b).

DEHALOGENASE ENZYMES FROM EXTREMOPHILIC BACTERIA AND ARCHAEA

L-Haloacid Dehalogenase from the Thermophilic Archaeon *Sulfolobus tokadii*

A thermophilic dehalogenase enzyme of industrial interest is found in the archaeon *Sulfolobus tokadaii*. This L-haloacid dehalogenase enzyme has been cloned and overexpressed in *E. coli* and has been characterized biochemically and structurally (Rye et al., 2007, 2009). This enzyme has applications for chiral halo-carboxylic acid production and bioremediation. Chiral halo-carboxylic acids are important intermediates in the fine chemical/pharmaceutical industries. The *Sulfolobus* dehalogenase enzyme has the potential to resolve racemic mixtures of bromocarboxylic acids and is able to catalyze the conversion of 2-halo-carboxylic acids to the corresponding hydroxyalkanoic acids. It has been shown to display activity towards longer chain substrates than the bacterial *Xanthomonas autotrophicus* dehalogenase (Van der Ploeg et al., 1991) with activity seen towards 2-chlorobutyric acid due to a more accessible active site (Rye et al., 2009). The enzyme has a maximum activity at 60°C and a half-life of over an hour at 70°C. It is stabilized by a salt bridge and hydrophobic interactions on the subunit interface, helix capping, a more compact subdomain than related enzymes, and shortening of surface loops. A related hyperthermophilic *Pyrococcus* dehalogenase (29% sequence identity) whose structure is available from a structural genomics project is a monomeric enzyme stabilized by a disulfide bond (Arai et al., 2006).

Dehalogenases from the Marine Environment

The marine environment has been recognized as a potential source of novel enzymes (Trincone, 2011). A novel L-haloalkane dehalogenase has been biochemically and structurally characterized from the psychrophilic bacterium *Psychromonas ingrahamii* (Novak et al., 2013a). This organism was originally isolated in 1991 from Elson Lagoon, Point Barrow Alaska. Original samples were collected from the sea ice interface, where temperatures can reach −10°C (Breezee et al., 2004). The *P. ingrahamii* is a non-motile, large, rod-shaped bacterium that can utilize glycerol as a sole carbon source. The *P. ingrahamii* genome has been shown to encode numerous genes that synthesize polysaccharides and betaine choline. These compounds are thought to aid survival of the organism at low temperatures (Riley et al., 2008). Studies into the structural properties of proteins from psychrophilic organisms have shown they have enhanced structural flexibility at low temperatures (Feller, 2003; Feller and Gerday, 2003). The fine balance between activity, stability, and flexibility of proteins which control enzyme kinetics has been reviewed by Georlette et al. (2004). When proteins from psychrophiles are compared with the equivalent proteins from mesophiles, they show a decrease in the number of ionic interactions, decreased number of hydrogen bonds, and fewer hydrophobic amino acid residues. The L-haloacid dehalogenase from *P. ingrahamii* has been cloned and overexpressed in *E. coli*. The recombinant protein has been biochemically and structurally characterized and compared with mesophilic and thermophilic L-haloacid dehalogenases. It shows activity towards monobromoacetic (100%), monochloroacetic acid (62%), *S*-chloropropionic acid (42%), *S*-bromopropionic acid (31%), dichloroacetic acid (28%), and 2-chlorobutyric acid (10%). The L-haloacid dehalogenase has highest activity towards substrates with shorter carbon chain lengths (≤C3), without preference towards a chlorine or bromine at the α-carbon position.

The enzyme has an optimal temperature for activity at 45°C and retains 70% of its activity after being incubated at 65°C for 90 min. The enzyme is relatively stable in organic solvents and therefore shows mesophilic properties despite being isolated from a psychrophilic bacterium. The relatively high thermal stability and optimal temperature for activity is surprising for an enzyme isolated from a psychrophilic bacterium. The thermal stability results show that the enzyme is stable beyond its catalytic temperature optimum. The "equilibrium model" has previously been described to explain the difference between apparent temperature optimum and higher thermostability for a range of psychrophilic, mesophilic, and thermophilic enzymes (Lee et al., 2007). This model includes an inactivated state of the enzyme at temperatures above the optimally active form, which are in reversible equilibrium. At sufficiently higher temperatures, the folded but inactive form of the enzyme can undergo irreversible thermal inactivation to the denatured state (Daniel and Danson, 2010).

Many reported psychrophilic enzymes have highest catalytic efficiency at low temperatures and have low thermal stability. However, some psychrophilic enzymes have been shown to denature at higher temperatures than that they appear to be inactive. For example, the *Pseudoalteromonas haloplanktis* DNA ligase is optimally active below 20°C, inactive above 25°C, but is not fully denatured until 35°C (Georlette et al., 2003). Also the citrate synthase from an Antarctic bacterium has been shown to decrease in enzyme activity at temperatures above its temperature optimum; however, this is not due to thermal denaturation of the enzyme since the activity loss can be reversed as the temperature decreases (Gerike et al., 1997, 2001). Further studies on psychrophilic enzymes will help to understand how these enzymes are adapted to function at low temperatures.

An homology model of the marine L-haloacid dehalogenase has been built based on the crystal structure of related enzymes. The active site pocket of the *P. ingrahamii* model and the *S. tokodaii* and *Burkholderia cepacia* enzymes are highly similar, with almost all residues in similar conformations. The observed thermostability of the enzyme is consistent with the conclusions drawn from homology modeling where no obvious psychrophilic adaptations were observed. At the *in vitro* optimal growth temperature of *P. ingrahamii*, L-haloacid dehalogenase would not be active. This could indicate that the enzyme has been acquired by horizontal gene transfer. This solvent-resistant and stable L-haloacid dehalogenase from *P. ingrahamii* has potential to be used as a biocatalyst in industrial processes.

Another novel marine dehalogenase from the Rhodobacteraceae family has been isolated from a polychaeta worm collected from Tralee beach, Argyll, UK. The enzyme tested positive for L-haloacid dehalogenase activity towards L-monochloropropionic acid (Novak et al., 2013b). A diagram of the overall two-domain structure is shown in **Figure 7** with the active site aspartic acid highlighted in the cleft between the domains. The active site of this dehalogenase shows significant differences from previously studied L-haloacid dehalogenases. The asparagine and arginine residues shown to be essential for catalytic activity in other L-haloacid dehalogenases are not present in this enzyme. The histidine residue that replaces the asparagine residue as shown in the structure was coordinated by a conformationally strained glutamate residue that replaces a conserved glycine residue. The His/Glu dyad is positioned for deprotonation of the catalytic water which attacks the ester bond in the reaction intermediate. The catalytic water in this novel enzyme is shifted by from its position in other L-haloacid dehalogenases. A similar His/Glu or Asp dyad is known to activate the catalytic water in haloalkane dehalogenases. The novel enzyme represents a new member within the L-haloacid dehalogenase family and appears to have evolved with properties of a mixture of a haloalkane dehalogenase and a haloacid dehalogenase, and it has the potential to be used as a commercial biocatalyst. It is not unusual to find such novel enzymes in extremophilic microorganisms.

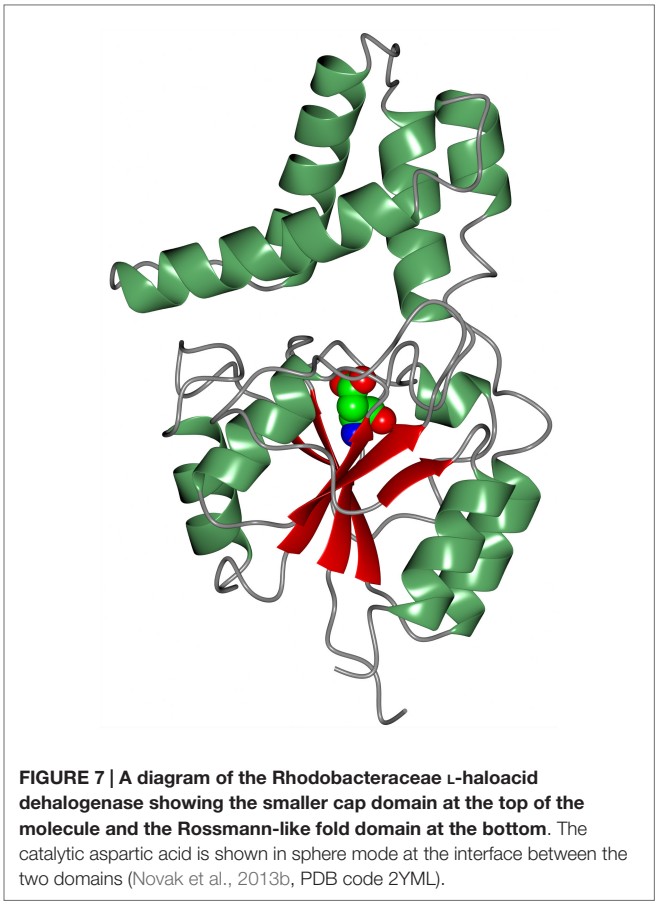

FIGURE 7 | A diagram of the Rhodobacteraceae L-haloacid dehalogenase showing the smaller cap domain at the top of the molecule and the Rossmann-like fold domain at the bottom. The catalytic aspartic acid is shown in sphere mode at the interface between the two domains (Novak et al., 2013b, PDB code 2YML).

The use of psychrophilic enzymes in industrial processes allows instability issues with reactants and products to be avoided and results in a reduction in cost because of the lower energy consumption. High catalytic efficiency at low temperatures makes psychrophilic enzymes attractive for use in biocatalytic processes (Gomes and Steiner, 2004; Novak and Littlechild, 2013).

CONCLUSION

Extremophilic enzymes are becoming an important source of new industrially robust biocatalysts. The use of nature's biodiversity provides an ever increasing resource of new genomes and metagenomes to identify useful activities which can carry out a variety of

chemical biotransformations of commercial interest. The activity of the enzymes can be identified by both bioinformatic techniques and screening of expression libraries. The enzymes can be cloned and overexpressed in easily grown hosts such as *E. coli* allowing access to sufficient quantities of the purified enzymes for detailed biochemical and structural characterization. The scale-up of the enzyme production required for commercial applications can be carried out by using a fungal host system that allows export of the proteins into the growth medium for easy downstream processing, if appropriate. The cost of the enzyme biocatalyst must be matched to the value of the end product. Higher value optically pure pharmaceutical intermediates which are used as building blocks for drug intermediates will allow a higher enzyme price than enzymes used for the production of bulk chemicals, additives for domestic products, food production, or biomass degradation processes. The stability of the biocatalyst is also an economic issue since if the enzyme is sufficiently robust under the industrial conditions it can be used for repeated cycles of the biocatalytic process thereby saving money. The use of enzymes isolated from extremophilic microorganisms offers the opportunity to access enzymes that are stable in a variety of different conditions such as high temperatures, low temperatures, high salt concentrations, high pressure, extremes of pH, and often a combination of these properties, which can make them more suited to the industrial environments.

The use of enzymes in "white biotechnology" is expected to grow with biobased materials and chemicals from emerging technologies predicted to rise globally to over 7.4 million metric tons in 2018 (Lux Research Analysis, www.luxresearchinc.com). Each industrial process is different and the correct biocatalyst needs to be identified and optimized for the industrial application. Many enzyme families have not realized their potential in this area and remain to be discovered. Enzymes that can catalyze reactions with non-natural substrates and under non-physiological conditions, which are often used in industry, can be found in the extremophile environment. Although the techniques available for enzyme engineering have improved recently, the enzyme discovery and optimization process is still a limiting factor for the adoption of new biobased industrial processes.

ACKNOWLEDGMENTS

The author would like to thank the University of Exeter, the Wellcome Trust, the BBSRC, the EPSRC, and the Technology Strategy Board, UK, for sponsoring research in the JL Laboratories at the Exeter Biocatalysis Centre. The EU Framework 7 grant "HotZyme" entitled Systematic Screening of Organisms from Hot Environments, Grant Number 265933, is thanked for supporting studies on the isolation of the metagenomes from Russia and China where the novel thermophilic limonene epoxide hydrolases were isolated and for the identification of the first thermophilic *Planctomycetes* species where the novel thermophilic esterase was identified. This EU project sponsored the research to clone, overexpress, and biochemically and structurally characterize these three new enzymes to allow their potential commercial exploitation. JL would like to thank all of the collaborators, postdoctoral fellows, and students who have contributed to the research work covered in this paper.

REFERENCES

Andreeva, A., Howorth, D., Chothia, C., Kulesha, E., and Murzin, A. G. (2014). SCOP2 prototype: a new approach to protein structure mining. *Nucleic Acids Res.* 42, D310–D314. doi:10.1093/nar/gkt1242

Arai, R., Kukimoto-Niino, M., Kuroishi, C., Bessho, Y., Shirouzu, M., and Yokoyama, S. (2006). Crystal structure of the probable haloacid dehalogenase PH0459 from *Pyrococcus horikoshii* OT3. *Protein Sci.* 15, 373–377. doi:10.1110/ps.051922406

Arand, M., Hallberg, B. M., Zou, J., Bergfors, T., Oesch, F., van der Werf, M. J., et al. (2003). Structure of *Rhodococcus erythropolis* limonene-1,2-epoxide hydrolase reveals a novel active site. *EMBO J.* 22, 2583–2592. doi:10.1093/emboj/cdg275

Bains, J., Kaufman, L., Farnell, B., and Boulanger, M. J. (2011). A product analog bound form of 3-oxoadipate-enol-lactonase (PcaD) reveals a multifunctional role for the divergent cap domain. *J. Mol. Biol.* 406, 649–658. doi:10.1016/j.jmb.2011.01.007

Baxter, S., Royer, S., Grogan, G., Brown, F., Holt-Tiffin, K., Taylor, I., et al. (2012). An improved racemase/acylase biotransformation for the amino acids. *J. Am. Chem. Soc.* 134, 19310–19313. doi:10.1021/ja305438y

Bommarius, A. S., Schwarm, M., and Drauz, K. (1998). Biocatalysis to aminoacid-based chiral pharmaceuticals: examples and perspectives. *J. Mol. Catal. B Enzym.* 5, 1–11. doi:10.1016/S1381-1177(98)00009-5

Breezee, J., Cady, N., and Staley, J. T. (2004). Subfreezing growth of the sea ice bacterium *Psychromonas ingrahamii*. *Microb. Ecol.* 47, 300–304. doi:10.1007/s00248-003-1040-9

Cheeseman, J. D., Tocilj, A., Park, S., Schrag, J. D., and Kazlauskas, R. J. (2004). Structure of an aryl esterase from *Pseudomonas fluorescens*. *Acta Crystallogr.* D60, 1237–1243. doi:10.1107/S0907444904010522

Chen, B. H., Sayar, A., Kaulmann, U., Dalby, P. A., Ward, J. M., and Woodley, J. M. (2006). Reaction modelling and simulation to assess the integrated use of transketolase and ω-transaminase for the synthesis of an aminotriol. *Biocatal. Biotransformation* 24, 449–457. doi:10.1080/10242420601068668

Daniel, R. M., and Danson, M. J. (2010). A new understanding of how temperature affects the catalytic activity of enzymes. *Trends Biochem. Sci.* 35, 584–591. doi:10.1016/j.tibs.2010.05.001

Di Fiore, A., Capasso, C., De Luca, V., Monti, S. M., Carginale, V., Supuran, C. T., et al. (2013). X-ray structure of the first 'extremo-α-carbonic anhydrase', a dimeric enzyme from the thermophilic bacterium *Sulfurihydrogenibium yellowstonense* YO3AOP1. *Acta Crystallogr.* D69, 1150–1159. doi:10.1107/S0907444913007208

Drauz, K. (1997). Chiral amino acids: a versatile tool in the synthesis of pharmaceuticals and fine chemicals. *Int J Chem Chimia* 51, 310–314.

Feller, G. (2003). Molecular adaptations to cold in psychrophilic enzymes. *Cell. Mol. Life Sci.* 60, 648–662. doi:10.1007/s00018-003-2155-3

Feller, G., and Gerday, C. (2003). Psychrophilic enzymes: hot topics in cold adaption. *Nat. Rev. Microbiol.* 1, 200–208. doi:10.1038/nrmicro773

Ferrandi, E. E., Sayer, C., Isupov, M. N., Annovazzi, C., Marchesi, C., Iacobone, G., et al. (2015a). Discovery and characterization of thermophilic limonene-1,2-epoxide hydrolases from hot spring metagenomics libraries. *FEBS J.* 282, 2879–2894. doi:10.1111/febs.13328

Ferrandi, E., Marchesi, C., Annovazzi, C., Riva, S., Monti, D., and Wohlgemuth, R. (2015b). Efficient epoxide hydrolase-catalyzed resolutions of (+)- and (-)-*cis*-/*trans*-limonene oxides. *ChemCatChem* doi:10.1002/cctc.201500608

Georlette, D., Blaise, V., Collins, T., D'Amico, S., Gratia, E., Hoyoux, A., et al. (2004). Some like it cold: biocatalysis at low temperatures. *FEMS Microbiol. Rev.* 28, 25–42. doi:10.1016/j.femsre.2003.07.003

Georlette, D., Damiens, B., Blaise, V., Depiereux, E., Uversky, V. N., Gerday, C., et al. (2003). Structural and functional adaptations to extreme temperatures in psychrophilic, mesophilic and thermophilic DNA ligases. *J. Biol. Chem.* 278, 37015–37023. doi:10.1074/jbc.M305142200

Gerike, U., Danson, M. J., and Hough, D. W. (2001). Cold-active citrate synthase: mutagenesis of active-site residues. *Protein Eng.* 14, 655–661. doi:10.1093/protein/14.9.655

Gerike, U., Danson, M. J., Russell, N. J., and Hough, D. W. (1997). Sequencing and expression of the gene encoding a cold active citrate synthase from an Antarctic bacterium, strain DS2 3R. *Eur. J. Biochem.* 248, 49–57. doi:10.1111/j.1432-1033.1997.00049.x

Gomes, J., and Steiner, W. (2004). The biocatalytic potential of Extremophiles and Extremozymes. *Food Technol. Biotechnol.* 42, 223–235.

Gonsalvez, I. S., Isupov, M., and Littlechild, J. A. (2001). Crystallization and preliminary X-ray analysis of a gamma-lactamase. *Acta Crystallogr.* D57, 284–286. doi:10.1107/S0907444900016838

Guler, O. O., Capasso, C., and Supuran, C. T. (2015). A magnificent enzyme superfamily: carbonic anhydrases, their purification and characterization. *J. Enzyme Inhib. Med. Chem.* doi:10.3109/14756366.2015.1059333

Hickey, A. M., Ngamsom, B., Wiles, C., Greenway, G. M., Watts, P., and Littlechild, J. A. (2009). A microreactor for the study of biotransformations by a cross-linked gamma-lactamase enzyme. *Biotechnol. J.* 4, 510–516. doi:10.1002/biot.200800302

Holt, K. (2004). Biocatalysis and chemocatalysis – a powerful combination for the preparation of enantiomerically pure α-amino acids. *Pharmachem* 3, 2–4. doi:10.1002/chin200542274

Hopmann, K. H., Hallberg, B. M., and Himo, F. (2005). Catalytic mechanism of limonene epoxide hydrolase, a theoretical study. *J. Am. Chem. Soc.* 127, 14339–14347. doi:10.1021/ja050940p

James, P., Isupov, M. N., Sayer, C., Saneei, V., Berg, S., Lioliou, M., et al. (2014). The structure of a tetrameric α-carbonic anhydrase from *Thermovibrio ammonificans* reveals a core formed around intermolecular disulfides that contribute to its thermostability. *Acta Crystallogr.* D70, 2607–2618. doi:10.1107/S1399004714016526

Kobayashi, M., Fujiwara, Y., Goda, M., Komeda, H., and Shimizu, S. (1997). Identification of active sites in amidase: evolutionary relationship between amide bond- and peptide bond-cleaving enzymes. *Proc. Natl. Acad. Sci. U.S.A.* 94, 11986–11991. doi:10.1073/pnas.94.22.11986

Kong, X.-D., Ma, Q., Zhou, J., Zeng, B.-B., and Xu, J.-H. (2014). A smart library of epoxide hydrolase variants and the top hits for synthesis of (*S*)-β-blocker precursors. *Angew. Chem. Int. Ed.* 53, 6641–6644. doi:10.1002/anie.201402653

Kotik, M., Archelas, A., and Wohlgemuth, R. (2012). Epoxide hydrolases and their application in organic synthesis. *Curr. Org. Chem.* 16, 451–482. doi:10.2174/138527212799499840

Lee, C. K., Daniel, R. M., Shepherd, C., Saul, D., Cary, S. C., Danson, M. J., et al. (2007). Eurythermalism and temperature dependence of enzyme activity. *FASEB J.* 8, 1934–1941. doi:10.1096/fj.06-7265com

Line, K., Isupov, M. N., and Littlechild, J. A. (2004). The crystal structure of a (−) γ-lactamase from an *Aureobacterium* species reveals a tetrahedral intermediate in the active site. *J. Mol. Biol.* 338, 519–532. doi:10.1016/j.jmb.2004.03.001

Littlechild, J., James, P., Novak, H., and Sayer, C. (2013). "Mechanisms of thermal stability adopted by thermophilic proteins and their use in white biotechnology," in *Thermophilic Microbes in Environmental and Industrial Biotechnology, Biotechnology of Thermophiles*, 2nd Edn, eds Satyanarayana T., Littlechild J., and Kawarabayasi Y. (London: Springer Publishers), 481–507.

Nestl, B. M., Hammer, S. C., Nebel, B. A., and Hauer, B. (2014). New generation of biocatalysts for organic synthesis. *Angew. Chem. Int. Ed.* 53, 3070–3095. doi:10.1002/anie.201302195

Ngamsom, B., Hickey, A. M., Greenway, G. M., Littlechild, J. A., Watts, P., and Wiles, C. (2010). Development of a high throughput screening tool for biotransformations utilising a thermophilic L-aminoacylase enzyme. *J. Mol. Catal. B Enzym.* 63, 81–86. doi:10.1016/j.molcatb.2009.12.013

Novak, H., and Littlechild, J. (2013). "Marine enzymes for biocatalysis. Sources, biocatalytic characteristics and bioprocesses of marine enzymes," in *Marine Enzymes with Applications for Biosynthesis of Fine Chemicals*, ed. Trincone A. (Cambridge: Woodhead Publishing Series in Biomedicine), 89–102.

Novak, H. R., Sayer, C., Panning, J., and Littlechild, J. A. (2013a). Characterisation of an L-haloacid dehalogenase from the marine psychrophile *Psychromonas ingrahamii* with potential industrial application. *Mar. Biotechnol.* 6, 695–705. doi:10.1007/s10126-013-9522-3

Novak, H. R., Sayer, C., Isupov, M. N., Paszkiewicz, K., Gotz, D., Mearns-Spragg, A., et al. (2013b). Marine *Rhodobacteraceae* L-haloacid dehalogenase contains a novel His/Glu dyad which could activate the catalytic water. *FEBS J.* 280, 1664–1680. doi:10.1111/febs.12177

Riley, M., Staley, J. T., Danchin, A., Wang, T. Z., Brettin, T. S., Hauser, L. J., et al. (2008). Genomics of an extreme psychrophile, *Psychromonas ingrahamii*. *BMC Genomics* 9:210. doi:10.1186/1471-2164-9-210

Rye, C. A., Isupov, M. N., Lebedev, A. A., and Littlechild, J. A. (2007). An order-disorder twin crystal of L-2-haloacid dehalogenase from *Sulfolobus tokodaii*. *Acta Crystallogr.* D63, 926–930. doi:10.1107/S0907444907026315

Rye, C. A., Isupov, M. N., Lebedev, A. A., and Littlechild, J. A. (2009). Biochemical and structural studies of a L-haloacid dehalogenase from the thermophilic archaeon *Sulfolobus tokodaii*. *Extremophiles* 13, 179–190. doi:10.1007/s00792-008-0208-0

Sayer, C., Bommer, M., Ward, J. M., Isupov, M. N., and Littlechild, J. A. (2012). Crystal structure and substrate specificity of the thermophilic serine:pyruvate aminotransferase from *Sulfolobus solfataricus*. *Acta Crystallogr.* D68, 763–772. doi:10.1107/S0907444912011274

Sayer, C., Isupov, M. N., Bonch-Osmolovskaya, E., and Littlechild, J. A. (2015). Structural studies of a thermophilic esterase from a new *Planctomycetes* species, *Thermogutta terrifontis*. *FEBS J.* 282, 2846–2857. doi:10.1111/febs.13326

Silverman, D. N., and Lindskog, S. (1988). The catalytic mechanism of carbonic anhydrase: implications of a rate-limiting protolysis of water. *Acc. Chem. Res.* 21, 30–36. doi:10.1021/ar00145a005

Singleton, M., Isupov, M., and Littlechild, J. (1999). X-ray structure of pyrrolidone carboxyl peptidase from the hyperthermophilic archaeon *Thermococcus litoralis*. *Structure* 7, 237–244. doi:10.1016/S0969-2126(99)80034-3

Smith, K. S., Jakubzick, C., Whittam, T. S., and Ferry, J. G. (1999). Carbonic anhydrase is an ancient enzyme widespread in prokaryotes. *Proc. Natl. Acad. Sci. U.S.A.* 96, 15184–15189. doi:10.1073/pnas.96.26.15184

Tanimoto, K., Higashi, N., Nishioka, M., Ishikawa, K., and Taya, M. (2008). Characterization of thermostable aminoacylase from hyperthermophilic archaeon *Pyrococcus horikoshii*. *FEBS J.* 275, 1140–1149. doi:10.1111/j.1742-4658.2008.06274.x

Taylor, S. J. C., McCague, R., Wisdom, R., Lee, C., Dickson, K., Ruecroft, G., et al. (1993). Development of the biocatalytic resolution of 2-azabicyclo [2.2.1] hept-5-en-3-one as an entry to single-enantiomer carbocyclic nucleosides. *Tetrahedron* 4, 1117–1128. doi:10.1016/S0957-4166(00)80218-9

Toogood, H. S., Brown, R. C., Line, K., Keene, P. A., Taylor, S. J. C., McCague, R., et al. (2004). The use of a thermostable signature amidase in the resolution of the bicyclic synthon (rac)-γ-lactam. *Tetrahedron* 60, 711–716. doi:10.1016/j.tet.2003.11.064

Toogood, H. S., Hollingsworth, E. J., Brown, R. C., Taylor, I. N., Taylor, S. J., McCague, R., et al. (2002a). A thermostable L-aminoacylase from *Thermococcus litoralis*: cloning, overexpression, characterization, and applications in biotransformations. *Extremophiles* 6, 111–122. doi:10.1007/s007920100230

Toogood, H. S., Taylor, I. N., Brown, R. C., Taylor, S. J. C., McCague, R., and Littlechild, J. A. (2002b). Immobilisation of the thermostable L-aminoacylase from *Thermococcus litoralis* to generate a reusable industrial biocatalyst. *Biocatal. Biotransformation* 20, 241–249. doi:10.1080/10242420290029472

Trincone, A. (2011). Marine biocatalysts: enzymatic features and applications. *Mar. Drugs* 9, 478–499. doi:10.3390/md9040478

Van der Ploeg, J., Van Hall, G., and Janssen, D. B. (1991). Characterization of the haloacid dehalogenase from *Xanthobacter autotrophicus* GJ10 and sequencing of the *dhlB* gene. *J. Bacteriol.* 173, 7925–7933.

Widersten, M., Gurell, A., and Lindberg, D. (2010). Structure-function relationships of epoxide hydrolases and their potential use in biocatalysis. *Biochim. Biophys. Acta* 1800, 316–326. doi:10.1016/j.bbagen.2009.11.014

Yin, D. L., Bernhardt, P., Morley, K. L., Jiang, Y., Cheeseman, J. D., Purpero, V., et al. (2010). Switching catalysis from hydrolysis to perhydrolysis in *P. fluorescens* esterase. *Biochemistry* 49, 1931–1942. doi:10.1021/bi9021268

Conflict of Interest Statement: The authors declare that the research was conducted in the absence of any commercial or financial relationships that could be construed as a potential conflict of interest.

frontiers in Bioengineering and Biotechnology

ORIGINAL RESEARCH
published: 13 July 2015
doi: 10.3389/fbioe.2015.00097

Biochemical and structural properties of a thermostable mercuric ion reductase from *Metallosphaera sedula*

*Jacob H. Artz[1], Spencer N. White[1], Oleg A. Zadvornyy[1], Corey J. Fugate[1], Danny Hicks[1], George H. Gauss[1], Matthew C. Posewitz[2], Eric S. Boyd[3,4] and John W. Peters[1]**

[1] Department of Chemistry and Biochemistry, Montana State University, Bozeman, MT, USA, [2] Department of Chemistry and Geochemistry, Colorado School of Mines, Golden, CO, USA, [3] Department of Microbiology and Immunology, Montana State University, Bozeman, MT, USA, [4] Thermal Biology Institute, Montana State University, Bozeman, MT, USA

OPEN ACCESS

Edited by:
Noha M. Mesbah, Suez Canal University, Egypt

Reviewed by:
Bing-Zhi Li, Tianjin University, China
Yasser Gaber, Beni-Suef University, Egypt

***Correspondence:**
John W. Peters, Department of Chemistry and Biochemistry, Montana State University, 224 Chemistry and Biochemistry Building, Bozeman, MT 59717, USA
john.peters@chemistry.montana.edu

Specialty section:
This article was submitted to Process and Industrial Biotechnology, a section of the journal Frontiers in Bioengineering and Biotechnology

Received: *10 April 2015*
Accepted: *19 June 2015*
Published: *13 July 2015*

Citation:
Artz JH, White SN, Zadvornyy OA, Fugate CJ, Hicks D, Gauss GH, Posewitz MC, Boyd ES and Peters JW (2015) Biochemical and structural properties of a thermostable mercuric ion reductase from Metallosphaera sedula. Front. Bioeng. Biotechnol. 3:97. doi: 10.3389/fbioe.2015.00097

Mercuric ion reductase (MerA), a mercury detoxification enzyme, has been tuned by evolution to have high specificity for mercuric ions (Hg^{2+}) and to catalyze their reduction to a more volatile, less toxic elemental form. Here, we present a biochemical and structural characterization of MerA from the thermophilic crenarchaeon *Metallosphaera sedula*. MerA from *M. sedula* is a thermostable enzyme, and remains active after extended incubation at 97°C. At 37°C, the NADPH oxidation-linked Hg^{2+} reduction specific activity was found to be 1.9 μmol/min·mg, increasing to 3.1 μmol/min·mg at 70°C. *M. sedula* MerA crystals were obtained and the structure was solved to 1.6 Å, representing the first solved crystal structure of a thermophilic MerA. Comparison of both the crystal structure and amino acid sequence of MerA from *M. sedula* to mesophillic counterparts provides new insights into the structural determinants that underpin the thermal stability of the enzyme.

Keywords: mercuric reductase, mercury detoxification, thermophile, thermostability, structure, biosensor, MerA

Introduction

The ionic form of mercury, which is one of the most toxic metals known to biology (Gertrud et al., 1989; Nies, 2003; Vetriani et al., 2005), is naturally present at elevated concentrations in many hydrothermal vents, hot springs, and acid mine drainage fluids (Batten and Scow, 2003; Simbahan et al., 2005; Vetriani et al., 2005; King et al., 2006; Boyd et al., 2009; Wang et al., 2011). In these environments, biology utilizes a finely tuned protein catalyst termed the mercuric reductase (MerA) (encoded by the *merA* gene) in order to reduce toxic ionic mercury (Hg^{2+}) to the far less toxic, volatile, and elemental form (Hg^0). The reaction catalyzed by MerA follows the reaction scheme of $NADPH + Hg^{2+} \rightarrow NADP^+ + Hg^0$ (Barkay et al., 2003). MerAs, which are part of the disulfide oxidoreductase (DSOR) family (Fox and Walsh, 1982), are ancient enzymes, having arisen in high temperature environments after the great oxidation event ~2.4 billion years ago (Barkay et al., 2010). Since that time, evolution has finely tuned MerA through recruitment of regulatory and transport proteins (Boyd and Barkay, 2012) to serve a diversity of organisms, including both Archaea and Bacteria, which encounter Hg^{2+} ions in less extreme mesophilic settings, while retaining extremely high stability and substrate specificity. These characteristics of mercuric reductases lend them to

possible sensor applications, wherein the redox properties of the enzyme could be coupled to an amplifiable electrical signal (Adami et al., 1995; Han et al., 2001; Zhang et al., 2011). A stable mercuric reductase may also be used to potentially mitigate mercury contamination (Nascimento and Chartone-Souza, 2003).

Metallosphaera sedula (*Mse*), isolated previously from Pisciarelli Solfatara in Naples, Italy (Gertrud et al., 1989), has a minimum and maximum temperature for growth range of 50–80°C (Auernik et al., 2008a). Pisciarelli Solfatara itself contains a variety of thermal features that range in temperature from ~30°C to nearly 100°C, and a pH range of 1.5 to around 6.0 with elevated concentrations of heavy metals, including Hg^{2+} at concentrations up to 0.005 g/kg (Huber et al., 2000). The genome sequence of *Mse* was completed in 2008, (Auernik et al., 2008b), making it possible to identify mechanisms of Hg^{2+} tolerance at the genomic level. The *mer* operon in *Mse* includes both MerA and MerH, where MerH may aid metal trafficking to the MerR transcription factor (Schelert et al., 2013).

A variety of MerAs have been characterized previously, most notably a protein encoded on a transposon isolated from *Pseudomonas aeruginosa*, which is termed Tn*501* (Fox and Walsh, 1982), as well as MerA from *Bacillus cereus* (*Bc*MerA) (Schiering et al., 1991) and a MerA from a deep brine environment, termed ATII-LCL (Sayed et al., 2013). Collectively, these biochemical studies have revealed MerAs that exhibit K_m values for Hg^{2+} that range from 9–70 μM and specific activities that range from 1.05–50 μmol/min·mg. Structural characterization was first carried out on *Bc*MerA (Schiering et al., 1991) and later on Tn*501* (Ledwidge et al., 2005). Most recently, the Tn*501* structure has been solved in complex with Hg^{2+} (Lian et al., 2014). Structural characterization confirmed that MerA is a member of the DSOR protein family, which adopts a βαββαβ fold, and which is known to catalyze pyridine-dependent substrate reduction with a characteristic active site CXXXXC motif (Argyrou and Blanchard, 2004). Some MerAs also harbor an additional N-terminal GMTCXXC motif (Boyd and Barkay, 2012) that assists in metal recruitment (Ledwidge et al., 2005). A third pair of conserved cysteines are located in a flexible region on the C-terminal domain, and are responsible for delivering mercuric ions to the active site of the opposing monomer (Lian et al., 2014).

Despite these advances, the structural characterization of a MerA from a thermophile has yet to be conducted, even though this is critical for understanding the properties of enzymes involved in mercury detoxification of high-temperature environments where mercury concentrations are very high. Structural characterization is important for both understanding the thermophilic origins of the protein (Barkay et al., 2010; Boyd and Barkay, 2012) as well as for possible incorporation into stable biotechnologies. Here, we report biochemical and structural characterization of a thermostable MerA from the aerobic thermoacidophilic Crenarchaeon *Mse* (*Mse*MerA).

Materials and Methods

Bioinformatics

MerA homologs were compiled from the Department of Energy-Integrated Microbial Genomes database using BLASTp and the *Tn501* MerA as a query. Representative homologs were screened for conserved residues that define MerA (as described above), and those protein sequences with these residues were aligned using CLUSTALX (version 2.0.8) specifying the Gonnet 250 protein substitution matrix and default gap extension and opening penalties (Larkin et al., 2007), with dihydrolipoamide dehydrogenase from *Magnetospirillum magneticum* AMB-1 (YP_423326), *Thermus thermophilus* HB27 (YP_005669), and *Pseudomonas fluorescens* Pf0-1 (YP_351398) serving as outgroups. N-terminal "NmerA" sequence was trimmed from the alignment block as previously described (Barkay et al., 2010) and the phylogeny of MerA was evaluated with PhyML (ver. 3.0.1) (Guindon et al., 2010) using the LG amino acid substitution matrix with a discrete four category gamma substitution model and a defined proportion of invariant sites. A consensus phylogenetic tree was projected from 100 bootstrap replications using FigTree (ver. 1.2.2) (http://tree.bio.ed.ac.uk/software/figtree/).

Structural superimpositions were generated by the program UCSF Chimera (Pettersen et al., 2004). The protein sequence of *Mse*MerA was blasted with NCBI BLASTp. The top eight hits were compared with mesophilic mercuric reductases from *Staphylococcus aureus*, *B. cereus*, *P. aeruginosa*, and a sequence from a hydrothermal deep-sea brine environment, ATII-LCL (Sayed et al., 2013). It should be noted that while the ATII-LCL sequence was isolated from a hydrothermal vent system with a temperature of 68°C, the optimum temperature for activity was shown to be 30–50°C (Sayed et al., 2013), indicating that it is not adapted to the thermal regime from where it was isolated or that the environment from where it was isolated is variable with respect to temperature. VADAR was used to evaluate the surface area and charged residue percentage of MerA homologs (Willard et al., 2003), while the ProtParam tool available from ExPASy was used to calculate the aliphatic index of MerA homologs (Gasteiger et al., 2005).

Expression and Purification

*Mse*MerA DSM 5348 sequence was codon-optimized and synthesized by GenScript USA Inc. with an N-terminal 6× His-tag (Data Sheet 1 in Supplementary Material). The gene was cloned into MCS1 of pETDuet-1 and transformed into *Escherichia coli* BL21DE3 cells (Novagen, EMD Millipore, USA). Sequence-based confirmation of *Mse*MerA transformation was performed by Davis Sequencing, Inc. (1450 Drew Ave, Suite 100, Davis, CA, USA).

Fifty milliliters of Luria-Bertani (LB) broth, supplemented with 0.5 mM riboflavin and 0.1 g/L ampicillin, were inoculated with recombinant *E. coli* cells containing *Mse*MerA and shaken at 250 rpm at room temperature overnight. One liter of LB medium, as described above, was inoculated with 2 mL from the overnight culture, and shaken at 250 rpm until an OD_{600} of 0.5–0.7 was reached. About 2 mM IPTG was added and expression was carried out for 4 h, after which the cultures were centrifuged at 6000 × *g* for 10 min (4°C), with the resultant cell pellet immediately being flash frozen in liquid nitrogen and stored at −80°C. Each liter of cell culture yielded 3.0–3.5 g of cell paste.

Cell paste was subjected to three freeze/thaw cycles to facilitate lysis, after which cells were re-suspended in 5 mL Buffer A (100 mM NaCl, 50 mM MOPS with a pH of 6.7, 25 mM imidazole)

per gram of cells. Lysozyme and deoxyribonuclease (DNase) were added to final concentrations of 0.1 mg/mL along with phenylmethylsulfonyl fluoride (PMSF)-saturated isopropanol to a final concentration of 0.1% v/v, and this mixture was incubated for 30 min at room temperature. Triton X-100 was then added to a final concentration of 1% v/v, and this was mixed for 30 min. The crude lysate was then clarified by centrifugation at 100,000 × *g* for 1 h (4°C). The resulting clarified lysate was observed to have a yellow color.

Purification of *Mse*MerA was carried out using a 75 mL gradient from 100% Buffer A to 100% Buffer B (100 mL NaCl, 50 mM MOPS with a pH 6.7, 250 mM imidazole) on a 2 mL Ni-NTA column (Qiagen) at 3 mL/min. Seven milliliter fractions were collected and further analyzed with an SDS-PAGE gel. Fractions containing pure protein were combined and concentrated to 10 mg/mL, buffer exchanged to Buffer C (10 mM MOPS pH of 6.7), and the protein was then concentrated to 30 mg/mL and flash-frozen in liquid nitrogen. Purity of the protein was confirmed by SDS- and Native PAGE (Figure S1 in Supplementary Material). A yield of 1.5 mg of pure protein per liter of growth culture was achieved.

Activity Assay

Activity assays were carried out in 100 mM NaCl, 50 mM MOPS with a pH of 6.7, 0.2 mg/mL *Mse*MerA, and 1 mM $HgCl_2$, and these were initiated by the addition of 0.2 mM NADPH, similar to previously established procedures (Fox and Walsh, 1982). For kinetic studies, the concentration of Hg^{2+} ranged from 28.6 μM to 2.77 mM. NADPH oxidation was monitored at 338 nm using a Cary 6000 UV/Vis spectrometer equipped with a 1 × 1 Peltier. Assays were conducted from 37 to 70°C, above which temperature the rate of non-enzymatic NADPH oxidation was too high to accurately measure enzymatic activity. In order to determine the thermostability of *Mse*MerA, an aliquot of the enzyme was assayed at 37°C and the remaining protein was boiled at 97°C for 100 min, after which the enzymatic activity was once again measured at 37°C.

Crystallization and Structure Determination

*Mse*MerA crystals were obtained using the hanging drop method. Crystallization drops contained 0.085M TRIS (pH 8.5), 15% v/v glycerol, 14% w/v PEG400, 0.19M $LiSO_4$, and 20 mg/mL protein. Crystals were obtained after 2 weeks, mounted on cryo loops, and shipped to the Stanford Synchrotron Radiation Lightsource for X-ray data collection. Diffraction data were collected at 100 K using the 12-2 beamline. Diffraction images were indexed, integrated, and scaled using HKL2000 (Otwinowski and Minor, 1997).

The structure of *Mse*MerA was solved to 1.6 Å using CCP4 molecular replacement (Cowtan et al., 2011) of Tn*501*MerA (PDB ID: 1ZK7), which shares 37% amino acid identity with *Mse*MerA. Model building was performed in Coot (Emsley et al., 2010) and coordinates were refined to reasonable stereochemistry at a resolution 1.6 Å (Figure S3 in Supplementary Material) using REFMAC5 (Murshudov et al., 1997). The structure was validated using MolProbity (Chen et al., 2010) and all molecular images were calculated in PyMol (Delano, 2002). Structural superimpositions were generated both with 1ZK7 (Ledwidge et al., 2005) and 4K7Z (Lian et al., 2014), in which the active site cysteines were substituted by alanines and could be solved in complex with the Hg^{2+} ion.

Results

Thermal Adaptation of *Mse*MerA

Phylogenetic reconstruction of representative core (NmerA trimmed) MerA sequences revealed a number of deeply branching lineages from thermophilic taxa, consistent with previous analyses that indicate MerA likely originated in a high temperature environment (Schelert et al., 2004; Barkay et al., 2010; Boyd and Barkay, 2012). *Mse*MerA clustered among MerA from thermophilic crenarchaeota (**Figure 1**). Sequence alignments reveal both the active site CXXXXC motif and C-terminal cysteines that are conserved among all MerA sequences. However, several key differences were observed that may be involved in conferring thermotolerance (**Figure 2**). Specifically, the thermophilic enzymes are missing regions corresponding to amino acids 66–71 and 130–134 Tn*501* (Tn*501*MerA numbering), suggesting a reduction in loop regions in comparison to the mesophilic enzymes (**Figure 2**). Two sets of residues, V317 and Y441, are within putative coordination distance of the active-site mercury. These residues are substituted for an E and F, respectively, in *Mse*MerA and other thermophiles with the exception of *Hydrogenobacter thermophilus* TK-6 (YNP_003432979) and *Hydrogenobaculum* sp. Y04AAS1 (YNP_002121876).

A comparison of the *Mse*MerA crystal structure to the previously determined Tn*501*MerA structure (PDB: 1ZK7) (Ledwidge et al., 2005) reveals that the two structures are highly similar, with an overall C-alpha deviation of 1.5 Å rmsd as calculated by Dali Lite (McWilliam et al., 2013). Two particular loop regions are shorter in *Mse*MerA (**Figure 3A**). This was further supported by VADAR (Willard et al., 2003), which calculated a 4% decrease in coil regions in *Mse*MerA. The calculated surface area of *Mse*MerA, 19,966.5 $Å^2$, is slightly reduced in comparison to Tn*501*MerA, with a surface area of 21,217.4 $Å^2$.

MEGA (Tamura et al., 2013) was used to compile an amino acid composition chart for the sequences examined. The thermophiles were observed to have a larger number of positively charged amino acids. VADAR calculated the total charged residues in *Mse*MerA to be 25% of residues compared to 21% of residues in *Tn501*MerA, and 24% in *Bc*MerA. An increase in ionic interactions may therefore represent a factor contributing to MerAs thermal stability (Szilágyi and Závodszky, 2000). The aliphatic index of *Mse*, Tn*501*, and *Bc* MerAs were calculated by ExPASy's ProtParam tool (Gasteiger et al., 2005), and found to be 101.63, 98.65, and 97.86, respectively, again in agreement with *Mse*MerA having higher thermostability (Ikai, 1980).

Biochemical Characterization

The specific activity of *Mse*MerA was examined from 37 to 70°C (**Figure 4**). One unit of activity was defined as 1 μmol NADPH oxidized per minute. At 37°C, the specific activity was found to be 1.9 U/mg, increasing up to 3.1 U/mg at 70°C. Mercury dependence of *Mse*MerA was determined, with K_m values of 400 and 150 μM at 37 and 70°C, respectively. Specific activity was not determined above 70°C due to the difficulty of discriminating between enzymatic and non-enzymatic NADPH oxidation

FIGURE 1 | Maximum-likelihood phylogenetic reconstruction of MerAs, with homologs from thermophilic taxa highlighted in red. *Mse*MerA is boldfaced. Bootstrap support is indicated by black (>90), gray (80–89), and open (70–79) circles. Nodes with no symbol exhibited bootstrap values of <70.

at high temperatures. The thermal stability of *Mse*MerA was tested by incubating the enzyme at 97°C for up to 100 min, followed by assessment of enzymatic activity at 37°C. Even after 100 min of incubation at 97°C, no decrease in overall activity was observed when compared to the untreated enzyme (Figure S2 in Supplementary Material). The K_{cat} at 70°C was found to be 23 s^{-1}, with a K_{cat}/K_m of 0.15 μM^{-1} s^{-1}.

Structural Characterization of *Mse*MerA

*Mse*MerA crystals were obtained using vapor diffusion in a precipitating solution of 14% polyethylene glycol 4000 and 0.19M lithium sulfate. These crystals belonged to space group $P22_12_1$ and contained two monomers per asymmetric unit, assembled into one homodimer (**Figure 3B**). The crystal structure of *Mse*MerA was solved to 1.6 Å, with R and R_{free} values of

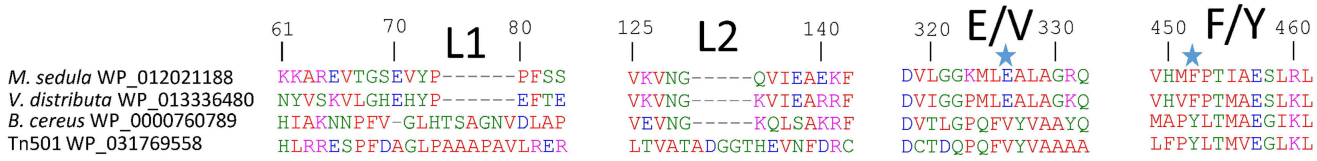

FIGURE 2 | *Mse*MerA aligned with other MerAs reveals two loop regions, L1 and L2, which may be involved in conferring thermostability, and two positions at 326 and 452 (highlighted with stars), where the active site region is different between thermophiles and mesophiles.

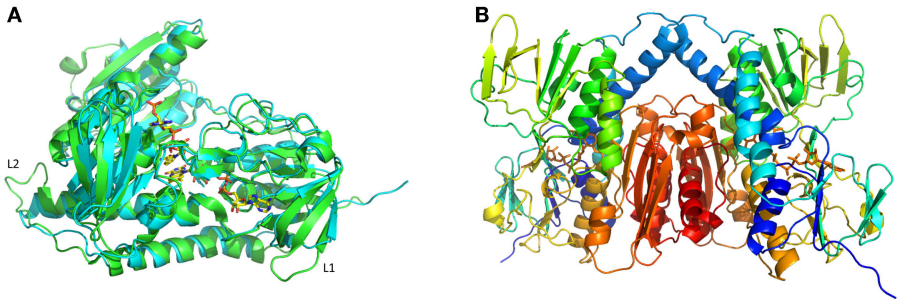

FIGURE 3 | (A) Structural superimposition of *Mse*MerA monomer (cyan) with Tn*501*MerA (green) reveals a decrease in loop regions (labeled L1 and L2) in *Mse*MerA. **(B)** Cartoon representation of a dimer of *Mse*MerA with bound FAD.

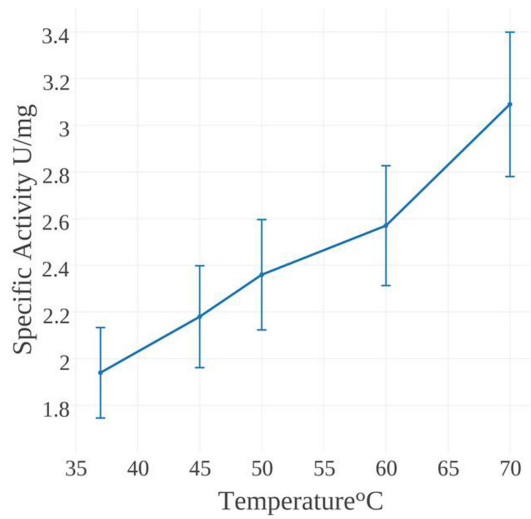

FIGURE 4 | NADPH oxidation activity of *Mse*MerA incubated at temperatures ranging from 37 to 70°C.

16.9 and 19.6%, respectively. Bound FAD was observed, suggesting that these molecules act to stabilize the structure. No mercury was observed in the active site. As expected based on the sequence alignment, a clear reduction in loop regions was observed in comparison to Tn*501*MerA (**Figure 3A**). No electron density for the carboxy terminus of *Mse*MerA was identified from 440 to 448, including the conserved pair of cysteines at residues 446 and 447. This is in agreement with the carboxy terminus being able to undergo conformational changes during the catalytic cycle (Lian et al., 2014). The solved structure has been deposited in the Protein Data Bank with the accession code 4YWO.

Discussion

Bioinformatic and phylogenetic data overwhelmingly support *Mse*MerA being a thermostable protein, as illustrated by features consistent with other enzymes from thermophiles, including a reduction in loop regions, a greater percent of charged amino acids, and an overall reduced surface area in comparison to its mesophilic counterpart. Collectively, these strategies are likely to interact synergistically to convey the high degree of thermostability observed. Retention of 100% activity after incubation at 97°C for 100 min further confirms the highly thermostable nature of *Mse*MerA.

Though practical constraints made measuring specific activity above 70°C impossible, catalytic activity was found to increase over the range of 37–70°C, with a V_{max} of 3.1 U/mg at 70°C. This places *Mse*MerA in the range of average activity when compared to other MerAs (**Table 1**). The K_m for Hg^{2+} of *Mse*MerA was found to decrease from 400 μM at 37°C to 150 μM at 70°C, indicating a higher affinity for Hg^{2+} ions at elevated temperatures. The K_m of *Mse*MerA is around an order of magnitude higher than that found for other MerAs (**Table 1**), and may be an adaptive strategy to cope with elevated Hg^{2+} concentrations commonly encountered in the acidic, high temperature environments where *Mse* resides (King et al., 2006; Boyd et al., 2009; Wang et al., 2011).

The K_{cat} of *Mse*MerA is 23 s^{-1}, which is very similar to the K_{cat} of ATII-LCL at 22.5 s^{-1} (Sayed et al., 2013) and also similar to *Bc*MerA at 12 s^{-1} (Rennex et al., 1994). The higher K_m value observed in *Mse*MerA translates to the lowest overall catalytic efficiency, with a K_{cat}/K_m of 0.15 μM^{-1} s^{-1}.

TABLE 1 | MerA comparison.

	Optimum growth temperature (°C)	Optimum temperature for enzyme activity (°C)	K_m (μM)		Specific activity (U/mg)	Amino acid substitution at the position V/Y 317/441 (Tn *501* numbering)	Reference
			Hg	NADPH			
M. sedula	50–79	>70	400[a]/150[b]	ND*	1.9[a]/3.1[b]	E/F	This work
*Pa*Tn*501*	25–42	55–65	12	6	12.7	V/Y	Fox and Walsh (1982)
ATII-LCL	~68	30–50	8.65	4.35	50	V/Y	Sayed et al. (2013)
Azotobacter Chroococcum	26	45	11.11	ND	25	ND	Ghosh et al. (1999)
Klebsiella pneumoniae	37	40	75	ND	9	V/Y	Zeroual et al. (2003)
B. cereus	37	ND	30	ND	ND	V/Y	Rennex et al. (1994)
E. coli R831	37	ND	13	6	1.05	ND	Schottel (1978)

*ND, not determined.
[a]Measured at 30°C.
[b]Measured at 70°C.

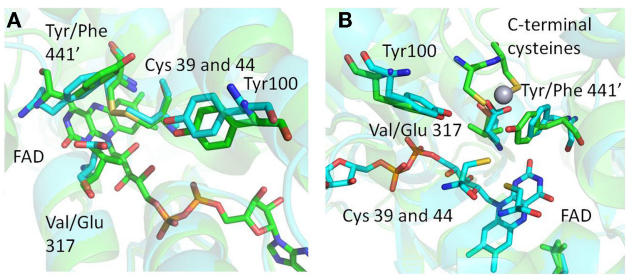

FIGURE 5 | (A) Structural superimposition of *Mse*MerA with Tn*501*MerA 1ZK7 shows the Y441′/V317 amino acids conserved in mesophiles and the F441/E317 amino acids conserved in thermophiles, suggesting an alternative Hg^{2+} coordination strategy in *Mse*MerA. **(B)** An alternative angle of the active site environment of *Mse*MerA superimposed onto Tn*501*MerA 4K7Z, which depicts the Hg^{2+} ion bound to the c-terminal cysteines. The monomer with the C-terminal cysteines is noted by a "prime" designation.

Though *P. aeruginosa* (*Pa*) from which the *Tn501* transposon was isolated is a mesophilic organism, the MerA enzyme was found to have optimal activity at 55–65°C, and retained full activity at 37°C even following a 10-min incubation at 100°C (Nakahara et al., 1985; Vetriani et al., 2005). Intriguingly, phylogenetic analysis indicates that *Tn501*MerA groups closely with the mesophiles (**Figure 1**). Conversely, phylogenetic analysis of MerA from a high temperature brine pool, ATII-LCL (Sayed et al., 2013), was found to group with MerA sequences from mesophilic organisms (**Figure 1**). While the environment from which ATII-LCL was isolated is at 68°C, the enzyme has maximum activity over a range of 30–50°C and, when measured at 37°C, was found to be half inactivated after a 10-min incubation at 75°C (Sayed et al., 2013). The ATII-LCLMerA is therefore not nearly as thermostable as *Mse*MerA, and is not adapted to its local environment, with respect to the thermal regime, but is adapted with respect to salinity regime.

The structure of *Mse*MerA reveals a dimeric biological assembly, as has been shown with previous structures (Schiering et al., 1991; Ledwidge et al., 2005; Lian et al., 2014). With this architecture, the active site cleft on one monomer interacts with the C-terminal domain of the opposing monomer (**Figure 5**; **Table 1**). This style of interaction is generally conserved among enzymes of the DSOR family. For example in glutathione reductase, His467, located near the *C*-terminus of one monomer, is necessary for catalytic function of the opposing monomer (Misra et al., 1985). In MerA, this has been substituted to a catalytically important tyrosine (Rennex et al., 1994).

Structural superimposition of *Mse*MerA (described here) with the recently solved Tn*501*MerA structure with bound mercury (4K7Z) reveals two specific amino acid substitutions, V317 to E, and Y441′ to F′, in the active site of *Mse*MerA compared to Tn*501*MerA (numbering is by Tn*501*MerA 4K7Z) (**Figure 5**). Another residue thought to be involved in metal coordination, Y100 (in *Bc* structure is Y264) (Schiering et al., 1991), is strictly conserved. For Tn*501*MerA and *Bc*MerA, the hydroxyl groups of Y441′ and Y100 likely act in concert to facilitate metal transfer from the C-terminal cysteines to the active site cysteines. In contrast, in *Mse*MerA, the F441′ in the position of tyrosine in Tn*501*MerA lacks a hydroxyl group to coordinate the Hg^{2+} ion, but a glutamic acid in place of the Tn*501*MerA V317 provides a different residue with which the Hg^{2+} ion could potentially be coordinated.

The conservation of either the V/Y′ in mesophiles or the E/F′ amino acid pair in thermophiles, along with the observed positions of the amino acids, is suggestive of an alternative metal binding strategy for Hg^{2+} ion transfer from the C′ cysteine pair to the active site cysteines C42 and C47. In Tn*501*MerA and *Bc*MerA, upon Hg^{2+} ion binding to the C′ cysteines, the C′ terminal region folds into the catalytic cleft, delivering the mercuric ion (Lian et al., 2014) to the conserved Y100 and Y441′, which facilitate transfer to the active site cysteines. Given that *Mse*MerA lacks the Y441 with which to coordinate the Hg^{2+} ion during active site delivery, the E317 is the most rational alternative.

Rennex et al. (1994) have previously substituted individual amino acids Y441F and Y100F in *Bc*MerA. The K_m for Hg^{2+} increased from 30 to 39 μM in the case of the Y441F variant, and decreased to 6 μM in the case of the Y100F variant. However, in both cases, the K_{cat}/K_m was decreased around 15-fold. It is therefore likely that the observed low catalytic efficiency

of the variant enzymes is due in part to a lack of a residue to coordinate the Hg^{2+} ion, such as the glutamic acid found in *Mse*MerA and other thermophiles. Moreover, Sayed et al. (2013) previously demonstrated that glutamic acid residues may play a role in Hg^{2+} ion coordination and transfer. However, the active site glutamic acid found in *Mse*MerA is a different site from what Sayed et al. (2013) have previously characterized. Furthermore, sequence alignment shows that the ATII-LCL enzyme has the V/Y amino acid pair (**Table 1**).

Both the Tn*501*MerA Y441′ and the *Mse*MerA E300 are about 5 Å from the active site cysteines, although they coordinate from different positions, with the Y441′ coordinating the Hg^{2+} ion almost perpendicular to E317. The different placement and nature of these side chains may help explain the higher K_m observed in *Mse*MerA relative to homologs from mesophilic organisms. Since the high Hg^{2+} concentrations are common features of high temperature environments, these differences may reflect adaptations to function at elevated Hg^{2+} concentrations and as such represent the structural determinants of specificity for mercuric reductases. Highly specific stable enzymes, especially those that catalyze oxidation-reduction reactions coupled to the specific molecular recognition, could potentially be used as chemical sensors in which the redox chemistry could be coupled to produce an amplifiable electrical signal.

In conclusion, here we present a characterization of the thermostable mercuric reductase from *M. sedula*. We show that the enzyme is highly resistant to heat treatment while retaining similar catalytic rates to other characterized MerAs. The enzyme appears to have a potentially different way of coordinating Hg^{2+} and has a lower affinity for Hg^{2+} ions than previously characterized enzymes. Considering that *Mse* is a thermophile and its MerA is likely to harbor properties more similar to those of primitive MerA that evolved in a high temperature environments (Barkay et al., 2010), these results may indicate that the activity of MerA has been refined through evolutionary time to successfully detoxify environmental Hg^{2+} at lower concentrations than those that are naturally present in thermal environments.

Acknowledgments

This work is supported by a grant from the Air Force Office of Scientific Research (FA9550-14-110147) to JP, MP, and EB. Portions of this research were carried out at the Stanford Synchrotron Radiation Laboratory (SSRL), a national user facility operated by Stanford University on behalf of the US Department of Energy, Office of Basic Energy Sciences. The SSRL Structural Molecular Biology program is supported by the US Department of Energy, Office of Biological and Environmental Research, the US National Institutes of Health, National Center for Research Resources, Biomedical Technology program, and the US National Institute of General Medical Sciences. EB acknowledges support from a grant from the National Science Foundation (EAR-1123689).

Supplementary Material

The Supplementary Material for this article can be found online at http://journal.frontiersin.org/article/10.3389/fbioe.2015.00097

References

Adami, M., Martini, M., and Piras, L. (1995). Characterization and enzymatic application of a redox potential biosensor based on a silicon transducer. *Biosens. Bioelectron.* 10, 633–638. doi:10.1016/0956-5663(95)96939-V

Argyrou, A., and Blanchard, J. S. (2004). Flavoprotein disulfide reductases: advances in chemistry and function. *Prog. Nucleic Acid Res. Mol. Biol.* 78, 89–142. doi:10.1016/s0079-6603(04)78003-4

Auernik, K. S., Cooper, C. R., and Kelly, R. M. (2008a). Life in hot acid: pathway analyses in extremely thermoacidophilic archaea. *Curr. Opin. Biotechnol.* 19, 445–453. doi:10.1016/j.copbio.2008.08.001

Auernik, K. S., Maezato, Y., Blum, P. H., and Kelly, R. M. (2008b). The genome sequence of the metal-mobilizing, extremely thermoacidophilic archaeon *Metallosphaera sedula* provides insights into bioleaching-associated metabolism. *Appl. Environ. Microbiol.* 74, 682–692. doi:10.1128/aem.02019-07

Barkay, T., Kritee, K., Boyd, E., and Geesey, G. (2010). A thermophilic bacterial origin and subsequent constraints by redox, light and salinity on the evolution of the microbial mercuric reductase. *Environ. Microbiol.* 12, 2904–2917. doi:10.1111/j.1462-2920.2010.02260.x

Barkay, T., Miller, S. M., and Summers, A. O. (2003). Bacterial mercury resistance from atoms to ecosystems. *FEMS Microbiol. Rev.* 27, 355–384. doi:10.1016/S0168-6445(03)00046-9

Batten, K. M., and Scow, K. M. (2003). Sediment microbial community composition and methylmercury pollution at four mercury mine-impacted sites. *Microb. Ecol.* 46, 429–441. doi:10.1007/s00248-003-1005-z

Boyd, E. S., and Barkay, T. (2012). The mercury resistance operon: from an origin in a geothermal environment to an efficient detoxification machine. *Front. Microbiol.* 3:349. doi:10.3389/fmicb.2012.00349

Boyd, E. S., King, S., Tomberlin, J. K., Nordstrom, D. K., Krabbenhoft, D. P., Barkay, T., et al. (2009). Methylmercury enters an aquatic food web through acidophilic microbial mats in Yellowstone National Park, Wyoming. *Environ. Microbiol.* 11, 950–959. doi:10.1111/j.1462-2920.2008.01820.x

Chen, V. B., Arendall, W. B. III, Headd, J. J., Keedy, D. A., Immormino, R. M., Kapral, G. J., et al. (2010). MolProbity: all-atom structure validation for macromolecular crystallography. *Acta Crystallogr. D Biol. Crystallogr.* 66, 12–21. doi:10.1107/S0907444909042073

Cowtan, K., Emsley, P., and Wilson, K. S. (2011). From crystal to structure with CCP4. *Acta Crystallogr. D Biol. Crystallogr.* 67, 233–234. doi:10.1107/S0907444911007578

Delano, W. L. (2002). *The PyMOL Molecular Graphics System*. San Carlos, CA: PyMol. Available at: http://www.pymol.org

Emsley, P., Lohkamp, B., Scott, W. G., and Cowtan, K. (2010). Features and development of Coot. *Acta Crystallogr. D Biol. Crystallogr.* 66, 486–501. doi:10.1107/S0907444910007493

Fox, B., and Walsh, C. T. (1982). Mercuric reductase. Purification and characterization of a transposon-encoded flavoprotein containing an oxidation-reduction-active disulfide. *J. Biol. Chem.* 257, 2498–2503.

Gasteiger, E., Hoogland, C., Gattiker, A., Duvaud, S. E., Wilkins, M., Appel, R., et al. (2005). "Protein identification and analysis tools on the ExPASy server," in *The Proteomics Protocols Handbook*, ed. J. Walker (Totowa, NJ: Humana Press), 571–607.

Gertrud, H., Carola, S., Agata, G., and Karl, O. S. (1989). *Metallosphaera sedula* gen, and sp. nov. Represents a new genus of aerobic, metal-mobilizing, thermoacidophilic archaebacteria. *Syst. Appl. Microbiol.* 12, 38–47. doi:10.1016/S0723-2020

Ghosh, S., Sadhukhan, P. C., Chaudhuri, J., Ghosh, D. K., and Mandal, A. (1999). Purification and properties of mercuric reductase from *Azotobacter chroococcum*. *J. Appl. Microbiol.* 86, 7–12. doi:10.1046/j.1365-2672.1999.00605.x

Guindon, S., Dufayard, J.-F., Lefort, V., Anisimova, M., Hordijk, W., and Gascuel, O. (2010). New algorithms and methods to estimate maximum-likelihood phylogenies: assessing the performance of PhyML 3.0. *Syst. Biol.* 59, 307–321. doi:10.1093/sysbio/syq010

Han, S. B., Zhu, M., Yuan, Z. B., and Li, X. (2001). A methylene blue-mediated enzyme electrode for the determination of trace mercury(II), mercury(I),

methylmercury, and mercury-glutathione complex. *Biosens. Bioelectron.* 16, 9–16. doi:10.1016/s0956-5663(00)00114-7

Huber, R., Huber, H., and Stetter, K. O. (2000). Towards the ecology of hyperthermophiles: biotopes, new isolation strategies and novel metabolic properties. *FEMS Microbiol. Rev.* 24, 615–623. doi:10.1111/j.1574-6976.2000.tb00562.x

Ikai, A. (1980). Thermostability and aliphatic index of globular proteins. *J. Biochem.* 88, 1895–1898.

King, S. A., Behnke, S., Slack, K., Krabbenhoft, D. P., Nordstrom, D. K., Burr, M. D., et al. (2006). Mercury in water and biomass of microbial communities in hot springs of Yellowstone National Park, USA. *Appl. Geochem.* 21, 1868–1879. doi:10.1016/j.apgeochem.2006.08.004

Larkin, M. A., Blackshields, G., Brown, N. P., Chenna, R., McGettigan, P. A., McWilliam, H., et al. (2007). Clustal W and Clustal X version 2.0. *Bioinformatics* 23, 2947–2948. doi:10.1093/bioinformatics/btm404

Ledwidge, R., Patel, B., Dong, A., Fiedler, D., Falkowski, M., Zelikova, J., et al. (2005). NmerA, the metal binding domain of mercuric ion reductase, removes Hg2+ from proteins, delivers it to the catalytic core, and protects cells under glutathione-depleted conditions†,‡. *Biochemistry* 44, 11402–11416. doi:10.1021/bi050519d

Lian, P., Guo, H.-B., Riccardi, D., Dong, A., Parks, J. M., Xu, Q., et al. (2014). X-ray structure of a Hg2+ complex of mercuric reductase (MerA) and quantum mechanical/molecular mechanical study of Hg2+ Transfer between the c-terminal and buried catalytic site cysteine pairs. *Biochemistry* 53, 7211–7222. doi:10.1021/bi500608u

McWilliam, H., Li, W., Uludag, M., Squizzato, S., Park, Y. M., Buso, N., et al. (2013). Analysis tool web services from the EMBL-EBI. *Nucleic Acids Res.* 41, W597–W600. doi:10.1093/nar/gkt376

Misra, T. K., Brown, N. L., Haberstroh, L., Schmidt, A., Goddette, D., and Silver, S. (1985). Mercuric reductase structural genes from plasmid R100 and transposon Tn501: functional domains of the enzyme. *Gene* 34, 253–262. doi:10.1016/0378-1119(85)90134-9

Murshudov, G. N., Vagin, A. A., and Dodson, E. J. (1997). Refinement of macromolecular structures by the maximum-likelihood method. *Acta Crystallogr. D Biol. Crystallogr.* 53, 240–255. doi:10.1107/S0907444996012255

Nakahara, H., Schottel, J. L., Yamada, T., Miyakawa, Y., Asakawa, M., Harville, J., et al. (1985). Mercuric reductase enzymes from *Streptomyces* species and group B Streptococcus. *J. Gen. Microbiol.* 131, 1053–1059.

Nascimento, A. M., and Chartone-Souza, E. (2003). Operon mer: bacterial resistance to mercury and potential for bioremediation of contaminated environments. *Genet. Mol. Res.* 2, 92–101.

Nies, D. H. (2003). Efflux-mediated heavy metal resistance in prokaryotes. *FEMS Microbiol. Rev.* 27, 313–339. doi:10.1016/S0168-6445(03)00048-2

Otwinowski, Z., and Minor, W. (1997). Processing of X-ray diffraction data collected in oscillation mode. *Macromol. Crystallogr. A* 276, 307–326. doi:10.1016/s0076-6879(97)76066-x

Pettersen, E. F., Goddard, T. D., Huang, C. C., Couch, G. S., Greenblatt, D. M., Meng, E. C., et al. (2004). UCSF Chimera – a visualization system for exploratory research and analysis. *J. Comput. Chem.* 25, 1605–1612. doi:10.1002/jcc.20084

Rennex, D., Pickett, M., and Bradley, M. (1994). In vivo and in vitro effects of mutagenesis of active site tyrosine residues of mercuric reductase. *FEBS Lett.* 355, 220–222. doi:10.1016/0014-5793(94)01180-X

Sayed, A., Ghazy, M. A., Ferreira, A. J. S., Setubal, J. C., Chambergo, F. S., Ouf, A., et al. (2013). A novel mercuric reductase from the unique deep brine environment of Atlantis II in the Red Sea. *J. Biol. Chem.* 289, 1675–1687. doi:10.1074/jbc.M113.493429

Schelert, J., Dixit, V., Hoang, V., Simbahan, J., Drozda, M., and Blum, P. (2004). Occurrence and characterization of mercury resistance in the hyperthermophilic archaeon *Sulfolobus solfataricus* by use of gene disruption. *J. Bacteriol.* 186, 427–437. doi:10.1128/JB.186.2.427-437.2004

Schelert, J., Rudrappa, D., Johnson, T., and Blum, P. (2013). Role of MerH in mercury resistance in the archaeon *Sulfolobus solfataricus*. *Microbiology* 159, 1198–1208. doi:10.1099/mic.0.065854-0

Schiering, N., Kabsch, W., Moore, M. J., Distefano, M. D., Walsh, C. T., and Pai, E. F. (1991). Structure of the detoxification catalyst mercuric ion reductase from *Bacillus* sp. strain RC607. *Nature* 352, 168–172. doi:10.1038/352168a0

Schottel, J. L. (1978). The mercuric and organomercurial detoxifying enzymes from a plasmid-bearing strain of *Escherichia coli*. *J. Biol. Chem.* 253, 4341–4349.

Simbahan, J., Kurth, E., Schelert, J., Dillman, A., Moriyama, E., Jovanovich, S., et al. (2005). Community analysis of a mercury hot spring supports occurrence of domain-specific forms of mercuric reductase. *Appl. Environ. Microbiol.* 71, 8836–8845. doi:10.1128/aem.71.12.8836-8845.2005

Szilágyi, A., and Závodszky, P. (2000). Structural differences between mesophilic, moderately thermophilic and extremely thermophilic protein subunits: results of a comprehensive survey. *Structure* 8, 493–504. doi:10.1016/S0969-2126(00)00133-7

Tamura, K., Stecher, G., Peterson, D., Filipski, A., and Kumar, S. (2013). MEGA6: molecular evolutionary genetics analysis version 6.0. *Mol. Biol. Evol.* 30, 2725–2729. doi:10.1093/molbev/mst197

Vetriani, C., Chew, Y. S., Miller, S. M., Yagi, J., Coombs, J., Lutz, R. A., et al. (2005). Mercury adaptation among bacteria from a deep-sea hydrothermal vent. *Appl. Environ. Microbiol.* 71, 220–226. doi:10.1128/aem.71.1.220-226.2005

Wang, Y. P., Boyd, E., Crane, S., Lu-Irving, P., Krabbenhoft, D., King, S., et al. (2011). Environmental conditions constrain the distribution and diversity of archaeal merA in Yellowstone National Park, Wyoming, U.S.A. *Microb. Ecol.* 62, 739–752. doi:10.1007/s00248-011-9890-z

Willard, L., Ranjan, A., Zhang, H., Monzavi, H., Boyko, R. F., Sykes, B. D., et al. (2003). VADAR: a web server for quantitative evaluation of protein structure quality. *Nucleic Acids Res.* 31, 3316–3319. doi:10.1093/nar/gkg565

Zeroual, Y., Moutaouakkil, A., Dzairi, F. Z., Talbi, M., Chung, P. U., Lee, K., et al. (2003). Purification and characterization of cytosolic mercuric reductase from *Klebsiella pneumoniae*. *Ann. Microbiol.* 53, 149–160.

Zhang, Z., Tang, A., Liao, S., Chen, P., Wu, Z., Shen, G., et al. (2011). Oligonucleotide probes applied for sensitive enzyme-amplified electrochemical assay of mercury(II) ions. *Biosens. Bioelectron.* 26, 3320–3324. doi:10.1016/j.bios.2011.01.006

Conflict of Interest Statement: The authors declare that the research was conducted in the absence of any commercial or financial relationships that could be construed as a potential conflict of interest.

frontiers in Bioengineering and Biotechnology

ORIGINAL RESEARCH
published: 16 June 2015
doi: 10.3389/fbioe.2015.00084

Highly thermostable xylanase production from a thermophilic *Geobacillus* sp. strain WSUCF1 utilizing lignocellulosic biomass

*Aditya Bhalla[1†], Kenneth M. Bischoff[2] and Rajesh Kumar Sani[1]**

[1] *Department of Chemical and Biological Engineering, South Dakota School of Mines and Technology, Rapid City, SD, USA,* [2] *Renewable Product Technology Research Unit, Agricultural Research Service, National Center for Agricultural Utilization Research, U.S. Department of Agriculture, Peoria, IL, USA*

OPEN ACCESS

Edited by:
Felipe Andres Sarmiento, Swissaustral USA LLC, USA

Reviewed by:
Hailan Piao, Washington State University Tri-Cities, USA
Noha M. Mesbah, Suez Canal University, Egypt

***Correspondence:**
Rajesh Kumar Sani, 501 East St. Joseph Street, Rapid City, SD, USA
rajesh.sani@sdsmt.edu

†Present Address:
Aditya Bhalla, DOE Great Lakes Bioenergy Research Center, Michigan State University, Lansing, MI, USA

Specialty section:
This article was submitted to Process and Industrial Biotechnology, a section of the journal Frontiers in Bioengineering and Biotechnology

Received: *31 March 2015*
Accepted: *22 May 2015*
Published: *16 June 2015*

Citation:
Bhalla A, Bischoff KM and Sani RK (2015) Highly thermostable xylanase production from a thermophilic Geobacillus sp. strain WSUCF1 utilizing lignocellulosic biomass. Front. Bioeng. Biotechnol. 3:84. doi: 10.3389/fbioe.2015.00084

Efficient enzymatic hydrolysis of lignocellulose to fermentable sugars requires a complete repertoire of biomass deconstruction enzymes. Hemicellulases play an important role in hydrolyzing hemicellulose component of lignocellulose to xylooligosaccharides and xylose. Thermostable xylanases have been a focus of attention as industrially important enzymes due to their long shelf life at high temperatures. *Geobacillus* sp. strain WSUCF1 produced thermostable xylanase activity (crude xylanase cocktail) when grown on xylan or various inexpensive untreated and pretreated lignocellulosic biomasses such as prairie cord grass and corn stover. The optimum pH and temperature for the crude xylanase cocktail were 6.5 and 70°C, respectively. The WSUCF1 crude xylanase was found to be highly thermostable with half-lives of 18 and 12 days at 60 and 70°C, respectively. At 70°C, rates of xylan hydrolysis were also found to be better with the WSUCF1 secretome than those with commercial enzymes, i.e., for WSUCF1 crude xylanase, Cellic-HTec2, and AccelleraseXY, the percent xylan conversions were 68.9, 49.4, and 28.92, respectively. To the best of our knowledge, WSUCF1 crude xylanase cocktail is among the most thermostable xylanases produced by thermophilic *Geobacillus* spp. and other thermophilic microbes (optimum growth temperature ≤70°C). High thermostability, activity over wide range of temperatures, and better xylan hydrolysis than commercial enzymes make WSUCF1 crude xylanase suitable for thermophilic lignocellulose bioconversion processes.

Keywords: biofuels, corn stover, xylanase, prairie cord grass, thermostable, untreated lignocellulose

Introduction

Lignocellulosic agricultural and forestry waste materials are the key substrates for second generation biofuels. Lignocellulose contains 20–40% of hemicellulose, which is a branched heteropolymer consisting of pentose (D-xylose and D-arabinose) and hexose (D-mannose, D-glucose, and D-galactose) sugars with xylose being most abundant (Cano and Palet, 2007; Kumar et al., 2008). Hemicelluloses are classified according to the main sugar in the backbone of the polymer, e.g., xylan (β-1,4-linked xylose) or mannan (β-1,4-linked mannose) (Jørgensen et al., 2007). To obtain these linked sugars, there is a need to effectively break the locked polysaccharides from recalcitrant lignocellulose. There have been various reports published on deconstruction of hemicellulose utilizing hemicellulases (Gao et al.,

2011). Among hemicellulases, endoxylanases and β-xylosidases are reported to be the main components responsible for effective conversion of xylan fraction of biomass to monomeric xylose (Qing and Wyman, 2011; Bhalla et al., 2014a,b).

Thermophiles have often been proposed as a potential source of industrially relevant thermostable enzymes (Turner et al., 2007; Viikari et al., 2007). For example, thermophilic microbes of various genera, including *Bacillus*, *Geobacillus*, *Acidothermus*, *Cellulomonas*, *Paenibacillus*, *Thermoanaerobacterium*, *Actinomadura*, *Alicyclobacillus*, *Anoxybacillus*, *Nesterenkonia*, and *Enterobacter* have been reported to produce thermostable xylanases (Bhalla et al., 2013). Thermostable enzymes have an obvious advantage as catalysts in the lignocellulose conversion processes due to better enzyme accessibility and cell-wall disorganization achieved at high-temperature reaction conditions (Paes and O'Donohue, 2006). Also, high temperature allows better solubility of reactants and products by lowering the viscosities, leading to faster hydrolysis (Viikari et al., 2007). Longer active life under high temperature conditions would make these enzymes favorable for enhanced and efficient biomass conversion. Therefore, to be an effective enzyme, thermostability is the most important attribute for the enzyme utilized under extreme bioprocessing conditions. The present work describes the characterization of highly thermostable endoxylanases (simply referred to as crude xylanase cocktail) produced by *Geobacillus* sp. strain WSUCF1. Hydrolytic activity of WSUCF1 crude xylanase cocktail was studied, and compared to commercially available enzyme cocktails.

Materials and Methods

Microorganism, Medium, and Inoculums

The WSUCF1 strain was identified as *Geobacillus* sp. and affiliated to phylum *Firmicutes* by 16S rDNA analysis (Rastogi et al., 2010). The WSUCF1 strain was grown at 60°C and pH 7.0 in a minimal medium supplemented with xylan (0.2%) or lignocellulosic substrates (1%) as carbon and energy source. The composition of the medium per liter: 0.1 g nitrilotriacetic acid, 0.05 g $CaCl_2 \cdot 2H_2O$, 0.1 g $MgSO_4 \cdot 7H_2O$, 0.01 g NaCl, 0.01 g KCl, 0.3 g NH_4Cl, 0.005 g methionine, 0.2 g yeast extract, 0.01 g casamino acid, 1.8 g of 85% H_3PO_4, 1 ml $FeCl_3$ solution (0.03%), and 1 ml of Nitsch's trace solution (Rastogi et al., 2009). Five percent of pre-culture grown was used to inoculate 100 ml of minimal medium containing carbon source in 500 ml Erlenmeyer flasks. The flasks were incubated in a shaker incubator at 60°C, 150 rpm for 96 h. Control flasks contained only carbon source without WSUCF1 cells, for each experiment. After every 12 h, 1 ml samples were removed aseptically, and analyzed. Growth was checked by measuring absorbance at 600 nm. Immediately after collection, the samples were centrifuged at 4°C and 10,000 × *g* for 10 min. Supernatant was analyzed for the endoxylanase activity as described below.

Enzyme Assay

The reaction mixtures contained 0.5 ml of 1% (w/v) Birchwood xylan (Sigma-Aldrich) in phosphate buffer (100 mM, pH 6.5) and 0.5 ml of an appropriate dilution of enzyme. The enzyme–substrate reaction was carried out at 70°C for 10 min and reaction was stopped by the addition of 1.5 ml 3,5-dinitrosalicylic acid (DNSA) solution, boiled for 10 min, and then cooled on ice for color stabilization. The optical absorbance was measured at 540 nm and the amounts of liberated reducing sugars (xylose equivalents) were estimated against a xylose standard curve.

Parametric Optimization for Xylanase Cocktail Production

Physical parameters for crude xylanase cocktail activity production were optimized by maintaining all factors constant except the one being studied. Effect of pH on enzyme production was assessed by cultivating the WSUCF1 strain in non-buffered growth media of pH 5.0–9.0, at 60°C for 96 h. The pH of the medium was adjusted using 5M NaOH or 6N HCl. The effect of temperature was studied by growing the microbe at different temperatures (50–80°C), pH 7.0 for 96 h. Effect of various easily available inexpensive carbon and energy sources including untreated prairie cord grass (PCG) 1%, untreated corn stover (CS) 1%, thermo-mechanically pretreated prairie cord grass (PPCG) 1%, or thermo-mechanically pretreated corn stover (PCS) 1% was studied for crude xylanase activity. Growth conditions for the WSUCF1 utilizing these substrates are described above under Section "Microorganism, Medium, and Inoculums." Thermo-mechanical pretreatment of the CS and PCG was carried out in a single-screw extruder as described earlier (Kannadhason et al., 2009).

Characterization of the Crude Xylanases

Sodium dodecyl sulfate-polyacrylamide gel electrophoresis (SDS-PAGE) was performed as described by Laemmli (1970). Ten milliliters of supernatant from each growth flask containing different substrates (xylan, CS, PCS, PCS, and PPCG as substrate) were passed through Amicon Ultra-15 – Millipore (3 kDa cut-off) to 10× concentrate the protein. To obtain zymogram of crude endoxylanase and β-xylosidase activity following SDS-PAGE, samples (10 µl of concentrated protein) were mixed with 10 µl 2× SDS sample buffer, and heated to 95°C for 1 min prior to loading on gel. For endoxylanase, sample was loaded onto a 12% SDS-PAGE gel containing 0.1% (w/v) oat spelt xylan (OSX) polymerized within the gel matrix whereas for β-xylosidase, gel was separately incubated with the substrate for 30 min, i.e., 0.1 mg/ml 4-methylumbelliferyl-β-d-xylopyranoside in phosphate buffered saline, pH 5.9. Current (150 V constant voltage) was passed through the gel until the bromophenol blue dye-front migrated to the bottom of the gel. The gel was washed successively with the following for 30 min each: 20% isopropanol in phosphate buffer saline (PBS, 100 mM, pH 5.9), 8M urea in PBS, and PBS (pH 5.9) three times. For endoxylanase, the gel was incubated in PBS (pH 5.9) overnight at 37°C. The gel was stained with Congo Red (1 mg/ml) for 30 min, and de-stained with 1M NaCl in PBS until clear bands indicating xylanase activity were visible. For the detection of β-xylosidase activity, gel was examined for fluorescence on a UV light box indicating β-xylosidase activity.

The relative xylanase activity using 1% (w/v) Birchwood xylan was determined at various pHs. The pH optimum of crude xylanase was estimated by carrying out the reactions in the pH range of

3.0–10.0 using different assay buffers, citrate buffer (50 mM, pH 3–6), phosphate buffer (50 mM, pH 6–7.5), Tris-HCl (50 mM, pH 7.5–9), and glycine–NaOH buffer (50 mM, pH 8.6–10) at 70°C for 20 min. The enzyme activity obtained at the pH optimum was used to calculate the relative enzyme activity at other pHs. The optimum pH of 6.5 was used to determine the optimum temperature for the crude xylanase. The optimal temperature for crude xylanase was obtained by performing the enzyme assays at different temperatures. The experiments were carried out in the temperature range of 40–90°C under assay conditions as described above.

Thermostability of xylanases was assessed by incubating the enzyme at different temperatures 50–100°C with increments of 10°C for a period of 19 days. Subsamples were removed at definite time intervals over the period of incubation. The residual activities were determined under optimum pH and temperature conditions using the DNSA method as described above. In all cases, the initial activity was assumed to be 100% and used to calculate the enzyme activities as percentages of the initial activity during the incubation period.

Hydrolysis of Birchwood Xylan

The hydrolysis of Birchwood xylan was carried out in 100 ml conical flask containing 50 ml sodium phosphate buffer (50 mM, pH 6.5), 1 g xylan, 0.03% (w/v) sodium azide, and 20 U xylanase/g xylan. The hydrolysis was performed for 48 h at different temperatures (50, 60, and 70°C) with a rotating speed of 150 rpm. Hydrolysis of xylan was also compared using commercial enzyme mix, Cellic HTec2 (Novozymes) and Accellerase XY (Genencor). Optimum pH of 5.0 was used for commercial enzymes to compare their hydrolytic potential at different temperatures. The amount of reducing sugar was measured by using DNS method as described above.

Results and Discussions

Thermophilic bacteria are excellent source of thermostable xylanases, which have the potential to be utilized in lignocellulose hydrolysis (Bhalla et al., 2013, 2014a,b). Thermostable xylanases, optimally active at high temperatures and wide range of pHs are useful under harsh industrial processing conditions (Turner et al., 2007). The production of total extracellular proteins and enzymes when WSUCF1 was grown on xylan is shown in Figure S1A in Supplementary Material. In general, the increase in enzyme activity is associated with an increase in total extracellular protein. The WSUCF1 strain produced maximum crude xylanase activity (14.6 U/ml) on day 4 when the culture had nearly reached to plateau phase. Further increase in the extracellular crude xylanase activity as well as total protein even after cessation of growth could be due to lysis of cells, which led to outflow of proteins into growth medium. Figure S1B in Supplementary Material suggests that maximum growth of WSUCF1 was achieved in ~60 h. Data on crude xylanase activities from WSUCF1 were generated from culture supernatants and under unoptimized medium conditions; therefore, further experiments were performed to optimize the xylanase activity.

Effects of Growth Medium pH and Temperature on Crude Xylanase Activity

Effect of growth medium pH is shown in **Figure 1A**. The pHs 6.0 and 7.0 adequately supported the xylanase activity with maximum at pH 7.0. It declined sharply when the pH was either decreased or increased around the optima. At pH 6.0, relative xylanase activity was 83% and it decreased to 30% at pH 8.0 whereas pH 5.0 and 9.0 did not support the production. It has been shown that growth medium pH strongly influences many enzymatic reactions by affecting the transport of a number of chemical products and enzymes across the cell membrane (Liang et al., 2010). Our results also confirmed that growth medium pH was an important factor affecting the crude xylanase activity in WSUCF1. Optimum xylanase activity near neutrality has been reported earlier for *Bacillus* sp. (Sapre et al., 2005), *Bacillus* SPS-0 (Bataillon et al., 2000), and *Bacillus thermoleovorans* strain K-3d (Sunna et al., 1997).

Growth medium temperature also impacted the production of xylanase activity (**Figure 1B**). WSUCF1 strain showed maximum amount of xylanase activity at 60°C and the activity decreased drastically when temperature was decreased below 55°C and increased above 65°C. Most of the known xylanase producing microbes have optimum growth pH between 5.5 and 9.5 (Kulkarni et al., 1999). Optimum growth temperature of 60°C has been reported for *Bacillus* SPS-0 (Bataillon et al., 2000) and *Bacillus stearothermophilus* (Khasin et al., 1993). *Bacillus thermantarcticus* (Lama et al., 2004) and *Bacillus* sp. JB 99 (Shrinivas et al., 2010) grew optimally at 65 and 55°C, respectively. Higher growth temperatures are industrially desirable because temperatures above 50°C could lead to significantly reduced risks of mesophilic microbial contamination (Yeoman et al., 2010).

Effects of Different Lignocellulosic Materials on Crude Xylanase Activity Production

The use of inexpensive agriculture residues as substrates for the production of industrial enzymes is a significant way to reduce cost of the overall process. WSUCF1 utilized a variety of inexpensive pretreated as well as untreated cellulosic substrates such as PCG, CS, PPCG, and PCS (**Figure 2**). Interestingly, in addition to xylan, all lignocellulosic substrates supported for xylanase activity. The crude xylanase activity was maximum (23.8 U/ml, 100%) for Birchwood xylan, followed by untreated CS (88%), untreated prairie cordgrass (84%), PPCG (76%), and PCS (72%). CS contributes roughly up to 80% of all agricultural residues produced in USA therefore considered as a feedstock of choice for various applications, including lignocellulosic ethanol production (Kadam and McMillan, 2003; Zhu et al., 2006; Balan et al., 2009). Kim and Dale (2004) have reported an estimated ethanol production from CS, i.e., 38.4 billion liters of ethanol per year. On the other hand, perennial grasses like prairie cordgrass is also considered as one of the most abundant biomass feedstocks in the Great Plains (Gonzalez-Hernandez et al., 2009; Rastogi et al., 2010; Zambare et al., 2011). Brito-Cunha et al. (2013) reported high xylanases production utilizing sugarcane bagasse and wheat bran as substrates from *Streptomyces* sp. Thermophilic xylanolytic *Thermoanaerobacter* strains have also been reported to produce xylanases with poplar, spruce, miscanthus, wheat

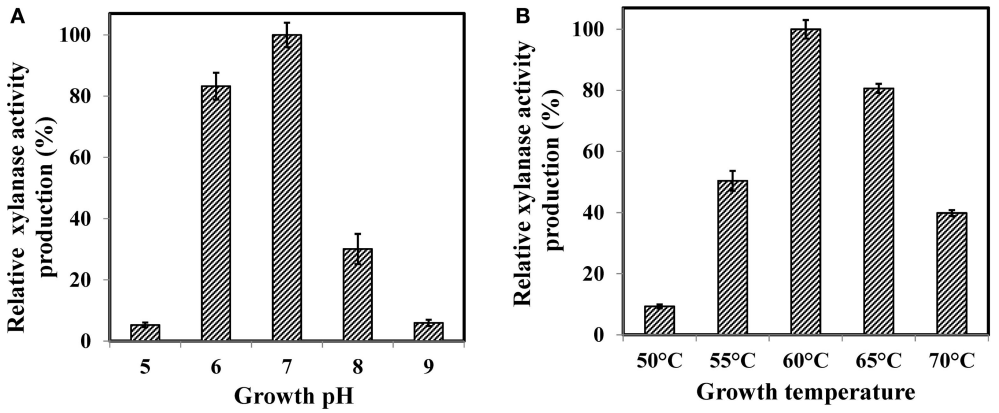

FIGURE 1 | Effect of (A) growth pH and (B) growth temperature on production of WSUCF1 xylanase. Enzyme production at optimum pH and optimum temperature was defined as 100% (19.3 and 18.7 U/ml, respectively). Values shown were the mean of duplicate experiments, and the variation about the mean was below 5%.

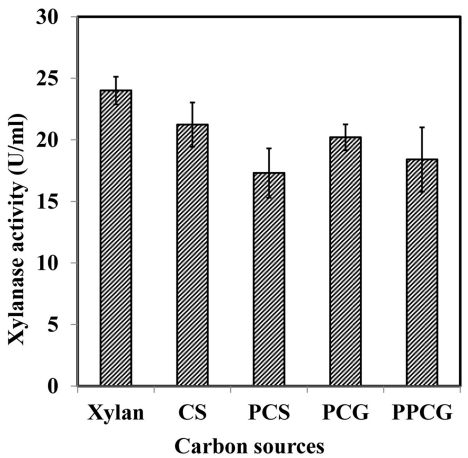

FIGURE 2 | Effects of xylan and various inexpensive lignocellulosics (prairie cordgrass – PCG, corn stover – CS, pretreated prairie cordgrass – PPCG, and pretreated corn stover – PCS) on xylanase production by WSUCF1.

straw, whole corn plants, corn cobs, corn stalks, sugarcane bagasse, sweet sorghum, or cotton stalks (Svetlitchnyi et al., 2013).

Literature shows that several microbial species have been reported to use lignocellulosics for xylanase production; however, there are not many reports on utilization of prairie cordgrass and CS as substrates. To reduce the cost of the enzymes needed for the hydrolysis, in-house production of xylanases on various substrates is beneficial. Producing thermostable lignocellulose deconstruction enzymes (crude xylanases) using untreated lignocellulosic biomasses (PCG and PCS) further shows the industrial potential of the WSUCF1 strain. The use of untreated lignocellulosic waste biomasses as substrates for the production of lignocellulolytic enzymes would have both economic and environmental advantages.

Characterization of Thermostable Crude Xylanase Cocktail

Crude xylanases were expressed at high levels in the production medium containing different carbon sources. A SDS zymogram analysis was performed to observe the expression of different xylanases in the crude extract obtained from the growth medium. **Figure 3A** demonstrates the activity bands for endoxylanase activity on OSX as substrate whereas **Figure 3B** shows β-xylosidase activity on 4-methylumbelliferyl-β-d-xylopyranoside (MUX) as a specific substrate.

On analyzing the activity bands obtained for endoxylanase activity (**Figure 3A**), five prominent activity bands were observed at 60, 45, 38, 34, and 17 kDa for the secretome obtained from growth on untreated CS whereas only two activity bands were obtained for PCS secretome, i.e., 34, and 17 kDa. Same trend was noticed for PCG where four activity bands were observed for untreated PCG (45, 38, 34, and 17 kDa) and two activity bands (34 and 17 kDa) for PPCG. On observing the activity bands for Birchwood xylan secretome, a high-density activity band smear was observed between 37 and 20 kDa. The observed trend very well explains the difference in expression of enzymes by a microbe when grown on differently treated complex substrates. On evaluating the activity bands obtained for β-xylosidase activity (**Figure 3B**), two bands were observed at 240 and 90 kDa for the secretomes obtained from growth on lignocellulosic substrates, whereas interestingly, one different band of 160 kDa along with 90 kDa band was observed for the secretome obtained from growth on pure substrate, i.e., Birchwood xylan. These results demonstrate the importance of variations in the enzyme expression by the same bacterium on different substrates.

Another hypothesis was tested to correlate the enzyme expression observed from zymography experiment with the data obtained on crude xylanase activity (**Figure 2**). Results showed that higher enzyme units obtained on untreated CS and PCG were positively correlated to the number of active enzymes from untreated CS and PCG zymograms, whereas for pretreated material, lesser enzyme activity was correlated with less enzyme expression.

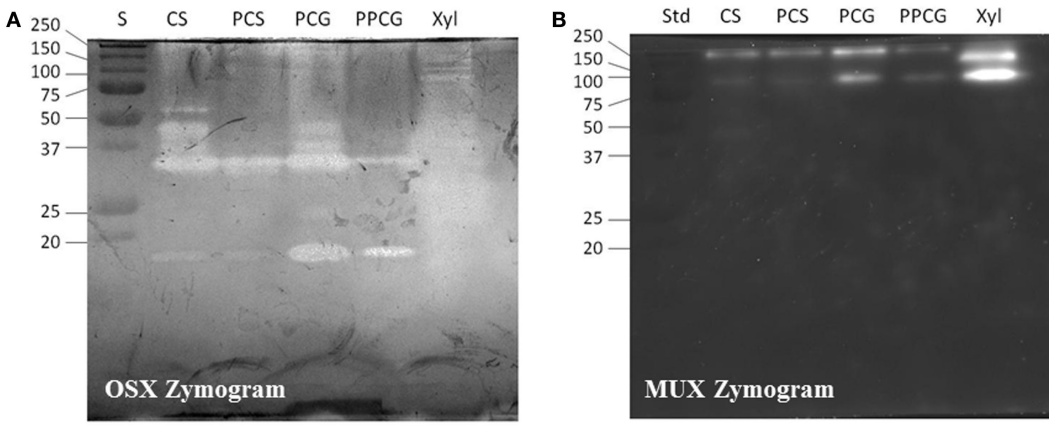

Sample	Masses (kDa) of xylanase
CS	60, 45, 38, 34, 17
PCS	34, 17
PCG	45, 38, 34, 17
PPCG	34, 17
Xyl	High density between 37-20

Sample	Masses (kDa) of xylosidase
CS	240, 90
PCS	240, 90
PCG	240, 90
PPCG	240, 90
Xyl	160, 90

FIGURE 3 | SDS-PAGE (12%) and zymogram of WSUCF1 (A) endoxylanase activity, (B) β-xylosidase activity. Lane S, precision plus protein standards (BioRad); Lane CS, corn stover; Lane PCS, pretreated corn stover; Lane PCG, prairie cord grass; Lane PPCG; pretreated prairie cord grass.

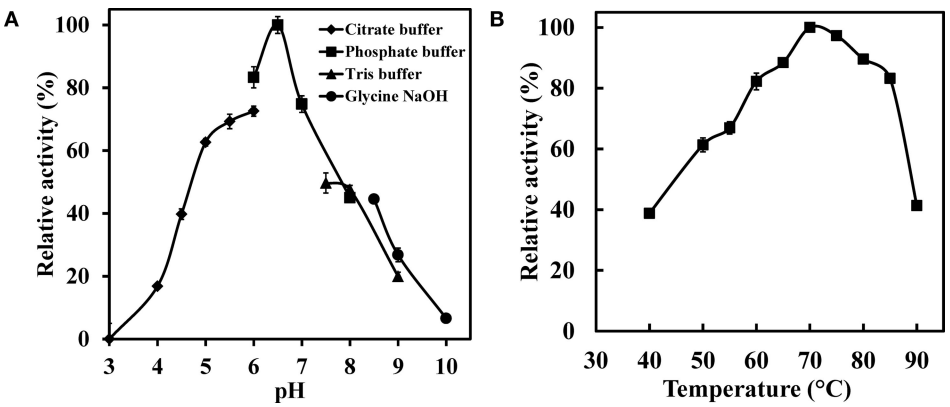

FIGURE 4 | Impact of (A) pH and (B) temperature on the xylanase activity of WSUCF1 isolate. The enzyme activity was expressed as percentages of the maximum activity. The points are the averages of triplicates, and error bars indicate ±SDs of the means (n = 3). Error bars smaller than the symbols are not shown.

To further characterize the enzyme, effect of the pH on the WSUCF1 crude xylanase activity was examined from pH 3.0 to 10.0 (**Figure 4A**). WSUCF1 produced maximum xylanase activity in sodium phosphate buffer at pH 6.5. WSUCF1 xylanase exhibited activity in broad pH range of 4.5–8.5 with more than 40% relative activity at pH 4.5 and 8.5. At pH range of 5.5–7.0, more than 70% relative activity was retained. Xylanases from *Thermoanaerobacterium saccharolyticum* NTOU1 (Hung et al., 2011), *Clostridium* sp. TCW1 (Lo et al., 2011), *Actinomadura* sp. S14 (Sriyapai et al., 2011), *Bacillus* sp. (Sapre et al., 2005), *Bacillus flavothermus* strain LB3A (Sunna et al., 1997), and *B. stearothermophilus* T-6 (Khasin et al., 1993) also showed their pH optima at 6.0–7.0.

The impact of different temperatures on the xylanase activity is shown in **Figure 4B**. Maximum xylanase activity was observed at 70°C. The xylanase activity increased linearly with increasing the temperature up to 70°C and thereafter it declined; however, at 85°C about 83% of its maximum activity was still retained. At lower temperatures, i.e., at 50 and 60°C, 61 and 82% of maximum xylanase activity was observed, respectively. Xylanases from *Geobacillus thermodenitrificans* TSAA1 (Verma et al., 2013), *Bacillus* sp. JB 99 (Shrinivas et al., 2010), *Bacillus licheniformis*

77-2 (Damiano et al., 2006), and *B. flavothermus* strain LB3A (Sunna et al., 1997) also showed their temperature optimum at 70°C. Results demonstrated that WSUCF1 xylanase activity was resistant to change in temperature and hence it is well suited for the harsh process conditions that lignocellulose bioprocessing entails.

Thermal stability profile of WSUCF1 xylanase activity was also observed (**Figure 5**). Enzyme retained about 70% of its original activity after incubating the enzyme at 50°C for 19 days. At 60 and 70°C, 50% of xylanase activity was retained after incubation for 19 and 12 days, respectively. With further increase in the incubation temperature, decreased enzyme activity was observed. At 80 and 90°C, complete enzyme activity was lost in 150 and 70 min, respectively (data not shown). Xylanase from *G. thermodenitrificans* TSAA1 (Verma et al., 2013) retained >85% activity after exposure to 70°C for only 180 min, xylanase from *Paenibacillus macerans* IIPSP3 exhibited half-life of 6 h at 60°C (Dheeran et al., 2012), *Bacillus subtilis* exhibited half-lives of 16.2, 9.6, and 2.8 h at 60, 70, and 80°C, respectively (Saleem et al., 2012), and *Enterobacter* sp. MTCC 5112 retained 85 and 64% of its activity for 18 h at 60 and 70°C, respectively (Khandeparkar and Bhosle, 2006). These results showed that WSUCF1 xylanase is highly thermostable as compared to the xylanases from other thermophiles. There is considerable interest in enzymes with high thermostability for industrial applications. There had been a number of studies published on enhancing thermal stability using genetic engineering. Stephens et al. (2009) reported the improvement in thermostability of xylanases from *Thermomyces lanuginosus* using error-prone PCR. Jeong et al. (2007) and Zhang et al. (2010) also reported improved thermostability in xylanases using site-directed mutagenesis whereas WSUCF1 is highly thermostable in its native form. Therefore, WSUCF1 xylanase warrants its application in biomass conversion processes, which are carried out at high temperatures.

Studies on Hydrolysis of Birchwood Xylan

Thermostable enzymes that hydrolyze lignocellulose to sugars have significant advantages for improving the conversion rate of biomass over their mesophilic counterparts. The hydrolysis rates for WSUCF1 xylanase were higher at 70°C as compared to 50 and 60°C. **Figure 6** shows the comparison of hydrolytic capability of WSUCF1 xylanase, Cellic HTec2 (optimum temperature 50°C) and Accellerase XY (optimum temperature 50°C). It can be seen from the figure that in opposed to commercial enzymes, with increase in temperature from 50 to 70°C hydrolysis rates of WSUCF1 xylanase were increased. At 70°C, higher conversions were obtained with WSUCF1 xylanase as compared to Cellic HTEc2 and Accellerase XY after 48 h of incubation. Percentage conversions were calculated on the basis of reducing sugars released from 1 g Birchwood xylan. At 70°C, WSUCF1 xylanase yielded higher conversions of 68.9% as compared to Cellic HTec2 (49.4%) and Accellerase XY (28.92%). However, lower conversion rates were obtained with WSUCF1 as compared to Cellic HTec2 and Accellerase XY at 50°C. The main objective of this experiment was to evaluate the potential of WSUCF1 xylanases at 70°C.

He et al. (2009) reported that the recombinant Xyn2 hydrolyzed <20% of Birchwood xylan when it was incubated at 50°C, but the hydrolysis rates linearly increased with the increasing of reaction time. The xylanase from *B. thermantarcticus* hydrolyzed 70% of Birchwood xylan (2% w/v) within 24 h of reaction time at 70°C, but the hydrolysis rates were <40% at 60 and 80°C (Lama et al., 2004). Our xylan hydrolysis results show that WSUCF1 crude xylanase cocktail performed better than Cellic-HTec2 and Accellerase XY at 70°C. These data suggest that xylanase cocktail produced by WSUCF1 strain is highly active and stable at high temperatures, and therefore, can be used as a part of the enzyme cocktail for efficient hemicellulose hydrolysis.

In summary, thermostable xylanases are the key enzymes for lignocellulosic deconstruction. The existing enzymatic hydrolysis

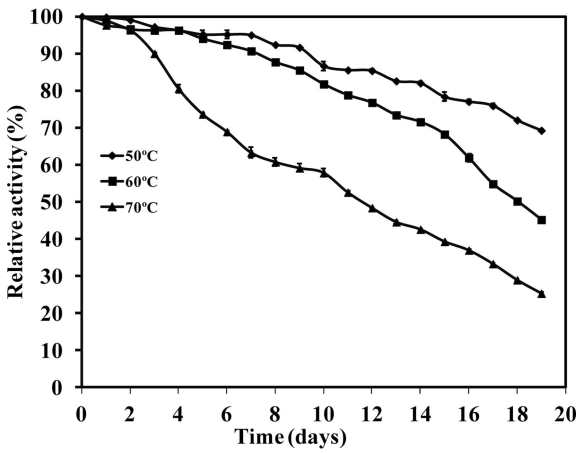

FIGURE 5 | Thermal stability of xylanase activity produced by WSUCF1 isolate. The enzyme activities were expressed as percentages of the initial activity. The points are the averages of triplicates, and error bars indicate ±SDs of the means (n = 3). Error bars smaller than the symbols are not shown.

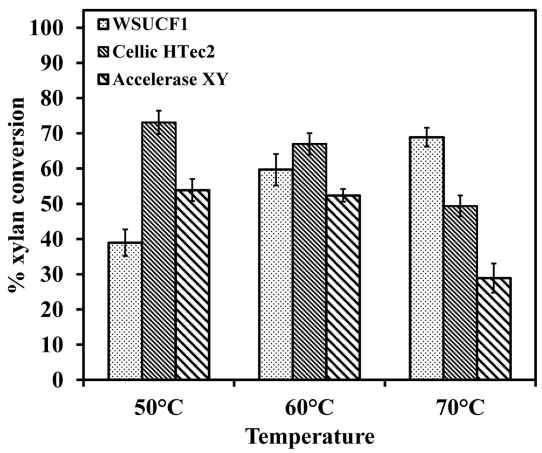

FIGURE 6 | Hydrolysis of Xylan from Birchwood – comparison of hydrolytic activity of WSUCF1 xylanase, Cellic HTec2, and Genencor Accellerase XY. The points are the averages of duplicates, and error bars indicate ±SDs of the means (n = 2). Error bars smaller than the symbols are not shown.

technologies of lignocellulose into sugars, which are carried out at ≤50°C, have several limitations, including very slow enzymatic hydrolysis rates, low yields of sugars from lignocellulose (often incomplete hydrolysis), high dosages of enzymes, and microbial contamination problems. It has repeatedly been suggested that these limitations could be overcome using thermophiles and thermostable enzymes (Viikari et al., 2007; Yeoman et al., 2010; Bhalla et al., 2013, 2014a,b). For instance, Ovissipour et al. (2009) showed that rates of hydrolysis of protein hydrolyzate from Persian Sturgeon (*Acipenser persicus*) using Alcalase^R were increased about three-times with increase in temperature from 35 to 55°C. The fact that the strain WSUCF1 thermophile can utilize untreated lignocellulosic substrates to produce xylanases will likely play a key role in reducing production costs of the enzymes. The low-cost enzymes, if made available to biofuel industries, will enable economic conversion of biomass to biofuels. Removal of the CS, PCG, and other biomass wastes will provide a social benefit of protecting the environment and cleaner surroundings. The local CS and prairie grass producers will benefit from an additional and continued income source.

Conclusions

Geobacillus sp. WSUCF1 produced highly active crude xylanase cocktail when grown on inexpensive renewable untreated feedstocks. The xylanase cocktail was found to be highly stable and active over wide range of pH and temperature. Zymography profiles showed an interesting correlation with the enzyme expression and differently treated or untreated lignocellulosic substrates. Higher xylan conversions were obtained at 70°C when compared with commercial enzymes. WSUCF1 crude xylanase is among the most thermostable xylanases produced by thermophilic *Geobacillus* spp. and other thermophilic microbes (optimum growth temperature ≤70°C). These unique properties make WSUCF1 xylanases suitable for thermophilic lignocellulose bioconversion processes.

Acknowledgments

The authors gratefully acknowledge the financial support provided by National Science Foundation – Industry/University Cooperative Research Center (NSF-I/UCRC, Grant # 441087). The support from the Department of Chemical and Biological Engineering at the South Dakota School of Mines and Technology is gratefully acknowledged.

Supplementary Material

The Supplementary Material for this article can be found online at http://journal.frontiersin.org/article/10.3389/fbioe.2015.00084

References

Balan, V., Bals, B., Chundawat, S. P., Marshall, D., and Dale, B. E. (2009). Lignocellulosic biomass pretreatment using AFEX. *Methods Mol. Biol.* 581, 61–77. doi:10.1007/978-1-60761-214-8_5

Bataillon, M., Cardinali, A. P. N., Castillon, N., and Duchiron, F. (2000). Purification and characterization of a moderately thermostable xylanase from *Bacillus* sp. strain SPS-0. *Enzyme Microb. Technol.* 26, 187–192. doi:10.1016/S0141-0229(99)00143-X

Bhalla, A., Bansal, N., Kumar, S., Bischoff, K. M., and Sani, R. K. (2013). Improved lignocellulose conversion to biofuels with thermophilic bacteria and thermostable enzymes. *Bioresour. Technol.* 128, 751–759. doi:10.1016/j.biortech.2012.10.145

Bhalla, A., Bischoff, K. M., and Sani, R. K. (2014a). Highly thermostable GH39 β-xylosidase from a *Geobacillus* sp. strain WSUCF1. *BMC Biotechnol.* 14:963. doi:10.1186/s12896-014-0106-8

Bhalla, A., Bischoff, K. M., Uppugundla, N., Balan, V., and Sani, R. K. (2014b). Novel thermostable endo-xylanase cloned and expressed from bacterium *Geobacillus* sp. WSUCF1. *Bioresour. Technol.* 165, 314–318. doi:10.1016/j.biortech.2014.03.112

Brito-Cunha, C. C., de Campos, I. T., de Faria, F. P., and Bataus, L. A. (2013). Screening and xylanases production by *Streptomyces* sp. grown on lignocellulosic wastes. *Appl. Biochem. Biotechnol.* 170, 598–608. doi:10.1007/s12010-013-0193-3

Cano, À., and Palet, C. (2007). Xylooligosaccharide recovery from agricultural biomass waste treatment with enzymatic polymeric membranes and characterization of products with MALDI-TOF-MS. *J. Membr. Sci.* 291, 96–105. doi:10.1016/j.memsci.2006.12.048

Damiano, V. B., Ward, R., Gomes, E., Alves-Prado, H. F., and Da Silva, R. (2006). Purification and characterization of two xylanases from alkalophilic and thermophilic *Bacillus licheniformis* 77-2. *Appl. Biochem. Biotechnol.* 12, 289–302. doi:10.1385/ABAB:129:1:289

Dheeran, P., Nandhagopal, N., Kumar, S., Jaiswal, Y. K., and Adhikari, D. K. (2012). A novel thermostable xylanase of *Paenibacillus macerans* IIPSP3 isolated from the termite gut. *J. Ind. Microbiol. Biotechnol.* 39, 851–860. doi:10.1007/s10295-012-1093-1

Gao, D., Uppugundla, N., Chundawat, S. P., Yu, X., Hermanson, S., Gowda, K., et al. (2011). Hemicellulases and auxiliary enzymes for improved conversion of lignocellulosic biomass to monosaccharides. *Biotechnol. Biofuels* 4, 5. doi:10.1186/1754-6834-4-5

Gonzalez-Hernandez, J. L., Sarath, G., Stein, J. M., Owens, V., Gedye, K., and Boe, A. (2009). A multiple species approach to biomass production from native herbaceous perennial feedstocks. *In vitro Cell. Dev. Biol. Plant* 45, 267–281. doi:10.1007/s11627-009-9215-9

He, J., Yu, B., Zhang, K., Ding, X., and Chen, D. (2009). Expression of endo-1, 4-beta-xylanase from *Trichoderma reesei* in *Pichia pastoris* and functional characterization of the produced enzyme. *BMC Biotechnol.* 9:56. doi:10.1186/1472-6750-9-56

Hung, K. S., Liu, S. M., Tzou, W. S., Lin, F. P., Pan, C. L., Fang, T. Y., et al. (2011). Characterization of a novel GH10 thermostable, halophilic xylanase from the marine bacterium *Thermoanaerobacterium saccharolyticum* NTOU1. *Process Biochem.* 46, 1257–1263. doi:10.1016/j.procbio.2011.02.009

Jeong, M. Y., Kim, S., Yun, C. W., Choi, Y. J., and Cho, S. G. (2007). Engineering a de novo internal disulfide bridge to improve the thermal stability of xylanase from *Bacillus stearothermophilus* no. 236. *J. Biotechnol.* 127, 300–309. doi:10.1016/j.jbiotec.2006.07.005

Jørgensen, H., Kristensen, J. B., and Felby, C. (2007). Enzymatic conversion of lignocellulose into fermentable sugars: challenges and opportunities. *Biofuels Bioprod. Biorefin.* 1, 119–134. doi:10.1002/bbb.4

Kadam, K. L., and McMillan, J. D. (2003). Availability of corn stover as a sustainable feedstock for bioethanol production. *Bioresour. Technol.* 88, 17–25. doi:10.1016/S0960-8524(02)00269-9

Kannadhason, S., Muthukumarappan, K., and Rosentrater, K. A. (2009). Effects of ingredients and extrusion parameters on aqua feed containing DDGS and tapioca starch. *J. Aquac. Feed Sci. Nutr.* 1, 6–21.

Khandeparkar, R., and Bhosle, N. B. (2006). Purification and characterization of thermoalkalophilic xylanase isolated from the *Enterobacter* sp. MTCC 5112. *Res. Microbiol.* 157, 315–325. doi:10.1016/j.resmic.2005.12.001

Khasin, A., Alchanati, I., and Shoham, Y. (1993). Purification and characterization of a thermostable xylanase from *Bacillus stearothermophilus* T-6. *Appl. Environ. Microbiol.* 59, 1725–1730.

Kim, S., and Dale, B. E. (2004). Global potential bioethanol production from wasted crops and crop residues. *Biomass Bioenergy* 26, 361–375.

Kulkarni, N., Shendye, A., and Rao, M. (1999). Molecular and biotechnological aspects of xylanases. *FEMS Microbiol. Rev.* 23, 411–456. doi:10.1111/j.1574-6976.1999.tb00407.x

Kumar, R., Singh, S., and Singh, O. (2008). Bioconversion of lignocellulosic biomass: biochemical and molecular perspectives. *J. Ind. Microbiol. Biotechnol.* 35, 374–379. doi:10.1007/s10295-008-0327-8

Laemmli, U. K. (1970). Cleavage of structural proteins during the assembly of the head of bacteriophage T4. *Nature* 227, 680–685. doi:10.1038/227680a0

Lama, L., Calandrelli, V., Gambacorta, A., and Nicolaus, B. (2004). Purification and characterization of thermostable xylanase and beta-xylosidase by the thermophilic bacterium *Bacillus thermantarcticus*. *Res. Microbiol.* 155, 283–289. doi:10.1016/j.resmic.2004.02.001

Liang, Y., Feng, Z., Yesuf, J., and Blackburn, J. W. (2010). Optimization of growth medium and enzyme assay conditions for crude cellulases produced by a novel thermophilic and cellulolytic bacterium, *Anoxybacillus* sp. 527. *Appl. Biochem. Biotechnol.* 160, 1841–1852. doi:10.1007/s12010-009-8677-x

Lo, Y. C., Huang, C. Y., Cheng, C. L., Lin, C. Y., and Chang, J. S. (2011). Characterization of cellulolytic enzymes and bioH2 production from anaerobic thermophilic *Clostridium* sp. TCW1. *Bioresour. Technol.* 102, 8384–8392. doi:10.1016/j.biortech.2011.03.064

Ovissipour, M., Abedian, A., Motamedzadegan, A., Rasco, B., Safari, R., and Shahiri, H. (2009). The effect of enzymatic hydrolysis time and temperature on the properties of protein hydrolysates from Persian sturgeon (*Acipenser persicus*) viscera. *Food Chem.* 115, 238–242. doi:10.1016/j.foodchem.2008.12.013

Paes, G., and O'Donohue, M. J. (2006). Engineering increased thermostability in the thermostable GH-11 xylanase from *Thermobacillus xylanilyticus*. *J. Biotechnol.* 25, 338–350. doi:10.1016/j.jbiotec.2006.03.025

Qing, Q., and Wyman, C. E. (2011). Supplementation with xylanase and β-xylosidase to reduce xylo-oligomer and xylan inhibition of enzymatic hydrolysis of cellulose and pretreated corn stover. *Biotechnol. Biofuels* 4, 18. doi:10.1186/1754-6834-4-18

Rastogi, G., Bhalla, A., Adhikari, A., Bischoff, K. M., Hughes, S. R., Christopher, L. P., et al. (2010). Characterization of thermostable cellulases produced by *Bacillus* and *Geobacillus* strains. *Bioresour. Technol.* 101, 8798–8806. doi:10.1016/j.biortech.2010.06.001

Rastogi, G., Muppidi, G. L., Gurram, R. N., Adhikari, A., Bischoff, K. M., Hughes, S. R., et al. (2009). Isolation and characterization of cellulose-degrading bacteria from the deep subsurface of the Homestake gold mine, Lead, South Dakota, USA. *J. Ind. Microbiol. Biotechnol.* 36, 585–598. doi:10.1007/s10295-009-0528-9

Saleem, M., Aslam, F., Akhtar, M. S., Tariq, M., and Rajoka, M. I. (2012). Characterization of a thermostable and alkaline xylanase from *Bacillus* sp. and its bleaching impact on wheat straw pulp. *World J. Microbiol. Biotechnol.* 28, 513–522. doi:10.1007/s11274-011-0842-z

Sapre, M. P., Jha, H., and Patil, M. B. (2005). Purification and characterization of a thermoalkalophilic xylanase from *Bacillus* sp. *World J. Microbiol. Biotechnol.* 21, 649–654. doi:10.1007/s12010-010-8980-6

Shrinivas, D., Savitha, G., Raviranjan, K., and Naik, G. R. (2010). A highly thermostable alkaline cellulase-free xylanase from thermoalkalophilic *Bacillus* sp. JB 99 suitable for paper and pulp industry: purification and characterization. *Appl. Biochem. Biotechnol.* 162, 2049–2057. doi:10.1007/s12010-010-8980-6

Sriyapai, T., Somyoonsap, P., Matsui, K., Kawai, F., and Chansiri, K. (2011). Cloning of a thermostable xylanase from *Actinomadura* sp. S14 and its expression in *Escherichia coli* and *Pichia pastoris*. *J. Biosci. Bioeng.* 111, 528–536. doi:10.1016/j.jbiosc.2010.12.024

Stephens, D. E., Singh, S., and Permaul, K. (2009). Error-prone PCR of a fungal xylanase for improvement of its alkaline and thermal stability. *FEMS Microbiol. Lett.* 293, 42–47. doi:10.1111/j.1574-6968.2009.01519.x

Sunna, A., Prowe, S. G., Stoffregen, T., and Antranikian, G. (1997). Characterization of the xylanases from the new isolated thermophilic xylan-degrading *Bacillus thermoleovorans* strain K-3d and *Bacillus flavothermus* strain LB3A. *FEMS Microbiol. Lett.* 148, 209–216. doi:10.1111/j.1574-6968.1997.tb10290.x

Svetlitchnyi, V. A., Kensch, O., Falkenhan, D. A., Korseska, S. G., Lippert, N., Prinz, M., et al. (2013). Single-step ethanol production from lignocellulose using novel extremely thermophilic bacteria. *Biotechnol. Biofuels* 6, 31. doi:10.1186/1754-6834-6-31

Turner, P., Mamo, G., and Karlsson, E. N. (2007). Potential and utilization of thermophiles and thermostable enzymes in biorefining. *Microb. Cell Fact.* 6, 9. doi:10.1186/1475-2859-6-9

Verma, D., Anand, A., and Satyanarayana, T. (2013). Thermostable and alkalistable endoxylanase of the extremely thermophilic bacterium *Geobacillus* thermodenitrificans TSAA1: cloning, expression, characteristics and its applicability in generating xylooligosaccharides and fermentable sugars. *Appl. Biochem. Biotechnol.* 170, 119–130. doi:10.1007/s12010-013-0174-6

Viikari, L., Alapuranen, M., Puranen, T., Vehmaanperä, J., and Siika-Aho, M. (2007). Thermostable enzymes in lignocellulose hydrolysis. *Adv. Biochem. Eng. Biotechnol.* 108, 121–145.

Yeoman, C. J., Han, Y., Dodd, D., Schroeder, C. M., Mackie, R. I., and Cann, I. K. (2010). Thermostable enzymes as biocatalysts in the biofuel industry. *Adv. Appl. Microbiol.* 70, 1–55. doi:10.1016/S0065-2164(10)70001-0

Zambare, V. P., Bhalla, A., Muthukumarappan, K., Sani, R. K., and Christopher, L. P. (2011). Bioprocessing of agricultural residues to ethanol utilizing a cellulolytic extremophile. *Extremophiles* 15, 611–618. doi:10.1007/s00792-011-0391-2

Zhang, Z. G., Yi, Z. L., Pei, X. Q., and Wu, Z. L. (2010). Improving the thermostability of *Geobacillus stearothermophilus* xylanase XT6 by directed evolution and site-directed mutagenesis. *Bioresour. Technol.* 101, 9272–9278. doi:10.1016/j.biortech.2010.07.060

Zhu, Y., Kim, T. H., Lee, Y. Y., Chen, R., and Elander, R. T. (2006). Enzymatic production of xylooligosaccharides from corn stover and corn cobs treated with aqueous ammonia. *Appl. Biochem. Biotechnol.* 12, 586–598. doi:10.1385/ABAB:130:1:586

Conflict of Interest Statement: The authors declare that the research was conducted in the absence of any commercial or financial relationships that could be construed as a potential conflict of interest.

frontiers in Bioengineering and Biotechnology

ORIGINAL RESEARCH
published: 03 June 2015
doi: 10.3389/fbioe.2015.00076

First glycoside hydrolase family 2 enzymes from *Thermus antranikianii* and *Thermus brockianus* with β-glucosidase activity

Carola Schröder†, *Saskia Blank*† *and Garabed Antranikian**

Institute of Technical Microbiology, Hamburg University of Technology, Hamburg, Germany

Two glycoside hydrolase encoding genes (*tagh2* and *tbgh2*) were identified from different *Thermus* species using functional screening. Based on amino acid similarities, the enzymes were predicted to belong to glycoside hydrolase (GH) family 2. Surprisingly, both enzymes (*Ta*GH2 and *Tb*GH2) showed twofold higher activities for the hydrolysis of nitrophenol-linked β-D-glucopyranoside than of -galactopyranoside. Specific activities of 3,966 U/mg for *Ta*GH2 and 660 U/mg for *Tb*GH2 were observed. In accordance, K_m values for both enzymes were significantly lower when β-D-glucopyranoside was used as substrate. Furthermore, *Ta*GH2 was able to hydrolyze cellobiose. *Ta*GH2 and *Tb*GH2 exhibited highest activity at 95 and 90°C at pH 6.5. Both enzymes were extremely thermostable and showed thermal activation up to 250% relative activity at temperatures of 50 and 60°C. Especially, *Ta*GH2 displayed high tolerance toward numerous metal ions (Cu^{2+}, Co^{2+}, Zn^{2+}), which are known as glycoside hydrolase inhibitors. In this study, the first thermoactive GH family 2 enzymes with β-glucosidase activity have been identified and characterized. The hydrolysis of cellobiose is a unique property of *Ta*GH2 when compared to other enzymes of GH family 2. Our work contributes to a broader knowledge of substrate specificities in GH family 2.

Keywords: β-glucosidase, glycoside hydrolase, thermostable, *Thermus antranikianii*, *Thermus brockianus*, cellobiose, truncated domains

OPEN ACCESS

Edited by:
Noha M. Mesbah, Suez Canal University, Egypt

Reviewed by:
Yasser Gaber, Beni-Suef University, Egypt
Satyanarayana Tulasi, University of Delhi, India

****Correspondence:***
Garabed Antranikian, Institute of Technical Microbiology, Hamburg University of Technology, Kasernenstr. 12, Hamburg D-21073, Germany
antranikian@tuhh.de

†*Carola Schröder and Saskia Blank have contributed equally to this work.*

Specialty section:
This article was submitted to Process and Industrial Biotechnology, a section of the journal Frontiers in Bioengineering and Biotechnology

Received: *09 March 2015*
Accepted: *10 May 2015*
Published: *03 June 2015*

Citation:
Schröder C, Blank S and Antranikian G (2015) First glycoside hydrolase family 2 enzymes from Thermus antranikianii and Thermus brockianus with β-glucosidase activity. Front. Bioeng. Biotechnol. 3:76. doi: 10.3389/fbioe.2015.00076

Introduction

Glycoside hydrolases (GHs) (EC 3.2.1.X) hydrolyze glycosidic bonds between carbohydrates or between carbohydrate and non-carbohydrate components, for instance alcohols or phenols. To date, enzyme classification is based on amino acid similarities rather than substrate specificity (Henrissat, 1991). GHs are assigned to different groups based on conserved domains, and the families are numbered from 1 to 131 that are listed in the Carbohydrate-Active Enzymes Database[1] (Lombard et al., 2014). Evolutionary or structurally unrelated β-glucosidases (EC 3.2.1.21) are found in six GH families (1, 3, 5, 9, 30, and 116). The majority of identified β-glucosidases is grouped in GH family 1 (Cairns and Esen, 2010). β-Galactosidase activity can be found in different GH families (1, 2, 3, 16, 20, 35, 42, 43, 50, and 59). In contrast to GH family 1, no β-glucosidase is found in GH family 2. So far, glycoside hydrolases classified as GH2 were described to function as β-galactosidase

[1]http://www.cazy.org/

(EC 3.2.1.23), β-mannosidase (EC 3.2.1.25), β-glucuronidase (EC 3.2.1.31), endo-β-mannosidase (EC 3.2.1.152), or as exo-β-glucosaminidase (EC 3.2.1.165). These enzymes hydrolyze their substrates through a retaining acid/base mechanism with two glutamic acid/glutamate residues involved. One residue acts as acid and base catalyst, whereas the other residue serves as nucleophile (Davies and Henrissat, 1995).

Glycoside hydrolases find a wide range of industrial applications. For instance, β-glucosidases are applied in biorefineries to reduce cellobiose-mediated product inhibition of endoglucanases. Thus, the addition of β-glucosidases leads to increased glucose concentrations during the enzymatic hydrolysis of cellulose, thereby increasing ethanol yields (Viikari et al., 2007). Furthermore, β-glucosidases and β-galactosidases are applied in the food industry to improve the aroma of juices and wine (Bhatia et al., 2002). Many industrial processes run at harsh conditions, e. g., elevated temperatures and extremes of pH. Hence, the demand for novel enzymes which function at high temperatures or acidic or alkaline pH values is growing (Antranikian and Egorova, 2007).

Bacteria belonging to the genus *Thermus* grow at temperatures between 53 and 86°C, and at pH values between 6.0 and 10.5 (Dworkin et al., 2006). Since the discovery of the type strain of this genus, *Thermus aquaticus* in 1969, numerous species have been isolated from hot environments (Brock and Freeze, 1969; Oshima and Imahori, 1974). Especially, the DNA polymerase from *T. aquaticus* (*Taq* DNA polymerase) became one of the key enzymes in molecular biology (Chien et al., 1976). Furthermore, thermostable DNA-processing enzymes such as ligases, helicases, or endonucleases have been identified (Pantazaki et al., 2002). Although *Thermus* spp. produce different hydrolytic enzymes like proteases or lipases, only few glycoside hydrolases have been characterized so far (Dion et al., 1999; Fridjonsson et al., 1999; Pantazaki et al., 2002; Kim et al., 2006; Nam et al., 2010; Blank et al., 2014).

In the current report, two genes coding for GHs (*Ta*GH2 and *Tb*GH2) were identified from *Thermus antranikianii* and *Thermus brockianus*. Conserved domains of GH2 were detected with incomplete motifs. The recombinant proteins showed highest activity toward 4-NP-β-D-glucopyranoside. The activity of *Ta*GH2 toward cellobiose makes this enzyme unique when compared to the GH family 2.

Materials and Methods

Bacterial Strains and Plasmids

Thermus antranikianii and *Thermus brockianus* were used as potential sources for the detection of β-glucosidase-encoding genes. Both strains were obtained from the collection of bacterial strains of the Institute of Technical Microbiology, Hamburg-Harburg. The strains *Escherichia coli* XL1-Blue MRF' [Δ(*mcr*A)*183* Δ(*mcr*CB-*hsd*SMR-*mrr*)*173* *end*A1 *sup*E44 *thi-1* *rec*A1 *gyr*A96 *rel*A1 *lac* [F' *pro*AB *lac*IqZΔM15 Tn10 (Tet^R)]] and *E. coli* XLOLR (Δ(*mcr*A)*183* Δ(*mcr*CB-*hsd*SMR-*mrr*)*173* *end*A1 *thi-1* *rec*A1 *gyr*A96 *rel*A1*lac* [F'*pro*AB *lac*IqZΔM15 Tn10 (Tet^R)] Su-(non-suppressing) λr) were obtained from the "ZAP Express Predigested Vector Kit" (Agilent Technologies, Waldbronn, Germany), and were utilized to construct and screen phagemid libraries using the vector pBK-CMV.

Escherichia coli Nova Blue Single™ (*end*A1 *hsd*R17(r^-_{K12} m^+_{K12}) *sup*E44 *thi-1* *rec*A1 *gyr*A96 *rel*A1 *lac* F'[*pro*A^+ B^+ *lacI*^{q} ZΔM15:Tn10 (Tc^R)]) (Novagen/Merck, Darmstadt, Germany) and *E. coli* BL21 Star™(DE3) [F^- *omp*T *hsd*SB (rB-mB-) *gal dcm* *rne*131 (DE3)] (Invitrogen, Karlsruhe, Germany) were used as hosts for cloned PCR products and expression using the plasmids pJet1.2/blunt (Fermentas, St.Leon-Rot, Germany) and pQE-80L (Qiagen, Hilden, Germany).

Media and Culture Conditions

The *Thermus* strains were grown at 70°C and 200 rpm for 16 h in *Thermus* 162 medium (DSMZ medium 878). *E. coli* strains were grown in LB medium at 30–37°C and 100–180 rpm for 16 h (Sambrook et al., 2001). LB medium was supplemented with selected antibiotics (ampicillin: 100 µg/mL, kanamycin: 50 µg/mL) when cultivating bacteria harboring appropriate plasmids. For gene expression, isopropyl-β-D-thiogalactopyranoside (IPTG) in concentrations of 0.5–1.0 mM were added.

Isolation of DNA, Construction and Screening of Gene Libraries

Genomic DNA from *Thermus* sp. was isolated according to the "Genomic DNA Handbook" (Qiagen, Hilden, Germany), and further purified by phenol/chloroform/isoamyl alcohol-extraction (25/24/1) and ethanol precipitation. Plasmid DNA was isolated using the "GeneJET™ Plasmid Miniprep Kit" (Fermentas, St. Leon-Rot, Germany).

Isolated genomic DNA from *Thermus* strains was partially digested with *Bam*HI to generate fragments of 5–10 kb. DNA fragments of the desired size were separated by agarose gel electrophoresis. To prepare an agarose gel of 1%, 1 g agarose was dissolved in 100 mL TAE buffer (40 mM Tris, 1 mM EDTA, 40 mM acetic acid, pH 8.5). The DNA was extracted from the gel by using the "GeneJet Gel Extraction Kit" (Fermentas, St. Leon-Rot, Germany). The ligation into the "ZAP Express Vector," as well as further steps for gene library construction were carried out according to the manufacturer's instructions.

To detect β-glucosidase-encoding genes, the gene libraries were plated on LB agar supplemented with 50 µg/mL kanamycin, and after growth over night the colonies were replicated on plates containing additionally 1 mM IPTG. The clones were overlayed with buffer (25 mM sodium acetate, 2.5 mM $CaCl_2 \times 2\ H_2O$, 170 mM NaCl, 1% agarose, pH 6.5) containing 2.5 mM esculin and 0.4 mM ammonium-iron(III)-citrate. After incubation at 70°C for 1–16 h, β-glucosidase positive clones were observed by the formation of a brown halo around the colonies. *E. coli* XLOLR pBK-CMV clones displaying β-glucosidase activity were conserved as cryostocks containing 25% glycerol.

Sequencing and Sequence Analysis

Plasmids were isolated ("GeneJET™ Plasmid Miniprep Kit", Fermentas, St. Leon-Rot, Germany) from selected clones, which conferred β-glucosidase activity. To determine the DNA-sequence of integrated DNA-fragments, the plasmids were sent to Eurofins MWG Operon (Ebersberg, Germany) for sequencing.

Putative open reading frames (ORF) were detected using the program "FramePlot 4.0beta."[2] The DNA- and amino acid-sequences were compared to the database of the "National Centre for Biotechnology Information" (NCBI[3]) using the "Basic Local Alignment Search Tool" (BLAST) (Altschul et al., 1997). Conserved domains were predicted using "InterProScan" (EMBL-EBI[4]) and the Conserved Domain Database (Marchler-Bauer et al., 2013). Glycoside hydrolase family 2 signatures were retrieved from http://prosite.expasy.org/PDOC00531. For multiple sequence alignments, ClustalW2 was employed (EMBL-EBI[5], 2013). Hypothetical models of protein structures, based on sequence homologies, were prepared with the program "SWISS-MODEL" (Gasteiger et al., 2003).

Cloning of Genes

To amplify the β-glucosidase-encoding genes, specific primers were obtained from Eurofins MWG Operon (Ebersberg). For the amplification of the gene *tagh2*, the primers *tagh2*_f_*Pae*I (5′-*GCATGC*AGGTGGGAAAGAGCTTGGTTTTTG-3′) and *tagh2*_r_*Sal*I*Hind*III (5′-*AAGCTTGTCGAC*TCACCAGGCCAC CCCCAGGG-3′) were used, while *tbgh*_f (*GGATCC*AGGCTA AAAAGCGCCCTTTTC) and *tbgh2*_r (*GTCGAC*CTACCAA GCCTCTCCAGG) were employed to amplify the gene *tbgh2*.

The PCRs were carried out in a thermocycler according to the manufacturer's instructions. A mixture of 20 µL contained 0.4 U "Phusion High-Fidelity DNA-Polymerase" (Fermentas, St. Leon-Rot, Germany), 0.2 mM dATP, dCTP, dGTP, dTTP, 0.5 µM of the forward and reverse primer, 10–300 ng template, reaction buffer, and distilled autoclaved water. The obtained PCR products were cloned into the pJet1.2/blunt vector (Fermentas, St. Leon-Rot, Germany), which was thereafter used to transform competent *E. coli* Nova Blue Single™ cells. Positive transformants were identified by colony PCR. Isolated pJet1.2/blunt plasmids were double digested with *Pae*I/*Sal*I or *Bam*HI/*Sal*I to excise the β-glucosidase-encoding genes. The purified genes were ligated into the *Pae*I/*Sal*I and *Bam*HI/*Sal*I digested expression vector pQE-80L, which was used to transform competent *E. coli* BL21 Star™(DE3) cells. Positive transformants were identified by colony PCR and conserved as cryostocks containing 25% glycerol.

Production and Purification of the Enzymes

E. coli BL21 Star™(DE3) harboring the recombinant pQE-80L plasmids were cultivated in 5 mL LB medium containing 100 µg/mL ampicillin at 37°C and 160 rpm for 16 h. The preculture was subcultivated in 500 mL LB medium containing 100 µg/mL ampicillin until the culture reached an optical density of $A_{600\,nm} = 0.5–0.7$. To induce protein production, 0.5 M IPTG was added. The cultivation was continued for 6 h, afterwards the cells were harvested by centrifugation at 13,000 rpm for 20 min at 4°C. The cell pellet was resuspended in lysis buffer (50 mM NaH_2PO_4, 300 mM NaCl, 10 mM imidazole, pH 8) in the ratio 5 mL buffer/1 g pellet. Cells were disrupted by French press (French® Pressure Cell Press, SLM-Aminco, MD, USA). Crude extracts with protein contents of 1.5 mg/mL (*Ta*GH2) and 1.07 mg/mL (*Tb*GH2) were obtained by centrifugation at 13,000 rpm at 4°C for 20 min.

For heat precipitation, the crude extract was incubated at 70°C for 15 min, and subsequently centrifuged at 13,000 rpm at 4°C for 20 min.

As a second purification step, a Ni^{2+}-nitrilic acid (Ni-NTA) affinity chromatography using a 1.5-mL Ni-NTA superflow column (Qiagen, Hilden, Germany) was conducted. About 2–5 mL of the crude extract was incubated with 1 mL of Ni-NTA-agarose (Qiagen, Hilden, Germany) at 4°C and 200 rpm for 1 h. Two washing steps were performed (50 mM NaH_2PO_4, 300 mM NaCl, 25 mM imidazole, pH 7.0). To elute the protein, six fractions of 500 µL elution buffer (50 mM NaH_2PO_4, 300 mM NaCl, 250 mM imidazole, pH 7.0) were added to the column. Fractions containing the protein were pooled.

In the case of *Tb*GH2, a gel filtration using the "ÄKTA™ Fast Protein Liquid Chromatography" (FPLC)-system (GE Healthcare, München, Germany) was carried out. One milliliter of the protein solution was load on a "HiLoad 16/60 Superdex 200 prep grade"-column (GE Healthcare, München, Germany) with a flow rate of 1 mL/min. The protein was eluted with a 1.5-fold column volume of 50 mM sodium phosphate buffer, pH 7.2, which contained 150 mM NaCl. Enzyme fractions were pooled.

The purified proteins were dialyzed against 20 mM citrate buffer (*Ta*GH2) or 20 mM maleate buffer (*Tb*GH2) and stored at 4°C.

The purity of the recombinant β-glucosidases was analyzed by sodium dodecyl sulfate polyacrylamide gel electrophoresis (SDS-PAGE, 12%) (Laemmli, 1970).

Protein concentrations were determined using the method described by Bradford (1976).

Determination of Enzyme Activity

Enzyme activity was determined by the released amounts of 2-nitrophenol (2-Np) and 4-nitrophenol (4-Np) from several nitrophenol-linked substrates (4-Np-β-D-glucopyranoside, 4-Np-α-D-glucopyranoside, 4-Np-β-D-glucuronid, 4-Np-β-D-galactopyranoside, 2-Np-β-D-galactopyranoside, 4-Np-α-D-galactopyranoside, 4-Np-β-D-xylopyranoside, 4-Np-β-D-manno pyranoside, 4-Np-β-D-cellobioside).

The reaction mixture of 1 mL contained 2 mM Np-substrate and 20 mM citrate buffer pH 6.5 (*Ta*GH2), or 20 mM maleate buffer pH 6.5 (*Tb*GH2). After preincubation of the reaction mixture for 5 min at 95°C (*Ta*GH2) or 90°C (*Tb*GH2), 10 µL of diluted enzyme solution were added. The hydrolysis was stopped after 10 min by adding 100 µL of 100 mM Na_2CO_3. The absorbance was measured at 410 nm. All measurements were determined in triplicates. About 1 U of enzyme activity was defined as the amount of enzyme needed for the release of 1 µmol 4-nitrophenol per minute. Kinetic parameters were determined according to Michaelis and Menten (1913).

Effect of pH and Temperature

Relative activities against 4-Np-β-D-glucopyranoside (2 mM) were measured in the range of pH 4.0–10.0 using 20 mM Britton–Robinson buffer (Britton and Robinson, 1931). To determine

[2]http://nocardia.nih.go.jp/fp4/
[3]http://www.ncbi.nlm.nih.gov/
[4]http://www.ebi.ac.uk/Tools/pfa/iprscan/
[5]http://www.ebi.ac.uk/Tools/msa/clustalw2/

the pH stability, both enzymes were preincubated in 20 mM Britton–Robinson buffer, pH 3.0–10.0 at 4°C for 24 h. To stabilize the enzymes, the concentration of the solution was adjusted to 0.1 mg/mL with BSA. After preincubation, the relative activity toward 4-Np-β-D-glucopyranoside (2 mM) was determined in 20 mM Britton–Robinson buffer pH 6.5 and 95°C (*Ta*GH2), or in 20 mM maleate buffer at 90°C (*Tb*GH2).

The influence of temperature was determined by measuring relative enzyme activities in the range of 10–115°C with 4-Np-β-D-glucopyranoside (2 mM) in 20 mM citrate buffer (*Ta*GH2) or 20 mM maleate buffer (*Tb*GH2), pH 6.5. To examine the temperature stability, both enzymes were preincubated at 50–90°C for 0–24 h in 20 mM citrate buffer (*Ta*GH2) or 20 mM maleate buffer (*Tb*GH2), pH 6.5. The protein concentration of the solution was adjusted to 0.1 mg/mL with BSA. After preincubation, the relative activity toward 4-Np-β-D-glucopyranoside (2 mM) was determined in 20 mM citrate buffer (*Ta*GH2) or 20 mM maleate buffer (*Tb*GH2), pH 6.5, at 95°C (*Ta*GH2) and 90°C (*Tb*GH2).

Determination of Hydrolysis Products

Hydrolysis products of 1% (w/v) cellobiose and lactose were examined by HPLC (Agilent Technology 1260 Infinity Quarternary LC system with 1260 ALS sampler, 1260 Quat pump and 1260 R_i detector). The enzymes were incubated with the substrates at 90°C for 1 h in 20 mM citrate buffer (*Ta*GH2) or 20 mM maleate buffer (*Tb*GH2), pH 6.5. After hydrolysis, 20 µL of the centrifuged and filtered solution was applied to a Hi-Plex H column (Agilent Technologies, Waldbronn, Germany). Water was used as solvent with a flowrate of 0.6 mL/min. To identify the hydrolysis products, the retention times (min) were compared to the standards cellobiose (9.433), lactose (9.789), and glucose (11.247).

Nucleotide Sequence Accession Number

DNA sequences of *tagh2* and *tbgh2* were deposited in GenBank (*tagh2*: HG969993, *tbgh2*: HG969994).

Results

Identification of Novel GH-Encoding Genes

Gene libraries were constructed from pure cultures of *T. antranikianii* and *T. brockianus*, and screened for genes coding for enzymes active toward esculin. One activity-conferring *E. coli* clone was detected from each library. The respective inserts of the phagemids (pBK-CMV:*Ta* and pBK-CMV:*Tb*) harbored *tagh2* and *tbgh2*. The nucleotide sequences of *tagh2* and *tbgh2* were 80% identical. GC contents of 68.4 and 66.7% with GC proportions in the third codon position (GC_3) of 86.3 and 82.3% were observed.

The deduced amino acid sequences *Ta*GH2 and *Tb*GH2 possessed theoretical isoelectric points (pI) of 6.1 (*Ta*GH2) and 5.99 (*Tb*GH2). Molecular masses of 79.0 kDa (*Ta*GH2) and 78.1 kDa (*Tb*GH2) were computed. The proteins were compared to proteins annotated in databases (GenBank). *Ta*GH2 exhibited highest identity (98%) to a putative β-galactosidase from *Thermus scotoductus* (YP_004203085, **Table 1**, Row 3). *Tb*GH2 showed 82% identity to a hypothetical protein from *Thermus* sp. (YP_005653839, **Table 1**, Row 4). The annotated proteins were deduced from ORFs identified in the course of whole genome sequencing projects of different *Thermus* species. Additionally, identities of 86% (*Ta*GH2) and 83% (*Tb*GH2) were obtained by comparison with a putative GH2 β-mannosidase from *Thermus thermophilus* (ACH89346, **Table 1**, Row 6). Identities to annotated proteins from *Thermus* sp. ranged from 83 to 98% (*Ta*GH2) and from 80 to 83% (*Tb*GH2). GH2 enzymes from genera other than *Thermus* were observed with identities of 38–42% (*Caldilinea aerophila*, YP_005442964 and *Alicyclobacillus pohlia*, WP_018133520.1; **Table 1**, Rows 7 and 8).

Notably, the Conserved Domain Database indicated two incomplete GH2 domains for both enzymes (**Figure 1**). A partial GH2 sugar-binding domain (pfam02837) in the protein sequence of *Ta*GH2 (aa 23–93) and *Tb*GH2 (aa 24–85), and an incomplete GH2 TIM-barrel domain (pfam02836) within *Ta*GH2 (aa 298–410) and *Tb*GH2 (aa 290–418) were predicted. Comparable domains were described for *E. coli* β-galactosidase LacZ in a complete form with low identities to the TIM-barrel domain ($\leq$ 30%) and to the sugar-binding domain ($\leq$ 20%) of *Ta*GH2 and *Tb*GH2 (**Figure 1**). Within LacZ, the consensus patterns N-X-[LIVMFYWD]-R-[STACN](2)-H-Y-P-X(4)-[LIVMFYWS](2)-x(3)-[DN]-X(2)-G-[LIVMFYW](4) and [DENQLF]-[KRVW]-N-[HRY]-[STAPV]-[SAC]-[LIVMFS]-[LIVMFSA]-[LIVMFS]-W-[GSV]-X(2,3)-N-E, which were described as conserved signatures of GH2, were identified[6] (**Figure 2**). Principally, these conserved signatures were also detected as variations within *Ta*GH2 and *Tb*GH2.

[6]http://prosite.expasy.org/PDOC00531

TABLE 1 | Identities of *Ta*GH2 and *Tb*GH2 to other GH2-proteins.

	1.	2.	3.	4.	5.	6.	7.	8.	9.
1. *T. antranikianii Ta*GH2	100%								
2. *T. brockianus Tb*GH2	80% (100)	100%							
3. *T. scotoductus* β-galactosidase (YP_004203085.1)	98% (100)	80% (100)	100%						
4. *Thermus* sp. hyp. Protein (YP_005653839.1)	83% (100)	82% (100)	83% (100)	100%					
5. *T. igniterrae* β-galactosidase (WP_018110934.1)	82% (100)	81% (100)	81% (100)	83% (100)	100%				
6. *T. thermophilus* put. β-mannosidase (ACH89346.1)	86% (92)	83% (93)	85% (99)	84% (99)	86% (87)	100%			
7. *A. pohliae* put. Protein (WP_018133520.1)	38% (97)	41% (83)	38% (90)	38% (95)	38% (94)	41% (92)	100%		
8. *C. aerophila* put. GH (YP_005442964.1)	41% (76)	42% (82)	41% (78)	41% (84)	42% (83)	41% (96)	45% (99)	100%	
9. *E. coli* LacZ (1HN1_D)	27% (35)	29% (32)	27% (37)	27% (32)	29% (46)	28% (46)	23% (61)	23% (58)	100%

Enzymes from Thermus spp. are highlighted in gray. Query-coverage values are indicated in % in brackets.
Numbers at the top are listed in the left column.

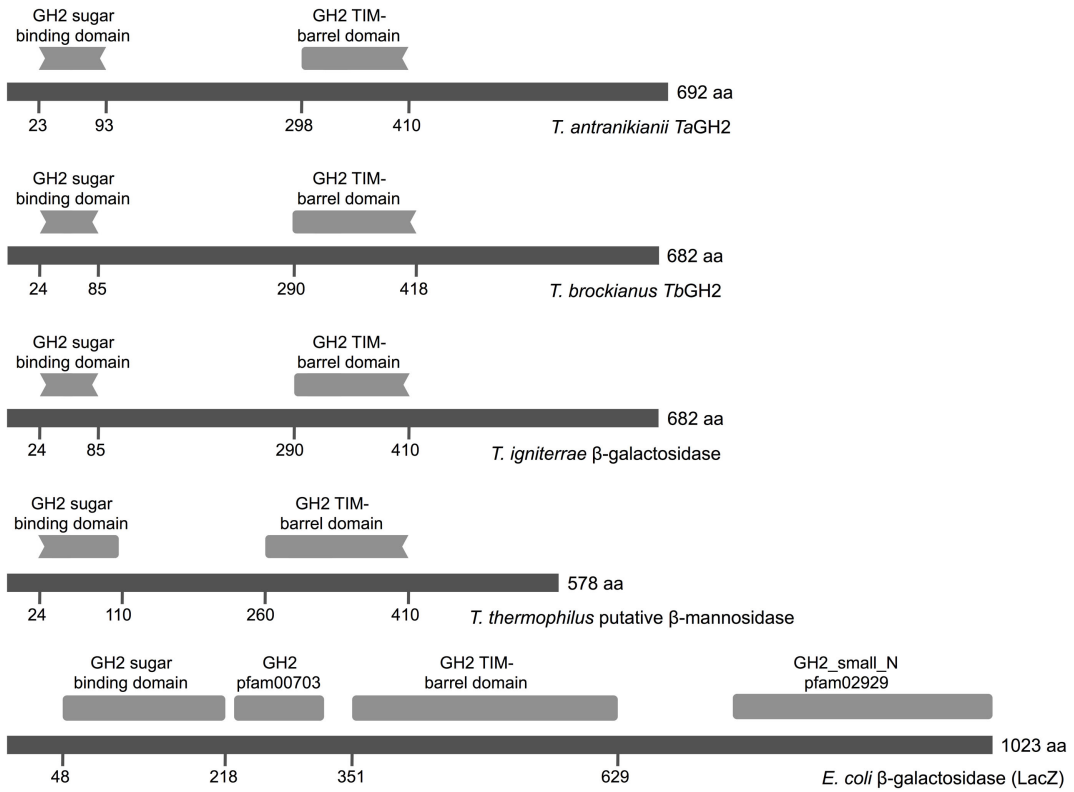

FIGURE 1 | Conserved domains of GH2 family enzymes. The amino acid sequences of *Ta*GH2 (*T. antranikianii*), *Tb*GH2 (*T. brockianus*), β-galactosidase (*T. igniterrae*, WP_018110934.1), putative β-mannosidase (*T. thermophilus*, ACH89346), and LacZ (*E. coli*, 1HN1_D) are depicted in dark gray with homologous predicted sugar-binding domain (pfam02837) and TIM-barrel domain (pfam02836, Conserved Domain Database) in light gray.

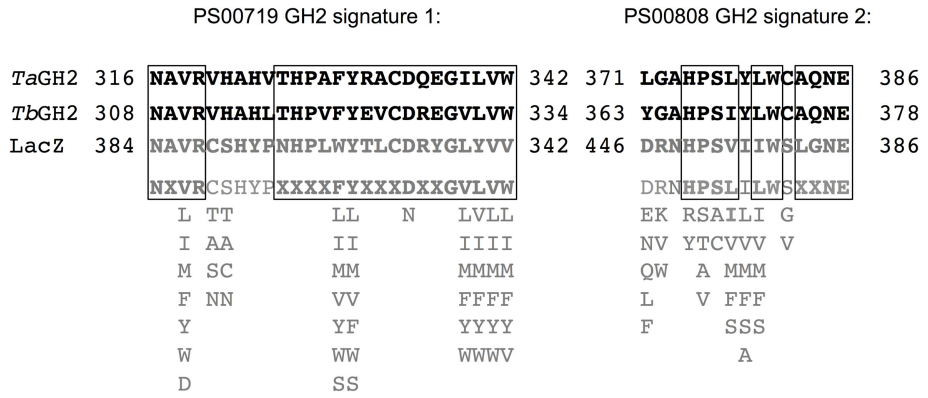

FIGURE 2 | Amino acid signatures of GH2 family enzymes. The amino acid sequences of *Ta*GH2 and *Tb*GH2 are shown in black and the sequence of LacZ (*E. coli*, 1HN1_D) and the consensus pattern of the two characteristic signatures of GH2 are depicted in gray with possible residue substitutions indicated below (http://prosite.expasy.org/PDOC00531). Corresponding amino acids are shown in bold characters and conformity within all sequences is framed.

Expression of *tagh2* and *tbgh2* and Protein Purification

The genes *tagh2* and *tbgh2* were amplified and expressed in *E. coli* BL21 Star™(DE3) using pQE-80L (**Figure 3**). A high proportion of *Tb*GH2 was produced in insoluble form. *Ta*GH2 and *Tb*GH2 were purified from soluble crude extracts. After heat precipitation and Ni-NTA affinity chromatography, *Ta*GH2 was homogenous with a yield of 17.3%, whereas *Tb*GH2 was subsequently subjected to size exclusion chromatography with a yield of 6.7%. The calculated molecular masses of 79.0 kDa (*Ta*GH2) and 78.1 kDa (*Tb*GH2) were confirmed by SDS gel analysis (**Figure 3**).

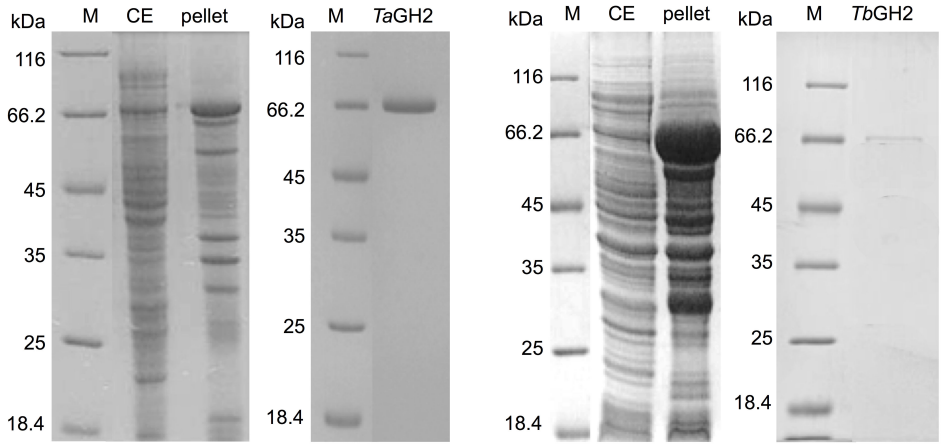

FIGURE 3 | SDS-PAGE analysis of crude extracts and purified *Ta*GH2 and *Tb*GH2. Soluble (CE) and insoluble (pellet) fractions of crude extracts and purified proteins were separated by SDS-PAGE (200 V, 50 min, M: Marker).

TABLE 2 | Kinetic parameters of *Ta*GH2 and *Tb*GH.

	4-Np-β-glucopyranoside		4-Np-β-galactopyranoside	
	***Ta*GH2**	***Tb*GH2**	***Ta*GH2**	***Tb*GH2**
K_m [mM]	0.73 ± 0.03	0.50 ± 0.02	2.20 ± 0.02	3.56 ± 0.07
V_{max} [μmol min^{-1} mg^{-1}]	4,028 ± 21	778 ± 22	2,615 ± 3	1,333 ± 11
k_{cat} [s^{-1}]	21,559	3,899	13,996	6,683
k_{cat}/K_m [mM^{-1} s^{-1}]	29,532	7,797	6,361	1,877

Activity of TaGH2 and TbGH2 was measured at 90°C in 20 mM citrate or maleate buffer (pH 6.5) with 0–10 mM 4-Np-β-D-glucopyranoside and 0–25 mM 4-Np-β-D-galactopyranoside for 10 min.

Substrate Conversion and Kinetics of *Ta*GH2 and *Tb*GH2

The purified enzymes *Ta*GH2 and *Tb*GH2 were analyzed regarding their substrate specificity. The predicted domains of GH2 and the highest homologies to annotated β-galactosidases suggested both enzymes being β-galactosidases. Nitrophenol-linked substrates were tested and in contrast to expectations, *Ta*GH2 and *Tb*GH2 exhibited highest activities toward 4-Np-β-D-glucopyranoside (*Ta*GH2: 3,966 U/mg and *Tb*GH2: 660 U/mg), and residual activities of 40 and 51% against 4-Np-β-D-galactopyranoside. In accordance, Michaelis constants (K_m) were lower when 4-Np-β-D-glucopyranoside was used as substrate (**Table 2**). The catalytic efficiency was 29,532 mM^{-1} s^{-1} for *Ta*GH2 and 7,797 mM^{-1} s^{-1} for *Tb*GH2. The maximum reaction rate (V_{max}) of *Ta*GH2 was higher when measured with 4-Np-β-D-glucopyranoside (4,028 ± 21 μmol min^{-1} mg^{-1}) compared to 4-Np-β-D-galactopyranoside (2,615 ± 3 μmol min^{-1} mg^{-1}). On the contrary, *Tb*GH2 exhibited a higher maximum reaction rate toward 4-Np-β-D-galactopyranoside (1,333 ± 11 μmol min^{-1} mg^{-1}) than toward 4-Np-β-D-glucopyranoside (778 ± 22 μmol min^{-1} mg^{-1}). Other nitrophenol-linked substrates were not converted. Furthermore, non-nitrophenolic substrates, such as cellobiose and lactose (1%, w/v), were tested. Interestingly, *Ta*GH2 converted cellobiose (**Figure 4**). *Tb*GH2 acted neither on cellobiose nor on lactose.

Influence of Temperature and pH

Highest activities toward 4-Np-β-D-glucopyranoside were observed at 95°C (*Ta*GH2) and 90°C (*Tb*GH2) at pH 6.5 (**Figures 5** and **6**). Residual activities of 83 ± 2% (*Ta*GH2) and 98 ± 4% (*Tb*GH2) were detected at 100°C. *Ta*GH2 showed no loss of activity when incubated at 50–90°C for 3 h (**Table 3**). By contrast, *Tb*GH2 was less stable and showed 17 ± 6% activity at 80°C after 3 h of incubation. At 70°C, *Ta*GH2 exhibited a half-life time of approximately 22 h and *Tb*GH2 of 12 h. In accordance, the predicted T_m was higher for *Ta*GH2 (>65°C) when compared to *Tb*GH2 (55–65°C) (Ku et al., 2009). Thermal activation was observed for both enzymes at 50 and 60°C. The enzyme *Ta*GH2 was stable when preincubated (4°C, 24 h) at pH values between 3.0 and 10.0 (81 ± 5-100 ± 2%). *Tb*GH2 was stable at pH 3.5–7.5 (71 ± 8-114 ± 13%) with residual activities of 63 ± 7 and 52 ± 11% at higher pH values (pH 8.5, 9.5).

Influence of Additives

The influence of different metal ions on the activity of *Ta*GH2 and *Tb*GH2 was tested (**Table 4**). K^+, Mg^{2+}, and Na^+ ions (1–10 mM) had no negative influence on the enzymatic performance of both enzymes. Furthermore, Ca^{2+}, Co^{2+}, Mn^{2+}, Ni^{2+}, Rb^+, and Sr^{2+} (1–10 mM) had no significant influence on the hydrolytic action of *Ta*GH2 (88 ± 4-104 ± 4%). The activity of *Tb*GH2 was reduced in presence of 10 mM $CaCl_2$ (56 ± 20%), $MnCl_2$ (64 ± 12%), RbCl (81 ± 5%), and $SrCl_2$ (67 ± 15%), or completely inhibited in presence of 5–10 mM $CoCl_2$ and $NiCl_2$. *Tb*GH2 was inactivated by 1 mM Ag^+, Cu^{2+}, and Zn^{2+}. *Ta*GH2 was exclusively inhibited by Ag^+. Fe^{2+} and Fe^{3+} (1 mM) had no influence on the enzymatic performance of both hydrolases (95 ± 2-120 ± 2%). *Tb*GH2 showed higher activity when 1 mM $AlCl_3$ (149 ±1%), $CrCl_3$ (139 ± 4%), KCl (146 ± 4%), $MgCl_2$ (136 ± 4%), NaCl (138 ± 11%), or RbCl (143 ± 10%) was added.

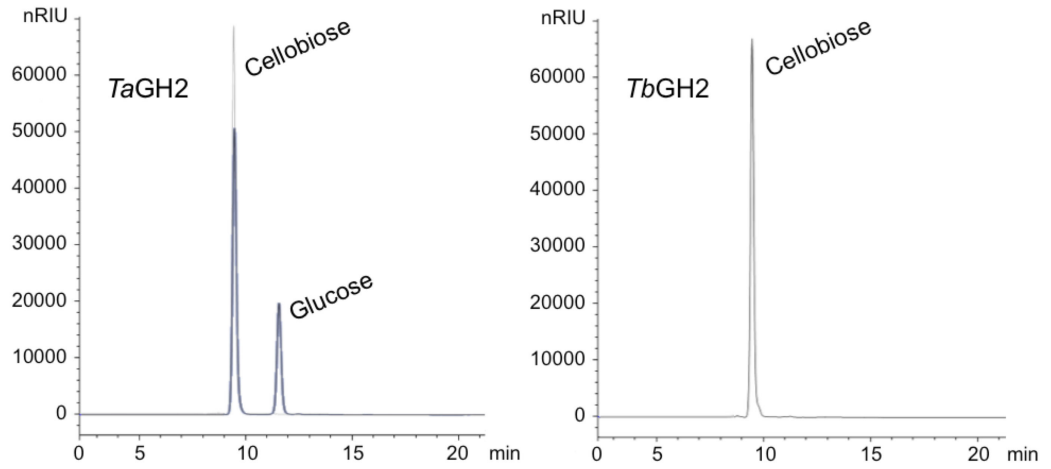

FIGURE 4 | HPLC analyses of cellobiose degradation. The degradation of cellobiose (1% w/v) by *Ta*GH2 and by *Tb*GH2 is depicted. The hydrolysis was carried out at 90°C for 1 h in 20 mM citrate or maleate buffer (pH 6.5). Subsequently, the samples were subjected to HPLC analyses using an Hi-Plex H column and water with a flow rate of 0.6 mL/min. Standards are shown in gray. nRIU, nano Refractive Index Units.

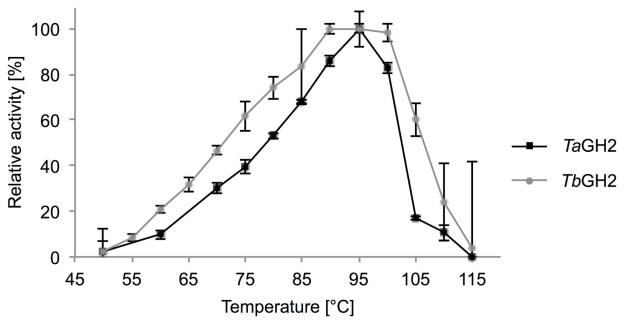

FIGURE 5 | Effect of temperature on activity of *Ta*GH2 and *Tb*GH2. Activity of *Ta*GH2 and *Tb*GH2 was measured at different temperatures (50–115°C) for 10 min in 20 mM citrate or maleate buffer (pH 6.5) with 2 mM 4-Np-β-D-glucopyranoside. Temperatures above 95°C were measured in heated oil.

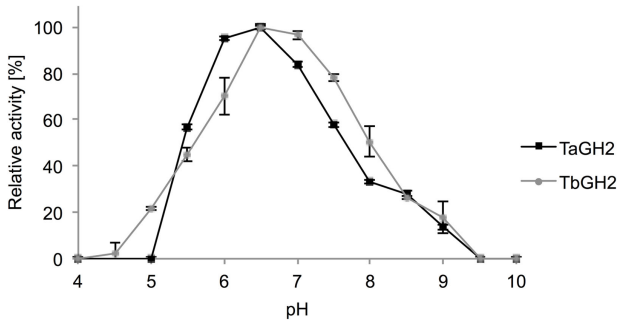

FIGURE 6 | Effect of pH on activity of *Ta*GH2 and *Tb*GH2. Activity of *Ta*GH2 and *Tb*GH2 was measured for 10 min at 95 or 90°C in 20 mM Britton–Robinson buffer (pH 4–10) with 2 mM 4-Np-β-D-glucopyranoside.

The presence of 5 mM additives, such as β-mercaptoethanol, DTT, EDTA, urea, iodoacetic acid, sodium azide, and Tween 80 did not decrease the activity of both enzymes. Moreover,

TABLE 3 | Effect of temperature on stability of *Ta*GH2 and *Tb*GH2.

	3 h		24 h	
	***Ta*GH2**	***Tb*GH2**	***Ta*GH2**	***Tb*GH2**
50°C	127 ± 5	129 ± 9	151 ± 4	246 ± 12
60°C	123 ± 2	199 ± 7	108 ± 8	202 ± 10
70°C	123 ± 4	94 ± 3	47 ± 3	0
80°C	128 ± 2	17 ± 6	15 ± 3	0
90°C	127 ± 3	0	0	0

Activity of TaGH2 and TbGH2 was measured at 90°C in 20 mM citrate or maleate buffer (pH 6.5) with 2 mM 4-Np-β-D-glucopyranoside for 10 min after preincubation for 3 or 24 h, respectively, at different temperatures (50–90°C). Activities determined at 0 h were set to 100%.

Triton X-100 and Tween 20 did not influence the performance of *Tb*GH2, whereas *Ta*GH2 exhibited 49 ± 2 and 76 ± 1% residual activity. Complete loss of activity for both glycoside hydrolases was detected when SDS or CTAB (5 mM) were added.

Discussion

Screening of gene libraries from *T. antranikianii* and *T. brockianus* on esculin resulted in the identification of two novel glycoside hydrolases (*Ta*GH2 and *Tb*GH2). Identities of amino acid sequences higher than 80% were observed to proteins from other *Thermus* species. The glycoside hydrolase family 2 domains (sugar binding domain and TIM-barrel domain) appeared to be incomplete. The domains are either truncated but functional or they are not recognized as domains due to large differences to other representatives of GH2. Comparison with the GH2 LacZ from *E. coli* (1HN1_D) showed low similarities within the corresponding domains. Additionally, conserved amino acid signatures typical for members of GH2 were partially identified (**Figure 2**). Similar hypothetical proteins with typical conserved domains from different genera were detected with identities of 39% (*Ta*GH2) and 42% (*Tb*GH2) or below. Thus, a differentiation of proteins produced from *Thermus* spp. would be suggested.

TABLE 4 | Effects of metal ions on the activity of *Ta*GH2 and *Tb*GH2.

Reagent	Relative activity of *Ta*GH2 (%)			Relative activity of *Tb*GH2 (%)		
	1 mM	5 mM	10 mM	1 mM	5 mM	10 mM
None	100 ± 3	100 ± 5	100 ± 2	100 ± 4	100 ± 4	100 ± 5
$AgNO_3$	0	0	0	0	0	0
$AlCl_3$	97 ± 4	53 ± 1	17 ± 5	149 ± 1	98 ± 13	0
$CaCl_2$	100 ± 3	100 ± 4	103 ± 4	93 ± 6	72 ± 5	56 ± 20
$CoCl_2$	99 ± 3	101 ± 2	97 ± 2	52 ± 7	0	0
$CrCl_3$	88 ± 2	43 ± 3	13 ± 5	139 ± 4	53 ± 11	0
$CuCl_2$	98 ± 4	64 ± 5	20 ± 4	0	0	0
$FeCl_2$	97 ± 1	42 ± 3	0	117 ± 3	31 ± 14	0
$FeCl_3$	95 ± 2	53 ± 4	12 ± 3	120 ± 2	37 ± 18	0
KCl	99 ± 3	98 ± 3	102 ± 4	146 ± 4	144 ± 7	83 ± 5
$MgCl_2$	99 ± 1	103 ± 2	103 ± 2	136 ± 4	117 ± 2	113 ± 7
$MnCl_2$	96 ± 3	98 ± 1	88 ± 4	94 ± 15	86 ± 3	64 ± 12
NaCl	97 ± 2	99 ± 4	100 ± 4	138 ± 11	129 ± 6	104 ± 10
$NiCl_2$	99 ± 3	104 ± 4	90 ± 3	61 ± 13	0	0
RbCl	96 ± 2	102 ± 1	98 ± 1	143 ± 10	143 ± 2	81 ± 5
$SrCl_2$	101 ± 3	104 ± 4	104 ± 2	127 ± 4	106 ± 9	67 ± 15
$ZnCl_2$	99 ± 2	97 ± 2	64 ± 3	0	0	0

Activity of TaGH2 and TbGH2 was measured at 90°C in 20 mM citrate or maleate buffer (pH 6.5) with 2 mM 4-Np-β-D-glucopyranoside for 10 min in presence or absence of metal ions.

Low sequence similarities within one protein superfamily could be the result of adaptation to different environmental conditions. Different enzymatic activities may have developed from a common ancestor (Galperin and Koonin, 2012). Structural diversification that preserved the active site residues may result in catalytically active enzymes with altered substrate specificity. Evolutionary pressure promotes functional and effective enzymes, which may result in reduction of conserved domains with remaining functionality (Juers et al., 1999). However, substrate specificity can be neglected for classification of glycoside hydrolases, since the structural homologies especially the motif forming the catalytic center is highly conserved (Henrissat and Davies, 1997). Homologies of up to 98 and 82%, respectively, were observed by comparison with annotated β-galactosidases or β-mannosidases from *Thermus* species. No similar characterized enzyme to *Ta*GH2 or *Tb*GH2 was detected in the NCBI database; thus, classification of similar proteins was achieved by domain prediction rather than by functional analyses. Highest catalytic efficiencies for *Ta*GH2 and *Tb*GH2 were observed toward 4-Np-β-D-glucopyranoside with residual activities toward 4-Np-β-D-galactopyranoside. Cellobiose conversion distinguishes *Ta*GH2 from *Tb*GH2. The hydrolysis characteristics may vary between artificial and natural substrates. This may be due to differences in size, charge, and binding properties of the artificial compound. Higher activity toward artificial substrates was also described as common phenomenon for α-galactosidases (Wang et al., 2014). Hydrolysis of cellobiose or lactose by *Tb*GH2 could not be detected, although high β-glucosidase activity was observed when the artificial substrate was used. β-Glucosidases are reported to often exhibit a broad substrate spectrum. A β-glucosidase from *Thermotoga neapolitana* hydrolyzed among others 4-Np-β-D-glucopyranoside, cellobiose, and lactose (Park et al., 2005). Likewise, a GH1-β-glucosidase derived from a hot-spring metagenome exhibited activity toward 4-Np-β-D-glucopyranoside, 4-Np-β-D-galactopyranoside, cellobiose, and lactose (Schröder et al., 2014). However, the newly discovered GH2 β-glucosidases *Ta*GH2 and *Tb*GH2 showed a narrow substrate range.

Protein production in the mesophilic host *E. coli* resulted in notable amount of inclusion bodies due to differences in genomic GC contents of the genus *Thermus*, as previously reported (Ishida and Oshima, 1994; Fridjonsson et al., 1999). The β-glucosidase *Ta*GH2 and the β-glucosidase/galactosidase *Tb*GH2 showed high activities at elevated temperatures. Other β-glycosidases from *Thermus thermophilus* also show activity at 88–90°C and pH 5.4–7.0 (Dion et al., 1999; Nam et al., 2010). A thermal activation was detected at 50 and 60°C, especially for *Tb*GH2 with 246 and 202% activity after 24 h, respectively. It was reported in the literature that enzymes from thermophilic organisms produced in mesophilic hosts may require thermal activation as demonstrated for a β-glycosidase from *T. thermophilus* at 70°C (Gerard et al., 2002). Specific activities were considered high with 3,966 and 660 U/mg, when compared to the majority of previously reported β-glucosidases and β-galactosidases with <1–100 U/mg[7]. Similar to GH family 1 β-glycosidases from *T. thermophilus*, significantly lower K_m values were observed with 4-Np-β-glucopyranoside when compared to -galactopyranoside (Dion et al., 1999; Nam et al., 2010). Highest substrate affinities for -glucopyranoside were also reported for other β-glucosidases from an uncultured soil bacterium and *Cellulomonas flavigena* with K_m-values of 0.16 and 7.1 mM, respectively (Barrera-Islas et al., 2007; Kim et al., 2007). Hence, the enzymes described here exhibit K_m-values in the range of other described GH1 β-glucosidases.

Ag^+, Cu^{2+}, and Fe^{3+} are most frequently described as glycoside hydrolase inhibitor (Cairns and Esen, 2010). By contrast, Fe^{3+} (1 mM) had no influence on the activity of both enzymes. Zinc ions inhibited *Tb*GH2 completely but had, interestingly, no effect on activity of *Ta*GH2. The surfactant CTAB (5 mM) inhibited both enzymes. The negatively charged catalytic amino acids in the active center might be covered by the positively charged additive. Moreover, negatively charged surface residues might be influenced resulting in structural destabilization of the enzyme. Although three cysteins are present in the amino acid sequence of both enzymes, reducing agents such as DTT and β-mercaptoethanol did not show a negative effect on the activity. Either no disulfide bond is formed or it is not affected by the prevalent conditions. It is a frequently described phenomenon that reducing agents can also have stabilizing effects on enzymes (Park et al., 2005). The influence of additives on β-glucosidases and β-galactosidases does not follow a certain pattern, and appears to be specific for each individual enzyme.

*Ta*GH2 and *Tb*GH2 were classified as members of glycoside hydrolase family 2 based on amino acid sequence similarities. Although GH family 2 comprises enzymes with different substrate specificities, β-glucosidase activity has not been reported in this family, yet (Henrissat, 1991). This finding proves the necessity of function-based screening to identify genes coding for proteins with unusual domain structures or unexpected activities. The

[7]http://www.brenda-enzymes.org

substrate specificity was reported to be less relevant than structural homologies for classification of members of glycoside hydrolase families (Henrissat and Davies, 1997).

In conclusion, our study demonstrates that enzymes structurally related to GH family 2 can exhibit more diverse substrate specificities than previously predicted. Therefore, we recommend to incorporate β-glucosidases into GH family 2 and consequently to evaluate activity on glucopyranosides including cellobiose for characterization of enzymes from this family.

References

Altschul, S. F., Madden, T. L., Schaffer, A. A., Zhang, J., Zhang, Z., Miller, W., et al. (1997). Gapped BLAST and PSI-BLAST: a new generation of protein database search programs. *Nucleic Acids Res.* 25, 3389–3402. doi:10.1093/nar/25.17.3389

Antranikian, G., and Egorova, K. (2007). "Extremophiles, a unique resource of biocatalysts for industrial biotechnlology," in *Physiology and Biochemistry of Extremophiles*, eds C. Gerday and N. Glansdorff (Washington, DC: ASM Press), 361–406. doi:10.1128/9781555815813.ch27

Barrera-Islas, G. A., Ramos-Valdivia, A. C., Salgado, L. M., and Ponce-Noyola, T. (2007). Characterization of a beta-glucosidase produced by a high-specific growth-rate mutant of *Cellulomonas flavigena*. *Curr. Microbiol.* 54, 266–270. doi:10.1007/s00284-006-0105-7

Bhatia, Y., Mishra, S., and Bisaria, V. S. (2002). Microbial beta-glucosidases: cloning, properties, and applications. *Crit. Rev. Biotechnol.* 22, 375–407. doi:10.1080/07388550290789568

Blank, S., Schröder, C., Schirrmacher, G., Reisinger, C., and Antranikian, G. (2014). Biochemical characterization of a recombinant xylanase from *Thermus brockianus*, suitable for biofuel production. *JSM Biotechnol. Biomed. Eng.* 2, 1027.

Bradford, M. M. (1976). A rapid and sensitive method for the quantitation of microgram quantities of protein utilizing the principle of protein-dye binding. *Anal. Biochem.* 72, 248–254. doi:10.1016/0003-2697(76)90527-3

Britton, H. T. S., and Robinson, R. A. (1931). Universal buffer solutions and the dissociation constant of veronal. *J. Chem. Soc.* 1456–1473. doi:10.1039/jr9310001456

Brock, T. D., and Freeze, H. (1969). *Thermus aquaticus* gen. n. and sp. n., a nonsporulating extreme thermophile. *J. Bacteriol.* 98, 289–297.

Cairns, J. R., and Esen, A. (2010). β-Glucosidases. *Cell. Mol. Life Sci.* 67, 3389–3405. doi:10.1007/s00018-010-0399-2

Chien, A., Edgar, D. B., and Trela, J. M. (1976). Deoxyribonucleic acid polymerase from the extreme thermophile *Thermus aquaticus*. *J. Bacteriol.* 127, 1550–1557.

Davies, G., and Henrissat, B. (1995). Structures and mechanisms of glycosyl hydrolases. *Structure* 3, 853–859. doi:10.1016/S0969-2126(01)00220-9

Dion, M., Fourage, L., Hallet, J. N., and Colas, B. (1999). Cloning and expression of a beta-glycosidase gene from *Thermus thermophilus*. Sequence and biochemical characterization of the encoded enzyme. *Glycoconj. J.* 16, 27–37. doi:10.1023/A:1006997602727

Dworkin, M., Falkow, S., Rosenberg, E., Schleifer, K. H., and Stackebrandt, E. (2006). *The Prokaryotes*. New York: Springer.

Fridjonsson, O., Watzlawick, H., Gehweiler, A., Rohrhirsch, T., and Mattes, R. (1999). Cloning of the gene encoding a novel thermostable alpha-galactosidase from *Thermus brockianus* ITI360. *Appl. Environ. Microbiol.* 65, 3955–3963.

Galperin, M. Y., and Koonin, E. V. (2012). Divergence and convergence in enzyme evolution. *J. Biol. Chem.* 287, 21–28. doi:10.1074/jbc.R111.241976

Gasteiger, E., Gattiker, A., Hoogland, C., Ivanyi, I., Appel, R. D., and Bairoch, A. (2003). ExPASy: the proteomics server for in-depth protein knowledge and analysis. *Nucleic Acids Res.* 31, 3784–3788. doi:10.1093/nar/gkg563

Gerard, F., Angelini, S., and Wu, L. F. (2002). Export of *Thermus thermophilus* cytoplasmic beta-glycosidase via the *E. coli* Tat pathway. *J. Mol. Microbiol. Biotechnol.* 4, 533–538.

Henrissat, B. (1991). A classification of glycosyl hydrolases based on amino acid sequence similarities. *Biochem. J.* 280(Pt 2), 309–316.

Henrissat, B., and Davies, G. (1997). Structural and sequence-based classification of glycoside hydrolases. *Curr. Opin. Struct. Biol.* 7, 637–644. doi:10.1016/S0959-440X(97)80072-3

Acknowledgments

This work was supported by the German Federal Ministry of Education and Research (BMBF) in the funding cluster "Biorefinery2021," and by Clariant Produkte (Deutschland) GmbH. This publication was supported by the German Research Foundation (DFG) and the Hamburg University of Technology (TUHH) in the funding program "Open Access Publishing". Thanks are also due to Bernard Henrissat for correspondence.

Ishida, M., and Oshima, T. (1994). Overexpression of genes of an extreme thermophile *Thermus thermophilus*, in *Escherichia coli* cells. *J. Bacteriol.* 176, 2767–2770.

Juers, D. H., Huber, R. E., and Matthews, B. W. (1999). Structural comparisons of TIM barrel proteins suggest functional and evolutionary relationships between beta-galactosidase and other glycohydrolases. *Protein Sci.* 8, 122–136. doi:10.1110/ps.8.1.122

Kim, D., Park, B. H., Jung, B. W., Kim, M., Hong, S., and Lee, D. (2006). Identification and molecular modeling of a family 5 endocellulase from *Thermus caldophilus* GK24, a cellulolytic strain of *Thermus thermophilus*. *Int. J. Mol. Sci.* 7, 571–589. doi:10.3390/i7120571

Kim, S. J., Lee, C. M., Kim, M. Y., Yeo, Y. S., Yoon, S. H., Kang, H. C., et al. (2007). Screening and characterization of an enzyme with beta-glucosidase activity from environmental DNA. *J. Microbiol. Biotechnol.* 17, 905–912.

Ku, T., Lu, P., Chan, C., Wang, T., Lai, S., Lyu, P., et al. (2009). Predicting melting temperature directly from protein sequences. *Comput. Biol. Chem.* 33, 445–450. doi:10.1016/j.compbiolchem.2009.10.002

Laemmli, U. K. (1970). Cleavage of structural proteins during the assembly of the head of bacteriophage T4. *Nature* 227, 680–685. doi:10.1038/227680a0

Lombard, V., Golaconda Ramulu, H., Drula, E., Coutinho, P. M., and Henrissat, B. (2014). The carbohydrate-active enzymes database (CAZy) in 2013. *Nucleic Acids Res.* 42, D490–D495. doi:10.1093/nar/gkt1178

Marchler-Bauer, A., Zheng, C., Chitsaz, F., Derbyshire, M. K., Geer, L. Y., Geer, R. C., et al. (2013). CDD: conserved domains and protein three-dimensional structure. *Nucleic Acids Res.* 41, D348–D352. doi:10.1093/nar/gks1243

Michaelis, L., and Menten, M. L. (1913). Die Kinetik der Invertinwirkung. *Biochem. Z.* 49, 333–369.

Nam, E. S., Kim, M. S., Lee, H. B., and Ahn, J. K. (2010). β-Glycosidase of *Thermus thermophilus* KNOUC202: gene and biochemical properties of the enzyme expressed in *Escherichia coli*. *Appl. Biochem. Microbiol.* 46, 515–524. doi:10.1134/S0003683810050091

Oshima, T. I., and Imahori, K. (1974). Description of *Thermus thermophilus* (Yoshida and Oshima) comb. nov., a nonsporulating thermophilic bacterium from a Japanese thermal spa. *Int. J. Syst. Bacteriol.* 24, 102–112. doi:10.1099/00207713-24-1-102

Pantazaki, A., Pritsa, D., and Kyriakidis, A. (2002). Biotechnologically relevant enzymes from *Thermus thermophilus*. *Appl. Microbiol. Biotechnol.* 58, 1–12. doi:10.1007/s00253-001-0843-1

Park, T. H., Choi, K. W., Park, C. S., Lee, S. B., Kang, H. Y., Shon, K. J., et al. (2005). Substrate specificity and transglycosylation catalyzed by a thermostable beta-glucosidase from marine hyperthermophile *Thermotoga neapolitana*. *Appl. Microbiol. Biotechnol.* 69, 411–422. doi:10.1007/s00253-005-0055-1

Sambrook, J., Fritsch, E., and Maniatis, T. (2001). *Molecular Cloning, A Laboratory Manual*, 3rd Edn. New York: Cold Spring Harbor Laboratory Press.

Schröder, C., Elleuche, S., Blank, S., and Antranikian, G. (2014). Characterization of a heat-active archaeal beta-glucosidase from a hydrothermal spring metagenome. *Enzyme Microb. Technol.* 57, 48–54. doi:10.1016/j.enzmictec.2014.01.010

Viikari, L., Alapuranen, M., Puranen, T., Vehmaanpera, J., and Siika-Aho, M. (2007). Thermostable enzymes in lignocellulose hydrolysis. *Adv. Biochem. Eng. Biotechnol.* 108, 121–145. doi:10.1007/10_2007_065

Wang, H., Ma, R., Shi, P., Xue, X., Luo, H., Huang, H., et al. (2014). A new alpha-galactosidase from thermoacidophilic alicyclobacillus sp. A4 with wide acceptor

specificity for transglycosylation. *Appl. Biochem. Biotechnol.* 174, 328–338. doi:10.1007/s12010-014-1050-8

Conflict of Interest Statement: The authors declare that the research was conducted in the absence of any commercial or financial relationships that could be construed as a potential conflict of interest.

frontiers in Bioengineering and Biotechnology

ORIGINAL RESEARCH
published: 29 February 2016
doi: 10.3389/fbioe.2016.00005

A New Thermophilic Nitrilase from an Antarctic Hyperthermophilic Microorganism

*Geraldine V. Dennett[1,2] and Jenny M. Blamey[1,2]**

[1] Fundación Científica y Cultural Biociencia, Santiago, Chile, [2] Doctorado en Biotecnología, Universidad de Santiago, Santiago, Chile

Several environmental samples from Antarctica were collected and enriched to search for microorganisms with nitrilase activity. A new thermostable nitrilase from a novel hyperthermophilic archaea *Pyrococcus sp*. M24D13 was purified and characterized. The activity of this enzyme increased as the temperatures rise from 70 up to 85°C. Its optimal activity occurred at 85°C and pH 7.5. This new enzyme shows a remarkable resistance to thermal inactivation retaining more than 50% of its activity even after 8 h of incubation at 85°C. In addition, this nitrilase is highly versatile demonstrating activity toward different substrates, such as benzonitrile (60 mM, aromatic nitrile) and butyronitrile (60 mM, aliphatic nitrile), with a specific activity of 3286.7 U mg^{-1} of protein and 4008.2 U mg^{-1} of protein, respectively. Moreover the enzyme NitM24D13 also presents cyanidase activity. The apparent Michaelis–Menten constant (K_m) and $V_{máx}$ of this Nitrilase for benzonitrile were 0.3 mM and 333.3 μM min^{-1}, respectively, and the specificity constant (k_{cat}/K_m) for benzonitrile was 2.05 × 10^5 s^{-1} M^{-1}.

Keywords: cyanidase, N-glycosylation, thermostable, nitriles, Antarctica

OPEN ACCESS

Edited by:
Noha M. Mesbah, Faculty of Pharmacy Suez Canal University, Egypt

Reviewed by:
Sam P. De Visser, University of Manchester, UK
Vasile I. Parvulescu, University of Bucharest, Romania
Michael Benedik, Texas A&M University, USA

***Correspondence:**
Jenny M. Blamey
jblamey@bioscience.cl

Specialty section:
This article was submitted to Process and Industrial Biotechnology, a section of the journal Frontiers in Bioengineering and Biotechnology

Received: *18 April 2015*
Accepted: *11 January 2016*
Published: *29 February 2016*

Citation:
Dennett GV and Blamey JM (2016) A New Thermophilic Nitrilase from an Antarctic Hyperthermophilic Microorganism. Front. Bioeng. Biotechnol. 4:5. doi: 10.3389/fbioe.2016.00005

INTRODUCTION

Chemical and pharmaceutical industries use a diversity of nitriles as feedstock material for the synthesis of a wide range of compounds, drug intermediates, pesticides (such as bromoxynil and dichlobenil), polymers and even solvents, such as acetonitrile (Jallageas et al., 1980; Cowan, et al., 1998; Prasad et al., 2007; DeSantis and DiCosimo, 2009). Nitriles are organic compounds containing in its structure a cyano group (-CN). They are transformed to carboxylic acids by several chemical processes, but these processes typically require strong acidic or basic conditions, high temperatures and usually produce unwanted byproducts and a lot of inorganic waste (Dash et al., 2009). This is not the case when this transformation is biocatalyzed by nitrilases making the transformation in a single step obtaining the respective carboxylic acid.

Nitriles (organic cyanide) are widely distributed in nature but most of them are chemically synthesized (Banerjee et al., 2002; Gong et al., 2012). Microorganism as well as plants are able to transform nitriles to the corresponding carboxylic acids and amides. These reactions are catalyzed by two different enzymes, nitrilase (EC 3.5.5.1) and nitrile hydratase (EC 4.2.1.84) (Arnaud et al., 1976).

In soil–water systems, the bioavailability and solubility of cyanide are also determining factors (Aronstein et al., 1994; Dash et al., 2006). Cyanide biodegradation can be carried out by more than one pathway in some organisms (Raybuck, 1992; Ezzi-Mufaddal and Lynch James, 2002; Akcil et al., 2003; Ebbs, 2004). Conditions such as oxygen, pH, and cyanide concentration determined

the metabolic pathway that will be involved in the degradation. Enzymes such as cyanide hydratase, forming formamide ($HCN + H_2O \rightarrow HCONH_2$), or cyanidase, which produces formate and ammonia ($HCN + 2H_2O \rightarrow HCOOH + NH_3$) (Ebbs, 2004) are involved in cyanide biodegradation.

Nitrilases are enzymes that catalyze the direct conversion of nitriles to their respective carboxylic acid with liberation of ammonia, while nitrile hydratase catalyze the formation of amides from nitriles.

Enzymatic biotransformation of nitriles has been considered an efficient alternative route with respect to chemical methods in industry, providing a very valuable alternative for efficiency, speed, and environmental friendliness. A great variety of nitrilases and nitrile hydratases and their applications in industry have been extensively studied (Arnaud et al., 1976; Mylerova and Martinkova, 2003; DeSantis and DiCosimo, 2009; Gong et al., 2012) for the production of amides and organic acid highly valued in industry (Ramakrishna et al., 1999) To perform the chemical synthesis of different compounds at elevated temperatures has many advantages for the industry, transfer rates improvement, substrate solubility enhancement, decrement in the viscosity of the solutions, and reducing the risk of contamination (Egorova and Antranikian, 2005). The relative instability of mesophilic nitrilases makes them to become inactivated at temperatures above 50°C (Harper, 1985; Kobayashi et al., 1990; Gong et al., 2012). For that reason, the interest in enzymes from thermophilic and hyperthermophilic microorganisms has increased and the fact that these proteins are resistant to chemical and physical denaturation and to proteolysis (Daniel et al., 1982; Egorova and Antranikian, 2005). Only two moderately thermo active nitrilases have been described so far. One of them was isolated from *Acidovorax facilis* 72W (Chauhan et al., 2003) and the second was isolated from *Bacillus pallidus* Dac521. This thermo active nitrilase has an optimum temperature of 65°C; however, after 13-min exposure to 70°C it is inactive (Almatawah et al., 1999). One thermostable recombinant nitrilase was isolated from *Pyrococcus abyssi* (Mueller et al., 2006). This nitrilase catalyzes the transformation of aliphatic nitriles mainly but inactive at concentrations above 12 mM of substrate malononitrile.

The growing need of new nitrile-degrading enzymes (Mathew et al., 1988; Wyatt and Linton, 1988) and the enzymatic detoxification of a nitrile-based herbicides (Harper, 1985; Stalker et al., 1988) along with the instability of mesophilic nitrile-metabolizing enzymes (Nagasawa et al., 1990) led us to investigate hyperthermophilic microorganisms as an alternative source of these activities (Cramp et al., 1997; Pereira et al., 1998; Mueller et al., 2006). In this work, we describe the purification and characterization of a new thermoactive nitrilase from the hyperthermophilic anaerobic archaeon *Pyrococcus* sp. M24D13 that it is able to use inorganic cyanides as substrate.

MATERIALS AND METHODS

Isolation of Microorganism and Culture Condition

Soil samples were collected from Fumarole Bay in Deception Island, Antarctica during the scientific expedition ECA 46. The nitrile-degrading microorganisms were isolated from these soil samples by serial dilutions using medium described by Mueller et al., 2006 containing nitriles.

The isolation of the microorganism was carried out under strict anaerobic conditions and has been identified through the analysis of its 16S rRNA gene complete sequence.

The microorganism M24D13 was cultivated anaerobically at 95°C in the following medium (pH 7.0) containing (per liter): 23.4 g NaCl, 10.8 g $MgCl_2 \times 6H_2O$, 4.0 g Na_2SO_4, 0.7 g KCl, 0.2 g $NaHCO_3$, 0.2 g $CaCl_2 \times 2H_2O$, 0.09 g KBr, 0.025 g $SrCl_2 \times 6H_2O$, 0.025 g H_3BO_3, 0.003 g NaF, 5 g elementary sulfur, 1 g yeast extract, 4 g peptone, 0.35 g KH_2PO_4, 0.7 g NH_4Cl, and 10 ml trace element solution according to Balch et al. (1979).

Phylogenetic Analysis of the 16S rRNA Gene Sequence and the Nitrilase NitM24D13 Sequence

Genomic DNA of the isolate was extracted using a phenol–chloroform protocol. The genomic DNA of the isolated microorganism was completely sequenced in Georgia Genomics Facility (GGF, University of Georgia, USA) obtaining from it the complete sequence of the 16S rRNA gene (GenBank, accession number SUB1008503 Pyrococcus_sp_M24D13 KT267175) and the NitM24D13 gene. Related sequences were obtained from GenBank database [National Center for Biotechnology Information (NCBI), Bethesda, MD, USA] PDB, SwissProt, PIR, and PRF using the BLAST search program. The sequences were aligned using multiple sequence alignment software, CLUSTAL W ver. 1.81. A phylogenetic tree was constructed with MEGA 5 software (Tamura et al., 2011) based on the information of complete 16S rRNA sequences of 13 strains similar to *Pyrococcus sp*. M24D13, using the method of *neighbor-joining* (Saitpu and Nei, 1987) with a bootstrap analysis of 1000 replicates.

Protein Assay

Protein was determined using the Bio-Rad Bradford kit according to Bradford (1976). Bovine serum albumin was used as standard.

Enzyme Assay

Nitrilase activity of the microbial enzyme was assayed by measuring the production of NH_3 during the hydrolysis of benzonitrile to benzoic acid by the method of Fawcett and Scott (1960). The standard assay was performed in duplicate at 80°C in tubes containing 0.9 ml of 30 mM benzonitrile in 100 mM phosphate buffer pH 8.0 with 2 mM EDTA, to which was added 0.1 ml of crude extract or purified protein. Mixtures were incubated for 5 min, after which time the reaction was terminated by the addition of 330 mM sodium phenoxide (1 ml), followed by 0.01% sodium nitroprusside (1 ml) and 20 mM sodium hypochlorite (1 ml). The assay mixture was thoroughly shaken, heated for 10 min at 95°C to allow color development, then diluted with water (6 ml), and the enzymatic activity was measured at an absorbance of 640 nm in a Shimadzu UV-VIS spectrophotometer.

For the measurement of cyanidase activity, potassium cyanide (KCN) was used as substrate replacing benzonitrilo to detect cyanidase in the standard assay shown above.

Purification of the Nitrilase from *Pyrococcus* sp. M24D13

All columns used in the protein purification were controlled by a Pharmacia FPLC (fast performance liquid chromatography) system.

Step I: Preparation of Cell-Free Extract

A cellular disruption method was specially designed for hyperthermophilic microorganisms. Washed cells (90 g) from 40 l of culture medium were suspended in 800 ml of 50 mM Tris–HCl buffer pH 7.0 containing 2 mM EDTA and lysozyme (3 mg ml^{-1}) and were incubated at 37°C for 60 min. Triton X100 was then added to a concentration of 4% v/v. The cell suspension was homogenized and incubated 15 min at 37°C. Then, it was disrupted by sonication for a total duration of 4 h using a sonicator bath (Branson sonifier 450). Cell debris was removed by centrifugation (17,968 × *g* for 40 min) and the supernatant solution was used as the crude extract for the purification. The crude extract was concentrated by ultrafiltration with Amicon cellulose membrane (M^r Cut-off 10,000).

Step II: Ammonium Sulfate Fractionation

Solid ammonium sulfate was added to the crude extract to give 55% saturation. After being stirred for 1 h, the suspension was centrifuged (17,968 × *g* for 20 min at 4°C), and the pellet was dissolved in Tris–HCl buffer (50 mM, pH 8.0), containing 2 mM EDTA (buffer A).

Step III: Hydrophobic Interaction Chromatography

After step II, ammonium sulfate was added to the protein solution in small portions with stirring to bring the solution to 1.6 M saturation. The enzyme solution was loaded onto a Octyl Sepharose column (GE Healthcare Life Sciences) pre-equilibrated with buffer A, containing 1.6 M $(NH_4)_2SO_4$. Bound proteins were eluted with a decreasing salt gradient (from 1 to 0 M) of $(NH_4)_2SO_4$ in buffer A, at a flow rate of 1 ml min^{-1}.

Step IV: Size Exclusion Chromatography

Active fractions were pooled, concentrated to a volume of 0.5 ml by ultrafiltration using an Amicon cellulose membrane (M^r cut-off 10,000), applied to a column (GE Healthcare, Tricorn 10/600) of Superdex-200 (Pharmacia Biotech), equilibrated with buffer A containing 0.2 M NaCl and eluted with the same buffer at a flow rate of 0.7 ml min^{-1}. The fractions with nitrilase activity were concentrated by ultrafiltration (PM-10 membrane filter; Amicon), and were stored at 4°C.

Step V: Ion Exchange Chromatography

The concentrated protein solution after size exclusion chromatography was applied to a 1 ml Q-HiTrap HP (GE Healthcare Life Sciences) anion exchange column. After loading the protein solution, the column was washed with buffer A until there was no further elution of protein. The enzyme was then eluted with a linear gradient of NaCl (from 0 to 1 M) in the same buffer for 90 min.

Protein fractions containing the nitrilase activity were analyzed by SDS-PAGE (polyacrylamide gel electrophoresis) according to Laemmli (1970) in 15% polyacrylamide gels with a Tris–Glycine buffer system.

Molecular Mass Determination

The apparent molecular mass of the native nitrilase was estimated by gel filtration chromatography on a column (GE Healthcare, Tricorn 10/600) of Superdex-200 (Pharmacia Biotech) equilibrated with buffer A containing 0.2 M NaCl and calibrated using urease 547 kDa, bovine glutamate dehydrogenase 300 kDa, bovine serum albumin 66 kDa, egg ovalbumin 45 kDa, and lysozyme 14.3 kDa as standard proteins. The void volume was determined using Blue dextran (2000 kDa). The enzyme relative molecular mass value under non-denaturating condition was determined from the semi-log plot of the standard protein molecular mass against K_{av} values. The subunit molecular mass of nitrilase was determined by SDS-PAGE (15%) according to the method of Laemmli (1970) using a BenchMark™ pre-stained protein ladder. SDS gel was stained for proteins with a silver stain protocol based on the method of Sammons et al. (1981).

Thermostability

For determination of nitrilase thermostability, the enzyme was placed in small tubes with O-ring-sealed caps and incubated for 14 h in a dry bath (Major Science, MD-02N-220) at 85°C. Samples were taken every hour and assayed for enzyme activity. Residual activity was determined at 80°C under the conditions described in Section "Enzyme Assay."

Effect of Metal Ions and Other Reagents

The effect of various reagents and salts of different metal ions (Ag^+ and Hg^{2+}) on the enzymatic activity was tested by pre-incubating the enzyme with these compounds in 100 mM phosphate buffer (pH 7.5) at room temperature for 5 min at a final concentration of 1–5 mM. Then, 3 mM benzonitrile was added and the standard activity was measured as described above.

RESULTS

Phylogenetic Analysis of the 16S rRNA Gene Sequence of M24D13

The phylogenetic analysis of complete 16S rRNA sequence of the isolated microorganism M24D13 shows that this microorganism belongs to the genus *Pyrococcus* and is related to the species *yayanossi*, as shown in the phylogenetic three (**Figure 1**).

Analysis of the Amino Acid Sequence of the Nitrilase NitM24D13 Gene

The complete amino acid sequence of the putative nitrilase present in the M24D13 genome was analyzed to verify that this sequence corresponds to a nitrilase. The conserved regions were detected at the positions of amino acids 41(E), 112(K), and 145(C). The cysteine residue (145 amino acid), which is involved in the currently known catalytic mechanism (Pace and Brenner, 2001) is absolutely conserved in all compared

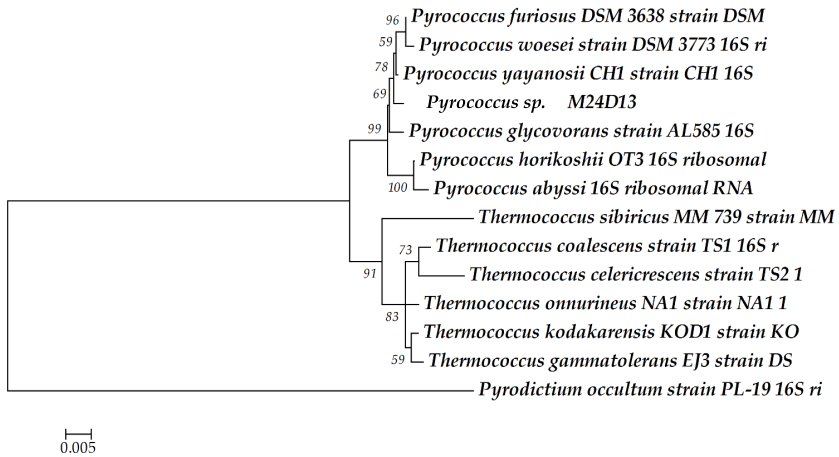

FIGURE 1 | Phylogenetic tree of the 16S rRNA gene sequence. The sequence obtained from the isolated microorganism M24D13 was compared with date base sequences available in GenBank to the Archaea domain, using *Pyrodictium occultum* as outgroup. The phylogenetic tree was made by Neighbor-joining method with 1000 bootstrap replicates.

sequences. Additionally, the N-terminal signature of already described microbial nitrilases KVA-x-VQ (Stalker et al., 1988; Hoyle et al., 1998; Mueller et al., 2006; Gong et al., 2012) was also identified in the sequence of nitrilase from the archaeal genome M24D13 (**Figure 2**). The results of the analyzed sequence allowed us to confirm that the examined gene corresponds to nitrilase.

Nitrilase Purification

A new nitrilase activity was purified to near homogeneity from benzonitrile-induced cells as described in methods using a combination of ammonium sulfate fractionation, hydrophobic interaction, gel filtration, and ion exchange chromatography. The nitrilase from *Pyrococcus sp*. M24D13 (NitM24D13) was purified 219-fold with a yield of approximately 4.7% from the cell-free extract using benzonitrile as substrate (**Table 1**) and SDS-PAGE analysis of fractions from the complete protocol are shown in **Figure 3**.

Molecular Mass Determination

The apparent molecular mass of the native nitrilase under non-denaturating condition was estimated in 38.5 kDa and the enzyme relative molecular mass of the subunit under denaturating condition was determine in 37 kDa.

Effect of Temperature, pH, and Thermostability

The influence of temperature on the specific activity was determined under standard assay conditions. The effect of pH on specific activity was measured as previously described at various pH values between 4.0 and 9.5 in EPPS (Sigma), CAPS (Sigma), phosphate (Winkler), and citrate (Winkler) buffers at the optimal temperature.

Optimal activity occurred at temperature of 85°C (at pH 7.5) and at pH around 5.5 (at 85°C) (**Figure 4**).The activity of the enzyme increased as the temperature changed from 70 to 85°C, diminishing at higher temperatures.

The thermostability of the nitrilase NitM24D13 was examined. **Figure 5** shows the remarkable resistance of this nitrilase to thermal inactivation. The enzyme retained more than 50% of its activity even after 8-h incubation at 85°C at an enzyme concentration of 0.035 mg ml^{-1}.

Substrate Specificity and Kinetic Behavior

The ability of the purified nitrilase from *Pyrococcus sp.* M24D13 to catalyze the hydrolysis of different nitriles was examined (**Figure 6**). The data indicate that nitrilase NitM24D13 can use a broad range of nitriles for its catalysis. There was a clear preference of the enzyme for phenylglycinonitrile and butyronitrile as substrates, suggesting that the enzyme is very versatile.

The specific activity of the purified nitrilase against benzonitrile was 3286.7 U mg^{-1} of protein. To study the affinity of the nitrilase from *Pyrococcus sp.* M24D13 toward benzonitrile, the kinetic parameters of the nitrilase were estimated over a range of benzonitrile concentration (0.5–3 mM) under standard assay condition. The maximal hydrolysis rate ($V_{máx}$) and apparent Michaelis–Menten constant (K_m) of nitrilase were calculated from Lineweaver Burk plot. K_m and $V_{máx}$ for benzonitrile were found to be 0.3 mM and 333.3 μM min^{-1}, respectively, and the specificity constant (k_{cat}/K_m) for benzonitrile was $2.05 \times 10^5\ s^{-1}\ M^{-1}$.

Effect of Metal Ions and Other Reagents

The enzyme shows high sensitivity for thiol binding metal ions such as Ag^+, Hg^{2+}. The relative activity was totally inhibited by Ag^+ and only 2.2% of its relative activity remained in the presence of Hg^{2+}. This indicates the importance of thiol group in the catalytic activity of this enzyme. The nitrilase of NitM24D13 exhibited great susceptibility to thiol-specific reagents, such as iodoacetamide (relative activity 18.5%).The presence of reducing agents, such as dithiothreitol (DTT) and glutathione, at a concentration

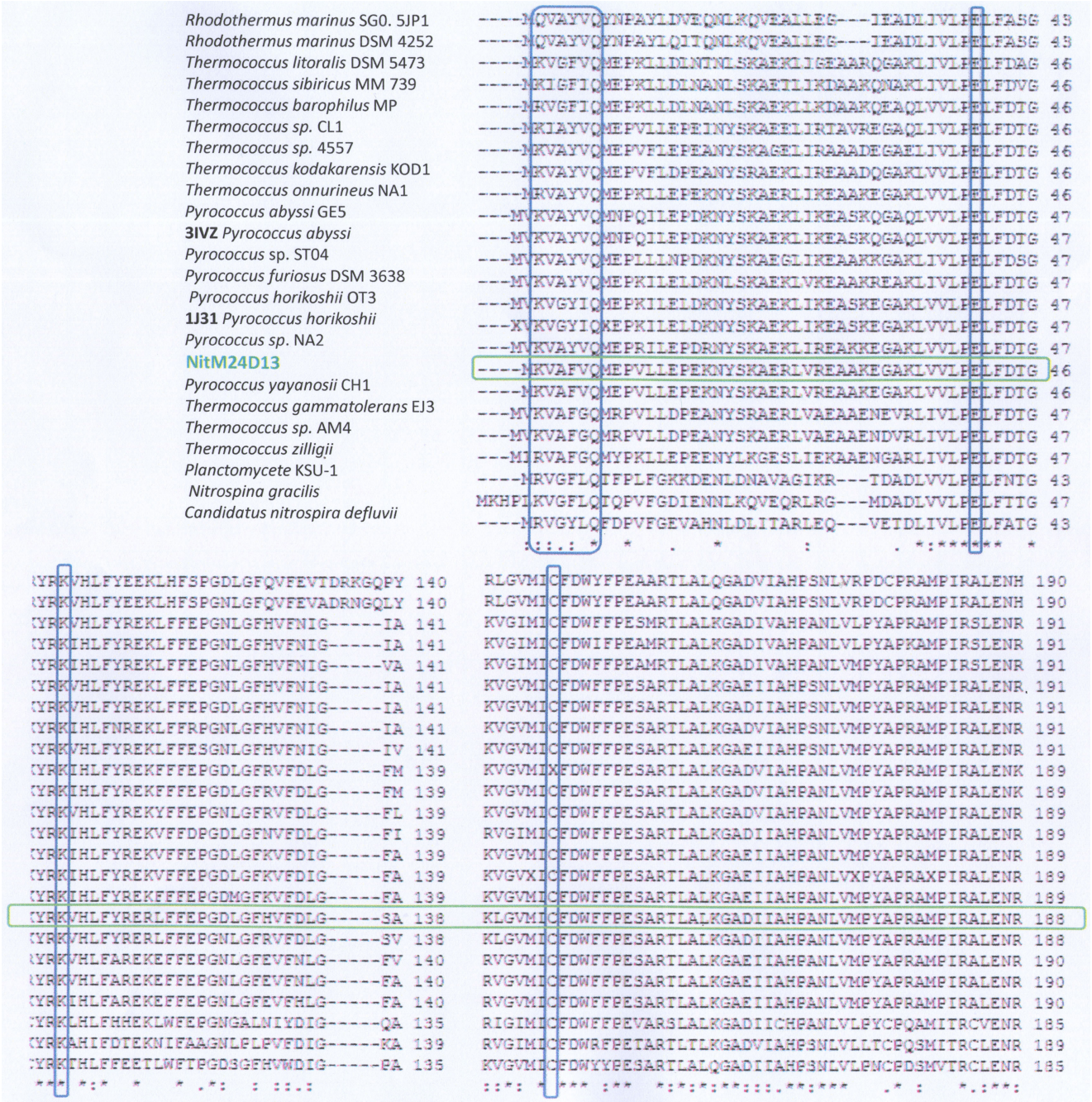

FIGURE 2 | Analysis of the amino acid sequence alignment of the nitrilase gene of M24D13 microorganism against GenBank, PDB, SwissProt, PIR, and PRF data bases using Clustal W software. The red marked columns indicate the amino acids that belong to the catalytic triad of the known nitrilase enzymes (E-K-C). The blue marked column corresponds to the consensus sequence present at the N-terminal for nitrilases. The green marked lane corresponds to the sequence of NitM24D13.

of 5 mM, was found to inactivate the nitrilase. These data indicate the involvement of the highly conserved cysteine residue in the catalytic mechanism (**Table 2**).

EDTA and KCN had no influence on the activity of the enzyme, suggesting that the nitrilase does not need divalent ions as cofactors for catalysis. Nitrilases are not metal-dependent enzymes that are consistent with the results obtained. In the presence of 5 mM KCN, a strong increase in the specific activity of 79.3% respect to the activity measured under standard conditions was observed, suggesting that the enzyme could also have cyanidase activity (**Table 2**). To verify this assumption, the nitrilase activity was determined using 1 and 5 mM KCN as sole substrate,

TABLE 1 | Summary of the purification protocol for nitrilase from M24D13.

Samples	Total activity (U)	U/ml	Total protein (mg)	Specific activity (U mg^{-1})	Volume (ml)	Yield (%)	Purification (fold)
Crude cell extract	4975.0	6.7	331.5	15.0	740	100	1
Ultrafiltrate crude cell extract (10 kDa)	3931.4	21.8	72.5	54.2	180	79	3.6
55% $(NH_4)_2SO_4$ fraction (p.p)	10,521.4	56.7	17.6	598.4	185.5	212	39.9
Octyl-Sepharose	5801.7	252.3	2.3	2533.2	23	117	168.8
Superdex-200	4388.9	319.2	1.7	2576.1	13.8	88	171.7
Q-Hi Trap HP	234.1	117.0	0.1	3286.7	2	5	219.0

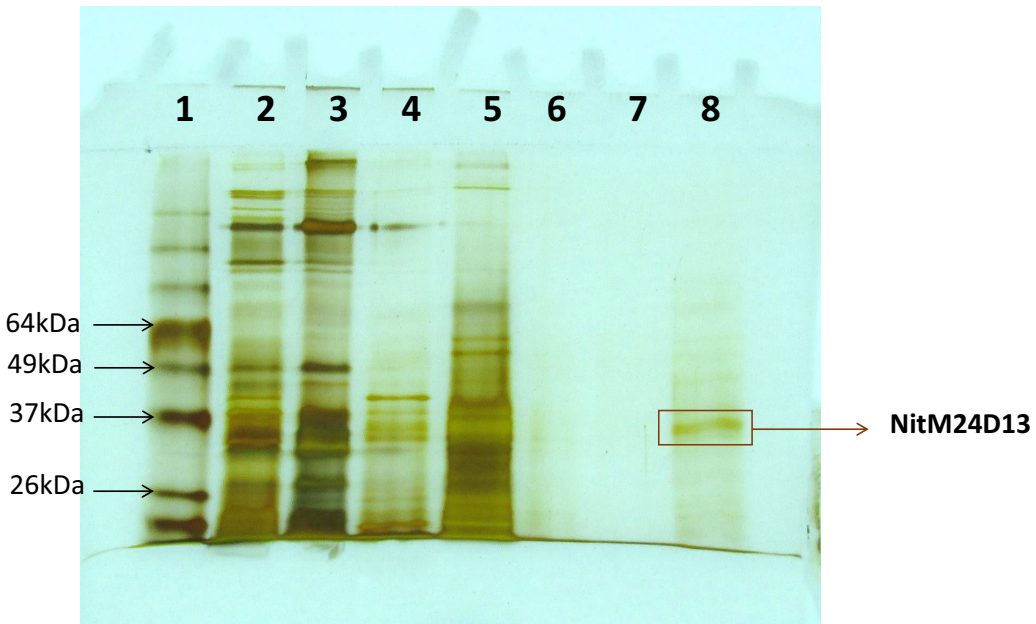

FIGURE 3 | SDS-PAGE (15%) gel electrophoresis of nitrilase fractions obtained from the purification protocol, stained with silver nitrate. The band marked on the gel corresponds to the band of interest. Lane 1, Bench Mark™ molecular weight marker (Invitrogen). Lane 2, Crude extract. Lane 3, concentrated crude extract. Lane 4, protein supernatant precipitated with 55% $(NH_4)_2SO_4$. Lane 5, fraction 10 from Octyl-Sepharose chromatography. Lanes 6 and 7 correspond to fractions 4 and 5 from Superdex-200 chromatography. Lane 8, fraction 4 from Q-HiTrap chromatography.

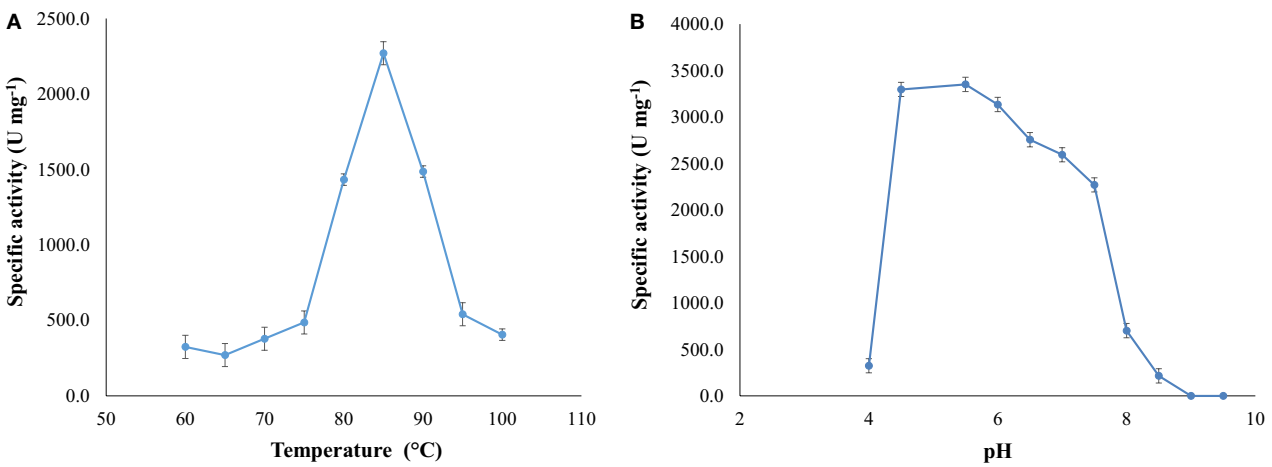

FIGURE 4 | (A) Optimal temperature for NitM24D13 nitrilase activity and **(B)** optimal pH for the NitM24D13 nitrilase activity. The error bars represent the SD of three independent experimental replicates.

obtaining 8954.8 and 13,245.6 U mg^{-1} of activity, respectively. The activity increased 256.1% and 426.7% respect to the activity measured under standard conditions, in the presence of 3 mM benzonitrile (**Table 3**).

DISCUSSION

The majority of currently known nitrilases from mesophilic bacterial species have been isolated from environmental samples in cultures grown using nitriles as sole nitrogen source (Layh et al., 1997). Most of them are often unstable at the temperatures optimal for growth of the microorganisms (Cowan, et al., 1998). The majority of nitrilases reported in the literature are quite labile at higher temperatures, like the *Rhodococcus rhodochrous* J1 nitrilase, which retains only 7% of its initial activity when incubated for 1 h at 50°C (Kobayashi et al., 1989). The enzymes derived from the hyperthermophilic microorganisms are more capable to do the catalysis at elevated temperatures as shown by the recombinant nitrilase from *P. abyssi* (Mueller et al., 2006). This enzyme exhibits high thermostability, after 9 h of incubation at 80°C, maintains 50% of its activity, being at 90°C the half-life of the enzyme 6 h. Due to that and to the constant demand by the industry, for new nitrilases with high stability toward temperature, substrate and product concentrations, we search for new hyperthermophilic microorganisms with potential nitrilase activity.

We found a new nitrilase that denominate NitM24D13. This enzyme has a maximum specific activity at 85°C. Thermostability of the purified nitrilase was also examined at 85°C. After 8 h of incubation at that temperature, the nitrilase NitM24D13 retains more than 50% of the specific activity. This observation indicates that the thermostability of NitM24D13 is very high and the enzyme is one of the two microbial nitrilases with highest values for activity compared to the half-life of nitrilase from *B. pallidus* Dac521 that is <3 min at 80°C (Almatawah, et al., 1999).

The majority of nitrilases described in the literature have a pH range for catalysis between 5.0 and 9.0 like nitrilases from *Alcaligenes faecalis* JM3 (Nagasawa, et al., 1990), *B. pallidus* Dac521 (Almatawah, et al., 1999), several *Rhodococcus* strains (Kobayashi, et al., 1992; Stevenson, et al., 1992), and *Pseudomonas fluorescens* DSM 7155 (Layh, et al., 1997). NitM24D13 has a tendency to catalyze the reaction at acid pH with an optimum at pH 5.5. However, the enzyme shows high activity in a wide pH range 4.5–7.5. This feature makes the enzyme suitable for the chemical industry.

The nitrilases described so far are homodimeric or multimeric, and some of them can be composed of 16 subunits (Kobayashi et al., 1990; Banerjee et al., 2002; Gong et al., 2012). Nitrilase from *Pyrococcus sp.* M24D13 was found to have a relative molecular mass of approximately 38.5 kDa as determined by size exclusion chromatography under non-denaturating conditions and the molecular mass determined in denaturing conditions was estimated as 37 kDa, which suggests that the enzyme is monomeric. Within the last few years only a few monomeric nitrilase has been described, one of them is from *R. rhodochrous* P34 and

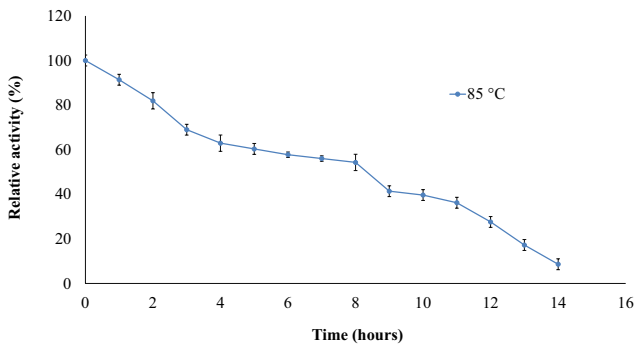

FIGURE 5 | Effect of temperature on the specific activity of NitM24D13 nitrilase as a function of time. The activity at initial time was considered as 100% of activity and correspond to 3135. 1 U mg^{-1}. The protein was maintained at 85°C. The error bars represent the SD of three independent experimental replicates.

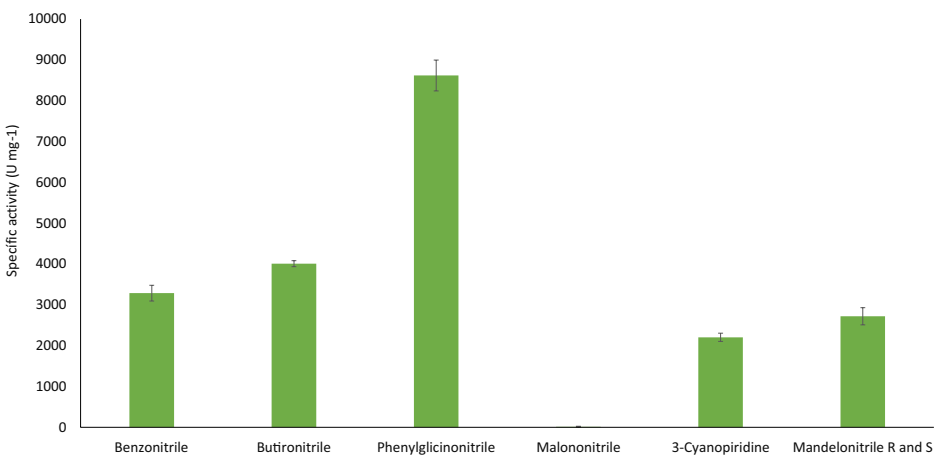

FIGURE 6 | NitM24D13 nitrilase specific activity in the presence of different substrates. The error bars represent the SD of three independent experimental replicates.

TABLE 2 | Effect of metallic ions and inhibitors on the NitM24D13 activity.

Inhibitor	Specific activity (U mg^{-1})	Residual activity (%)	Percentage of inhibition
None	2514.6	100.0	0
DTT 1 mM	1564.6	62.2	37.8
DTT 5 mM	0	0	100
Glutathione (reduced) 1 mM	1788.1	71.1	28.9
Glutathione (reduced) 5 mM	0	0	100.0
Iodoacetamide 1 mM	1490.1	59.3	40.7
Iodoacetamide 5 mM	4,65.7	18.5	81.5
$HgCl_2$ 1 mM	260.8	10.4	89.6
$HgCl_2$ 5 mM	55.9	2.2	97.8
$AgNO_3$ 5 mM	0	0	100.0
KCN 1 mM	2756.7	109.6	0
KCN 5 mM	4507.6	179.3	0

TABLE 3 | Cyanidase activity of NitM24D13 with KCN as substrate in the absence and presence of benzonitrile.

	Specific activity (U/mg)	%
Benzonitrile 3 mM	2514.6	100
Benzonitrile 3 mM + KCN 5 mM	4507.6	179.3
Benzonitrile 3 mM + KCN 1 mM	2756.7	109.6
KCN 5 mM	13,245.6	526.7
KCN 1 mM	8954.8	356.1

the other one is from *Arthrobacter* sp. J1 (Bandyopadhyay et al., 1986; Gong et al., 2012); for this reason, NitM24D13 is a different nitrilase to those already described enzymes. Nevertheless, it is necessary to determine the molecular mass of this protein in the presence of the substrate, by size exclusion chromatography under non-denaturating conditions to confirm if the active form of the enzyme is monomeric.

The molecular mass estimated by bioinformatic analysis of the amino acid sequence of NitM24D13 gives a mass value of approximately 30 kDa. This difference could be due to post-translational glycosylation in the microorganism increasing the molecular mass of the enzyme. It has been described the presence of glycosyltransferases in thermophilic and hyperthermophilic archaea that glycosylate proteins (Magidovich and Eichler, 2009; Calo et al., 2010). Although the N-glycosylation pathway in archaea is not yet fully understood, it is known that have certain similarities to the found in eukaryotic organisms. Oligosaccharides are transferred to the nascent protein in an asparagine residue (Asp) specifically located in an N-X-S/T motif characteristic for N-glycosylation, where X can be any amino acid except proline (Pro) (Yurist-Doutsch et al., 2008). This motif has also been identified in the amino acid sequence of NitM24D13 enzyme. Additionally, when the M24D13 genome of the microorganism was analyzed, the presence of several glycosyltransferases sequences was found. These glycosylations favor protein packaging, providing greater stability at elevated temperatures explaining the high thermostability of the enzyme at 85°C. In addition, protein glycosylation modified enzyme kinetics and decreases the effect of proteolysis on proteins (Shental-Bechor and Levy, 2008). These facts support the possibility that the enzyme NitM24D13 is glycosylated and, hence, the difference in molecular mass between the theoretical and experimental value is probably due to the presence of oligosaccharides in the protein structure. It is necessary to do further experimental studies to corroborate this assumption.

NitM24D13 nitrilase also presents a cyanidase activity by showing activity in the presence of KCN as sole substrate (**Table 3**), being a new hyperthermophilic enzyme that displays this type of behavior. This provides an added value to this enzyme for the biotechnological industry.

REFERENCES

Akcil, A., Karaham, A. G., Ciftci, H., and Sagdic, O. (2003). Biological treatment of cyanide by natural isolated bacteria (*Pseudomonas* sp). *Miner. Eng.* 16, 643–649. doi:10.1016/S0892-6875(03)00101-8

Almatawah, Q. A., Cramp, R., and Cowan, D. (1999). Characterization of an inducible nitrilase from a thermophilic bacillus. *Extremophiles* 3, 283–291. doi:10.1007/s007920050129

Arnaud, A., Galzy, P., and Jallageas, J. (1976). Nitrilase activity in several bacteria. *C. R. Acad. Sci. Hebd. Seances Acad. Sci.* 283, 571–573.

Aronstein, B. N., Maka, A., and Srivastava, V. J. (1994). Chemical and biological removal of cyanides from aqueous and soil-containing systems. *Appl. Biochem. Microbiol.* 41, 700–707. doi:10.1007/BF00167288

Balch, W. E., Fox, C. E., Magrun, L. G., Woese, C. R., and Wolfe, R. S. (1979). Methanogens: reevaluation of a unique biological group. *Microbiol. Rev.* 43, 260–296.

Bandyopadhyay, A., Nagasawa, T., Asano, Y., Fujishiro, K., Tani, Y., and Yamada, H. (1986). Purification and characterization of benzonitrilases from *Arthrobacter* sp. Strain J-1. *Appl. Environ. Microbiol.* 51, 302–306.

Banerjee, A., Sharma, R., and Banerjee, U. C. (2002). The nitrile-degrading enzymes: current status and future prospects. *Appl. Microbiol. Biotechnol.* 60, 33–44. doi:10.1007/s00253-002-1062-0

Bradford, M. (1976). A rapid and sensitive method for quantitation of microgram quantities of protein utilizing the principle of protein-dye-binding. *Anal. Biochem.* 72, 248–254. doi:10.1016/0003-2697(76)90527-3

Calo, D., Kaminski, L., and Eichler, J. (2010). Protein glycosylation in Archaea: sweet and extreme. *Glycobiology* 20, 1065–1076. doi:10.1093/glycob/cwq055

Chauhan, S., Wu, S., Blumerman, S., Fallon, R. D., Gavagan, J. E., DiCosimo, R., et al. (2003). Purification, cloning, sequencing and overexpression in *Escherichia coli* of a regioselective aliphatic nitrilase from *Acidovorax facilis* 72W. *Appl. Microbiol. Biotechnol.* 61, 118–122. doi:10.1007/s00253-002-1192-4

Cowan, D., Cramp, R., Pereira, R., Graham, D., and Almatawah, Q. (1998). Biochemistry and biotechnology of mesophilic and thermophilic nitrile metabolizing enzymes. *Extremophiles* 2, 207–216. doi:10.1007/s007920050062

Cramp, R., Gilmour, M., and Cowan D. A. (1997). Novel thermophilic bacteria producing nitrile-degrading enzymes. *Microbiol.* 143, 2313–2320. doi:10.1099/00221287-143-7-2313

Daniel, R., Cowan, D., Morgan, H., and Curran, M. (1982). A correlation between protein thermostability and resistance to proteolysis. *Biochem. J.* 207, 641–644.

Dash, R., Balomajumder, C., and Kumar, A. (2006). Cyanide removal by combined adsorption and biodegradation process. *Iran. J. Enviro. Health. Sci. Eng.* 3, 91–96.

Dash, R., Gaur, A., and Balomajumder, C. (2009). Cyanide in industrial wastewaters and its removal: A review on biotreatment. *J. Haz. Mat.* 163, 1–11. doi:10.1016/j.jhazmat.2008.06.051

DeSantis, G., and DiCosimo, R. (2009). "Aplications of nitrile hydratases and nitrilases," in *Biocatalysis for the Pharmaceutical Industry: Discovery,*

Development and Manufacturing, Vol. 8, eds J. Tao, G.-Q. Lin, and A. Lies (Singapore: John Wiley and Sons, Asia), 153–181.

Ebbs, S. (2004). Biological degradation of cyanide compounds. *Curr. Opin. Biotechnol.* 15, 231–236. doi:10.1016/j.copbio.2004.03.006

Egorova, K., and Antranikian, G. (2005). Industrial relevance of thermophilic Archaea. *Curr. Opin. Microbiol.* 8, 649–655. doi:10.1016/j.mib.2005.10.015

Ezzi-Mufaddal, I., and Lynch James, M. (2002). Cyanide catabolizing enzymes in *Trichoderma* spp. *Enzyme Microb. Technol.* 31, 1042–1047. doi:10.1016/S0141-0229(02)00238-7

Fawcett, J. K., and Scott, J. E. (1960). A rapid and precise method for the determination of urea. *J. Clin. Pathol.* 13, 156–159. doi:10.1136/jcp.13.2.156

Gong, J. S., Lu, Z. M., Li, H., Shi, J. S., Zhou, Z. M., and Xu, Z. H. (2012). Nitrilases in nitrile biocatalysis: recent progress and forthcoming research. *Microb. Cell Fact.* 11, 142–159. doi:10.1186/1475-2859-11-142

Harper, D. (1985). Characterization of a nitrilase from *Nocardia* sp. (*Rhodococcus* group) NCIB 11215, using *p*-hydroxybenzonitrile as sole carbon source. *Int. J. Biochem.* 17, 677–683. doi:10.1016/0020-711X(85)90364-7

Hoyle, A. J., Bunch, A. W., and Knowles, C. J. (1998). The nitrilases of *Rhodococcus rhodochrous* NCIMB 11216. *Enzyme. Microb. Technol.* 23, 475–482. doi:10.1016/S0141-0229(98)00076-3

Jallageas, A. C., Arnaud, A., and Galzy, P. (1980). Bioconversions of nitriles and their applications. *Adv. Biochem. Eng.* 14, 1–32. doi:10.1007/BFb0007187

Kobayashi, M., Nagasawa, T., and Yamada, H. (1989). Nitrilase of *Rhodococcus rhodochrous* J1. Purification and characterization. *Eur. J. Biochem.* 182, 349–356. doi:10.1111/j.1432-1033.1989.tb14837.x

Kobayashi, M., Yanaka, N., Nagasawa, T., and Yamada, H. (1990). Purification and characterization of a novel nitrilase of *Rhodococcus rhodochrous* K22 that acts on aliphatic nitriles. *J. Bacteriol.* 172, 4807–4815.

Kobayashi, M., Yanaka, N., Nagasawa, T., and Yamada, H. (1992). Primary structure of an aliphatic nitrile-degrading enzyme, aliphatic nitrilase, from *Rhodococcus rhodochrous* K22 and expression of its gene and identification of its active site residue. *Biochemistry* 31, 9000–9007. doi:10.1021/bi00152a042

Laemmli, U. K. (1970). Cleavage of structural proteins during the assembly of the head of bacteriophage T4. *Nature* 227, 680–685. doi:10.1038/227680a0

Layh, N., Hirrlinger, B., Stolz, A., and Knackmuss, H. J. (1997). Enrichment strategies for nitrile-hydrolysing bacteria. *Appl. Microbiol. Biotechnol.* 47, 668–674. doi:10.1007/s002530050993

Magidovich, H., and Eichler, J. (2009). Glycosyltransferases and oligosaccharyltransferases in Archaea: putative components of the N-glycosylation pathway in the third domain of life. *FEMS Microbiol. Lett.* 300, 122–130. doi:10.1111/j.1574-6968.2009.01775.x

Mathew, C., Nagasawa, T., Kobayashi, M., and Yamada, H. (1988). Nitrilase catalyzed production of nicotinic acid from 3-cyanopyridine in *Rhodococcus rhodochrous* J1. *Appl. Environ. Microbiol.* 54, 1030–1032.

Mueller, P., Egorova, K., Vorgias, C. E., Boutou, E., Trauthwein, H., Verseck, S., et al. (2006). Cloning, overexpression, and characterization of a thermoactive nitrilase from the hyperthermophilic archaeon *Pyrococcus abyssi*. *Protein Expr. Purif.* 47, 672–681. doi:10.1016/j.pep.2006.01.006

Mylerova, V., and Martinkova, L. (2003). Synthetic application of nitrile converting enzyme. *Curr. Org. Chem.* 7, 1279–1295. doi:10.2174/1385272033486486

Nagasawa, T., Mauger, J., and Yamada, H. (1990). A novel nitrilase, arylacetonitrilase of *Alcaligenes faecalis* JM3 purification and characterization. *Eur. J. Biochem.* 194, 765–772. doi:10.1111/j.1432-1033.1990.tb19467.x

Pace, H. C., and Brenner, C. (2001). The nitrilase superfamily: classication, structure and function. *Genome Biol.* 2, 1–9. doi:10.1186/gb-2001-2-1-reviews0001

Pereira, R., Graham, D., Rainey, F., and Cowan, D. (1998). A novel thermostable nitrile hydratase. *Extremophiles* 2, 347–357. doi:10.1007/s007920050078

Prasad, S., Misra, A., Jangir, V., Awasthi, A., Raj, J., and Bhalla, T. (2007). A propionitrile-induced nitrilase of *Rhodococcus* sp. NDB 1165 and its application in nicotinic acid synthesis. *World J. Microbiol. Biotechnol.* 23, 345–353. doi:10.1007/s11274-006-9230-5

Ramakrishna, C., Dave, H., and Ravindranathan, M. (1999). Microbial metabolism of nitriles and its biotechnological potential. *J. Sci. Ind. Res.* 58, 925–947.

Raybuck, S. A. (1992). Microbes and microbial enzymes for cyanide degradation. *Biodegradation* 3, 3–18. doi:10.1007/BF00189632

Saitpu, N., and Nei, M. (1987). The neighbor-joining method: a new method for reconstructing phylogenetic trees. *Mol. Biol. Evol.* 4, 406–425.

Sammons, D. W., Adams, L. D., and Nishizawa, E. E. (1981). Ultrsensitive silver-based color staining of peptides in poliacrilamide gel electroforesis. *Electrophoresis* 2, 135–141. doi:10.1002/elps.1150020303

Shental-Bechor, D., and Levy, Y. (2008). Effect of glycosylation on protein folding: a close look at thermodynamic stabilization. *Proc. Natl. Acad. Sci. U.S.A.* 105, 8256–8261. doi:10.1073/pnas.0801340105

Stalker, D. M., Malyj, L. D., and McBride, K. E. (1988). Purification and properties of a nitrilase specific for the herbicide bromoxynil and corresponding nucleotide sequence analysis of the *bxn* gene. *J. Biol. Chem.* 263, 6310–6314.

Stevenson, D., Feng, R., Dumas, F., Groleau, D., Mihoc, A., and Storer, A. (1992). Mechanistic and structural studies on *Rhodococcus* ATCC 39484 nitrilase. *Biotechnol. Appl. Biochem.* 15, 283–302.

Tamura, K., Peterson, D., Stecher, G., Nei, M., and Kumar, S. (2011). MEGA5: molecular evolutionary genetics analysis using maximun likelihood, evolutionary distance, and maximum parsimony methods. *Mol. Biol. Evol.* 28, 2731–2739. doi:10.1093/molbev/msr121

Wyatt, J. M., and Linton, E. A. (1988). "The industrial potencial of microbial nitrile biochemistry," in *Cyanide Compounds in Biology*, Vol. 140. eds D. Evered and S. Harnett (Chichester: Ciba foundation symposium, Wiley), 32–48.

Yurist-Doutsch, S., Chaban, B., VanDyke, D. J., Jarrell, K. F., and Eichler, J. (2008). Sweet to the extreme: protein glycosylation in Archaea. *Mol. Microbiol.* 68, 1079–1084. doi:10.1111/j.1365-2958.2008.06224.x

Conflict of Interest Statement: The authors declare that the research was conducted in the absence of any commercial or financial relationships that could be construed as a potential conflict of interest.

frontiers in Bioengineering and Biotechnology

ORIGINAL RESEARCH
published: 01 June 2015
doi: 10.3389/fbioe.2015.00074

Biochemical and structural characterization of enolase from *Chloroflexus aurantiacus:* evidence for a thermophilic origin

*Oleg A. Zadvornyy[1,2], Eric S. Boyd[3], Matthew C. Posewitz[4], Nikolay A. Zorin[2] and John W. Peters[1]**

[1] Department of Chemistry and Biochemistry, Montana State University, Bozeman, MT, USA, [2] Institute of Basic Biological Problems, Russian Academy of Sciences, Pushchino, Russia, [3] Department of Microbiology and Immunology, Montana State University, Bozeman, MT, USA, [4] Department of Chemistry and Geochemistry, Colorado School of Mines, Golden, CO, USA

Enolase catalyzes the conversion of 2-phosphoglycerate to phosphoenolpyruvate during both glycolysis and gluconeogenesis, and is required by all three domains of life. Here, we report the purification and biochemical and structural characterization of enolase from *Chloroflexus aurantiacus*, a thermophilic anoxygenic phototroph affiliated with the green non-sulfur bacteria. The protein was purified as a homodimer with a subunit molecular weight of 46 kDa. The temperature optimum for enolase catalysis was 80°C, close to the measured thermal stability of the protein which was determined to be 75°C, while the pH optimum for enzyme activity was 6.5. The specific activities of purified enolase determined at 25 and 80°C were 147 and 300 U mg^{-1} of protein, respectively. K_m values for the 2-phosphoglycerate/phosphoenolpyruvate reaction determined at 25 and 80°C were 0.16 and 0.03 mM, respectively. The K_m values for Mg^{2+} binding at these temperatures were 2.5 and 1.9 mM, respectively. When compared to enolase from mesophiles, the biochemical and structural properties of enolase from *C. aurantiacus* are consistent with this being thermally adapted. These data are consistent with the results of our phylogenetic analysis of enolase, which reveal that enolase has a thermophilic origin.

Keywords: enolase, thermal stability, origin, evolution, hydropathy, green sulfur bacteria

OPEN ACCESS

Edited by:
Noha M. Mesbah, Suez Canal University, Egypt

Reviewed by:
Luigi Mandrich, National Research Council, Italy
Chiranjeevi Thulluri, Jawaharlal Nehru Technological University Hyderabad, India

****Correspondence:***
John W. Peters, Department of Chemistry and Biochemistry, Montana State University, 230 Chemistry and Biochemistry Building, Bozeman, MT 59717, USA
john.peters@chemistry.montana.edu

Specialty section:
This article was submitted to Process and Industrial Biotechnology, a section of the journal Frontiers in Bioengineering and Biotechnology

Received: *30 March 2015*
Accepted: *08 May 2015*
Published: *01 June 2015*

Citation:
Zadvornyy OA, Boyd ES, Posewitz MC, Zorin NA and Peters JW (2015) Biochemical and structural characterization of enolase from Chloroflexus aurantiacus: evidence for a thermophilic origin. Front. Bioeng. Biotechnol. 3:74. doi: 10.3389/fbioe.2015.00074

Introduction

Enolase (2-phospho-D-glycerate hydrolyase, EC 4.2.1.11) catalyzes the conversion of 2-phosphoglycerate (2-PGA) to phosphoenolpyruvate (PEP) during both glycolysis and gluconeogenesis in all three domains of life (Ballou and Wold, 1957; Wold, 1971). Enolase is a metalloenzyme activated by cations of bivalent metals (Brewer, 1981), such as magnesium (Mg^{2+}). In bacteria, enolases are highly conserved enzymes and commonly exist as homodimers

Abbreviations: EnoCa, enolase-1 from *Chloroflexus aurantiacus*; FIRST, floppy inclusion rigid substructure topography; 2-PGA, 2-phosphoglycerate; PEP, phosphoenolpyruvate; PAGE, polyacrylamide gel electrophoresis; PEG, polyethylene glycol; PDB, protein data bank; R.m.s.d.s, root-mean-square deviations; SDS-PAGE, sodium dodecyl sulfate polyacrylamide gel electrophoresis.

with molecular weights in the range of 80–100 kDa; the mass of a single subunit ranges from 40 to 50 kDa. Intriguingly, purified enolase from the thermophilic bacteria *Thermotoga maritima* (Schurig et al., 1995) and *Thermus aquaticus* (Stellwag et al., 1973) have been reported to be octamers. However, enolase from the anaerobic, hyperthermophilic archaeon *Pyrococcus furiosus* was reported as a homodimer (Peak et al., 1994).

Crystal structures of enolase from a variety of taxonomic sources have been examined; however, the majority of studies have been focused on the structure of the homodimeric enolase from *Saccharomyces cerevisiae* (Chin et al., 1981; Lebioda et al., 1991; Wedekind et al., 1995; Brewer et al., 1998; Sims et al., 2006; Schreier and Hocker, 2010). In the *S. cerevisiae* enolase dimeric structure, each monomer consists of a carboxyl terminal catalytic site (Lebioda and Stec, 1988; Lebioda et al., 1989; Stec and Lebioda, 1990; Lebioda and Stec, 1991; Zhang et al., 1994), which is highly conserved in enolases from different microorganisms. In addition, upon binding of the substrate to the active site, several conformations of the loop regions near the active site have been observed in the structures of this enzyme. When co-crystallized with Mg^{2+} and 2-PGA or PEP, the *S. cerevisiae* enolase structure adopts a completely "closed" state. In the closed state, the flexible active site loops L1 (residues 36–43) from the lid domain and the L2 (residues 153–169) and L3 (residues 251–277) loops from the barrel domain are all in a closed conformation (**Figure 3**) (Larsen et al., 1996; Zhang et al., 1997; Sims et al., 2006). In contrast, in the apo state, the L1 motif is far removed from the active site and the L2 and L3 loops are in the "open" conformation (Lebioda and Stec, 1991). In addition to the dimeric structure described above, enolase has been shown to form asymmetric dimers in which the subunits adopt two different conformations (Sims et al., 2006; Schulz et al., 2011).

The catalytic mechanism of enolase has been studied in a number of phylogenetically distinct organisms, including representatives from Archaea, Bacteria, and Eukarya (Wold and Ballou, 1957b; Brewer, 1981; Reed et al., 1996; Zhang et al., 1997). From such studies, it is clear that all members of this superfamily share a common initial reaction step: the abstraction of the *R*-proton of a carboxylate substrate by a general base (Babbitt et al., 1996; Gerlt et al., 2005), represented by lysine 345 in *S. cerevisiae* enolase (Poyner et al., 1996). The resulting enolic intermediate is stabilized by a magnesium ion [Mg^{2+}(I)], in the conserved active site that interacts with the intermediate carboxylate group. Enolase is unique in that it is the only member of the enolase superfamily in which a reaction intermediate is coordinated by a second catalytic magnesium ion [Mg^{2+}(II)]. Mg^{2+}(II) interacts with one carboxylate oxygen and a phosphate group oxygen of the substrate 2-PGA. In *S. cerevisiae* enolase, serine 39 in the L1 motif of the lid domain is the only residue that directly interacts with Mg^{2+}(II), while two water molecules positioned by aspartate 321 complete the coordination sphere of Mg^{2+}(II) (Zhang et al., 1994; Larsen et al., 1996). Both magnesium ions [e.g., Mg^{2+}(I) and Mg^{2+}(II)] are thought to participate in the crucial first step of the enolase reaction, the ionization of 2-PGA to give the negatively charged enolic intermediate and the stabilization thereof.

In the second step of the enolase reaction, the general acid glutamate 211 facilitates the dissociation of the hydroxide to form PEP (Larsen et al., 1996; Poyner et al., 1996; Reed et al., 1996). Enolase mutants in which serine at the position 39 in the L1 loop is substituted for asparagine retain basal catalytic enolase activity with coordination of Mg^{2+}(I) and 2-PGA in an "open" active site that does not require the Mg^{2+}(II) coordination residues (Schreier and Hocker, 2010). Interestingly, a structure of enolase from the anaerobic protozoan *Entamoeba histolyca* contains 2-PGA in the active site and exists in the open conformation; the Mg^{2+}(II) ion is absent from the active site (Schulz et al., 2011).

The widespread taxonomic distribution of enolase in Bacteria and Archaea (Tracy and Hedges, 2000), coupled with its fundamental role in glycolysis and gluconeogenesis (Wold, 1971; Fothergill-Gilmore and Michels, 1993; Ronimus and Morgan, 2003), strongly suggests that enolase was present in the Last Universal Common Ancestor (LUCA) of Bacteria and Archaea. Evidence derived from the characteristics of deeply branching taxa on the universal tree of life suggests that LUCA may have been a thermophile (Pace, 1991; Ronimus and Morgan, 2003; Lineweaver and Schwartzman, 2003). Proteins isolated from thermophilic microorganisms exhibit properties relative to their mesophilic counterparts that allow them to function in these extreme environments (Miller, 2003).

In the present study, we purified enolase-1 from *Chloroflexus aurantiacus* (EnoCa), a thermophilic green non-sulfur bacterium that grows photosynthetically under anaerobic conditions. Members of the green sulfur bacteria are thought to have emerged early in the evolution of photosynthetic metabolisms, whereby green sulfur bacteria gave rise to gram positive *Heliobacteriales* capable of photosynthesis, followed by the emergence of photosynthesis in cyanobacteria (Gupta et al., 1999; Xiong et al., 2000). Detailed biochemical and structural analysis of EnoCa reveal features that are consistent with adaptation to high temperature. These results, in the context of our phylogenetic work indicating enolase has a thermophilic origin, confirm adaptation of this enzyme to high temperature and suggest that EnoCa emerged from a thermophilic ancestor. Comparison of biochemical and structural features of EnoCa with enolase from phylogenetically diverse microorganisms reveal a number of common features that are likely to confer thermostability to members of this enzyme superfamily.

Materials and Methods

Growth Conditions of *C. aurantiacus*

Chloroflexus aurantiacus strain J.10.fl. (courtesy of Dr. Mikhail F. Yanyushin) was grown in 1 L screw-capped bottles illuminated by two pairs of 100 W incandescent lamps at 56°C in a modified Castenholz Medium (Castenholz, 1969; Yanyushin, 1988) (Tables S1 and S2 in Supplementary Material), or in 100 L fermenters stirred at 200 rpm and bubbled with nitrogen gas passed through a 0.2 μm filter (Fisher Scientific, Ireland). Fermenters were illuminated by five 150 W incandescent lamps.

Purification of EnoCa

Cultures of *C. aurantiacus* were harvested in mid-exponential growth phase by centrifugation (6,000 × *g*, 25 min). Cell pellets (100 g) were washed twice with Tris-HCl buffer (50 mM, pH 8.0). Following washing, the cell pellet was re-suspended in Tris-HCl

buffer (50 mM, pH 8.0) and sonicated using a Branson Sonifier 450 (VWR Scientific, USA) at 40% power for 5 min at 4°C. This process was repeated two additional times. Unbroken cells and cell fragments were pelleted by centrifugation (14,000 × *g*, 40 min, 4°C). Following centrifugation, the cell free extract was diluted 10-fold with Tris-HCl buffer (5 mM, pH 8.0), and ~570 mg were applied to Q-sepharose column (GE Healthcare, Sweden) equilibrated with Tris-HCl buffer (50 mM, pH 8.0). A linear gradient of 0.05–1.00M NaCl in Tris-HCl buffer (50 mM, pH 8.0) was applied to the column at a flow rate of 3.5 ml min^{-1}. Enolase fractions with activity eluted at ~0.5M NaCl. These fractions were combined and concentrated using a Molecular Stirred cell (Spectrum Laboratories, Inc., USA). Concentrated protein (~250 mg) was loaded onto a Sephacryl S-300 (Pharmacia, Sweden) gel filtration column (2.5 × 100 cm) at a flow rate 1 ml min^{-1}. Fractions that exhibited enolase activity were combined and subjected to further purification using a hydrophobic Octyl Sepharose column (GE Healthcare, Sweden). The column was equilibrated with 0.8M NaCl in Tris-HCl buffer (50 mM, pH 8.0). A linear gradient of 0.8–0.0M NaCl was applied to the column with a flow rate 2.5 ml min^{-1}. The active enolase fractions were combined and desalted using a Sephadex G-25 (GE Healthcare, Sweden). The purity of protein sample was confirmed by SDS-PAGE. Purified enolase was stored in liquid nitrogen until further biochemical and structural characterization.

EnoCa Protein Concentration and Kinetic Assays

The concentration of protein in these samples was determined using the Bradford Assay (Bradford, 1976) with bovine serum albumin as a standard. The activity of purified EnoCa was determined by monitoring the conversion of 2-PGA to PEP. PEP absorbs at 240 nm and was quantified over time in a temperature-controlled assay using a Cary50-Bio-UV-Visible spectrophotometer. The assay contained 1.5 mM PGA, 5 mM $MgCl_2$ in Bis-Tris propane (50 mM, pH 6.5), and enolase (12 µg), unless otherwise stated. The change in PEP concentration was determined using an absorption coefficient ($\varepsilon_{240\text{-}25t}$) = 1.7 mM^{-1} cm^{-1} at 25°C and ($\varepsilon_{240\text{-}80t}$) = 1.2 at mM^{-1} cm^{-1} at 80°C. The absorption coefficient of PEP varies with pH, concentration of Mg^{2+}, and temperature. Corrected molar absorptivity for PEP was used in experiments where pH, Mg^{2+} concentration, and temperature were varied (Wold and Ballou, 1957a,b). One unit (U) of the enzyme activity was defined as the amount of enolase that converts 1 µmol of 2-PGA into PEP in 1 min at 80°C, unless otherwise stated. Michaelis–Menten kinetic parameters were determined from curves generated by plotting the concentration of substrate p as a function of reaction velocity. The standard reaction mixture contained 1.5 mM 2-PGA, 5 mM $MgCl_2$ in 50 mM Bis-Tris propane (pH 6.5), and enolase sample (12 µg). The 2-PGA concentrations varied from 0.04 to 12 mM, while Mg^{2+} concentrations ranged from 0.05 to 20 mM. The reaction was initiated by the addition of 12 µg of enzyme. To determine the Mg^{2+} kinetic parameters, the enzyme was subjected to an additional round of purification using a PD-10 (Sephadex™ G-25, GE Healthcare, Sweden) desalting column equilibrated with Bis-Tris propane buffer (50 mM, pH 6.5) free of Mg^{2+}. To investigate the effect of the Tris-HCl (50mM, pH 8.0), HEPES (50 mM, pH 8.0), or Bis-Tris propane (50 mM, pH 8.0) buffer on the enolase activity, the protein was exchanged on Sephadex G-25 column equilibrated with the corresponding buffer.

Thermal Stability and Temperature Optimum of Enzyme

To investigate the thermal stability of the EnoCa, protein samples were heated for 5 min at the specified temperature (25–90°C), and then placed immediately on ice before being added to the reaction mixture. The activity of heat-treated enzymes was determined using the methods described above at a temperature of 25°C. The optimum temperature for the activity of enolase was determined by evaluating activity over the range of temperatures spanning 25–90°C. Three replicate measurements for each of the experiments described above were made at each sampling interval, and replicate measurements did not vary by more than 5%.

Crystallization and Data Collection

Crystals of EnoCa were obtained by the hanging drop vapor diffusion method at 18°C in 2 µl drops containing a 1:1 protein:reservoir solution ratio. The reservoir solution contained 0.8 ml of Bis-Tris propane buffer (0.1M, pH 9.0), 0.21M NaCl, and 28% PEG 1500. Crystals were cryoprotected by soaking them in the reservoir solution containing an additional 20% (v/v) glycerol, and they were then flash frozen in liquid nitrogen prior to data collection. The crystal composition was confirmed by SDS-PAGE and liquid chromatography–mass spectrometry analysis. Diffraction data were collected at 100 K at the Stanford Synchrotron Radiation Lightsource beamline 9-2, using the MARmosaic 325 CCD Detector (Menlo Park, CA). Data collected from EnoCa crystals were processed and scaled by XDS (Kabsch, 2010).

The structure was solved by molecular replacement (Winn et al., 2011) using the *Enterococcus hirae* enolase structure [PDB entry 1IYX (Hosaka et al., 2003)] as a search model. Model building was performed in Coot (Emsley et al., 2010). Coordinates were refined to reasonable stereochemistry at a resolution 2.30–3.04 Å using REFMAC5 (Murshudov et al., 1997). The structure was validated using MolProbity (Chen et al., 2010). All molecular images were calculated in PyMol (Delano, 2002). Calculation of root-mean-square deviations (r.m.s.d) was performed with the program LSQKAB (Winn et al., 2011). Structures are submitted to PDB entry 4YWS (native), 4Z17 (with PEP), 4Z1Y (with PGA).

Amino Acid Sequence Comparison and Homology Modeling

Amino acid sequences of enolases from *P. furiosus* (NP_577944), *T. maritima* (NP_228685), *T. aquaticus* (ZP_03497734), *Plasmodium falciparum* (XP_001347440), *Escherichia coli* (1E9I_A), *Candida albicans* (XP_711912), *S. cerevisiae* (1EBG_A), and *Trypanosoma brucei* (2PTW_A) were obtained from the NCBI/BLAST/BLASTP server.[1] The ProtParam tool, available from the ExPASy server,[2] was used to calculate the percentage amino acid composition (Gasteiger et al., 2003). Homology models containing one subunit of enolase from *P. furiosus*, *T. maritima*, *T. aquaticus*, *P. falciparum*, *C. albicans*,

[1] http://blast.ncbi.nlm.nih.gov
[2] http://web.expasy.org/protparam/

S. cerevisiae, and *T. brucei* were generated by SWISS-MODEL (Arnold et al., 2006).

Structural Rigidity Analysis

Homology models were used to perform structural rigidity analysis. The program Floppy Inclusion Rigid Substructure Topography (FIRST) (Jacobs et al., 2001) was used to perform flexibility analysis and to calculate the number of probable (i) hydrogen bonds, (ii) rigid clusters, (iii) sites in the largest rigid cluster, and (iv) the total independent degrees of freedom. Using covalent bonds, hydrophobic tethers, hydrogen bonds, and salt bridges, FIRST defines the constraint network. Based on the constraint network, the program identifies compared parameters of rigid and flexible regions of the protein (Jacobs et al., 2001; Rader et al., 2002). Relationships between calculated and measured protein parameters and optimal growth temperature were determined using XL Stat (ver. 2008.7.03). Pearson correlation coefficients and *P*-values were generated from 1000 permutations of the data.

Evolutionary Analyses

Enolase-1 sequences were compiled from the DOE-IMG database using enolase-1 sequence from *E. coli* K12 (NP_417259) as a query. All representative sequences were aligned using ClustalX (ver. 2.0) (Larkin et al., 2007) employing the Gonnett substitution matrix with default parameters. A neighbor-joining tree was used to empirically identify sequences that represent the primary phylogenetic lineages. Representative enolase-1 sequences were realigned as described above and the alignment block was subjected to evolutionary model prediction using ProtTest (ver. 2.4).(Abascal et al., 2005) Phylogenetic reconstruction was performed with the neighbor-joining method specifying the JTT substitution matrix and gamma distributed rate variation ($\gamma = 0.93$) with MEGA4 (Tamura et al., 2007) The pairwise deletion option was specified and enolase-2 sequences from *Methanothermobacterium thermoautotrophicum* strain delta H and *Archaeoglobus fulgidus* DSM 4304 served as out groups. The phylogenetic tree was projected from 100 bootstrap replicates using FigTree (ver. 1.2.2).[3]

Results

Thermophilic Origin and Properties of Thermal Adaptation of Enolase from *C. aurantiacus*

EnoCa shares significant sequence identity with enolases from other organisms distributed across Bacteria and Archaea (alignment not shown). Phylogenetic reconstruction of representative bacterial and archaeal enolase-1 sequences, when rooted with enolase-2, reveal a number of early branching lineages that are derived from thermophilic or hyperthermophilic organisms (**Figure 1**). Such an observation is consistent with a thermophilic origin for enolase-1. EnoCa-1 from *C. aurantiacus*, which is characterized here, forms a lineage with other green non-sulfur bacteria that branches late among thermophilic enolase. Nevertheless, these results suggest that the properties of EnoCa are likely to reflect those of the thermophilic ancestor to a greater extent than more recently derived mesophilic representatives.

[3]http://tree.bio.ed.ac.uk/software/figtree/

The amino acid composition and flexibility analysis of EnoCa together with enolases from *P. furiosus*, *T. maritima*, *T. aquaticus*, *P. falciparum*, *C. albicans*, *S. cerevisiae*, and *T. brucei* are given in **Table 1**. Despite the high level of sequence conservation among enolases, EnoCa has a higher percentage of aliphatic amino acids when compared to enolases from non-thermophilic taxa. The Pearson correlations (r) between optimal growth temperature of microorganisms and parameters associated with EnoCa properties have been calculated to establish positive and negative relationships between these parameters. The results indicate that hydrophobocity indices, aliphatic indices, the total number of sites in the rigid cluster, and the total independent degrees of freedom varied positively and to a significant extent ($P < 0.05$) with the optimal growth temperature of the strains. In contrast, the relative abundance of polar amino acids, hydrogen bonds, and total number of clusters in the rigid cluster varied inversely with the optimal growth temperature of the strains (Table S3 in Supplementary Material). In addition, the EnoCa structure reveals differences relevant to thermostable proteins, such as the residues that form the loops (138–143, 189–207, and 247–268 in EnoCa) being shorter than the corresponding residues of *S. cerevisiae* enolase (**Figure 3**; Figure S6 in Supplementary Material).

Biochemical Characterization of Enolase from *C. aurantiacus*

EnoCa was purified as a dimer with a molecular weight of ~92–96 kDa (**Table 2**; Figures S1–S3 in Supplementary Material). The subunit molecular weight of enolase was determined to be ~46.0 kDa using SDS-gel electrophoresis (Figure S2 in Supplementary Material). The activity of EnoCa was highest (124 ± 5 U mg^{-1} of protein at 25°C) in Bis-Tris propane buffer, with roughly a 25 and 47% decrease in activity when the enzyme was exchanged in Tris-HCl and HEPES, respectively. EnoCa activity was examined over a pH range of 6.0–10.0 in 50 mM Bis-Tris propane; the optimum pH for the catalytic activity of enolase was determined to be 6.5 (**Figure 2A**). EnoCa exhibited thermostability at temperatures up to 90°C, as indicated by retention of ~45% of the activity at this temperature when compared to that at 75°C. The temperature optimum for the assay reactions in 50 mM Bis-Tris propane buffer (pH 6.5) was 80°C in comparison to 55°C for the *S. cerevisiae* enolase (**Figures 2B,C**).

The K_m of EnoCa for 2-PGA and Mg^{2+} at 25 and 80°C were determined from measurements of initial rates of the reactions using the Lineweaver-Burk method (Lineweaver and Burk, 1934). EnoCa displayed classical Michaelis–Menten kinetics for both 2-PGA and Mg^{2+}. The enzyme had a lower K_m for both 2-PGA (0.035 ± 0.00 mM) and Mg^{2+} (1.9 ± 0.3 mM) at 80°C, when compared to the K_m for these substrates as determined at 25°C (0.16 ± 0.01 and 2.5 ± 0.2 mM, respectively). As expected, the V_{max} for 2-PGA (50 ± 1 μmol min^{-1} mg^{-1}) and Mg^{2+} (36 ± 2 μmol min^{-1} mg^{-1}) was higher at 80°C, when compared to that at 25°C (9 ± 1 μmol min^{-1} mg^{-1} and 17 ± 2 μmol min^{-1} mg^{-1}, respectively) (**Table 3**; Figures S4 and S5 in Supplementary Material). It should be noted that concentrations of at least 10 mM Mg^{2+} inactivated EnoCa (data not shown).

FIGURE 1 | Phylogenetic reconstruction of representative enolase-1 sequences as determined using the neighbor-joining method. Lineages represented by thermophiles are colored red. Parsimony was used to designate thermophilic lineages in cases where both thermophilic and non-thermophilic taxa were present. Bootstrap support values are designated at nodes.

Structural Characterization of Enolase from *C. aurantiacus*

EnoCa was crystallized under multiple conditions; however, the best crystals were obtained using 0.21M NaCl and 28% PEG 1500. High-resolution crystal structures were obtained for the apo protein as well as proteins with 2-PGA and PEP bound in the active site. The enolase crystals belonged to space group *I*4, which contained two monomers per asymmetric unit assembled

TABLE 1 | Amino acid composition and flexibility analysis of enolases from different microorganisms.

Organism	Growth temp, °C	pI	Amino acid composition, %							Flexibility analysis			
			Amino acids				Residues		AI[f]	H bonds	Rc	#Rc	df
			Hydrophobic[a]	Charged[b]	Polar[c]	Gly	Neg[d]	Pos[e]					
P. furiosus	100	4.98	48.8	27.4	14.7	9.1	64	45	97.74	295	1657	155	622
T. maritima	80	4.93	47.2	28	16.6	8.2	66	48	98.01	290	1575	526	656
T. aquaticus	70	5.01	47.5	27.7	13.7	11.1	64	47	98.27	296	1590	496	590
C. aurantiacus	**55**	**4.99**	**48.3**	**25.1**	**17.4**	**9.2**	**58**	**42**	**99.25**	**354**	**915**	**3405**	**525**
E. coli	37	5.32	45.6	26.4	17.1	10.9	59	48	89.12	344	1468	908	535
C. difficile	37	4.58	46.7	26	16.3	10.9	68	41	96.42	343	1389	1608	496
P. falciparum	37	6.21	45.8	25.1	21.7	7.4	55	53	97.35	361	905	3980	502
C. albicans	37	5.54	46.5	25.7	18.9	8.9	57	49	92.09	392	911	3620	455
S. cerevisiae	30	6.17	46	27.1	18.4	8.5	56	51	90.69	405	852	3826	406
T. brucei	27	5.93	43.8	26.6	20	9.6	56	51	84.41	399	589	4647	386

[a] *Total number of hydrophobic amino acids: alanine, leucine, isoleucine, valine, proline, phenylalanine, tyrosine, tryptophan, and methionine.*
[b] *Total number of charged amino acids: asparagine, glutamate, arginine, and lysine.*
[c] *Total number of polar amino acids: asparagine, glutamine, serine, threonine, and cysteine.*
[d] *Total number of negatively charged amino acids: asparagine and glutamate.*
[e] *Total number of positively charged amino acids: arginine and lysine.*
[f] *AI – The aliphatic index of proteins is defined as the relative volume occupied by aliphatic side chains (alanine, valine, isoleucine, and leucine)*
pI, principle isoelectric point; neg, negative; pos, positive; AI, aliphatic index; H bonds, hydrogen bonds; Rc, rigid clusters; #Rc, total number of sites in rigid cluster; df, total independent degrees of freedom.
Bold font indicates that the data presented in the tables are from this work.

TABLE 2 | The purification of EnoCa.

Stages of purification	Total protein, mg	Activity			Degree of purification
		Specific[a], U/mg	Total, units	Yield, %	
Crude extract	570.1 ± 13.5	0.76 ± 0.03	433 ± 15	100	1
Chromatography on Q-sepharose	250.3 ± 9.8	1.28 ± 0.05	320 ± 12	74 ± 2	2 ± 0
Gel filtration on sephacryl S-300	20.8 ± 0.8	12.4 ± 0.3	258 ± 11	59 ± 2	16 ± 1
Chromatography on octyl-sepharose	1.1 ± 0.1	147 ± 6	162 ± 7	37 ± 1	213 ± 2

[a] *1 unit of enolase activity (μmol PEP min^{-1}) was measured at 25°C.*

into one homodimer (Table S4 in Supplementary Material). Each monomer of EnoCa contains an amino terminal domain that consists of a three-stranded β-sheet packed against three α-helices and a carboxy terminal domain that consists of an eightfold α/β-barrel (**Figure 3**); both domain features are typical of the enolase superfamily.

The structure of the apo protein and that containing 2-PGA (2-PGA EnoCa structure) of EnoCa exhibits the so-called "open" conformation, where the L1 loop is away from the active site. The EnoCa structure containing PEP (PEP EnoCa structure) exhibits the so-called "closed" conformation, where the L1 loop is located closer to the active site (**Figures 4A,B**). Upon superposition with the apo EnoCa structure in the open conformation, the L1 loop in the 2-PGA EnoCa structure (open conformation) displays an r.m.s.d. of 0.38 Å, whereas the PEP EnoCa structure superimposed on the apo EnoCa structure (closed conformation) has r.m.s.d. 3.1 Å.

The remaining electron density was visible in the active site, after refinement of all protein structures. In the beginning of the apo EnoCa structure refinement, the difference map peaks were refined placing Mg^{2+}(I) atom in coordination with Asp241, Glu285, and Asp313, and then three water molecules in an octahedral manner (**Figures 5A,B**). The nature of the metal ion could not be unambiguously determined from the metal–oxygen distances of between 2.4 and 2.5 Å (Dokmanic et al., 2008). Hence, the octahedral coordination sphere, the presence of Mg^{2+} in the crystallization buffer, and the fact that Mg^{2+} is the natural ligand of enolase, is consistent with the modeling of the difference density peak as an Mg^{2+} ion (Brewer, 1981; Wedekind et al., 1995; Larsen et al., 1996). Like the apo EnoCa structure, a metal ion was mapped to the active site in the 2-PGA and PEP structures. However, for the same reasons described above for the apo EnoCa structure, unambiguous determination of the metal ion was not possible in the 2-PGA and PEP EnoCa structures.

The presence of 2-PGA and PEP in the active site of EnoCa was confirmed by calculation of a simulated-annealing OMIT map. The simulated-annealing OMIT map shows electron density that correlates with the presence of 2-PGA and PEP molecules (data not shown). As was mentioned before, the L1 loop in 2-PGA EnoCa structure was refined in the open conformation. 2-PGA in the active site is coordinated with Glu165, Glu206, Lys338, Arg367, and Ser368. Additionally, 2-PGA interacts with water molecules, and the carboxyl molecule involved in coordination of conformational Mg^{2+}(I) (**Figures 5C,D**).

In contrast to the 2-PGA EnoCa structure, PEP was coordinated with the second catalytic metal atom in the active site. The second atom was identified as Mg^{2+}. Mg^{2+}(II) was coordinated with Ser43, water molecules, and phosphate atoms from PEP supporting the octahedral coordination sphere. PEP itself is bound by Glu165, Glu206, Lys338, Arg367, and Ser368

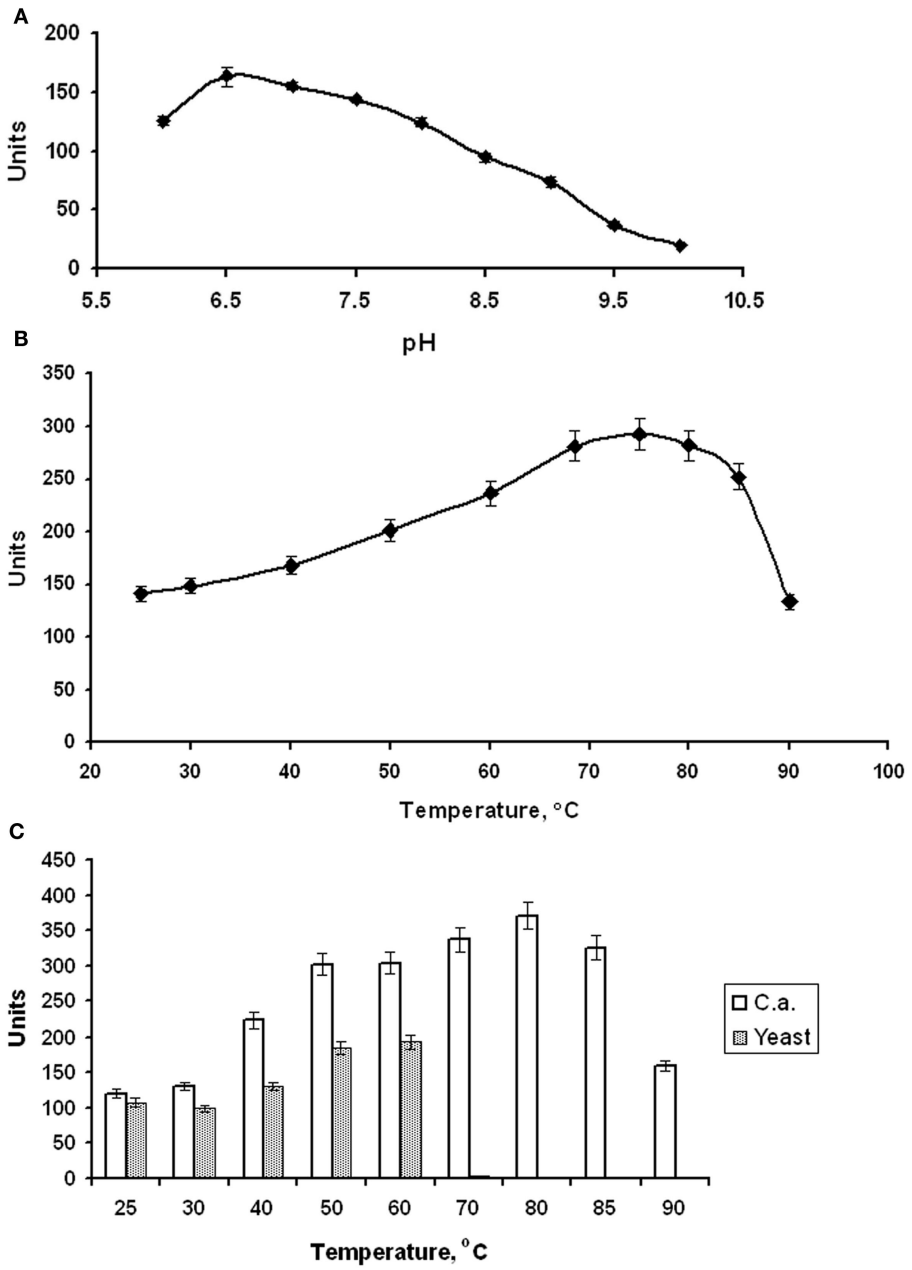

FIGURE 2 | Properties of *C. aurantiacus* enolase. **(A)** Determination of pH optimum. **(B)** Thermostability of *C. aurantiacus* enolase. **(C)** Comparison of temperature optimum of *C. aurantiacus* and *Saccharomyces cerevisiae* enolases.

(**Figures 5E,F**). It should be noted that the electron density was absent for the Ser43 in subunit A of the PEP EnoCa structure due to instability of the L1 region. Nevertheless, the Ser43 was modeled in subunit A with reduced occupancy (0.5).

Discussion

Evolutionary analysis of archaeal and bacterial enolase-1 protein representatives, when rooted with representative enolase-2 proteins, indicate that the earliest branching lineages derive from thermophilic taxa indicating that the enzyme likely has a thermophilic origin. Enolase-1 from the thermophile *C. aurantiacus*, as characterized here, branches late among the thermophilic ancestry of the enzyme, but prior to when the widespread diversification of organisms harboring this enzyme into lower temperature environments. Thus, it is likely that enolase-1 isolated from *C. aurantiacus* harbors biochemical and structural properties that are more reflective of the thermophilic ancestor than mesophilic enzymes.

Despite the clear indication that EnoCa is derived from a thermophilic ancestor, the molecular properties of the enzyme exhibit a number of similarities with characterized enzymes

TABLE 3 | Properties of organisms from which enolase have been characterized, and properties of the purified enzymes.

Organism	Growth temperature, °C	Specific activity, U/mg	MW, kDa		K_m, 10^{-3}M		pH_{opt}	Temperature, °C	
			Subunit	Total	PGA	Mg^{2+}		Opt	Stab
P. furiosus	100	14	45	90	0.4	n/a[a]	8.1	>90	100
T. maritima	80	250	48	345[b]	0.07	0.03	7.5	90	94
T. aquaticus	70	450–900	44	352[b]	2.8[c]/3.5[d]	1.5[c]/0.9[d]	7.2[e]/8.5[f]	70	100
C. aurantiacus	**55**	**150–300**	**46**	**92**	**0.158[c]/0.035[d]**	**2.5[c]/1.9[d]**	**6.5**	**80**	**75**
E. coli	37	180	46	90	0.1	2.0	8.1	n/a	n/a
C. difficile	37	450	50	300[b]	3	2.0	7.6	55	70
P. falciparum[e]	37	30	50	100	0.041	0.18	7.4–7.6	n/a	n/a
C. albicans	37	35	46	100	0.38	0.286	6.8	n/a	n/a
S. cerevisiae	30	130	46	90	0.057	0.43	7.5	50	n/a
T. brucei	27	85	46	90	0.054	0.36	7.7	n/a	n/a

[a]*Not applicable.*
[b]*Total molecular weight for octameric structure.*
[c]*Measured at 25°C.*
[d]*Measured at optimum temperature.*
[e]*Expressed in E. coli.*
[f]*Obtained at the optimum temperature.*
MW, molecular weight; Opt, optimum; Stab, temperature stability.
Bold font indicates that the data presented in the tables are from this work.

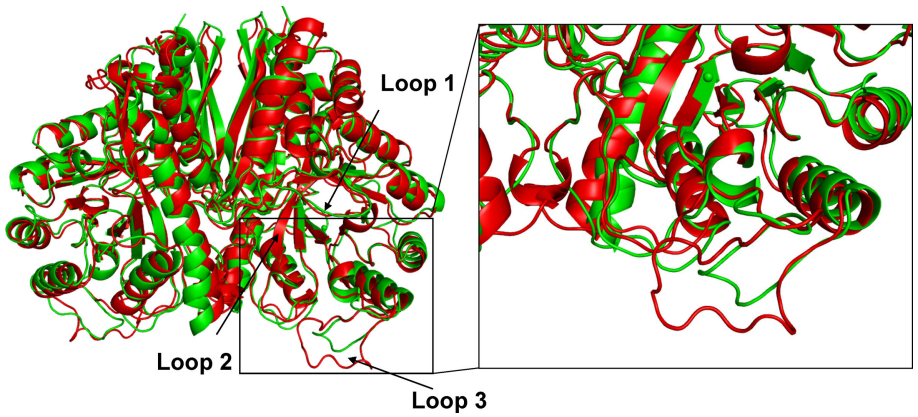

FIGURE 3 | Comparison of crystal structure of *C. aurantiacus* and *Saccharomyces cerevisiae* enolase. Difference in the secondary-structure elements of *C. aurantiacus* enolase (in green) and *S. cerevisiae* enolase (1EBH; in red). The two structures are superimposed and the difference in the loop with residues 189–207 and L3 loop (residues 247–268) are shown. Insert shows close-up view of the loop L3.

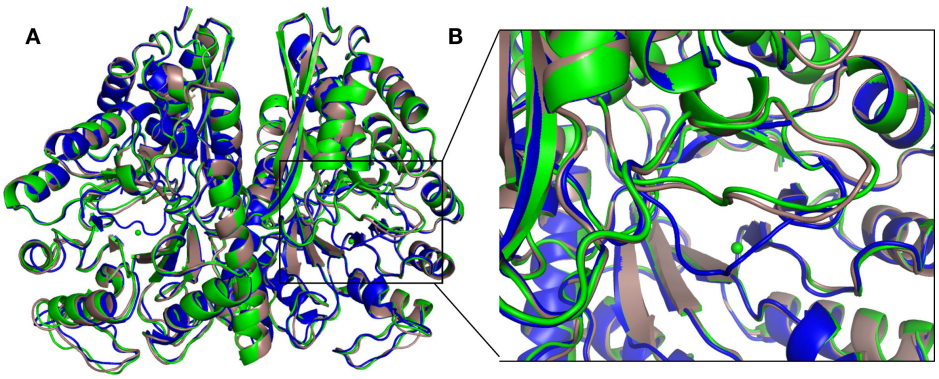

FIGURE 4 | Differences in the overall crystal structures of *C. aurantiacus* enolase. Superposition of apo (green), 2-PGA (gray), and PEP (blue) structures **(A)**. Close-up view of the L1 loop. In the PEP structure, the L1 loop is shown in close conformation **(B)**.

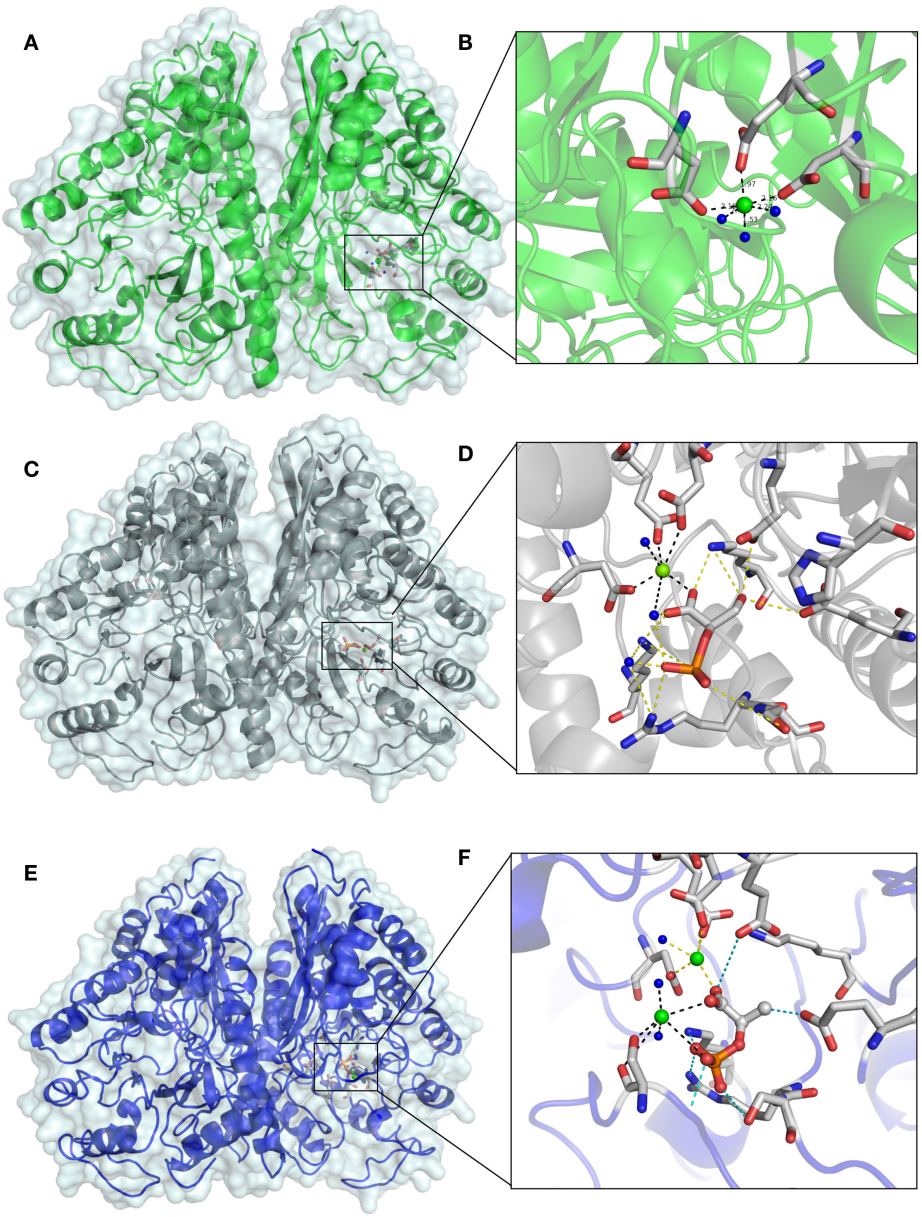

FIGURE 5 | Differences in the active site of crystal structures of *C. aurantiacus* enolase. The active sites of native EnoA in green **(A,B)** 2-PGA structure in gray **(C,D)**, and PEP structure in blue **(E,F)** are shown in overall **(A,C,E)** and close view **(B,D,F)**.

from mesophiles. For example, the subunit molecular weights are similar in enolase from *E. coli* (Wold and Ballou, 1957a), *P. furiousus* (Peak et al., 1994), *S. cerevisiae* (Chin et al., 1981), *T. brucei* (Hannaert et al., 2000), and *P. falciparum* (Pal-Bhowmick et al., 2004), all of which vary from 45.0 to 46.4 kDa. Moreover, the pH optima of enolases from various organisms are also similar among enzymes (Wold, 1971; Kustrzeba-Wojcicka and Golczak, 2000) and tend to fall within the ~6 to 7 range with activity decreasing sharply in more acidic medium and less so in more alkaline solutions. Since enolase is a cytoplasmic enzyme, this finding likely reflects similar cytoplasmic pH in these organisms and may indicate similar cytoplasmic pH since early in life history.

The K_m value for 2-PGA as a substrate for EnoCa is 0.16 mM at 25°C and 0.03 mM at 80°C, which compares well with the K_m value for *S. cerevisiae* enolase (0.12 mM) at 25°C (Wold and Ballou, 1957b). Enolase from *T. aquaticus* and *C. difficile* have K_m values for 2-PGA of 2.8 and 3.0 mM respectively (Stellwag et al., 1973; Green et al., 1993), which is one order of magnitude higher than that observed for *C. aurantiacus* and *S. cerevisiae*.

Bivalent metal ions have been shown to be necessary for the activation of enolase. Specifically, Mg^{2+} has shown to be the strongest activator for all known enolases (Wold and Ballou, 1957b; Faller et al., 1977). Other bivalent metal ions activated homologous enolase enzymes to varying extents (Faller et al.,

1977; Brewer, 1981). K_m values for the $MgCl_2$ for EnoCa are 2.5 (at 25°C) and 1.5 mM (at 80°C), similar to those from *E. coli* and *C. difficile* which are 2.0 mM (at 25°C) but an order magnitude higher than for mesophilic bacteria (**Table 3**). The decrease in the K_m values for 2-PGA and Mg^{2+} with an increase of the temperature approaching the temperature optimum of the catalytic reaction has been shown for enolase from *T. quaticus* (Stellwag et al., 1973) and *T. maritima* (Schurig et al., 1995). Together, these observations indicate adaptation of the thermostable enzymes with respect to their structural properties and activity, showing maximum catalytic efficiency and stability at high temperatures. Similar to the effect of Mg^{2+} on activity of *S. cerevisiae* enolase (Faller et al., 1977; Vinarov and Nowak, 1998), the increase in the Mg^{2+} concentration (higher than 10 mM) inhibited the activity of EnoCa. The inhibitory metal binding site has been identified in structural studies conducted on enolase from *T. brucei* (Giotto et al., 2003).

Enolase from the thermophile *C. aurantiacus* (growth optimum = 55°C) exhibits thermostability and a higher temperature optimum (enolase T_{opt} = 80°C) than enolase from the thermophile *T. aquaticus* (growth optimum = 70°C; enolase T_{opt} = 70°C), but a lower temperature optimum than enolase from the hyperthermophiles *P. furiosus* (growth optimum = 100°C; enolase T_{opt} = >90°C) and *T. maritima* (growth optimum = 80; enolase T_{opt} = 90°C) (**Table 3**). There are several differences in the properties of enolase proteins observed in the primary sequence and structure that may account for the differences in the observed thermostability. For example, the optimal growth temperature of strains significantly correlates with the hydrophobicity index (e.g., number of hydrophobic residues in the protein sequence), aliphatic index (Ikai, 1980), number of rigid clusters in inferred structures, and total independent degree of freedom. These differences would support enhanced thermal stability, since bulkier hydrophobic amino acid side-chains can support stronger hydrophobic interactions in the protein interior (Jaenicke, 1991; Vieille and Zeikus, 2001). Similar adaptations at the structural level have been observed in ribulose-1,5-bisphosphate carboxylase/oxygenase in response to temperature (Miller, 2003). The conformational entropy of the protein molecule increases with elevated temperatures, and this can be attributed to the high degree of disorder observed in the protein–solvent interactions. Therefore, the increase in conformational entropy may have deleterious effects on the structure of the protein molecule by altering its active configuration and leading to its denaturation at elevated temperatures. Hence, to maintain the structural integrity, the thermophilic protein needs to adopt certain strategies that will act as a control mechanism to lower the conformational entropy and prevent it from denaturing at higher temperatures (Kumar and Nussinov, 2001). Increased rigidity of the thermophilic proteins can be considered the first step toward the reduction of the conformational disorder of the protein molecule. This can be achieved by stronger interactions within the protein interior. The rigid clusters, calculated by the FIRST software, are formed from a collection of atoms connected by non-rotatable bonds varying in size from hundreds and thousands of atoms forming a rigid protein core, down to a single atom (Jacobs et al., 2001). Thus, a high temperature stability is the result of adaptation at the structural level in the response to high temperature (Ikai, 1980; Kumar and Nussinov, 2001; Vieille and Zeikus, 2001; Miller, 2003).

In conclusion, the results from the structural analysis of *C. aurantiacus* enolase presented here are consistent with its thermophilic ancestry. For example, the *C. aurantiacus* enolase has a decreased number of amino acids that comprise flexible loops (**Figure 3**). Among proteins that are isolated from thermophiles, it is common to observe an overall greater proportion of amino acids involved in well-defined secondary structure (Ikai, 1980; Vieille and Zeikus, 2001). This is manifested not only in the lack of extensive solvent-exposed loop regions, but also in a greater extent of secondary structure. Increase in the helical content along with shortening of loop regions results in a decrease in conformational entropy. The other feature that was identified in the structural analysis is the absence of second, catalytic Mg^{2+}(II) atom at the active site in the structures containing 2-PGA. It has been reported that the *S. cerevisiae* and *E. histolytica* enolase structures contain the 2-PGA that was not coordinated with Mg^{2+}(II) in the active site. This fact might be explained by the pre-catalytic step of the reaction sequence prior to binding of metal II and closure of L1.

Acknowledgments

A culture of *C. aurantiacus* was kindly provided by Dr. Mikhail F. Yanyushin. We thank Dr. Larisa Serebriakova, Dr. Charles M. Lawrence, Jacob H. Artz, Dr. Anoop K. Sendamarai, Dr. George Gauss, and Brian J. Eilers for valuable advice and suggestions. This work supported by a grant from the Air Force Office of Scientific Research (FA9550-14-110147) to JP, EB, and MP. The authors also acknowledge funding for the establishment and operation of the Environmental and Biofilm Mass Spectrometry Facility at Montana State University (MSU) through the Defense University Research Instrumentation Program (DURIP, Contract Number: W911NF0510255) and the MSU Thermal Biology Institute from the NASA Exobiology Program (Project NAG5-8807). Portions of this research were carried out at the Stanford Synchrotron Radiation Laboratory (SSRL), a national user facility operated by Stanford University on behalf of the US Department of Energy, Office of Basic Energy Sciences under Contract No. DE-AC02-76SF00515. The SSRL Structural Molecular Biology program is supported by the US Department of Energy, Office of Biological and Environmental Research, the US National Institutes of Health, National Center for Research Resources, Biomedical Technology program, and the US National Institute of General Medical Sciences (including P41GM103393). EB acknowledges support from a grant from the NASA Astrobiology Institute (NNA 15BB02A).

Supplementary Material

The Supplementary Material for this article can be found online at http://journal.frontiersin.org/article/10.3389/fbioe.2015.00074/abstract

References

Abascal, F., Zardoya, R., and Posada, D. (2005). ProtTest: selection of best-fit models of protein evolution. *Bioinformatics* 21, 2104–2105. doi:10.1093/bioinformatics/bti263

Arnold, K., Bordoli, L., Kopp, J., and Schwede, T. (2006). The SWISS-MODEL workspace: a web-based environment for protein structure homology modelling. *Bioinformatics* 22, 195–201. doi:10.1093/bioinformatics/bti770

Babbitt, P. C., Hasson, M. S., Wedekind, J. E., Palmer, D. R., Barrett, W. C., Reed, G. H., et al. (1996). The enolase superfamily: a general strategy for enzyme-catalyzed abstraction of the alpha-protons of carboxylic acids. *Biochemistry* 35, 16489–16501. doi:10.1021/bi9616413

Ballou, C. E., and Wold, F. (1957). Studies on enolase. *Fed. Proc.* 16, 150–150.

Bradford, M. M. (1976). A rapid and sensitive method for the quantitation of microgram quantities of protein utilizing the principle of protein-dye binding. *Anal. Biochem.* 72, 248–254. doi:10.1016/0003-2697(76)90527-3

Brewer, J. M. (1981). Yeast enolase: mechanism of activation by metal ions. *CRC Crit. Rev. Biochem.* 11, 209–254. doi:10.3109/10409238109108702

Brewer, J. M., Glover, C. V., Holland, M. J., and Lebioda, L. (1998). Significance of the enzymatic properties of yeast S39A enolase to the catalytic mechanism. *Biochim. Biophys. Acta.* 1383, 351–355. doi:10.1016/S0167-4838(98)00004-1

Castenholz, R. W. (1969). Thermophilic blue-green algae and the thermal environment. *Bacteriol. Rev.* 33, 476–504.

Chen, V. B., Arendall, W. B. III, Headd, J. J., Keedy, D. A., Immormino, R. M., Kapral, G. J., et al. (2010). MolProbity: all-atom structure validation for macromolecular crystallography. *Acta Crystallogr. D Biol. Crystallogr.* 66, 12–21. doi:10.1107/S0907444909042073

Chin, C. C., Brewer, J. M., and Wold, F. (1981). The amino acid sequence of yeast enolase. *J. Biol. Chem.* 256, 1377–1384.

Delano, W. L. (2002). *The PyMOL Molecular Graphics System*. Version 1.7.4. San Carlos, CA: Schrödinger, LLC.

Dokmanic, I., Sikic, M., and Tomic, S. (2008). Metals in proteins: correlation between the metal-ion type, coordination number and the amino-acid residues involved in the coordination. *Acta Crystallogr. D Biol. Crystallogr.* 64, 257–263. doi:10.1107/S090744490706595X

Emsley, P., Lohkamp, B., Scott, W. G., and Cowtan, K. (2010). Features and development of Coot. *Acta Crystallogr. D Biol. Crystallogr.* 66, 486–501. doi:10.1107/S0907444910007493

Faller, L. D., Baroudy, B. M., Johnson, A. M., and Ewall, R. X. (1977). Magnesium-ion requirements for yeast enolase activity. *Biochemistry* 16, 3864–3869. doi:10.1021/bi00636a023

Fothergill-Gilmore, L. A., and Michels, P. A. (1993). Evolution of glycolysis. *Prog. Biophys. Mol. Biol.* 59, 105–235. doi:10.1016/0079-6107(93)90001-Z

Gasteiger, E., Gattiker, A., Hoogland, C., Ivanyi, I., Appel, R. D., and Bairoch, A. (2003). ExPASy: the proteomics server for in-depth protein knowledge and analysis. *Nucleic Acids Res.* 31, 3784–3788. doi:10.1093/nar/gkg563

Gerlt, J. A., Babbitt, P. C., and Rayment, I. (2005). Divergent evolution in the enolase superfamily: the interplay of mechanism and specificity. *Arch. Biochem. Biophys.* 433, 59–70. doi:10.1016/j.abb.2004.07.034

Giotto, M. T. D., Hannaert, V., Vertommen, D., Navarro, M. V. D. S., Rider, M. H., Michels, P. A. M., et al. (2003). The crystal structure of *Trypanosoma brucei* enolase: visualisation of the inhibitory metal binding site III and potential as target for selective, irreversible inhibition. *J. Mol. Biol.* 331, 653–665. doi:10.1016/S0022-2836(03)00752-6

Green, G. A., Girardot, R., Baldacini, O., Ledig, M., and Monteil, H. (1993). Characterization of enolase from *Clostridium difficile*. *Curr. Microbiol.* 26, 53–56. doi:10.1007/BF01577243

Gupta, R. S., Mukhtar, T., and Singh, B. (1999). Evolutionary relationships among photosynthetic prokaryotes (*Heliobacterium chlorum*, *Chloroflexus aurantiacus*, cyanobacteria, *Chlorobium tepidum* and proteobacteria): implications regarding the origin of photosynthesis. *Mol. Microbiol.* 32, 893–906. doi:10.1046/j.1365-2958.1999.01417.x

Hannaert, V., Brinkmann, H., Nowitzki, U., Lee, J. A., Albert, M. A., Sensen, C. W., et al. (2000). Enolase from *Trypanosoma brucei*, from the amitochondriate protist *Mastigamoeba balamuthi,* and from the chloroplast and cytosol of *Euglena gracilis*: pieces in the evolutionary puzzle of the eukaryotic glycolytic pathway. *Mol. Biol. Evol.* 17, 989–1000. doi:10.1093/oxfordjournals.molbev.a026395

Hosaka, T., Meguro, T., Yamato, I., and Shirakihara, Y. (2003). Crystal structure of *Enterococcus hirae* enolase at 2.8 A resolution. *J. Biochem.* 133, 817–823. doi:10.1093/jb/mvg104

Ikai, A. (1980). Thermostability and aliphatic index of globular-proteins. *J. Biochem.* 88, 1895–1898.

Jacobs, D. J., Rader, A. J., Kuhn, L. A., and Thorpe, M. F. (2001). Protein flexibility predictions using graph theory. *Proteins* 44, 150–165. doi:10.1002/prot.1081

Jaenicke, R. (1991). Protein stability and molecular adaptation to extreme conditions. *Eur. J. Biochem* 202, 715–728. doi:10.1111/j.1432-1033.1991.tb16426.x

Kabsch, W. (2010). Xds. *Acta Crystallogr. D Biol. Crystallogr.* 66, 125–132. doi:10.1107/S0907444909047337

Kumar, S., and Nussinov, R. (2001). How do thermophilic proteins deal with heat? *Cell. Mol. Life Sci.* 58, 1216–1233. doi:10.1007/PL00000935

Kustrzeba-Wojcicka, I., and Golczak, M. (2000). Enolase from *Candida albicans*–purification and characterization. *Comp. Biochem. Physiol. B Biochem. Mol. Biol.* 126, 109–120. doi:10.1016/S0305-0491(00)00169-3

Larkin, M. A., Blackshields, G., Brown, N. P., Chenna, R., Mcgettigan, P. A., Mcwilliam, H., et al. (2007). Clustal W and Clustal X version 2.0. *Bioinformatics* 23, 2947–2948. doi:10.1093/bioinformatics/btm404

Larsen, T. M., Wedekind, J. E., Rayment, I., and Reed, G. H. (1996). A carboxylate oxygen of the substrate bridges the magnesium ions at the active site of enolase: structure of the yeast enzyme complexed with the equilibrium mixture of 2-phosphoglycerate and phosphoenolpyruvate at 1.8 A resolution. *Biochemistry* 35, 4349–4358. doi:10.1021/bi952859c

Lebioda, L., and Stec, B. (1988). Crystal structure of enolase indicates that enolase and pyruvate kinase evolved from a common ancestor. *Nature* 333, 683–686. doi:10.1038/333683a0

Lebioda, L., and Stec, B. (1991). Mechanism of enolase: the crystal structure of enolase-$Mg^{2(+)}$-2-phosphoglycerate/phosphoenolpyruvate complex at 2.2-A resolution. *Biochemistry* 30, 2817–2822. doi:10.1021/bi00225a013

Lebioda, L., Stec, B., and Brewer, J. M. (1989). The structure of yeast enolase at 2.25-A resolution. An 8-fold beta + alpha-barrel with a novel beta beta alpha alpha (beta alpha)6 topology. *J. Biol. Chem.* 264, 3685–3693.

Lebioda, L., Stec, B., Brewer, J. M., and Tykarska, E. (1991). Inhibition of enolase: the crystal structures of enolase-$Ca^{2(+)}$-2-phosphoglycerate and enolase-$Zn^{2(+)}$-phosphoglycolate complexes at 2.2-A resolution. *Biochemistry* 30, 2823–2827. doi:10.1021/bi00225a013

Lineweaver, C. H., and Schwartzman, D. (2003). "Seckbach part of a series on cellular origins and life in extreme habitats," in *Origins*, ed. J. Seckbach (Dordrecht: Kluwer Academic), 233–248.

Lineweaver, H., and Burk, D. (1934). The determination of enzyme dissociation constants. *J. Am. Chem. Soc.* 56, 658–666. doi:10.1021/ja01318a036

Miller, S. R. (2003). Evidence for the adaptive evolution of the carbon fixation gene rbcL during diversification in temperature tolerance of a clade of hot spring cyanobacteria. *Mol. Ecol.* 12, 1237–1246. doi:10.1046/j.1365-294X.2003.01831.x

Murshudov, G. N., Vagin, A. A., and Dodson, E. J. (1997). Refinement of macromolecular structures by the maximum-likelihood method. *Acta Crystallogr. D Biol. Crystallogr.* 53, 240–255. doi:10.1107/S0907444996012255

Pace, N. R. (1991). Origin of life–facing up to the physical setting. *Cell* 65, 531–533. doi:10.1016/0092-8674(91)90082-A

Pal-Bhowmick, I., Sadagopan, K., Vora, H. K., Sehgal, A., Sharma, S., and Jarori, G. K. (2004). Cloning, over-expression, purification and characterization of *Plasmodium falciparum* enolase. *Eur. J. Biochem.* 271, 4845–4854. doi:10.1111/j.1432-1033.2004.04450.x

Peak, M. J., Peak, J. G., Stevens, F. J., Blamey, J., Mai, X., Zhou, Z. H., et al. (1994). The hyperthermophilic glycolytic enzyme enolase in the archaeon, *Pyrococcus furiosus*: comparison with mesophilic enolases. *Arch. Biochem. Biophys.* 313, 280–286. doi:10.1006/abbi.1994.1389

Poyner, R. R., Laughlin, L. T., Sowa, G. A., and Reed, G. H. (1996). Toward identification of acid/base catalysts in the active site of enolase: comparison of the properties of K345A, E168Q, and E211Q variants. *Biochemistry* 35, 1692–1699. doi:10.1021/bi952186y

Rader, A. J., Hespenheide, B. M., Kuhn, L. A., and Thorpe, M. F. (2002). Protein unfolding: rigidity lost. *Proc. Natl. Acad. Sci. U.S.A.* 99, 3540–3545. doi:10.1073/pnas.062492699

Reed, G. H., Poyner, R. R., Larsen, T. M., Wedekind, J. E., and Rayment, I. (1996). Structural and mechanistic studies of enolase. *Curr. Opin. Struct. Biol.* 6, 736–743. doi:10.1016/S0959-440X(96)80002-9

Ronimus, R. S., and Morgan, H. W. (2003). Distribution and phylogenies of enzymes of the Embden-Meyerhof-Parnas pathway from archaea and hyperthermophilic bacteria support a gluconeogenic origin of metabolism. *Archaea* 1, 199–221. doi:10.1155/2003/162593

Schreier, B., and Hocker, B. (2010). Engineering the enolase magnesium II binding site: implications for its evolution. *Biochemistry* 49, 7582–7589. doi:10.1021/bi100954f

Schulz, E. C., Tietzel, M., Tovy, A., Ankri, S., and Ficner, R. (2011). Structure analysis of *Entamoeba histolytica* enolase. *Acta Crystallogr. D Biol. Crystallogr.* 67, 619–627. doi:10.1107/S0907444911016544

Schurig, H., Rutkat, K., Rachel, R., and Jaenicke, R. (1995). Octameric enolase from the hyperthermophilic bacterium *Thermotoga maritima*: purification, characterization, and image processing. *Protein Sci.* 4, 228–236. doi:10.1002/pro.5560040209

Sims, P. A., Menefee, A. L., Larsen, T. M., Mansoorabadi, S. O., and Reed, G. H. (2006). Structure and catalytic properties of an engineered heterodimer of enolase composed of one active and one inactive subunit. *J. Mol. Biol.* 355, 422–431. doi:10.1016/j.jmb.2005.10.050

Stec, B., and Lebioda, L. (1990). Refined structure of yeast apo-enolase at 2.25 A resolution. *J. Mol. Biol.* 211, 235–248. doi:10.1016/0022-2836(90)90023-F

Stellwag, E., Cronlund, M. M., and Barnes, L. D. (1973). Thermostable enolase from extreme thermophile *Thermus aquaticus* Yt-1. *Biochemistry* 12, 1552–1559. doi:10.1021/bi00732a014

Tamura, K., Dudley, J., Nei, M., and Kumar, S. (2007). MEGA4: molecular evolutionary genetics analysis (MEGA) software version 4.0. *Mol. Biol. Evol.* 24, 1596–1599. doi:10.1093/molbev/msm092

Tracy, M. R., and Hedges, S. B. (2000). Evolutionary history of the enolase gene family. *Gene* 259, 129–138. doi:10.1016/S0378-1119(00)00439-X

Vieille, C., and Zeikus, G. J. (2001). Hyperthermophilic enzymes: sources, uses, and molecular mechanisms for thermostability. *Microbiol. Mol. Biol. Rev.* 65, 1–43. doi:10.1128/MMBR.65.1.1-43.2001

Vinarov, D. A., and Nowak, T. (1998). pH dependence of the reaction catalyzed by yeast Mg-enolase. *Biochemistry* 37, 15238–15246. doi:10.1021/bi981047o

Wedekind, J. E., Reed, G. H., and Rayment, I. (1995). Octahedral coordination at the high-affinity metal site in enolase – crystallographic analysis of the mg-ii-enzyme complex from yeast at 1.9 angstrom resolution. *Biochemistry* 34, 4325–4330. doi:10.1021/bi00013a022

Winn, M. D., Ballard, C. C., Cowtan, K. D., Dodson, E. J., Emsley, P., Evans, P. R., et al. (2011). Overview of the CCP4 suite and current developments. *Acta Crystallogr. D Biol. Crystallogr.* 67, 235–242. doi:10.1107/S0907444910045749

Wold, F. (1971). "Enolase," in *The Enzymes*, 3rd Edn, ed. P. D. Boyer (New York, London: Academic Press), 499–519.

Wold, F., and Ballou, C. E. (1957a). Studies on the enzyme enolase. I. Equilibrium studies. *J. Biol. Chem* 227, 301–312.

Wold, F., and Ballou, C. E. (1957b). Studies on the enzyme enolase. II. Kinetic studies. *J. Biol. Chem* 227, 313–328.

Xiong, J., Fischer, W. M., Inoue, K., Nakahara, M., and Bauer, C. E. (2000). Molecular evidence for the early evolution of photosynthesis. *Science* 289, 1724–1730. doi:10.1126/science.289.5485.1724

Yanyushin, M. F. (1988). Isolation and characterization of f1-atpase from the green nonsulfur photosynthesizing bacterium *Chloroflexus aurantiacus*. *Biochemistry (Moscow)* 53, 1120–1127.

Zhang, E., Brewer, J. M., Minor, W., Carreira, L. A., and Lebioda, L. (1997). Mechanism of enolase: the crystal structure of asymmetric dimer enolase-2-phospho-D-glycerate/enolase-phosphoenolpyruvate at 2.0 A resolution. *Biochemistry* 36, 12526–12534. doi:10.1021/bi9712450

Zhang, E., Hatada, M., Brewer, J. M., and Lebioda, L. (1994). Catalytic metal ion binding in enolase: the crystal structure of an enolase-Mn^{2+}-phosphonoacetohydroxamate complex at 2.4-A resolution. *Biochemistry* 33, 6295–6300. doi:10.1021/bi00186a032

Conflict of Interest Statement: The authors declare that the research was conducted in the absence of any commercial or financial relationships that could be construed as a potential conflict of interest.

frontiers in Bioengineering and Biotechnology

ORIGINAL RESEARCH
published: 01 July 2015
doi: 10.3389/fbioe.2015.00095

Functional screening of hydrolytic activities reveals an extremely thermostable cellulase from a deep-sea archaeon

*Benedikt Leis[1†], Simon Heinze[1†], Angel Angelov[1], Vu Thuy Trang Pham[1], Andrea Thürmer[2], Mohamed Jebbar[3], Peter N. Golyshin[4], Wolfgang R. Streit[5], Rolf Daniel[2] and Wolfgang Liebl[1]**

[1] Department of Microbiology, School of Life Sciences Weihenstephan, Technische Universität München, Freising-Weihenstephan, Germany, [2] Göttingen Genomics Laboratory, Department of Genomic and Applied Microbiology, Georg-August University Göttingen, Göttingen, Germany, [3] Laboratoire de Microbiologie des Environnements Extrêmes-UMR 6197 (CNRS-Ifremer-UBO), Institut Universitaire Européen de la Mer, Université de Bretagne Occidentale, Plouzané, France, [4] School of Biological Sciences, Bangor University, Bangor, UK, [5] Fakultät für Mathematik, Informatik und Naturwissenschaften Biologie, Biozentrum Klein Flottbek, Universität Hamburg, Hamburg, Germany

OPEN ACCESS

Edited by:
Noha M. Mesbah,
Suez Canal University, Egypt

Reviewed by:
Franz Josef St John,
United States Department of Agriculture, USA
Yasser Gaber,
Beni-Suef University, Egypt

***Correspondence:**
Wolfgang Liebl,
Department of Microbiology, School of Life Sciences Weihenstephan, Technische Universität München, Emil-Ramann-Strasse 4, Freising-Weihenstephan D-85354, Germany
wliebl@wzw.tum.de

[†]Benedikt Leis and Simon Heinze have contributed equally to this work.

Specialty section:
This article was submitted to Process and Industrial Biotechnology, a section of the journal Frontiers in Bioengineering and Biotechnology

Received: 11 March 2015
Accepted: 17 June 2015
Published: 01 July 2015

Citation:
Leis B, Heinze S, Angelov A, Pham VTT, Thürmer A, Jebbar M, Golyshin PN, Streit WR, Daniel R and Liebl W (2015) Functional screening of hydrolytic activities reveals an extremely thermostable cellulase from a deep-sea archaeon. Front. Bioeng. Biotechnol. 3:95. doi: 10.3389/fbioe.2015.00095

Extreme habitats serve as a source of enzymes that are active under extreme conditions and are candidates for industrial applications. In this work, six large-insert mixed genomic libraries were screened for hydrolase activities in a broad temperature range (8–70°C). Among a variety of hydrolytic activities, one fosmid clone, derived from a library of pooled isolates of hyperthermophilic archaea from deep sea vents, displayed hydrolytic activity on carboxymethyl cellulose substrate plates at 70°C but not at lower temperatures. Sequence analysis of the fosmid insert revealed a gene encoding a novel glycoside hydrolase family 12 (GHF12) endo-1,4-β-glucanase, termed Cel12E. The enzyme shares 45% sequence identity with a protein from the archaeon *Thermococcus sp*. AM4 and displays a unique multidomain architecture. Biochemical characterization of Cel12E revealed a remarkably thermostable protein, which appears to be of archaeal origin. The enzyme displayed maximum activity at 92°C and was active on a variety of linear 1,4-β-glucans like carboxymethyl cellulose, β-glucan, lichenan, and phosphoric acid swollen cellulose. The protein is able to bind to various insoluble β-glucans. Product pattern analysis indicated that Cel12E is an endo-cleaving β-glucanase. Cel12E expands the toolbox of hyperthermostable archaeal cellulases with biotechnological potential.

Keywords: functional screenings, extreme thermostable protein, archaeal endoglucanase, enzymatic characterization

Introduction

The search for novel enzymes for biotechnological and pharmaceutical applications must focus on proteins displaying the desired properties under process-relevant conditions, which are often harsh, especially with regard to salt or solvent concentrations, pH, and temperature. In this regard, process conditions resemble the conditions in extreme environments. Microorganisms inhabit a multitude of such environments, characterized by high temperature, salinity, or extreme pH (Grant et al., 2004; Li et al., 2014). Accordingly, extreme habitats represent a good source for enzymes active under

extreme conditions (Simon et al., 2009; Delavat et al., 2012). Two distinct strategies are available for the identification of enzymes from extreme environments. While metagenomics enable the exploration of phylogenetic and biochemical characteristics of microbial consortia without the need for cultivation (Handelsman et al., 1998), culture-based approaches overcome restrictions of metagenomic screening.

The choice of an appropriate sampling environment is generally important when screening for certain enzymatic activities (Taupp et al., 2011) but interesting enzymes have also been discovered in samples from environments in which the respective functions were initially not expected or observed (Voget et al., 2003; Delavat et al., 2012). Therefore, it has been suggested to broaden functional screenings, for example, to include more than one specific enzymatic activity (Leis et al., 2013). Although sequence similarity and functional screenings are both well established, functional screens appear to be better suited for the discovery of completely new enzymatic functions encoded by the genetic material (Langer et al., 2006; Liebl et al., 2014).

In this study, we performed a functional screening of fosmid expression libraries in order to identify hydrolytic activities for biotechnological applications. The fosmid inserts were derived from mixed genomes originating from mesophilic and thermophilic bacteria as well as hyperthermophilic archaeal (HA) isolates (deep sea environments), enrichment cultures from ship worm digestive tracts, and uncultured microorganisms (river sediment, elephant feces). The screening was performed at different temperatures, ranging from 8 to 70°C. The application of the same expanded temperature range for all functional screenings, independent of the nature of the source of the genomic DNA, increased the number of unique identified proteins. By this route, we were able to identify a total of 60 different activities (esterases, lipases, and glycoside hydrolases). One cellulolytic clone from a library of uncharacterized archaeal isolates cultivated from hydrothermal vents was of particular interest due to its activity at elevated temperatures. Sequence analysis and biochemical characterization revealed an extremely thermostable endoglucanase, termed Cel12E, which was able to hydrolyze a variety of β-1,4-linked polysaccharides. The high thermostability and broad substrate specificity of Cel12E make this enzyme a promising candidate for industrial degradation of lignocellulosic biomass.

Materials and Methods

Bacterial Strains and Vectors

Escherichia coli EPI300-T1 (Epicentre, Madison, USA) was used for screening the genomic libraries cloned in pCC1FOS large insert fosmids (Epicentre). The *E. coli* strains XL1-Blue (Stratagene, La Jolla, USA) and DH10B (Invitrogen, Carlsbad, USA) were used for transformation and propagation of recombinant plasmids. *E. coli* strain BL21(DE3) was used as the host for pET21a(+) expression vector. *E. coli* was grown and maintained on LB media with appropriate antibiotic supplementation with ampicillin (100 μg/ml) and chloramphenicol (12.5 μg/ml) at 37°C overnight.

Generation of Genomic DNA Libraries and Activity-Based Screenings

Three metagenomic DNA libraries were available for functional screenings: low-to-mid temperature libraries were derived from sediments from the river Elbe (Rabausch et al., 2013), elephant feces and ship worm enrichment cultures on CMC (Ilmberger et al., 2012), each containing 960 fosmid clones. Three further fosmid libraries contained inserts of mixed genomic DNA of enrichment cultures from deep sea hydrothermal vents. A total of 788 uncharacterized, individually grown strains were subdivided into three physiological groups (251 thermophilic bacteria, 194 mesophilic bacteria, and 343 hyperthermophilc archaea) and used to prepare these "mixed genome" libraries. Each library represented one of the three physiological groups. Cells from 20 to 30 ml culture volume were harvested by centrifugation at 8,000 × rpm at 4°C for 5 min. For cell lysis, 100 μl 10% sarkosyl, 100 μl 10% SDS, and 50 μl proteinase K (20 mg/ml stock) were added and mixed gently. The lysis reaction was incubated for 1 h at 55°C and slowly stirred several times. RNase A was added (20 μl of 50 μg/ml stock) and incubated for 20–30 min at 37°C. After cell lysis, the genomic DNA of each strain was isolated. The best DNA yield and quality were obtained with the standard phenol-chloroform method according to Sambrook et al. (1989). To obtain the three "mixed genome" DNA libraries, the DNA extracts of all isolates belonging to the same physiological group were mixed using equal DNA amounts and subjected to further cloning into pCC1FOS fosmids (according to the Epicentre manufacturer instructions). The isolated microorganisms are deposited as -80°C DMSO-stocks in the UBO Culture Collection UBOCC[1] of the laboratory of Microbiology of Extreme Environments at IUEM-UBO (Plouzané, France).

Escherichia coli EPI300-T1 transformed with the fosmid library was grown on LB agar plates at 37°C overnight to yield single colonies. Next, replica plating was used to transfer the library colonies on LB agar indicator plates containing Fosmid Autoinduction Solution (Epicentre, Madison, USA) for activation of the *oriV* origin and different substrates: 1.0% (v/v) tributyrin, 1.0% (v/v) triolein supplemented with rhodamine B [according to Kouker and Jaeger (1987)], 0.1% (w/v) xylan (from oat spelts), 0.1% (w/v) carboxymethyl cellulose (CMC, sodium salt, low viscosity), 0.3% (w/v) starch (soluble). All substrates were purchased from Sigma-Aldrich (Germany). The original LB agar plates were stored at 4°C to enable the identification of positive clones after the functional screenings. After growth at 37°C overnight, the replicated colonies on the LB agar indicator plates were subjected to functional screenings for 1 week at temperatures from 8 to 20°C or for 2–3 days when incubating at temperatures from 30 to 70°C. Agar plate screening for (hemi-) cellulose degradation was monitored using Congo red staining solution of 0.1% (w/v) followed by repeated washing with 1.0M sodium chloride solution (Wood et al., 1988). Halo formation around the colonies indicated degradation of substrates due to hydrolytic activity. Functional screening in microtiter plates was performed with Cibacron red dyed substrates (xylan and CMC) according to Ten et al. (2005). Starch degradation was visualized

[1]http://www.univ-brest.fr/souchotheque/Collection+LM2E

by the addition of Lugol's iodine solution (0.33% w/v elemental iodine and 0.66% w/v potassium iodide). DNA from positive fosmid clones was isolated and re-transformed in *E. coli* EPI300 cells to confirm the observed activity. Cloning of fosmid fragments was performed with pCR®2.1-XL-TOPO® (Invitrogen, USA) for confirmation of the phenotype and for sequencing purposes.

Sequence Analysis

Complete sequencing of selected DNA inserts was performed in the Göttingen Genomics Laboratory (G_2L) using a combination of Sanger and 454-pyrosequencing technology. The generation of 454 shotgun libraries was performed following the manufacturer instructions (Roche, 454 Life Sciences, Branford). Libraries were sequenced using the FLX Titanium chemistry and 25,591 single reads were generated. The shotgun reads were assembled *de novo* with Newbler Assembler V2.6 (Roche, Branford), resulting in 153 contigs (>500 bp). Fosmid mapping was achieved by sequencing from both fosmid ends using oligonucleotide primers abi-for (5′-ACGACGTTGTAAAACGACGGCCAG-3′) and abi-rev (5′-TTCACACAGGAAACAGCTATGACC-3′) with Sanger technology. ORF prediction and annotation was performed with SEED (Overbeek et al., 2005), SignalP (Petersen et al., 2011) was used for the prediction of signal peptides. BlastP (Altschul et al., 1990) was used for sequence similarity search against the *nr* database, conserved protein domains were searched in the Pfam database version 27.0 (Punta et al., 2012). The prediction of domain linkers was performed with the DLP-SVM web service (Ebina et al., 2009).

Construction of Expression Vectors

Gene *cel12E* of fosmid HA-cmc-1 was amplified by PCR with Phusion F530S DNA polymerase (ThermoFisher Scientific, Waltham, MA, USA) according to the manufacturer's instructions. The PCR product of *cel12E* was cloned in pET21a(+) expression vector using Gibson Assembly™ (New England Biolabs, Ipswich, MA, USA). Amplicons obtained with primers SP-HACMC-F (5′-TTTAAGAAGGAGATATACAATGAAAAGCATTGCACTTG-3′) and HACMC-R (5′-GTGGTGCTCGAGTGCGGCC TCACTGTGGCGTCCAGATA-3′) were full-length Cel12E with the predicted signal peptide encoded at the N-terminus. A truncated version of Cel12E omitting the signal peptide sequence was obtained with HACMC-F (5′-TTTAAGAAGGAGATATA CAATGCAGGAGACAACAGTGCTGGA-3′) and HACMC-R.

Expression and Purification of Recombinant Cel12E

Escherichia coli cultures (500 ml) were grown in Erlenmeyer flasks to mid-log phase (absorbance at 600 nm wavelength ranging from 0.6 to 0.7) and induced with isopropyl-β-D-thiogalactopyranoside (IPTG) at a final concentration of 1.0 mM. After 4 h at 37°C, the cultures were harvested by centrifugation (5,000 × *g* for 5 min) and disrupted by French pressure cell (SLM Aminco, Urbana, IL, USA). EDTA-free Protease Inhibitor Cocktail Tablets (Roche Diagnostics, Mannheim, Germany) were used during protein purification to prevent degradation of the target protein. After removal of the cell debris by centrifugation (21,000 × *g* for 15 min), the lysate was subjected to heat treatment (80°C for 20 min). The supernatant containing the thermostable and soluble protein of interest was purified using an Äkta Explorer fast protein liquid chromatography system (GE Healthcare, Little Chalfont, UK) with a SOURCE™ 15Q anion exchange column in 50 mM Tris-HCl buffer, pH 8.0 (buffer A) and sodium chloride gradient (buffer B, 50 mM Tris-HCl, pH 8.0, 1.0 M NaCl). Gel filtration on Superdex 200 column for Cel12E was performed in buffer A supplemented with 150 mM NaCl. Protein separation and purity were determined with sodium dodecyl sulfate polyacrylamide gel electrophoresis (SDS-PAGE) based on Laemmli (1970).

Enzyme Assays

Microcrystalline cellulose (Avicel PH-101), CMC (low viscosity), hydroxyethyl cellulose (HEC), xylan (from oat spelts, birchwood, and larchwood), chitin, chitosan, lichenan (from *Cetraria islandica*), laminarin (from *Laminaria digitata*), and starch (from potato) were purchased from Sigma (St. Louis, MO, USA); β-glucan (from barley), pachyman (from *Poria cocos*), xyloglucan (from tamarind), arabinoxylan (medium viscosity and insoluble form, from wheat), arabinan (from sugar beet), arabinogalactan (from larch wood), galactan and pectic galactan (from potato and lupine), glucomannan (from konjac), galactomannan (from guar), and mannan (from ivory nut) were obtained from Megazyme (Wicklow, Ireland). Phosphoric acid swollen cellulose (PASC) was prepared from Avicel (Wood, 1988). Activity of recombinant proteins was determined using the 3,5-dinitrosalicylic acid (DNS) colorimetric assay (Miller, 1959). One unit of enzymatic activity was defined as the amount of enzyme which liberates 1.0 µmol of reducing sugar ends per minute from the substrate. The standard enzyme activity assay was performed with 0.1 µg/ml of Cel12E in 50 mM MES buffer 2-(N-morpholino)ethanesulfonic acid, pH 5.5 at 92°C in an oil bath rotary shaker (Infors HT Aquatron, Bottmingen, Switzerland). The pH optimum for activity was determined using different buffers (each at 50 mM): glycin-HCl (pH 2–3), sodium acetate buffer (pH 4–6), and phosphate buffer (pH 5.5–8). For enzyme thermoinactivation kinetics, 0.5 µg/ml of Cel12E were incubated over various time intervals at 80, 92, and 97°C. Residual enzymatic activity was assessed using 0.1 µg/ml of Cel12E in 50 mM MES buffer (pH 5.5) on 1.4% (w/v) CMC.

Analysis of Polysaccharide Degradation Products

The degradation products of enzymatic hydrolysis of PASC and cellodextrins were analyzed using thin layer chromatography (TLC). Two microliters of samples with cellodextrins (from cellobiose to celloheptaose) and 22.5 µl of samples with PASC were spotted on silica gel type 60 F254 aluminium plates (Merck, Darmstadt, Germany). The mobile phase consisted of acetonitrile/water (80:20 v/v). The separation was carried out twice (with thorough drying of the plates between consecutive separation steps to remove any residual mobile phase), before the degradation products were visualized by spraying the plates with a freshly prepared mixture of 10 ml stock solution (1 g diphenylamine and 1 ml aniline dissolved in 100 ml acetone) and 1 ml 85% phosphoric acid followed by incubating the plates at 120°C for 15 min.

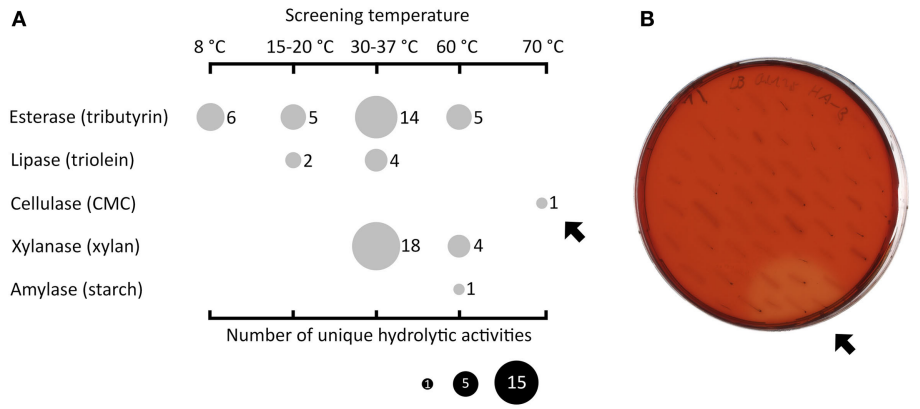

FIGURE 1 | Summary of functional screenings of diverse fosmid libraries in *E. coli*. Esterase activity was determined by the presence of clear hydrolysis halos around the colonies on LB agar indicator plates containing tributyrin (1% v/v). Lipase-active clones gave a fluorescent halo on plates with trioleine (1% v/v) supplemented with Rhodamine B when exposed to UV light (Kouker and Jaeger, 1987). (Hemi-)cellulolytic activities were visible by release of Cibacron red from dyed insoluble substrates or clear hydrolysis halos on LB substrate indicator plates containing 0.1% (w/v) carboxymethyl cellulose or oat spelt xylan. Amylolytic activity was visualized by staining the 0.3% (w/v) starch plates with Lugol's iodine solution. **(A)** Overview of all hydrolytic activities (vertical axis) identified at different incubation temperatures (horizontal axis). The size of the filled circles indicates the number of unique clones in dependence of the substrate and screening temperatures used. The black arrows indicate one particular fosmid clone termed HA-cmc-1 that was active on CMC at 70°C after 2 days of incubation **(B)**.

Substrate Binding Assays

Insoluble polysaccharides (0.5% final concentration) were mixed with 1.5 µg/µL purified Cel12E in 50 mM MES buffer containing 200 mM NaCl and incubated overnight at 6°C in a Thermomixer Comfort (Eppendorf, Germany). Protein bound on the insoluble substrate was centrifuged (21,000 × *g* for 30 min) and washed four times; bound proteins were then eluted with addition of protein loading buffer containing SDS and loaded on SDS-PAGE gels.

Results

Screening of Metagenomic Libraries for Hydrolytic Activities

Fosmid libraries containing genomic DNA derived from different habitats were functionally screened for hydrolytic activities in the mesophilic screening host *E. coli*. In order to reflect the conditions of the respective sources of the libraries, the functional screening was performed at four different temperature ranges (8°C, 15–20°C, 30–37°C, and 60–70°C). **Figure 1A** displays the types and number of discovered activities depending on the screening temperatures. The highest number of active fosmid clones was found in the mesophilic range (n = 36). Below 30°C, 13 positive clones were detected and above 37°C, 11 positive clones were found. In particular, one fosmid clone (named HA-cmc-1) was only active at 70°C, the highest temperature used in the screening. When incubated at 70°C for 2 days, colonies of *E. coli* carrying HA-cmc-1 showed a clear hydrolysis halo after Congo red staining when grown on agar plates containing CMC (**Figure 1B**). This indicated the presence of a thermophilic cellulase encoded by the fosmid insert. This fosmid contained a DNA insert derived from HA enrichment cultures, which originated from deep sea hydrothermal vents.

Sequencing and Bioinformatic Analysis of Fosmid HA-Cmc-1

In order to reveal the gene(s) carried on the cellulase activity-encoding fosmid HA-cmc-1, the fosmid was sequenced using a combination of Sanger and 454-sequencing. Assembly of the obtained sequence reads resulted in a fosmid insert of 38,175 bp DNA (Genbank/EMBL/DDBJ accession no. LN850140). Sequence analysis revealed 48 putative open reading frames (ORFs) that are represented in the fosmid map on **Figure 2A**. All predicted ORFs encoded proteins with highest similarity to *Thermococcus* species. Inspection of the predicted ORFs for the presence of glycoside hydrolase domains revealed that ORF 23 encodes a predicted glycoside hydrolase family 12 (GHF12, pfam family pf01670) protein of 566 amino acids with a predicted molecular mass of 62.3 kDa and an isoelectric point of 4.26. The protein showed amino acid sequence similarity to endo-1,4-β-glucanase b of *Thermococcus sp.* AM4 (Genbank accession no. YP_002581913.2, 45% identity, blastp E-value of $2 \times e^{-82}$). Analysis of the domain structure of this ORF revealed one GH12 module followed by two separated carbohydrate binding modules (CBMS) of family 2 (CBM2) (**Figure 2B**). Multiple sequence alignments revealed two conserved glutamates as catalytic residues in the active site (nucleophile Glu-171 and the acid-base Glu-266). CBM2 members are known to bind cellulose, chitin, and xylan[2] (Lombard et al., 2014). A signal peptide sequence motif could be predicted with a suggested signal peptidase cleavage between the residues Ala-24 and Gln-25.

Expression and Purification of Cel12E

The gene sequences encoding the entire preprotein and a N-terminally truncated form lacking the predicted signal peptide

[2]http://www.cazy.org

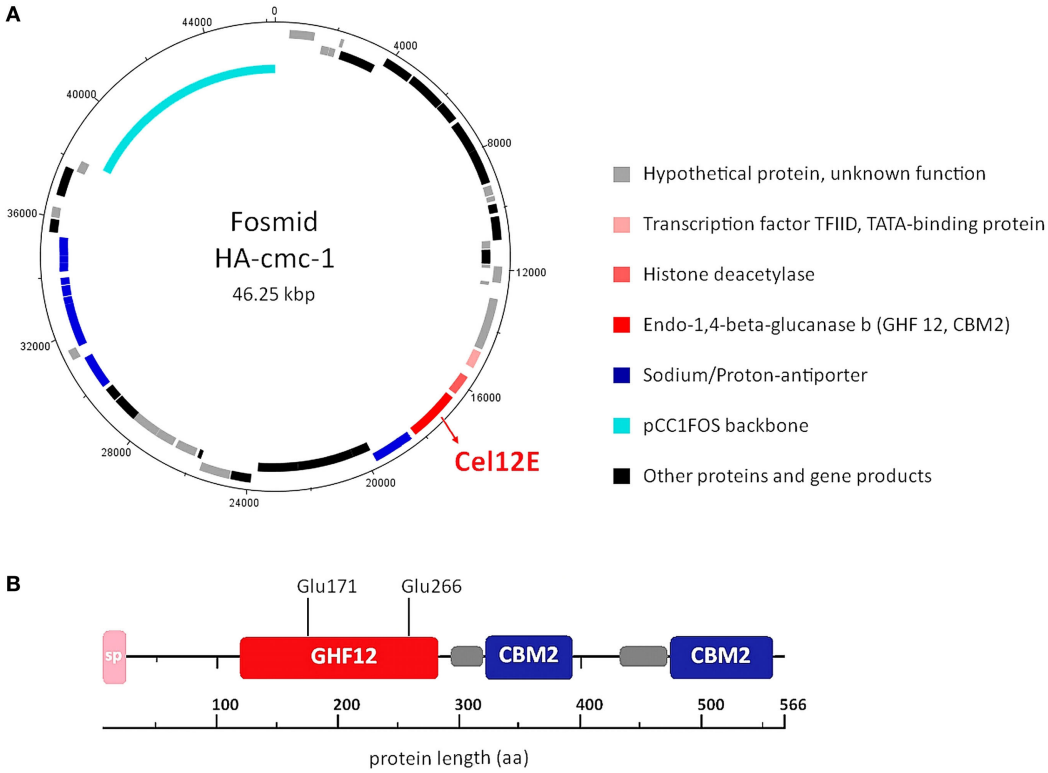

FIGURE 2 | DNA and amino acid sequence analysis of the cellulase active-fosmid HA-cmc-1 and of the Cel12E protein. (A) Predicted ORFs in forward direction (outermost ring) and reverse direction (second ring). Possible biological functions are depicted in different colors. **(B)** Multidomain architecture of Cel12E. A signal peptide (24 amino acids), the catalytic GHF12 domain, and two carbohydrate binding modules (CBM2) at the C-terminus were predicted. The predicted catalytic nucleophile Glu-171 and acid-base residue Glu-266 are indicated. Possible domain linker regions that could be predicted are shown as gray boxes.

were cloned into the pET21a(+) expression vector without the addition of any purification tag sequences. Although both enzyme variants were functionally expressed in *E. coli* BL21(DE3), the N-terminally truncated form (termed Cel12E) yielded 2.3 times higher functional protein production levels. Cel12E displayed hydrolytic activity toward CMC at temperatures above 80°C. Due to the inherent thermostable nature of the target protein, no affinity tag was needed for purification purposes. Protein purification was achieved by heat treatment of *E. coli* proteins at 80°C, followed by anion exchange chromatography and size exclusion chromatography (purification details are provided in **Table 1**). SDS-PAGE analysis (**Figure 3**) revealed a band corresponding to the expected 59.96 kDa molecular mass. Subsequently, the expressed and purified target protein was characterized biochemically.

Substrate Specificity and Product Pattern

Cel12E showed highest specific activity against β-1,4-glycosidic bonds of various linear glucan polysaccharides like PASC, barley β-glucan, lichenan, and modified soluble cellulose substrates (CMC, hydroxylethyl cellulose). In contrast to this, the activity of Cel12E toward microcrystalline cellulose was relatively low (**Table 2**). In addition to these cellulosic substrates, Cel12E also displayed side activities toward xyloglucan, glucomannan, and different types of xylans (approximately, 0.1–2.9% relative activity compared with lichenan). In order to determine intermediate and final products of the hydrolysis of PASC and various cellulose oligosaccharides (DP 2: cellobiose to DP 6: cellohexaose), TLC analysis was performed. Cellobiose and cellotriose accumulated as products when PASC was used as substrate at a Cel12E concentration of 0.2 μg per ml, whereas cellotetraose was only visible to a lesser extent. High-molecular weight intermediate products were not visible. Also, no glucose spots were detected. On the other hand, the hydrolysis of soluble cello-oligosaccharides at a high Cel12E concentration (52 μg per ml) showed degradation of cellotriose, cellotetraose, cellopentaose, and cellohexaose to monomeric glucose and cellobiose, showing that the enzyme can liberate glucose from cellotriose and larger cello-oligosaccharides under these conditions. Cellobiose was not hydrolyzed by Cel12E (**Figure 4**). Furthermore, the binding properties of Cel12E toward insoluble polysaccharides were studied. The enzyme was shown to bind to microcrystalline and amorphous cellulose as well as mixed linkage β-glucan and chitin. Binding of xylan was not observed.

Biochemical Characterization of Cel12E

Enzyme activity measurements were carried out at various temperatures and pH values. Cel12E was found to be a highly

TABLE 1 | Purification table for Cel12E.

Fraction of purification	Volume (ml)	Total protein (mg)	Total activity (U) × 10^3	Specific CMCase activity (U/mg)	Yield (%)	Fold purification
Crude cell extract	27.5	361.1 ± 3.9	14.2 ± 2.6	39.3 ± 7.5	100 ± 18.6	1.0 ± 0.2
Heat treated extract	22.5	60.3 ± 3.7	9.8 ± 0.9	162.3 ± 9.5	68.9 ± 6.1	4.1 ± 0.2
Anion exchange chromatography	0.4	17.7 ± 0.1	7.8 ± 0.6	440.2 ± 31.9	53.9 ± 6.0	11.2 ± 0.8
Gel filtration chromatography	1.6	8.0 ± 1.1	5.6 ± 1.1	700.4 ± 75.8	39.6 ± 7.9	17.8 ± 1.9

Values are average values ± 1 × SD from two independent purifications.

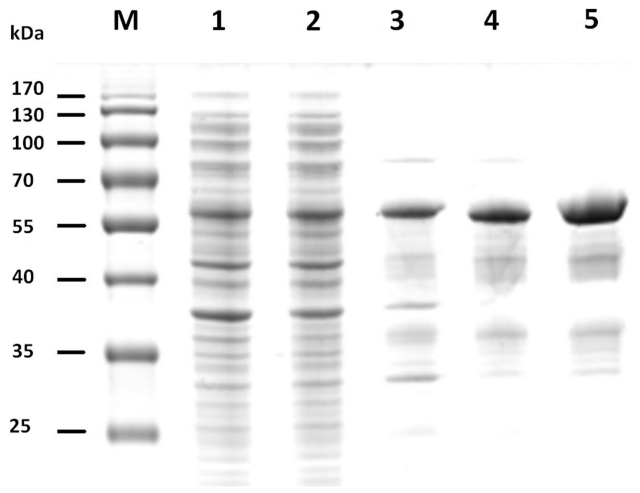

FIGURE 3 | SDS-PAGE of fractions of recombinant Cel12E throughout the purification steps. The figure shows the untreated raw extract of *E. coli* BL21 after protein expression (lane 1), the soluble fraction (lane 2), heat-treated supernatant (lane 3), collected fractions after SOURCE 15Q anion exchange (lane 4), and Superdex 200 gel filtration chromatography (lane 5). M, molecular size marker.

thermostable protein that was most active between 90 and 95°C (10 min activity assay at pH 5.5, **Figure 5A**) with an optimal pH value around 5.5. The enzyme's half-life of thermoinactivation at 92°C was approximately 2 h, while the enzyme retained more than 80% of its activity even after 4.5 h of incubation at 80°C (**Figure 5B**). Enzyme kinetics assays, performed with CMC as the substrate, revealed an apparent V_{max} value of 1,025 U/mg protein and an apparent K_m-value of 2.35 mg/ml. The influence of several salts and additives on the enzymatic activity was examined at pH 5.5 and 92°C (Table S1 in Supplementary Material). It is noteworthy that the addition of the reducing agent dithiothreitol (DTT) improved enzymatic activity by 65.9–146.2% when added at final concentrations of 10 and 1.0 mM, respectively. An activity increase of about 75% was observed in the presence of 500 mM NaCl or KCl. Interestingly, supplementation with $CoCl_2$ and $MnCl_2$ at low concentrations led to an increase of the enzymatic activity. The strongest effects were observed with concentrations of 0.5 mM $CoCl_2$ (210.9 ± 5.1% relative activity) or 1.0–2.0 mM $MnCl_2$ (188.5 ± 22.6% relative activity). Higher concentrations of these bivalent heavy metal ions caused inhibitory effects (data not shown). The promoting effect of these ions at concentrations of 1.0 mM was shown to be selective and reversible by complexation of the ions with excess amounts of EDTA (10 mM) (Table S2 in Supplementary Material). The order of the supplementation of ions and chelating agent did not have an influence on this result. Interestingly, the activating effects of monovalent salts and bivalent metal ions were additive: a combination of 0.4 M NaCl and 0.3 M KCl increased the enzyme's specific activity by a factor of 1.56, which could be boosted by the addition of 0.2 mM $CoCl_2$ to 430% of the control without supplementations (data not shown).

Discussion

Recent examples of extremely thermostable hydrolases, isolated via functional screenings, include esterases and lipases from hot solfataric springs and compost samples (Rhee et al., 2005; Leis et al., 2015), esterases from hypersaline deep sea brines (Alcaide et al., 2015a), carboxyl esterases from microbial communities inhabiting the shrimp *Rimicaris exoculata* dominating the fauna in deep-sea hydrothermal vent sites along the Mid-Atlantic Ridge (Alcaide et al., 2015b), an amylase from hydrothermal deep sea vents (Wang et al., 2011), and cellulolytic and hemicellulolytic enzymes from a naturally heated volcano site (Mientus et al., 2013).

In this study, we uncovered various hydrolase enzymes from diverse environments by functional screenings of mixed genomic DNA libraries from mesophilic, thermophilic, and hyperthermophilic microorganisms in the expression host *E. coli* at various temperatures. From 60 active clones, the majority (60%) of the enzymatic activities were observed when screening was performed at *E. coli*'s optimal growth temperature between 30 and 37°C, and a fraction of 40% was found to be active at lower or higher screening temperatures. Out of 20,000 single fosmid clones, one originating from a HA library screened at 70°C carried a particularly interesting fosmid encoding cellulolytic activity. Sequence analysis and subcloning experiments revealed that the gene responsible for this activity encoded a GHF12 endoglucanase termed Cel12E, which was characterized in more detail. The deduced Cel12E primary structure as well as the neighboring ORFs on the fosmid insert suggested that the gene originated from an extremely thermophilic archaeon possibly related to the genus *Thermococcus*.

A surprisingly low number of GHF12 proteins from hyperthermophilic archaea (*Sulfolobus solfataricus* P2, *Pyrococcus furiosus* DSM 3638, and *Caldivirga maquilingensis* IC-167) have been identified and characterized so far. They are all remarkably thermostable proteins with extremely high temperature optima between 80 and 100°C, while pH optima,

TABLE 2 | Substrate specificity of Cel12E.

Substrate (% concentration, w/v)	Type(s) of glycosidic linkage and main sugar monomers	Specific activity (U/mg protein ± SD)	Binding
POLYSACCHARIDES FROM GLUCOSEMONOMERS			
Carboxymethyl cellulose (2.0%)	β-1,4 only	692.3 ± 55.7	
β-glucan from Barley (2.0%)	Mixed β-1,3 and β-1,4	317.7 ± 3.8	Yes
Lichenan (0.5%)	Mixed β-1,3 and β-1,4	272.0 ± 6.9	
Hydroxyethyl cellulose (2.0%)	β-1,4 only	107.7 ± 8.8	
PASC (2.0%)	β-1,4 only	33.6 ± 3.8	Yes
Avicel PH-101 (2.0%)	β-1,4 only	0.03 ± 0.01	Yes
Pachyman	β-1,3 only	Not detected	Yes
Laminarin	β-1,3 and β-1,6	Not detected	
Starch	Mixed α-1,4 and α-1,6	Not detected	
POLYSACCHARIDES FROM VARIOUS SUGAR MONOMERS			
Xyloglucan from tamarind (0.5%)	β-1,4 glucose backbone, xylose sidechains	2.9 ± 0.2	
Glucomannan from konjac (0.125%)	β-1,4 glucose and mannose backbone galactose sidechains	2.8 ± 0.1	
Arabinoxylan from oat spelts (0.5%)	β-1,4 xylose backbone, arabinose and xylose sidechains	0.38 ± 0.01	No
Arabinoxylan from wheat (0.5%) iinsoluble		0.12 ± 0.02	
Arabinoxylan from wheat (0.5%) medium viscosity		0.10 ± 0.01	
Glucuronoxylan (0.5%) from birch wood (0.5%)	β-1,4 xylose backbone, 4-O-methyl-glucuronic acid sidechains	0.20 ± 0.04	
Chitin	β-1,4 *N*-acetyl-glucosamine backbone	Not detected	Yes
Chitosan	β-1,4 glucosamine and *N*-acetyl-glucosamine backbone	Not detected	No

Activities were determined at 92°C, pH 5.5. No hydrolytic activity of Cel12E could be detected toward the following polysaccharides (incubation overnight at 60°C, pH 6.0): arabinan (from sugar beet), arabinogalactan (from larch wood), galactans and pectic galactans (from lupine and potato), galactomannan (from guar), and mannan (from ivory nut).

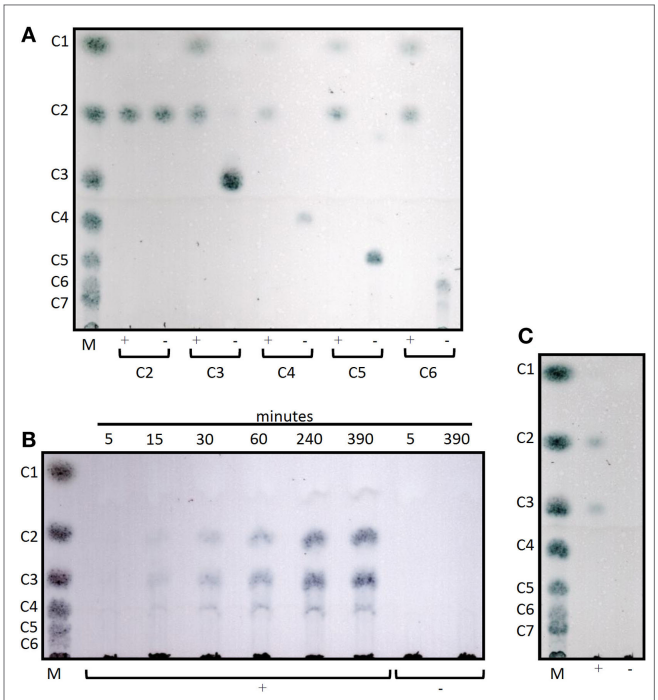

FIGURE 4 | Thin layer chromatograms of the hydrolysis products of Cel12E. (A) 0.1% (w/v) of cello-oligosaccharides from cellobiose (C2) to cellohexaose (C6) were incubated in 50 mM MES buffer pH 5.5 at 92°C for 6 h, followed by incubation at 60°C for 2 days with Cel12E at 52 μg per ml (+) or without enzyme (-, negative control) Cel12E. Samples were taken at the indicated time points and 2 μL were spotted onto a TLC plate. **(B)** Time course of the hydrolysis of PASC by Cel12E. 0.5% (w/v) PASC was incubated in 50 mM MES buffer pH 5.5 at 80°C with Cel12E at 0.2 μg per ml (+) or without enzyme (-, negative control) Cel12E. Samples were taken at the indicated time points and 22.5 μL were spotted onto a TLC plate. The incubation of the reaction mix was continued for 2 days at 60°C **(C)**. The marker (M) contains cello-oligosaccharides from glucose (DP = 1) to cellohexaose [DP = 6, **(B)**] or celloheptaose [DP = 7, **(A,C)**].

substrate specificities, and activities can vary substantially (Bauer et al., 1999; Limauro et al., 2001; Huang et al., 2005; Girfoglio et al., 2012).

The GHF12 (formerly known as cellulase family H) belongs to glycoside hydrolase clan C, the members of which have a β-jelly roll structure with two glutamate residues serving as catalytic nucleophile/base and catalytic proton donor in a retaining mechanism of hydrolysis. According to the CAZy database[2] (Lombard et al., 2014), GHF12 family proteins with endoglucanase activity (EC 3.2.1.4) are found in all domains of life, while β-1,3-1,4-glucanase (EC 3.2.1.73), xyloglucan hydrolase (EC 3.2.1.151), and xyloglucan endotransglycosylase (EC 2.4.1.207) activities seem mainly to be restricted to eukaryotes. The substrate spectrum of Cel12E determined by us confirmed the predicted endoglucanase activity, as it was able to hydrolyze mainly β-1,4-glycosidic cellulosic polysaccharides like CMC, β-glucan, hydroxyethylcellulose, and PASC, with only little activity on microcrystalline cellulose. It is interesting to note that Cel12E displays activity toward xyloglucan and xylans, which has not been previously reported for prokaryotic GH12 enzymes. The *in silico* characterization of the Cel12E protein revealed the presence of two CBMs at the C-terminus, which both belong to the CBM2 family. CBMs of this family can be divided into two types, based on the structural properties of the substrate they bind (Simpson et al., 2000). Cel12E was found to bind to cellulose but not to xylans. The presence of two CBMs can be explained as an adaptation to efficiently bind polysaccharides at extremely high temperatures. Tandem CBMs increase the affinity for polysaccharides by a factor of 10 to 100 compared to single CBMs, and since glycoside hydrolases with multiple CBMs occur most frequently in thermo- or hyperthermophilic organisms, CBM duplication may be a way to compensate for the loss of binding affinity that is observed with most molecular interactions at higher temperatures (Boraston et al., 2004).

Cel12E has a unique multidomain architecture that does not seem to exist in known proteins from other organisms.

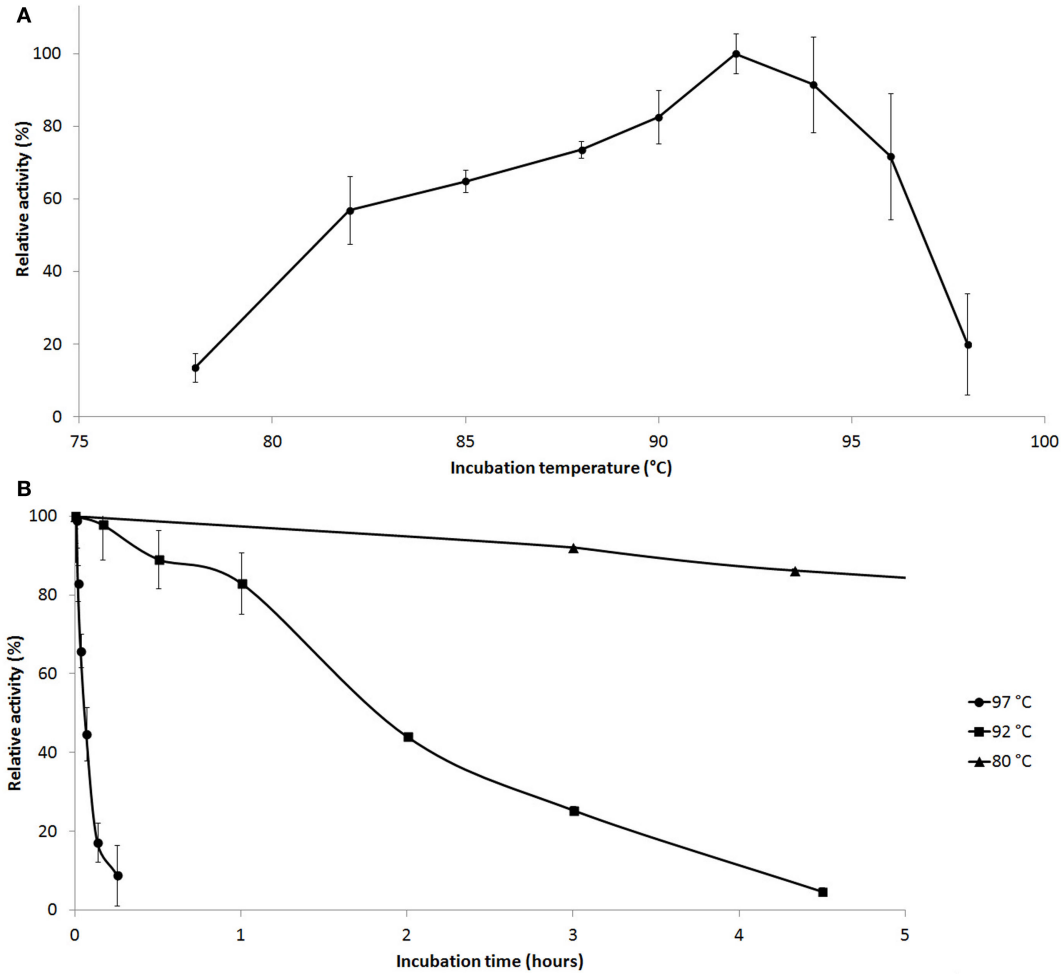

FIGURE 5 | **Effect of temperature on Cel12E activity**. **(A)** Influence of the temperature on the activity of Cel12E toward CMC at pH 5.5 in a 10-min assay. **(B)** Thermal inactivation kinetics of Cel12E at various temperatures. The purified enzyme was incubated at a concentration of 0.5 μg/ml at 80°C (triangles), 92°C (squares), or 97°C (circles) for different periods of time before determining the residual activity at 92°C in 50 mM MES buffer, pH 5.5 with CMC as substrate. Activity data are represented as relative activity from duplicate measurements (±SD).

Other archaeal proteins comprising CBM2 domains seem to be exclusively connected to GH18 catalytic modules, as in the case of *P. furiosus* DSM3638 chitinase ChiA and ChiB (Oku and Ishikawa, 2006; Nakamura et al., 2008) and *Thermococcus kodakarensis* KOD1 ChiA (Tanaka et al., 1999). Interestingly, Cel12E also displayed chitin-binding ability, which presumably is brought about by its CBM2 modules, although no chitin-degrading activity was observed. Future experiments will help to clarify if the Cel12E CBM2 modules are responsible for the observed binding to cellulose, or if this capacity is due to other parts of the protein.

The supplementation with ions has been shown to specifically inhibit or enhance enzymatic activities observed in glycoside hydrolases from thermophilic organisms, although the mechanism is not well understood. For example, the presence of certain divalent metal ions was found to be essential for activity stimulation (Gargallo et al., 2006) and/or (thermal) stabilization of other enzymes (Morag et al., 1991; Abou-Hachem et al., 2002; Santos et al., 2012). In the case of the GH12 endocellulase EGPf of *P. furiosus*, crystallographic data and examination of thermostability showed a binding motif for divalent ions (Ca^{2+}), which plays a functional role in thermostability (Kim et al., 2012). The mechanism of activation of CelE12 by low concentrations of manganese or cobalt ions remains to be elucidated.

Our data demonstrate that Cel12E is a cellulose-/β-glucan-specific endoglucanase, and based on sequence similarity of the neighboring ORFs found on the fosmid insert, we conclude that it originates from one of the uncharacterized hyperthermophilic archaea strains that were cultivated from deep sea vents. The enzyme may indicate the presence of certain β-glucan polysaccharides in the native environment, which are directly utilized by the organism, or which serve as storage polysaccharides. Another function of Cel12E may be in the metabolism of extracellular polysaccharides (EPS), which have been found in many marine organisms including hyperthermophilic archaea (Rinker and Kelly, 1996). EPS are high molecular weight carbohydrates that

form complex heteropolysaccharides containing mainly mannose, glucose, galactose, and *N*-acetylglucosamin (Poli et al., 2011). EPS serve for cell attachment onto surfaces and protect the encapsulated cells from different types of environmental stress.

Although the physiological role of Cel12E remains unclear (its natural producer organism has not been characterized yet), its unique properties make this enzyme an interesting candidate for applications such as the degradation of cellulosic biomass under harsh reaction conditions.

Acknowledgments

The authors gratefully acknowledge the support by the Faculty Graduate Center Weihenstephan of TUM Graduate School at Technische Universität München, Germany. We thank Marie Roumagnac and Nadège Bienvenu for performing growth experiments and DNA preparation from strains deposited in the UBO Culture Collection UBOCC (http://www.univ-brest.fr/souchotheque/Collection+LM2E). This work was funded by the German Federal Ministry of Education and Research (BMBF) in the collaborative project ExpresSys within the funding measure GenoMik-Transfer. PG acknowledges EU FP7 Project MicroB3 (FP7- OCEAN.2011 287589), PG and MJ acknowledge EU FP7 Project MAMBA (FP7-KBBE-2008-226977). Publication of this work was supported by the German Research Foundation (DFG) and the Technische Universität München within the funding program Open Access Publishing. The authors would like to thank Dr. Vladimir V. Zverlov for discussions and advice concerning the interpretation of the thin layer chromatograms.

Supplementary Material

The Supplementary Material for this article can be found online at http://journal.frontiersin.org/article/10.3389/fbioe.2015.00095

References

Abou-Hachem, M., Karlsson, E. N., Simpson, P. J., Linse, S., Sellers, P., Williamson, M. P., et al. (2002). Calcium binding and thermostability of carbohydrate binding module CBM4-2 of Xyn10A from *Rhodothermus marinus*. *Biochemistry* 41, 5720–5729. doi:10.1021/bi012094a

Alcaide, M., Stogios, P. J., Lafraya, Á, Tchigvintsev, A., Flick, R., Bargiela, R., et al. (2015a). Pressure adaptation is linked to thermal adaptation in salt-saturated marine habitats. *Environ. Microbiol.* 17, 332–345. doi:10.1111/1462-2920.12660

Alcaide, M., Tchigvintsev, A., Martínez-Martínez, M., Popovic, A., Reva, O. N., Lafraya, Á, et al. (2015b). Identification and characterization of carboxyl esterases of gill chamber-associated microbiota in the deep-sea shrimp *Rimicaris exoculata* by using functional metagenomics. *Appl. Environ. Microbiol.* 81, 2125–2136. doi:10.1128/AEM.03387-14

Altschul, S. F., Gish, W., Miller, W., Myers, E. W., and Lipman, D. J. (1990). Basic local alignment search tool. *J. Mol. Biol.* 215, 403–410. doi:10.1016/S0022-2836(05)80360-2

Bauer, M. W., Driskill, L. E., Callen, W., Snead, M. A., Mathur, E. J., and Kelly, R. M. (1999). An endoglucanase, EglA, from the hyperthermophilic archaeon *Pyrococcus furiosus* hydrolyzes beta-1,4 bonds in mixed-linkage (1 – 3),(1 – 4)-beta-D-glucans and cellulose. *J. Bacteriol.* 181, 284–290.

Boraston, A. B., Bolam, D. N., Gilbert, H. J., and Davies, G. J. (2004). Carbohydrate-binding modules: fine-tuning polysaccharide recognition. *Biochem. J.* 382, 769–781. doi:10.1042/BJ20040892

Delavat, F., Phalip, V., Forster, A., Plewniak, F., Lett, M.-C., and Lièvremont, D. (2012). Amylases without known homologues discovered in an acid mine drainage: significance and impact. *Sci. Rep.* 2, 354. doi:10.1038/srep00354

Ebina, T., Toh, H., and Kuroda, Y. (2009). Loop-length-dependent SVM prediction of domain linkers for high-throughput structural proteomics. *Biopolymers* 92, 1–8. doi:10.1002/bip.21105

Gargallo, R., Cedano, J., Mozo-Villarias, A., Querol, E., and Oliva, B. (2006). Study of the influence of temperature on the dynamics of the catalytic cleft in 1,3-1,4-beta-glucanase by molecular dynamics simulations. *J. Mol. Model.* 12, 835–845. doi:10.1007/s00894-006-0110-6

Girfoglio, M., Rossi, M., and Cannio, R. (2012). Cellulose degradation by *Sulfolobus solfataricus* requires a cell-anchored endo-β-1-4-glucanase. *J. Bacteriol.* 194, 5091–5100. doi:10.1128/JB.00672-12

Grant, S., Sorokin, D. Y., Grant, W. D., Jones, B. E., and Heaphy, S. (2004). A phylogenetic analysis of Wadi el Natrun soda lake cellulase enrichment cultures and identification of cellulase genes from these cultures. *Extremophiles* 8, 421–429. doi:10.1007/s00792-004-0402-7

Handelsman, J., Rondon, M. R., Brady, S. F., Clardy, J., and Goodman, R. M. (1998). Molecular biological access to the chemistry of unknown soil microbes: a new frontier for natural products. *Chem. Biol.* 5, R245–R249. doi:10.1016/S1074-5521(98)90108-9

Huang, Y., Krauss, G., Cottaz, S., Driguez, H., and Lipps, G. (2005). A highly acid-stable and thermostable endo-β-glucanase from the thermoacidophilic archaeon *Sulfolobus solfataricus*. *Biochem. J.* 385, 581. doi:10.1042/BJ20041388

Ilmberger, N., Meske, D., Juergensen, J., Schulte, M., Barthen, P., Rabausch, U., et al. (2012). Metagenomic cellulases highly tolerant towards the presence of ionic liquids – linking thermostability and halotolerance. *Appl. Microbiol. Biotechnol.* 95, 135–146. doi:10.1007/s00253-011-3732-2

Kim, H.-W., Kataoka, M., and Ishikawa, K. (2012). Atomic resolution of the crystal structure of the hyperthermophilic family 12 endocellulase and stabilizing role of the DxDxDG calcium-binding motif in *Pyrococcus furiosus*. *FEBS Lett.* 586, 1009–1013. doi:10.1016/j.febslet.2012.02.029

Kouker, G., and Jaeger, K. E. (1987). Specific and sensitive plate assay for bacterial lipases. *Appl. Environ. Microbiol.* 53, 211–213.

Laemmli, U. K. (1970). Cleavage of structural proteins during the assembly of the head of bacteriophage T4. *Nature* 227, 680–685. doi:10.1038/227680a0

Langer, M., Gabor, E. M., Liebeton, K., Meurer, G., Niehaus, F., Schulze, R., et al. (2006). Metagenomics: an inexhaustible access to nature's diversity. *Biotechnol. J.* 1, 815–821. doi:10.1002/biot.200600111

Leis, B., Angelov, A., and Liebl, W. (2013). Screening and expression of genes from metagenomes. *Adv. Appl. Microbiol.* 83, 1–68. doi:10.1016/B978-0-12-407678-5.00001-5

Leis, B., Angelov, A., Mientus, M., Li, H., Pham, V. T., Lauinger, B., et al. (2015). Identification of novel esterase-active enzymes from hot environments by use of the host bacterium *Thermus thermophilus*. *Front. Microbiol.* 6:275. doi:10.3389/fmicb.2015.00275

Li, S.-J., Hua, Z.-S., Huang, L.-N., Li, J., Shi, S.-H., Chen, L.-X., et al. (2014). Microbial communities evolve faster in extreme environments. *Sci. Rep.* 4, 6205. doi:10.1038/srep06205

Liebl, W., Angelov, A., Juergensen, J., Chow, J., Loeschcke, A., Drepper, T., et al. (2014). Alternative hosts for functional (meta)genome analysis. *Appl. Microbiol. Biotechnol.* 98, 8099–8109. doi:10.1007/s00253-014-5961-7

Limauro, D., Cannio, R., Fiorentino, G., Rossi, M., and Bartolucci, S. (2001). Identification and molecular characterization of an endoglucanase gene, celS, from the extremely thermophilic archaeon *Sulfolobus solfataricus*. *Extremophiles* 5, 213–219. doi:10.1007/s007920100200

Lombard, V., Golaconda Ramulu, H., Drula, E., Coutinho, P. M., and Henrissat, B. (2014). The carbohydrate-active enzymes database (CAZy) in 2013. *Nucleic Acids Res.* 42, D490–D495. doi:10.1093/nar/gkt1178

Mientus, M., Brady, S., Angelov, A., Zimmermann, P., Wemheuer, B., Schuldes, J., et al. (2013). Thermostable xylanase and β-glucanase derived from the metagenome of the Avachinsky crater in Kamchatka (Russia). *Curr. Biotechnol.* 2, 284–293. doi:10.2174/22115501029991311281502 57

Miller, G. L. (1959). Use of dinitrosalicylic acid reagent for determination of reducing sugar. *Anal. Chem.* 31, 426–428. doi:10.1021/ac60147a030

Morag, E., Halevy, I., Bayer, E. A., and Lamed, R. (1991). Isolation and properties of a major cellobiohydrolase from the cellulosome of *Clostridium thermocellum*. *J. Bacteriol.* 173, 4155–4162.

Nakamura, T., Mine, S., Hagihara, Y., Ishikawa, K., Ikegami, T., and Uegaki, K. (2008). Tertiary structure and carbohydrate recognition by the chitin-binding domain of a hyperthermophilic chitinase from *Pyrococcus furiosus*. *J. Mol. Biol.* 381, 670–680. doi:10.1016/j.jmb.2008.06.006

Oku, T., and Ishikawa, K. (2006). Analysis of the hyperthermophilic chitinase from *Pyrococcus furiosus*: activity toward crystalline chitin. *Biosci. Biotechnol. Biochem.* 70, 1696–1701. doi:10.1271/bbb.60031

Overbeek, R., Begley, T., Butler, R. M., Choudhuri, J. V., Chuang, H.-Y., Cohoon, M., et al. (2005). The subsystems approach to genome annotation and its use in the project to annotate 1000 genomes. *Nucleic Acids Res.* 33, 5691–5702. doi:10.1093/nar/gki866

Petersen, T. N., Brunak, S., von Heijne, G., and Nielsen, H. (2011). SignalP 4.0: discriminating signal peptides from transmembrane regions. *Nat. Methods* 8, 785–786. doi:10.1038/nmeth.1701

Poli, A., Di Donato, P., Abbamondi, G. R., and Nicolaus, B. (2011). Synthesis, production, and biotechnological applications of exopolysaccharides and polyhydroxyalkanoates by archaea. *Archaea* 2011, 1–13. doi:10.1155/2011/693253

Punta, M., Coggill, P. C., Eberhardt, R. Y., Mistry, J., Tate, J., Boursnell, C., et al. (2012). The Pfam protein families database. *Nucleic Acids Res.* 40, D290–D301. doi:10.1093/nar/gkr1065

Rabausch, U., Juergensen, J., Ilmberger, N., Bohnke, S., Fischer, S., Schubach, B., et al. (2013). Functional screening of metagenome and genome libraries for detection of novel flavonoid-modifying enzymes. *Appl. Environ. Microbiol.* 79, 4551–4563. doi:10.1128/AEM.01077-13

Rhee, J.-K., Ahn, D.-G., Kim, Y.-G., and Oh, J.-W. (2005). New thermophilic and thermostable esterase with sequence similarity to the hormone-sensitive lipase family, cloned from a metagenomic library. *Appl. Environ. Microbiol.* 71, 817–825. doi:10.1128/AEM.71.2.817-825.2005

Rinker, K. D., and Kelly, R. M. (1996). Growth physiology of the hyperthermophilic archaeon *Thermococcus litoralis*: development of a sulfur-free defined medium, characterization of an exopolysaccharide, and evidence of biofilm formation. *Appl. Environ. Microbiol.* 62, 4478–4485.

Sambrook, J., Fritsch, E. F., and Maniatis, T. (1989). *Molecular Cloning: A Laboratory Manual*, 2nd Edn. New York, NY: Cold Spring Harbor Laboratory Press.

Santos, C. R., Paiva, J. H., Sforça, M. L., Neves, J. L., Navarro, R. Z., Cota, J., et al. (2012). Dissecting structure-function-stability relationships of a thermostable GH5-CBM3 cellulase from *Bacillus subtilis* 168. *Biochem. J.* 441, 95–104. doi:10.1042/BJ20110869

Simon, C., Herath, J., Rockstroh, S., and Daniel, R. (2009). Rapid identification of genes encoding DNA polymerases by function-based screening of metagenomic libraries derived from glacial ice. *Appl. Environ. Microbiol.* 75, 2964–2968. doi:10.1128/AEM.02644-08

Simpson, P. J., Xie, H., Bolam, D. N., Gilbert, H. J., and Williamson, M. P. (2000). The structural basis for the ligand specificity of family 2 carbohydrate-binding modules. *J. Biol. Chem.* 275, 41137–41142. doi:10.1074/jbc.M006948200

Tanaka, T., Fujiwara, S., Nishikori, S., Fukui, T., Takagi, M., and Imanaka, T. (1999). A unique chitinase with dual active sites and triple substrate binding sites from the hyperthermophilic archaeon *Pyrococcus kodakaraensis* KOD1. *Appl. Environ. Microbiol.* 65, 5338–5344.

Taupp, M., Mewis, K., and Hallam, S. J. (2011). The art and design of functional metagenomic screens. *Curr. Opin. Biotechnol.* 22, 465–472. doi:10.1016/j.copbio.2011.02.010

Ten, L. N., Im, W.-T., Kim, M.-K., and Lee, S.-T. (2005). A plate assay for simultaneous screening of polysaccharide- and protein-degrading micro-organisms. *Lett. Appl. Microbiol.* 40, 92–98. doi:10.1111/j.1472-765X.2004.01637.x

Voget, S., Leggewie, C., Uesbeck, A., Raasch, C., Jaeger, K.-E., and Streit, W. R. (2003). Prospecting for novel biocatalysts in a soil metagenome. *Appl. Environ. Microbiol.* 69, 6235–6242. doi:10.1128/AEM.69.10.6235-6242.2003201203

Wang, H., Gong, Y., Xie, W., Xiao, W., Wang, J., Zheng, Y., et al. (2011). Identification and characterization of a novel thermostable gh-57 gene from metagenomic fosmid library of the Juan de Fuca Ridge hydrothemal vent. *Appl. Biochem. Biotechnol.* 164, 1323–1338. doi:10.1007/s12010-011-9215-1

Wood, P. J., Erfle, J. D., and Teather, R. M. (1988). Use of complex formation between Congo red and polysaccharides in detection and assay of polysaccharide hydrolases. *Meth. Enzymol.* 160, 59–74. doi:10.1007/s00284-008-9276-8

Wood, T. M. (1988). Preparation of crystalline, amorphous, and dyed cellulase substrates. *Meth. Enzymol.* 160, 19–25.

Conflict of Interest Statement: The authors declare that the research was conducted in the absence of any commercial or financial relationships that could be construed as a potential conflict of interest.

frontiers in Bioengineering and Biotechnology

REVIEW
published: 03 June 2015
doi: 10.3389/fbioe.2015.00075

Alkaliphilic bacteria with impact on industrial applications, concepts of early life forms, and bioenergetics of ATP synthesis

*Laura Preiss[1], David B. Hicks[2], Shino Suzuki[3,4], Thomas Meier[1] and Terry Ann Krulwich[2]**

[1] *Department of Structural Biology, Max Planck Institute of Biophysics, Frankfurt, Germany,* [2] *Department of Pharmacology and Systems Therapeutics, Icahn School of Medicine at Mount Sinai, New York, NY, USA,* [3] *Geomicrobiology Group, Kochi Institute for Core Sample Research, Japan Agency for Marine-Earth Science and Technology, Nankoku, Japan,* [4] *Microbial and Environmental Genomics, J. Craig Venter Institutes, La Jolla, CA, USA*

OPEN ACCESS

Edited by:
Noha M. Mesbah, Suez Canal University, Egypt

Reviewed by:
Aharon Oren, The Hebrew University of Jerusalem, Israel
Isao Yumoto, National Institute of Advanced Industrial Science and Technology, Japan

***Correspondence:**
Terry Ann Krulwich, Department of Pharmacology and Systems Therapeutics, Icahn School of Medicine at Mount Sinai, Box 1603, 1468 Madison Avenue, New York, NY 10029, USA
terry.krulwich@mssm.edu

Specialty section:
This article was submitted to Process and Industrial Biotechnology, a section of the journal Frontiers in Bioengineering and Biotechnology

Received: *30 March 2015*
Accepted: *10 May 2015*
Published: *03 June 2015*

Citation:
Preiss L, Hicks DB, Suzuki S, Meier T and Krulwich TA (2015) Alkaliphilic bacteria with impact on industrial applications, concepts of early life forms, and bioenergetics of ATP synthesis. Front. Bioeng. Biotechnol. 3:75. doi: 10.3389/fbioe.2015.00075

Alkaliphilic bacteria typically grow well at pH 9, with the most extremophilic strains growing up to pH values as high as pH 12–13. Interest in extreme alkaliphiles arises because they are sources of useful, stable enzymes, and the cells themselves can be used for biotechnological and other applications at high pH. In addition, alkaline hydrothermal vents represent an early evolutionary niche for alkaliphiles and novel extreme alkaliphiles have also recently been found in alkaline serpentinizing sites. A third focus of interest in alkaliphiles is the challenge raised by the use of proton-coupled ATP synthases for oxidative phosphorylation by non-fermentative alkaliphiles. This creates a problem with respect to tenets of the chemiosmotic model that remains the core model for the bioenergetics of oxidative phosphorylation. Each of these facets of alkaliphilic bacteria will be discussed with a focus on extremely alkaliphilic *Bacillus* strains. These alkaliphilic bacteria have provided a cogent experimental system to probe adaptations that enable their growth and oxidative phosphorylation at high pH. Adaptations are clearly needed to enable secreted or partially exposed enzymes or protein complexes to function at the high external pH. Also, alkaliphiles must maintain a cytoplasmic pH that is significantly lower than the pH of the outside medium. This protects cytoplasmic components from an external pH that is alkaline enough to impair their stability or function. However, the pH gradient across the cytoplasmic membrane, with its orientation of more acidic inside than outside, is in the reverse of the productive orientation for bioenergetic work. The reversed gradient reduces the trans-membrane proton-motive force available to energize ATP synthesis. Multiple strategies are hypothesized to be involved in enabling alkaliphiles to circumvent the challenge of a low bulk proton-motive force energizing proton-coupled ATP synthesis at high pH.

Keywords: alkaliphiles, biotechnology, serpentinization, ATP synthase, *Bacillus pseudofirmus* OF4, bioenergetics, proton-motive force

Introduction to Alkaliphilic Bacteria

The term alkaliphilic microorganisms or "alkaliphiles," generally refers to microorganisms that grow well at pH values exceeding pH 9, often in the 10–13 range of pH (Horikoshi, 1999). Obligate alkaliphiles is a term used for alkaliphiles that grow only at pH values of ~pH 9 and above, while

facultative alkaliphiles are strains that grow optimally under stringent alkaline conditions but are also capable of growing near neutral pH (Guffanti et al., 1986). Professor Koki Horikoshi, who has played a major role in developing interest in alkaliphilic bacteria and their capabilities, noted that only 16 papers on alkaliphilic bacteria had been published when he began his extensive studies of them in 1968 (Horikoshi, 1999). Since then, alkaliphiles have gained much more attention because of major contributions they make via the natural products they produce and the impact they have on diverse ecological settings. Interestingly, highly alkaliphilic bacteria, including some obligate alkaliphiles, have also been isolated from garden soils or other non-extremophilic settings. This suggests that these soils harbored niches that provided the necessary conditions for the persistence of such alkaliphiles (Horikoshi, 2006). Alkaliphilic bacteria are an important source of useful, stable enzymes and novel chemicals, including antimicrobials (Joshi et al., 2008; Fujinami and Fujisawa, 2010; Horikoshi, 2011; Sarethy et al., 2011; Ibrahim et al., 2012). Also, alkaliphile cells with specific capabilities can be used to carry out particular processes that benefit from the alkaline *milieu*, such as removing H_2S from "sour" gas streams produced in the petrochemical industry (Sorokin et al., 2008). The ecological niches of alkaliphiles are remarkably diverse, e.g., ranging from alkaline soda lakes (Jones et al., 1998; Grant et al., 2004), the hind-gut of insects (Thongaram et al., 2003, 2005), to soils subjected to ammonification and human industrial processes that generate high pH (Jones et al., 1998). Other interesting environments are the alkaline hydrothermal vents, which have been proposed to recapitulate conditions that existed during formation of early life forms (Martin and Russell, 2007; Mulkidjanian et al., 2007; Martin et al., 2008; Lane and Martin, 2012; Herschy et al., 2014). The microbial activities impact the properties of their ecological niches and the niches impact the bacteria, as the evolutionary dance between the niche and the microbial population unfolds.

The next two sections will first amplify biotechnological contributions of alkaliphiles and the soda lakes in which many of those alkaliphiles are found (Jones et al., 1998; Grant, 2003; Sorokin et al., 2011, 2014), and then expand upon additional alkaline ecosystems that are "early earth analogs" (Suzuki et al., 2013). The extremophile enzyme that will then be highlighted in the final section is the F_1F_o-ATP synthase that is found in Gram-positive alkaliphilic *Bacillus* strains, such as *Bacillus pseudofirmus* OF4 (Janto et al., 2011) and *B. halodurans* C-125 (Takami et al., 2000). These alkaliphiles carry out oxidative phosphorylation in support of non-fermentative growth. The finding that such alkaliphilic aerobes use proton-coupled ATP synthases was a surprising finding, since the apparently low bulk proton-motive force (PMF) had led to the expectation that synthesis would be coupled to larger bulk sodium-ion gradients (Hicks and Krulwich, 1990; Krulwich, 1995). The use of protons at low bulk PMF has led to re-consideration of the idea that the PMF, which drives ATP synthesis, is the electrochemical gradient of protons between the bacterial cytoplasm and the bulk external *milieu* as envisioned in Peter Mitchell's ground-breaking work (Mitchell, 1961). More localized models have gained ground (Williams, 1978; Slater, 1987; Heberle et al., 1994; Krulwich, 1995; Yumoto, 2002; Goto et al., 2005; Krulwich and Ito, 2013). As will be discussed, these models include fast movement of protons along the outer surface of the coupling membrane between proton pumps and ATP synthases. Other models include membrane properties that can increase proximity between pumps and synthases. A variety of emerging new findings now provide new opportunities to explore features that may together circumvent the "bioenergetic challenge" of proton-coupled ATP synthesis at low bulk PMF.

Applications of Alkaliphilic Bacteria and Their Enzymes

A comprehensive review of established and proposed applications of alkaliphilic cells and alkaliphile enzymes to industrial uses is beyond the scope of this review; several such reviews have already been mentioned above. The aim of this section is, rather, to present a selection of applications in order to underscore the breadth of alkaliphile contributions for those whose interest in alkaliphiles are attuned mostly to the ecological or bioenergetic aspects of bacterial alkaliphily.

A major contribution of alkaliphiles to enzymes used in industry is the diversity of enzymes with activity optima shifted to the alkaline pH region. Mesophilic bacteria produce enzymes with similar activities but without enzymatic capacity at elevated pH. Alkaliphile enzymes from aerobic and anaerobic alkaliphilic bacteria tend, as expected, to have activity profiles that included higher pH values than displayed by mesophile enzymes. The added attraction was that they also often had additional capacities, e.g., some with high temperature optima and others with low temperature optima that increased the range of environments in which they were catalytically competent (Kumar and Takagi, 1999; Fujinami and Fujisawa, 2010; Horikoshi, 2011; Sarethy et al., 2011). Examples of alkaliphile enzymes and their uses include alkaline proteases, which are used as detergent additives and for removing hair from hides; starch-degrading amylases with elevated pH optima are also suitable for laundry use and debranching enzymes, together with amylase, play a role in stain removal (Ito et al., 1989; Gessesse et al., 2003; Sarethy et al., 2011); alkaline keratinases can degrade feathers that are often unwanted by-products of other processes (Kojima et al., 2006); and cyclomaltodextrin glucanotransferases (CGTases) from alkaliphilic strains enhance the production of cyclodextrins (CDs), which are used in pharmaceuticals, foodstuffs, and for chemical interactions (Horikoshi, 1999; Qi and Zimmermann, 2005; Fujinami and Fujisawa, 2010). Alkaliphiles also produce useful metabolites, including antibiotics. Among other metabolites, carotenoids are worth mentioning. They are for example responsible for the yellow color of many alkaliphilic *Bacillus* strains (Aono and Horikoshi, 1991).

In addition to useful alkaliphile enzymes and metabolites, there are many processes that can utilize these extremophiles, sometimes a mixture of alkaliphiles and other bacterial cells, to produce the desired changes. A classic example is the presence of *Alkalibacterium* strains as part of the microbiota involved in production of indigo blue dye from various plants in Europe, Japan, Korea, and elsewhere. Successive oxidation and reduction steps occur in a dye vat, in which the alkaliphile strains

have important roles in the reducing phases (Aino et al., 2010; Park et al., 2012). Another example involving participation of alkaliphilic bacterial cells in a reduction process is the Fe(III)-reducing bacterium "*Alkaliphilus metalliredigens* QYMF" which could have useful applications to metal-contaminated alkaline environments (Ye et al., 2004; Roh et al., 2007). In another scenario, thermo-alkaliphilic *Bacillus* strains isolated from a textile wastewater drain were found to grow at pH 9.3–10 at 60–65°C (Paar et al., 2001). The most stable catalase among the strains was isolated from a strain designated *Bacillus* SF. This catalase was biochemically characterized and immobilized in order to recycle the remaining textile bleaching effluent without free enzyme contamination. A different situation is found when H_2S is present in fuel gases and needs to be removed before combustion can proceed. Lithoautotrophs (sometimes called chemoautotrophs) can oxidize inorganic substrates such as H_2S as an energy source. H_2S-oxidizing bacteria of the genus *Thioalkalivibrio* were used in "lab-scale sulfide-removing bioreactors." The results suggest that members of the *Thioalkalivibrio* genus have significant potential to oxidize sulfide under haloalkaline conditions in which desulfurization of natural gas is needed (Sorokin et al., 2008).

A final example of biotechnological deployment of alkaliphiles are microbial fuel cells (MFCs) (Logan et al., 2006). In the developing area of MFC devices, bacteria oxidize organic or inorganic substrates and generate current. As electrons are produced during the oxidation reactions, they are transferred to the anode, the negative terminal. They then flow to the cathode, the positive terminal, via conductive material whose properties support conditions for producing electricity. Among the bacteria that have been used for MFCs is a psychrophilic alkaliphile from seawater, *Pseudomonas alcaliphila* MBR (Yumoto et al., 2001), which releases phenazine-1-carboxylic acid under alkaline conditions (Zhang et al., 2011). A second, Gram-positive alkaliphile has been used to generate "bioelectricity" in an MFC. It is *Corynebacterium* sp. strain MFC03, which uses organic compounds, e.g., glucose, as electron donors at pH 9. The electron transfer mechanism which it employs appears to rely primarily on redox compounds that are excreted into the medium (Liu et al., 2010).

The examples given here underline the diversity of alkaliphile enzymes that have potential applications to industrial settings. Those applications continue to be identified with an increasing pace.

Association of Alkaliphiles with Soda Lakes, Alkaline Hydrothermal Vents, and Other Serpentinizing Ecosystems

Many of the diverse alkaliphiles that display novel physiological features and potential applications were isolated from soda lakes found in various continents and settings (Borkar, 2015). Their properties, in addition to alkaliphily, cover wide tolerance ranges for salinity, temperature, and/or hydrogen levels. Soda lake alkaliphiles also participate in biogeochemical redox cycles of carbon, sulfur, and nitrogen (Sorokin et al., 2008, 2011, 2014), exhibiting capacities that are not found in alkaliphiles from other environments. Soda lake alkaliphiles are found extensively in parts of Asia (e.g., China and Russia) and in Africa (Jones et al., 1998; Sorokin et al., 2011), but there are other well-studied alkaliphiles that were found in places where soda lakes are less frequent, e.g., Lake Mono in California (Humayoun et al., 2003). As noted, the alkaliphiles isolated from soda lakes are often poly-extremophiles, e.g., *Natranaerobius thermophilus*, an anaerobe, which was isolated from the hypersaline lake Wadi El Natrun, Egypt and is resistant to high sodium-ion concentrations, pH, and temperature (Mesbah et al., 2009). The haloalkalithermophile *N. thermophilus* is an example of poly-extremophiles. In general, each of the individual resistances of a poly-extremophile is less extreme than the resistance observed for singly extremophilic bacteria, but the trade-off enables viability under multiple simultaneous stresses (Bowers et al, 2009; Mesbah et al., 2009; Mesbah and Wiegel, 2012).

Hydrothermal chimneys and black smoker vents that support biological communities were found in 1979 associated with mid-ocean ridges that have underlying layers of magma, whose cooling was a source of energy (Spiess et al., 1980). Subsequent findings of numerous vent fields were reported, followed by reports of the "Lost City Hydrothermal Field," which was found at a different water depth and was shown to have novel properties. It is now recognized as a serpentinizing ecosystem (Kelley et al., 2005) with active carbonate structures and a broad range of springs, including some that have high temperatures and others that are in somewhat cooler settings. Their microbial cohort includes a dominant number of Archaea, and its bacterial cohort includes Gram-negative Epsilonproteobacteria and Gammaproteobacteria as well as Gram-positive Firmicutes that are relatives of known Firmicute sulfur- and methane-oxidizers (Schrenk et al., 2004). Brazelton et al. (2013) noted that the ultrabasic serpentinite springs can provide "windows" into the marine sub-surface, in an analogous way to the information obtained from deep hydrothermal vents. Recently, models of proton-based chemiosmosis were described that included a potential alkaline compartment for which there is a natural chemical origin. In turn, this model led to proposals that the alkaline hydrothermal vents could be a site for early development of cells (Martin and Russell, 2007; Martin et al., 2008; Lane et al., 2010; Lane and Martin, 2012). Others have characterized different ecological settings, which are terrestrial but anoxic geothermal fields; they proposed that these might be possible sites of the earliest life, based more on sodium-ion-coupling, which has been found in bacteria that have sodium pumps but are lower energy-consumers than bacteria that use proton-based oxidative phosphorylation, e.g., *Ilyobacter tartaricus* and *Propionigenium modestum* (Dimroth, 1997). Proton-coupling may have emerged early in alkaline hydrothermal vents, but may not have been immediately able to make levels of available energy comparable to levels made available by oxidative phosphorylation which involves electron transport by respiratory chain complexes and oxygen reduction, as it provides energy for proton-coupled ATP synthesis (Dimroth and Cook, 2004; Mulkidjanian et al., 2008, 2012). Questions regarding whether either Na^+ or H^+ coupling came "first" in evolutionary terms, or whether it is possible that they may have evolved in parallel in different niches, will not be addressed here. However, findings that indicate early presence of alkaliphilic bacteria are emerging from studies of specific serpentinizing ecosystems, and will be described.

FIGURE 1 | *Serpentimonas* strains have been isolated from the Barnes springs at The Cedars. The images show Barnes spring complex (left) and Barns spring 5 (right). The Cedars is an area in northern California noted for the presence of abundant ultrabasic, highly alkaline, springs (pH 11–12) as the product of serpentinization. Serpentinization is a process involving reaction of water with ultramafic minerals, which have low silica content but are rich in minerals such as olivine. The interaction leads to formation of a new set of minerals including serpentine along with methane, hydrogen, and alkaline fluids. Barnes spring complex is one of the largest complexes in this site. The spring waters discharged from the sub-surface contain calcium as the result of serpentinization. The calcium reacts with carbonate at the surface of the spring, producing calcium carbonate precipitate that covers the surface of the springs (Frost and Beard, 2007; Suzuki et al., 2013).

Like The Lost City Hydrothermal Fields, which were noted earlier, The Cedars is an active serpentinization site, but it is located on the coast of northern California and is fed by deep groundwater (Suzuki et al., 2013) (**Figure 1**). The Cedars comprises highly basic and reducing springs with low salinity and has bacteria from various phyla, including clostridia and Betaproteobacteria. A highly alkaliphilic, hydrogen-oxidizing Gram-negative Betaproteobacterium was isolated from a spring with a pH of 11.6. It displays a pH optimum for growth of pH 11 and it exhibits autotrophic growth on hydrogen, calcium carbonate, and oxygen. The name "*Serpentinomonas raichei* A1" has been proposed for this extremely alkaliphilic organism and its gene sequence indicates that it has an ATP synthase that couples to protons rather than sodium ions (Suzuki et al., 2014). As discussed in the final section of this review, *S. raichei* A1 and several other Gram-negative alkaliphiles that couple ATP synthesis to protons differ from Gram-positive alkaliphiles in the amino acid sequence motifs of two key subunits of the ATP synthase. This difference may provide clues to the range of adaptations that enable proton-coupled ATP synthesis to proceed under the adverse conditions of a low "bulk" PMF. More interesting observations may arise from an increasing number of alkaline ground water (Roadcap et al., 2006) and serpentinite sites whose bacterial cohort can be studied (Crespo-Medina et al., 2014; Meyer-Dombard et al., 2015).

The Bioenergetic Challenge Imposed upon Alkaliphiles That Carry Out Proton-Coupled Oxidative Phosphorylation

A Schematic Profile of Bioenergetic Cycles and Related Cell Structures of Extremely Alkaliphilic *Bacillus* Strains

The central challenge for extremely alkaliphilic bacteria is the maintenance of a cytoplasmic pH that is significantly lower than the highly alkaline external *milieu* in which they grow. As depicted in **Figure 2**, *B. pseudofirmus* OF4 grows in media with a pH of 10.5. Under these conditions, alkaliphilic *Bacillus* strains use antiporters to catalyze an electrogenic exchange of outwardly moving sodium ions, or in some instances potassium ions, for a greater number of entering protons. The multi-subunit Mrp-type of antiporter comprises 7 hydrophobic gene products, or a 6-subunit version in which MrpA and MrpB are fused. This membrane-embedded antiporter plays an essential role in catalyzing the electrogenic antiport in support of alkaliphily in intensively studied organisms such as *B. pseudofirmus* OF4 (Janto et al., 2011) and *B. halodurans* C-125 (Takami et al., 2000) and *B. alcalophilus*, which appears to have a potassium ion cycle that includes at least one of its two Mrp antiporters (Attie et al., 2014). A point mutation that rendered *B. halodurans* C-125 non-alkaliphilic led to characterization of the Mrp-type antiporters (Hamamoto et al., 1994), which are also found in both Gram-positive and Gram-negative non-alkaliphiles. Among the bacteria in which Mrp antiporters have been found to have important roles are non-alkaliphiles that are able to grow under moderately alkaline conditions, e.g., *B. subtilis*, *P. aeruginosa*, *Rhizobium meliloti*, *Vibrio cholerae*, and *Staphylococcus aureus* (Hiramatsu et al., 1998; Putnoky et al., 1998; Ito et al., 1999; Kosono et al., 1999, 2005; Swartz et al., 2005; Dzioba-Winogrodzki et al., 2009). In addition to one or more Mrp cation/proton antiporters, alkaliphilic bacteria generally have a robust cohort of additional antiporters encoded by single genes (Takami et al., 2000; Janto et al., 2011).

It is crucial for maintenance of pH homeostasis in extreme alkaliphiles that there is continuous availability of the efflux cation so that the cation/proton antiporters have a substrate, be it sodium- or potassium-ions, to exchange with cell-external protons (Krulwich et al., 1985). The cation/proton antiporters are indispensable in enabling alkaliphiles to sustain a cytoplasmic pH that is often more than two pH units below the pH of the medium (Krulwich, 1995). For example, *B. pseudofirmus* OF4 maintains a cytoplasmic pH of ≤8.3 at an external pH of 10.8 and has an upper pH limit for growth at about pH 11.4 (Sturr et al., 1994). In addition to the cation/proton antiporters, several other paths for cation entry play roles in ensuring that sufficient cytoplasmic substrate for the antiporters is present at high pH. A major additional route of cation uptake is provided by the numerous solute uptake pathways that take up solutes together with sodium ions, which is energetically favorable because of the inwardly directed sodium-ion gradient (**Figure 2**). Also shown in **Figure 2** are two additional entry routes for cations that contribute to pH homeostasis in alkaliphiles under high pH conditions. One route is provided by the cation uptake channels that power flagellar rotation, e.g., the MotPS sodium-ion channel in extremely alkaliphilic *Bacillus* strains including *B. halodurans* C-125 and *B. pseudofirmus* OF4 (Fujinami et al., 2009). Interestingly, some neutrophilic *Bacillus* strains, including *B. subtilis,* have a proton-conducting MotAB motility channel as well as a sodium-ion-conducting MotPS type (Ito et al., 2004a). A second group of channels that support cation uptake in alkaliphilic *Bacillus* strains are voltage-gated cation channels (**Figure 2**). A voltage-gated sodium-ion channel from *B. halodurans* C-125 was first noted by Durell and Guy (2001) and hypothesized to be a calcium ion channel. When subsequently

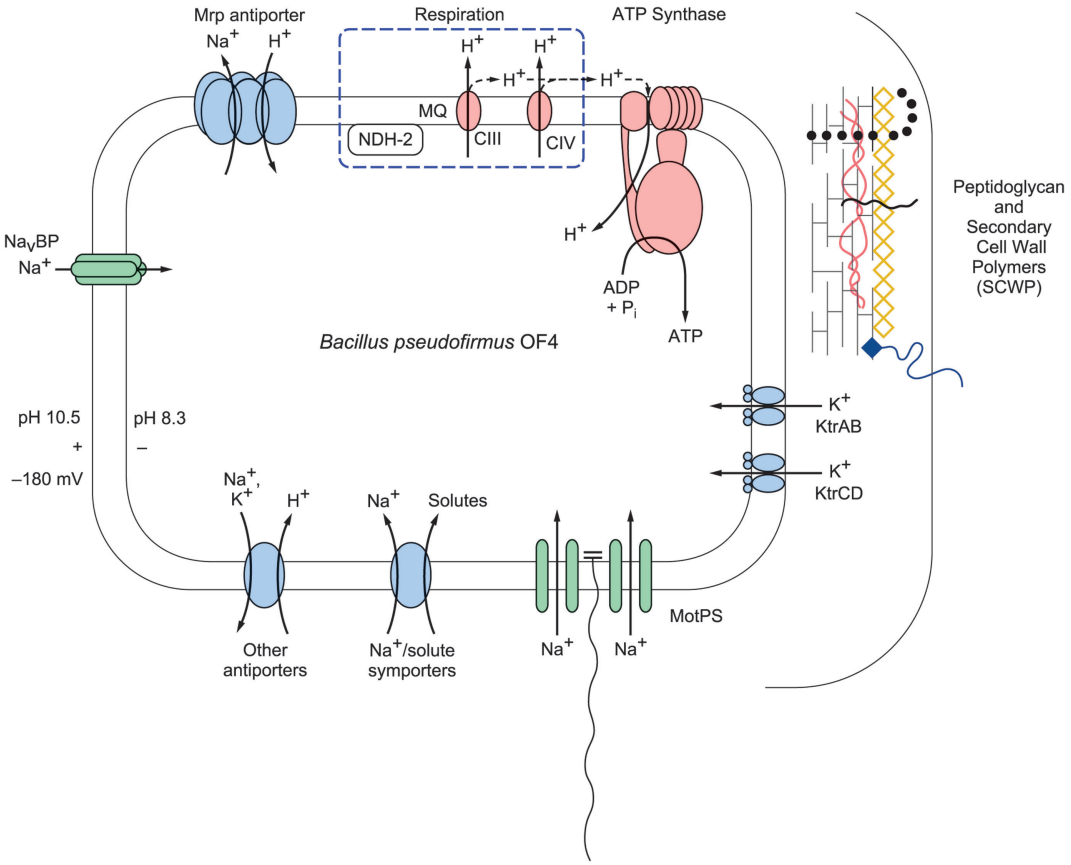

FIGURE 2 | A schematic representation of selected bioenergetic and cell surface properties of alkaliphilic *Bacillus pseudofirmus* OF4. Electron transfer is initiated by dehydrogenases such as NADH dehydrogenase (designated NDH-2), a non-proton-pumping enzyme that replaces complex I in many bacteria. The dehydrogenases donate electrons to the menaquinone (MQ) pool in the membrane. From reduced MQ, the electrons move on through the two proton-pumping complexes, the menaquinol:cytochrome *c* oxidoreductase (complex III, labeled CIII in the figure) and cytochrome *c* oxidase (complex IV, labeled CIV in the figure), which pump protons out of the cell into the bulk medium as molecular oxygen is reduced. These protons are shown with the solid line. Evidence has been presented for retention of other protons on or near the membrane where they move laterally and may reach PMF users such as ATP synthase before equilibrating with the bulk medium outside the cell (Heberle et al., 1994; Sandén et al., 2010; Rieger et al., 2014). These protons are shown with a dashed line. The bioenergetic impact and possible mechanisms of that delay of proton equilibration will be discussed in the final section of this review. In addition to energizing ATP synthesis, the proton-motive force (PMF) generated by respiration energizes the cation/proton antiporters that catalyze electrogenic import of more protons than the number of sodium ions that are exported in the antiporter turnover. The inward movement of protons contributes to the maintenance of a low pH inside the alkaliphile cytoplasm relative to the pH in the medium. This facilitates maintenance of a cytoplasmic pH of 8.3 while the external pH is 10.5, an "inverted" ΔpH. Additional sodium ions enter through the MotPS sodium-ion channels (Ito et al., 2004a) that power motility and through a voltage-gated sodium-ion channel, Na_VBP (Ito et al., 2004b); the influxes of sodium ions complete a sodium-ion cycle, enabling continued uptake of protons via antiporters. Ktr potassium ion importers similarly contribute to completion of a potassium ion cycle. The net chemiosmotically productive, trans-membrane potential ($\Delta\Psi$) is substantial, so that the total of the inverted ΔpH and the $\Delta\Psi$ yields a low but productively oriented bulk PMF.

cloned and characterized, it was found to be a voltage-gated sodium-ion channel and was designated NaChBac (Ren et al., 2001). Structural insights followed from studies of related proteins from a marine Alphaproteobacterium (Zhang et al., 2012) and from *Arcobacter butzleri* (Payandeh et al., 2012). Studies of the NaChBac homolog from alkaliphilic *B. pseudofirmus* OF4, Na_VBP, revealed a sodium-ion-specific channel that is potentiated at high pH and has a role in chemotaxis as well as in cytoplasmic pH homeostasis (Ito et al., 2004b). By contrast, the *B. alcalophilus* member of the voltage-gated channel family has been shown to be a voltage-gated channel that is remarkably non-specific with respect to multiple monovalent and divalent cation substrates (DeCaen et al., 2014). This characteristic is consistent with the hypothesis that *B. alcalophilus* transporters can couple solute to diverse cation gradients (Attie et al., 2014).

When the pH of the outside medium of extreme alkaliphiles is raised to very high alkaline levels, the capacity to maintain a steady cytoplasmic pH below pH 8.5 is lost and an upward creep in the cytoplasmic pH is observed. For example, at the high end of the growth range for alkaliphilic *B. pseudofirmus* OF4, e.g., ≥11.2, the cytoplasmic pH rises to ~9.5 (Sturr et al., 1994). The basis for resistance to this unusually high cytoplasmic pH is not yet fully understood and is an intriguing part of alkaliphiles' extremophilic capacity (Janto et al., 2011; Krulwich et al., 2011).

Another major problem is raised by the substantial "reversed" proton gradient (i.e., a significantly more acidic cytoplasm than the pH of the medium). This orientation of the pH gradient reduces the total PMF that drives proton-coupled processes such as proton-coupled ATP synthesis, and in many bacteria, proton-coupled uptake of solutes as well as motility. The productive orientation of the PMF, which is an electrochemical gradient, consists of an inwardly directed chemical gradient of protons (ΔpH) and a trans-membrane potential oriented with the positive side on the outside (ΔΨ) across the bacterial membrane. While the reversal of the ΔpH is accompanied by a rise in the ΔΨ, the increment does not fully compensate for the reversal of the ΔpH (Krulwich, 1995). Therefore, the net PMF available for bioenergetic work is significantly reduced. How then, do aerobic alkaliphiles carry out robust PMF-dependent work? The expected answer was that the low inwardly directed PMF would not be used by alkaliphiles but that the larger sodium-ion gradient could energize ATP synthesis just as it energizes alkaliphiles' solute uptake systems and motility (**Figure 2**). As mentioned earlier, there are indeed F_1F_o-ATP synthases that are coupled to sodium ions. However, these synthases are found in bacteria such as *I. tartaricus* and *P. modestum* but not in bacteria that derive energy from electron transport during oxidative phosphorylation, such as aerobic alkaliphiles (Dimroth and Cook, 2004). *B. pseudofirmus* OF4, which was originally named *B. firmus* OF4, was the first alkaliphile found to use a proton-coupled ATP synthase, in experiments using purified synthase reconstituted and assayed in proteoliposomes (Hicks and Krulwich, 1990). It was also noted that there was barely detectable hydrolytic activity, a typical feature of alkaliphile ATP synthases. Without suppression of ATP hydrolysis by alkaliphile synthases, alkaliphiles would be susceptible to loss of ATP via hydrolysis when the low PMF dipped stochastically. A study of the molar growth yields of *B. pseudofirmus* OF4 was conducted in a continuous culture that was held at a range of specific pH values between pH 7.5 and 11.2, with vigorous aeration. The results showed that *B. pseudofirmus* OF4 grew throughout that range, with higher molar growth yields at pH 10.5 than at pH 7.5 (Sturr et al., 1994). Subsequently, the expected use of protons by *B. alcalophilus* was reported (Hoffmann and Dimroth, 1991), and, since then, other aerobic and alkaliphilic strains have similarly exhibited proton-coupling, e.g., thermo-alkaliphilic *Caldalkalibacillus thermarum* strain TA2.A1, which only exhibits non-fermentative growth at alkaline pH values and couples the ATP synthase to protons (Cook et al., 2003; McMillan et al., 2009).

Alkaliphile F_1F_o-ATP Synthases and an Overview of Adaptations That Support Their Function at Low PMF

The model of an F_1F_o-ATP synthase in **Figure 3A** is based on work by other investigators who have developed key features

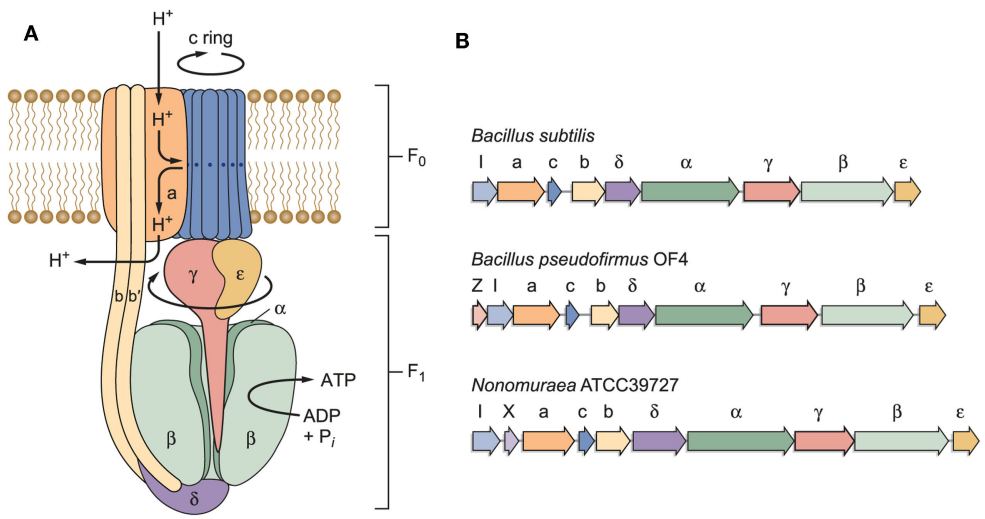

FIGURE 3 | **(A)** A model of a bacterial F_1F_o-ATP synthase and **(B)** schematic examples of bacterial *atp* operons. The F_1 sector containing the α/β catalytic sites is bound by stator elements to the membrane-embedded F_o portion of the complex. The F_o sector contains the proton-conducting elements utilized to transform proton electrochemical gradients into rotational energy that supports ATP synthesis. Of special interest here are the *a*- and *c*-subunits in the F_o that work together to convert the proton electrochemical gradient into *c*-ring rotation, ultimately leading to ATP synthesis. Non-fermentative alkaliphilic *Bacillus* strains have adaptations in both subunits that are hypothesized to help capture protons and to facilitate the binding of those protons to the essential carboxylate in the *c*-subunit (E54 in *B. pseudofirmus* OF4). Pathway(s) for proton uptake and exit are hypothesized to be comprised of two half-channels in the *a*-subunit (Angevine and Fillingame, 2003). One half-channel is an uptake channel that delivers protons from the outside down their electrochemical gradient to the essential carboxylate in the *c*-subunit. The other half-channel is an exit pathway, ultimately releasing protons in the cytoplasm. As detailed further in the text, roles have been hypothesized and in some instances assigned to the "alkaliphile-specific motifs" that are found in the trans-membrane helices (TMH) of the *c*-subunit, in TMH1: AxAxAVA and in TMH2: PxxExxP. **(B)** Schematic examples of bacterial *atp* operons. The *atp* operon of *B. subtilis* is typical of many *atp* operons from neutralophilic bacteria, with one gene, *atpI*, just upstream of the eight structural genes of the enzyme complex. Another type is found in a variety of Gram-positive species, especially *Bacillus* species. The *atp* operon of alkaliphilic *B. pseudofirmus* OF4 is similar to the *B. subtilis* example, but has a small additional gene just upstream of *atpI*, designated *atpZ*. This gene encodes a hydrophobic protein that has a role in Mg^{2+} homeostasis (Hicks et al., 2003). An example of a non-alkaliphile *atp* operon, from actinomycete *Nonomuraea* sp. ATCC 39727, also includes a gene predicted to encode a hydrophobic protein, *orfX*, which is found between *atpI* and the gene encoding the *a*-subunit (Gaballo et al., 2006).

of this rotary machine (Stock et al., 2000; Yoshida et al., 2001; Boyer, 2002; Walker, 2013). The model indicates a path of protons through a "half-channel" of the membrane-embedded *a*-subunit, which leads to an interface that enables the proton to move from the *a*-subunit to the *c*-rotor ring, and subsequently be released through another half-channel into the bacterial cytoplasm after it has completed a full rotation (Angevine and Fillingame, 2003; Dong and Fillingame, 2010). Recently, a structural study of the *a*-subunit from the algae *Polytomella* sp., which has a dimeric F-type ATP synthase structure, has shown that the membrane-embedded helices of the *a*-subunit stator are horizontal relative to the *c*-ring (Allegretti et al., 2015). When the sequences of the proton-conducting *a*- and *c*-subunits of both *B. pseudofirmus* OF4 and *B. alcalophilus* were first obtained, it was evident that there were sequence deviations from neutralophilic bacterial homologs (Ivey and Krulwich, 1991, 1992). It was anticipated that these "alkaliphile motifs" would turn out to be adaptive to the challenges of the alkaliphile setting. In addition to the major problem of an insufficient PMF to account for the ATP synthesis observed, challenges that were likely to require special adaptations included the risk of proton loss to an alkaline environment before the protons reach a proton binding site on the rotor ring or while the rotor ring is in rotation within the lipid *milieu*. In **Figure 3B**, the operons encoding three different F_1F_o-ATP synthases, from *B. subtilis*, alkaliphilic *B. pseudofirmus* OF4, and an actinomycete example, *Nonomuraea* ATCC39727 are compared. Like neutralophilic *B. subtilis*, alkaliphilic strain *B. pseudofirmus* OF4, has an *atp* operon with the expected eight structural, ATP synthase protein-encoding genes and an *atpI* gene whose protein product contributes to stability and assembly of the synthase (Suzuki et al., 2007; Liu et al., 2013). However, the *B. pseudofirmus* OF4 operon has an additional gene, designated *atpZ*, that is operon-associated but is absent in *B. subtilis* (**Figure 3B**). Some other *atp* operons have an additional gene, as shown for the actinomycete *Nonomuraea* which also has a ninth gene (designated as *orfX*) as does *B. pseudofirmus* OF4 (**Figure 3B**). But the predicted product of *Nonomuraea orfX* is different in sequence, size, and location relative to the alkaliphile AtpZ (Liu et al., 2013). In *B. pseudofirmus* OF4, the *atpZ* gene has been shown to enhance the ability of the alkaliphile to acquire sufficient magnesium, which is challenging at elevated pH (Hicks et al., 2003). Lee et al. (2014) suggested that *atpZ* might have an evolutionary link to mitochondrial calcium uniporters (MCUs) (De Stefani et al., 2011).

Adaptations of the *a*-Subunit in Support of ATP Synthesis in Alkaliphilic Bacteria

Aligned amino acid sequences of the *a*-subunits from several alkaliphilic *Bacillus* species are shown in **Figure 4** along with those from thermo-alkaliphilic *C. thermarum* TA2.A1, three non-alkaliphilic *Bacillus* strains, and *Escherichia coli.* When the alkaliphiles were first studied, there were enough sequences available to unequivocally identify K180 of trans-membrane helix-4 (TMH4) as a residue of interest and G212 of TMH5 as a possible interacting partner for K180. Their hypothesized function was to act as an important impediment to proton loss from the entry half-channel of the *a*-subunit and thus promote successful movement of protons to the ion-binding sites of the *c*-ring. In the earliest mutagenesis study, the K180 residue was replaced by glycine, the consensus residue for non-alkaliphiles,

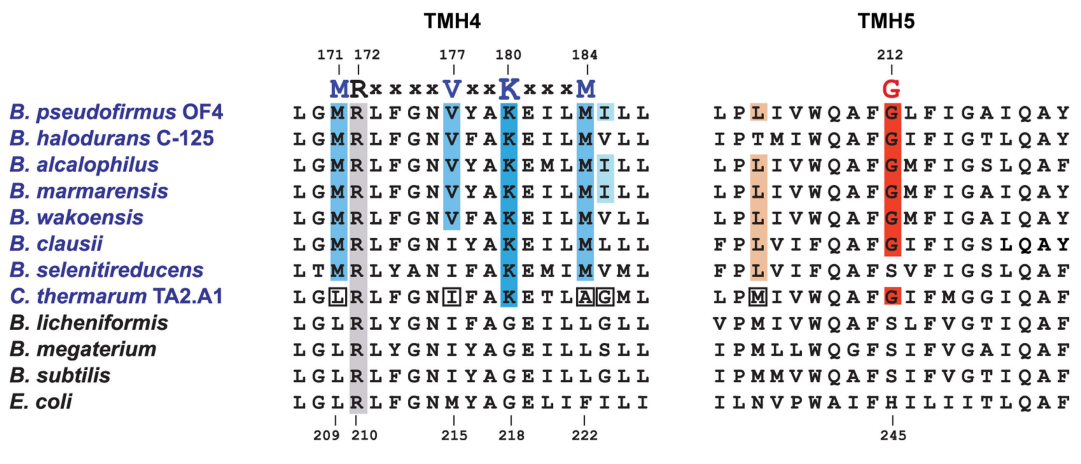

FIGURE 4 | Special features of alkaliphilic *Bacillus* ATP synthase *a*-subunits. Portions of trans-membrane helices (TMH) 4 and 5 contain many of the residues that form the putative aqueous channels through which protons are delivered to a deprotonated, key carboxylate in the *c*-ring and subsequently exit from the *c*-ring to the cytoplasm. Alkaliphilic species are in blue. The essential arginine that is conserved in all *a*-subunits is highlighted in gray (position 172 in *B. pseudofirmus* OF4 and 210 in *E. coli*). In TMH4, alkaliphiles have a generally conserved motif of M(R)xxxxVxxKxxxM shown in blue, with the critical lysine in a darker blue. V177 and K180 are positioned to be part of the putative proton uptake pathway from the periplasm in analogy to the equivalent *E. coli* residues (Dong and Fillingame, 2010). The glycine at position 212 in *B. pseudofirmus* OF4 (in red) is conserved in alkaliphiles and is likely to be a key residue in the uptake pathway. A few alkaliphiles lack V177 or G212 and are hypothesized to be more moderately alkaliphilic. This is the case here for the poly-extremophilic *C. thermarum* TA2.A1, which is the only alkaliphile in a group of 21 *a*-subunits (not shown) that lacks M171 and M184, as well as the generally conserved V177. The *C. thermarum* TA2.A1 residues that deviate from the alkaliphile consensus are in white boxes. The isoleucine at 185 (pale blue) and the leucine at 205 (brown) are less conserved than the other relevant residues. See **Table 1** for a summary of the conservation of the alkaliphile-specific residues and **Table 2** for the phenotypes of relevant mutants.

TABLE 1 | The sequence similarity among 21 *Bacillus* alkaliphiles in identified alkaliphile amino acid variants in the ATP synthase *a*-subunit.

***Bacilluspseudofirmus* OF4 residue**	**M171**	**V177**	**K180**	**M184**	**I185**	**L205**	**G212**
Bacillus alkaliphile conservation	20/21	17/21	21/21	20/21	9/21	9/21	17/21
Bacillus neutralophile consensus	L	I	G	L	G (S/T)	M (T/F)	S
C. thermarum TA2.A1 residue	L	I	K[a]	A	G	M	G[a]

[a]*This residue matches the alkaliphile consensus. The other residues of C. thermarum TA2.A1 deviate from the alkaliphile consensus (and, for the most part, correspond to the Bacillus neutralophile consensus).*

resulting in major loss of growth on malate at pH 10.5 but not 7.5 and major loss of ATP synthesis by ADP + P_i-loaded membrane vesicles while replacement of G212 by serine had a much smaller defect (Wang et al., 2004). In a later study, K180 was replaced by alanine, glycine, cysteine, arginine, and histidine. The resulting ATP synthases were all defective in their ability to grow on malate and carry out ATP synthesis. It was also noted that the alanine-, glycine-, and histidine-containing mutants were considerably more sensitive to the uncoupler carbonyl cyanide *m*-chlorophenyl hydrazone (CCCP) than the WT strain (Fujisawa et al., 2010). The synthase in which K180 was changed to arginine exhibited no synthesis under any tested conditions, although the same substitution in *C. thermarum* TA2.A1 was functional (McMillan et al., 2007).

At the time of this initial work, it was noted that additional motifs were probably present in the different *a*-subunits. The larger data base of alkaliphile sequences now confirms that the motifs associated with the alkaliphile *a*-subunits are more comprehensive. Again, the alkaliphile motifs are distinct from those of neutralophilic *Bacillus* strains as well as *C. thermarum* TA2.A1, and some of the *Bacillus* alkaliphiles that are somewhat less alkaliphilic than the top five strains in the alignment (**Figure 4**; **Table 1**). Subsequently, when more sequences became available, multiple alkaliphile sequences revealed other residues in membrane segments that were hypothesized to be in or very close to the *a*-subunit proton pathway. These were M171, V177, M184, I185, and L205 (Fujisawa et al., 2010) (**Table 1**). Except for *C. thermarum* TA2.A1, the two methionines are conserved in all *Bacillus* alkaliphiles, and their mutation to the sequence found in neutralophiles resulted in impaired growth on malate (**Table 2**). The mutation of V177 to the neutralophile consensus also resulted in a significant loss of growth on malate, as did the mutations of the two other flagged residues of potential interest, I185 and I205 (**Tables 1** and **2**). No clear notion of the basis for their functional importance has yet emerged but as soon as more structural data become available in the future, a more detailed hypothesis will likely become feasible.

TABLE 2 | Phenotypes of *B. pseudofirmus* OF4 ATP synthase *a*-subunit mutants.

Mutation	**Growth at pH 10.5 with malate (% of WT)**	**Growth at pH 7.5 with malate (% of WT)**
M171L	49	78
V177I	32	55
K180G	18	86
M184L	20	30
I185G	49	84
G212S	100	86
L205M	30	33

Data are from Wang et al. (2004) and Fujisawa et al. (2010). Growth was for 16 h. The mutations were based on the equivalent consensus Bacillus neutralophile a-subunit residues. Standard deviations can be found in those references. Although the G212S mutant did not show a defect when grown in malate-replete media, the mutant exhibited defects when it was starved extensively and reenergized with malate compared to the wild-type. Whereas the WT after 1 h of re-energization showed an increased ΔGp/Δp and lowered cytoplasmic pH, the G212S mutant exhibited the opposite pattern, with a decreased ΔGp/Δp and an increased cytoplasmic pH from time 0 (Wang et al., 2004). The ΔGp is the phosphorylation potential ($\Delta G'_o$+RT ln[ADP][Pi]/[ATP]) *and the Δp is the proton-motive force (arithmetic sum of ΔpH in mV and the membrane potential).*

Adaptations of the *c*-Subunit That Support ATP Synthesis by Alkaliphilic Bacteria

Two Major Motifs of the *c*-Subunit of Alkaliphiles

In comparison with neutralophiles, alkaliphilic *Bacillus* strains have two major motifs in their *c*-subunit amino acid sequences. First, and located on the N-terminal helix of the hairpin like *c*-subunit, there is a 16AxAxAVA22 motif (using *B. pseudofirmus* OF4 numbering), which replaces the GxGxGNG motif found in neutralophilic *Bacillus* strains (**Figure 5**). However, only *B. pseudofirmus* OF4 has the full set of four alanines in the motif. Second, located on the C-terminal helix, a proline at position 51 appears. This proline is an alkaliphile-specific residue that is three residues in front of the critical, ion-binding glutamic acid residue, E54. In some cases, a second proline residue appears equidistantly positioned after E54. Together they form the motif 51PxxExxP57 (Arechaga and Jones, 2001). Mutagenesis studies on the two motifs showed that a quadruple mutant in which the four alanines of the AxAxAVA motif were changed to glycines resulted in loss of only 50% of the WT hydrolytic activity but loss of over 80% of the enzyme's ATP synthesis capacity (Liu et al., 2009). A mutation of P51 to alanine led to a very significant loss in the ability to grow non-fermentatively at pH 10.5, while replacement of P51 with glycine led to mutants with growth deficits and proton leakiness (Liu et al., 2009). A mutation of the E54 residue, which is expected to have a central role in the ion-binding site, to D54, led to acute proton leakiness accompanied by almost total loss of the ability to grow on malate (Liu et al., 2009).

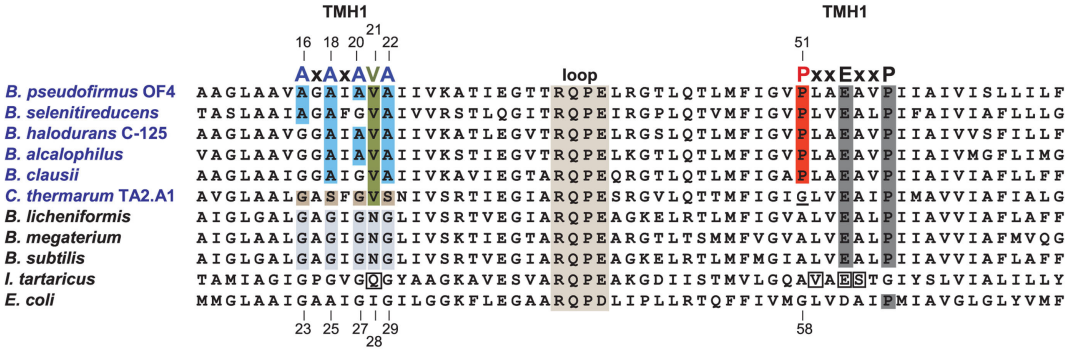

FIGURE 5 | Alignment of the *Bacillus* alkaliphiles *c*-subunits with those from *Bacillus* neutralophiles, the Na^+-binding *c*-subunit of *I. tartarticus* and the *c*-subunit from *E. coli*. Neutralophilic *Bacillus* species have a well-conserved TMH1 motif of GxGxGNG, which is shaded in gray. *Bacillus* alkaliphiles names are in blue. The TMH1 motif of these alkaliphiles, shown in blue, is AxAxA(V)A. The valine (V21) is highlighted in green. A different deviation from the non-alkaliphilic bacteria TMH1 motif, is the GxSxGVS sequence found in the poly-extremophilic, thermo-alkaliphilic *C. thermarum* TA2.A1, as highlighted in brown. The second TMH2 alkaliphile motif is PxxExxP, which includes the unique alkaliphile proline (P51 in *B. pseudofirmus* OF4) shown in red. P51 is indirectly required for water coordination within the active site and may play a role in how protons are moved to the cytoplasm after complete *c*-ring rotation, in analogy to the proposed function of the equivalent *E. coli* residue, G58 (Steed and Fillingame, 2009). *C. thermarum* TA2.A1 is the only *Bacillus* alkaliphile among a group of 19 aligned alkaliphilic *Bacillus* *c*-subunits (not shown) that lacks this proline, instead containing a glycine (which is underlined) at this position. The direct Na^+-coordinating residues of the *I. tartarticusc*-subunit are boxed (Meier et al., 2005, 2009); these are Q32, V63, E65, and S66. The numbering at top is from *B. pseudofirmus* OF4 while the bottom numbering is from *E. coli*. To improve the clarity of the figure, a number of residues at the N-terminus and C-terminus of the different *c*-subunits were omitted. Mutant strains were constructed based on the consensus *Bacillus* neutralophile residues. The relevant phenotypes of mutant strains are as follows. In the AXAXA(V)A motif, single alanine to glycine mutants are reduced in pH 10.5 malate growth approximately 30–40% compared to WT (Liu et al., 2009, 2011). The double mutants A18G/A22G and A20G/A22G were modestly impaired in high pH malate growth compared to the single A18G, A20G, or A22G mutants. In contrast, the double mutants that included an A16G mutation were significantly reduced in malate-dependent growth at high pH, with the A16G/A18G mutant exhibiting just 36% of WT growth while the growth of the A16G/A20G mutant was only 9% of WT growth. The ATP synthase from the A16G mutant in the *c*-subunit displayed *c*-rings with both a *c*13 (WT) and *c*12 stoichiometry while double A16G/A20G mutants displayed *c*-rings with only a *c*12 stoichiometry (Liu et al., 2010). The V21N mutant grew at similar rates to the WT under all tested conditions except at pH 10.5 with malate, where its doubling time, 3.7 h, was 2.5 times slower than the WT (Preiss et al., 2014). The proline mutant, P51A, exhibited a small reduction in malate growth at pH 7.5, which was 75% of WT, but was very sensitive to malate growth at pH 10.5, only 23% of WT (Liu et al., 2009).

The Stoichiometry of the *c*-Rotor Ring and Impact of the Motifs

The stoichiometry of the *c*-rotor ring as well as the basis for the apparent impact of the *c*-subunit motifs were clarified when the crystal structure of the purified *c*-subunit rotor ring from alkaliphilic *B. pseudofirmus* OF4 was solved at 2.5 Å (Preiss et al., 2010). The stoichiometry of *c*-rotor rings from various organisms, i.e., the number of *c*-subunits in each ring, is in a range from 8 subunits in vertebrates to 13–15 in various photosynthetic organisms (Watt et al., 2010; Meier et al., 2011). Alkaliphilic bacteria such as *B. pseudofirmus* OF4 and thermoalkaliphilic *C. thermarum* TA2.A1 both have 13-subunits, near the upper end of the observed range (Meier et al., 2007; Matthies et al., 2009; Preiss et al., 2010). The *c*-rings from each bacterial species, plant, or animal, have a constant *c*-subunit stoichiometry, with each *c*-subunit coordinating one proton (or sodium ion, where applicable) via the glutamate or aspartate in each of the ion-binding sites. During the 360° rotation of the rotor ring, with the attached central stalk γϵ subunits, three ATPs are synthesized in the F_1 sector β subunits. The number of coupling ions translocated for synthesis of the three molecules of ATP is determined by the *c*-ring stoichiometry: a larger *c*-ring is beneficial under circumstances of a lower PMF and vice versa; this notion is consistent with results of engineering of rotor ring stoichiometries both in upward and downward directions (Pogoryelov et al., 2012; Preiss et al., 2013).

Mutations that reduce the number of alanine residues in the 16AxAxAVA22 motif of alkaliphilic *B. pseudofirmus* OF4 by replacing them with glycine residues were found to increase the mobility of the *c*-ring on SDS-PAGE when the first alanine (A16) was among the residues that was replaced (Liu et al., 2011). The A16 residue was shown to have more hydrophobic interactions than the other three alanines in a network in which the alanine methyl side chains interact with atoms from other residues (Preiss et al., 2013). Mutants were constructed in which either a single A16G mutation or a double A16G/A20G mutation were present. The single mutant displayed two bands on SDS-PAGE, suggesting that both a significant amount of *c*-ring with WT stoichiometry and *c*-ring with a lower than WT stoichiometry was present (Liu et al., 2011). The *c*-ring of the double mutant, showing only the faster migrating band, putatively had a lower stoichiometry. Subsequent atomic force microscopy (AFM) studies showed the presence of a mix of 12- and 13-subunits in the single mutant and of 12-subunits in the double mutant (Preiss et al., 2013). As confirmed by X-ray crystallography, the WT *c*-ring has 13-subunits, while the A16G/A20G double mutant displays a 12-subunit ring (**Figure 6**). Changing the stoichiometry from 13 to 12 resulted in a *c*-ring with a significantly smaller circumference and diameter (**Figure 6**). In support of these reported structural changes, the molar growth yield of the single A16G mutant was modestly reduced at pH 10.5 while

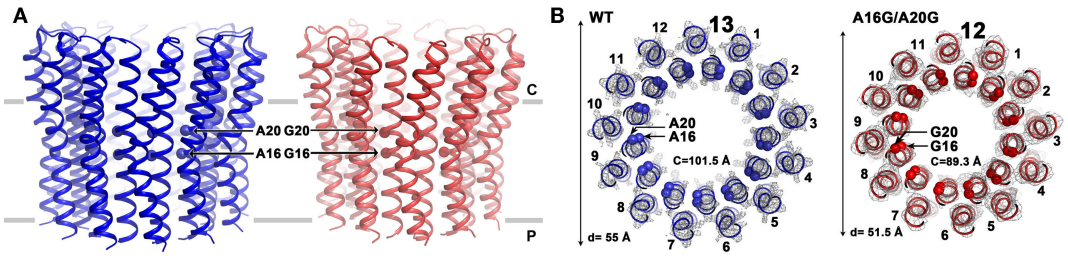

FIGURE 6 | Comparison of the structures of the *B. pseudofirmus* OF4 wild-type (WT) and the A16G/A20G mutant *c*-ring. Side views **(A)** and top views **(B)** are shown for the WT and the double A16G/A20G mutant *c*-rings at the level of residue A16 and G16. Alanine and glycine residues 16 and 20 are located in the inner N-terminal helix at the middle region of the membrane. A mutation of A16G/A20G alters the *c*-ring stoichiometry from 13 (WT, blue, pdb code: 2 × 2v) to 12 (A16G/A20G mutant, red, pdb code: 3zo6) as visualized by atomic force microscopy and X-ray crystallography (Preiss et al., 2013). The mutations further reduced *c-to-c*-subunit distances at the level of A16 and A20, resulting in a smaller ring circumference (*C*) of only 89.3 Å (on level of G16) and a ring diameter of 51.5 Å. Helices are shown in cartoon representation, Cα of WT with both A16 and A20 shown as blue spheres and the double mutant with G16 and G20 shown as red spheres. Electron densities ($2F_{obs}–F_{calc}$) are shown as gray mesh at σ = 2.5 (WT) and σ = 1.7 (A16/20G mutant). Membrane borders are indicated as gray bars, cytoplasmic and periplasmic sites are labeled with C and P, respectively.

that of the double mutant was reduced by almost 50% (Preiss et al., 2013).

Studies of the ion-binding site of the *c*-subunit of *B. pseudofirmus* OF4 have revealed features that are clearly adaptations to alkaliphily. A side view and a top view of the rotor ring is shown in **Figures 7A,B**, respectively. In **Figure 7C** (top two panels), binding sites of wild-type (WT) *c*-subunit structures that were crystallized at different pH values; and below them, the consequences of a P51A mutation of the 51PxxExxP motif (lower left) and a V21-to-N mutation in the 16AxAxAVA22 motif (lower right) are shown (Preiss et al., 2014). The top two panels of **Figure 7C** show that the structure of the ion-binding site is essentially identical in crystals that were prepared at pH 4.4 vs. pH 9.0, highlighting the high affinity H^+ binding propensity of the c-ring over a wide pH range. The structure of the P51A mutant binding site illustrates the role of the first proline of the PxxExxP motif of the C-terminal *c*-subunit helix in binding a water molecule in the ion-binding site of each subunit. The retention of the water molecule depends upon the presence of P51 and appears to play an important role in preventing proton loss from the ion-binding site during rotation. The V21N mutated *c*-ring had to be modeled since its instability prevented the determination of its crystal structure. The final panel illustrates subtle but important changes that significantly compromise the ion-binding E54 WT conformation upon mutation of valine (conserved in alkaliphiles) to asparagine (conserved in neutralophilic *Bacillus* species). The coordination network of the ion-binding site slightly changes as a result of this mutation, impacting the proton-binding affinity of E54, in agreement with the observed impaired growth phenotype on malate medium at pH 10.5 (Preiss et al., 2014).

In contrast to the scenario with aerobic alkaliphiles that couple *c*-rotor rotation exclusively to proton movements, it is worth noting that some anaerobic alkaliphiles, which are fermentative and do not carry out oxidative phosphorylation, can couple their ATPase (in this case a hydrolase) to pump sodium ions uphill against the trans-membrane ion gradient. This property was exemplified by the rotor ring of *Clostridium paradoxum*, which was found to be coupled to sodium ions and which has an undecameric (c_{11}) rotor ring (Meier et al., 2006).

Strategies That May Help Resolve the Thermodynamic Challenge of Proton-Coupled ATP Synthesis at High pH

After proton-coupling of alkaliphile ATP synthases was clearly established, a major focus was set next on elements and hypotheses that rationalize the thermodynamic challenge of an apparently insufficient bulk PMF to account for the observed synthesis. Much of the effort and hypotheses have focused on rapid movement of protons from the proton-pumping complexes to the proton-coupled ATP synthase. Studies in support of a more localized movement near the membrane surface included observations by Heberle of proton transfer across bacteriorhodopsin that then extended along the membrane (Heberle, 2000). Proposals of near-membrane barriers to proton equilibration with the bulk phase include compartmentalization and aspects of proton-electrostatics (Mulkidjanian et al., 2006; Liu et al., 2007; Ojemyr et al., 2010; Sandén et al., 2010; Lee, 2012; Wilkens et al., 2013; Rieger et al., 2014). These proposals all have a major focus on the near-membrane environment. However, a comparison of the sequences of *c*-subunits from Gram-negative alkaliphiles with those from Gram-positive alkaliphiles, as shown in **Figure 8**, suggests that there may be additional cellular factors besides F_o adaptations that may have roles in maintaining pumped protons in the periplasm or, perhaps, in some instance, enhancing the ability of a particular strain to maintain a lower periplasmic pH. The alignment in **Figure 8** includes examples of both Gram-positive and Gram-negative aerobic alkaliphiles as well as neutralophiles from both groups. It is striking that none of the Gram-negative alkaliphiles requires any of the C-terminal PxxExxP motif adaptations within the *c*-ring that are crucial in Gram-positive alkaliphiles. Moreover, only *Alkalimonas amylolytica* N10, an aerobic Gram-negative, NaCl-dependent alkaliphile isolated from Lake Chahanor in China (Ma et al., 2004) has the suite of four N-terminal alanines, but without the V21 that plays an important

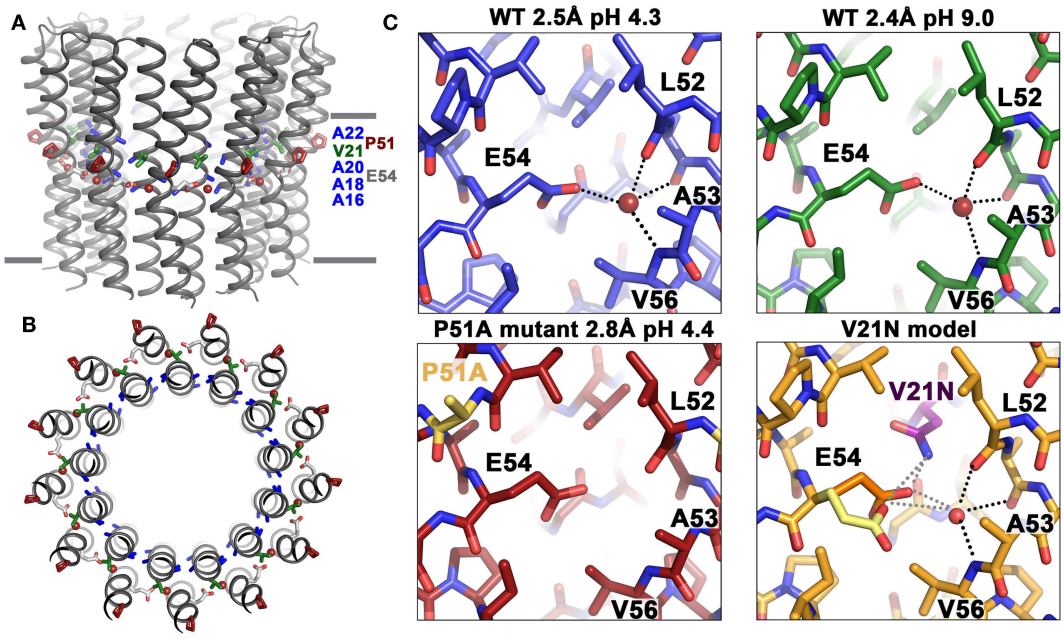

FIGURE 7 | Structural adaptations of the *B. pseudofirmus* OF4 *c*-ring to an alkaliphilic lifestyle. The *c*-ring of *B. pseudofirmus* OF4 is shown **(A)** in side view, perpendicular to the membrane and **(B)** in top view. Amino acids that were found to be adapted to the alkaliphilic lifestyle are highlighted in blue (alanine motif), red (Pro51, from the PxxExxP motif), and green (Val21, within the alanine motif AxAxAVA). Membrane borders are indicated by gray bars. **(C)** X-ray crystallographic structures of the *B. pseudofirmus* OF4 *c*-ring ion-binding sites at pH 4.3 (blue), at pH 9.2 (green), the mutant P51A (red), and the mutant model V21N (orange) (Preiss et al., 2010, 2014). H-bonds around the conserved E54 residue (responsible for reversible H^+ binding, see text) are indicated by dashed lines. The water molecule in the ion-binding site is shown as a red sphere. The V21N model shows E54 in *I. tartaricus*-like conformation (1yce, yellow, Meier et al., 2005) in addition to the WT *B. pseudofirmus* OF4 conformation (orange). The *I. tartaricus*-like conformation might be energetically favorable in the V21N mutant due to the formation of an additional H-bond between N21 and E54 [for details see Preiss et al. (2014)].

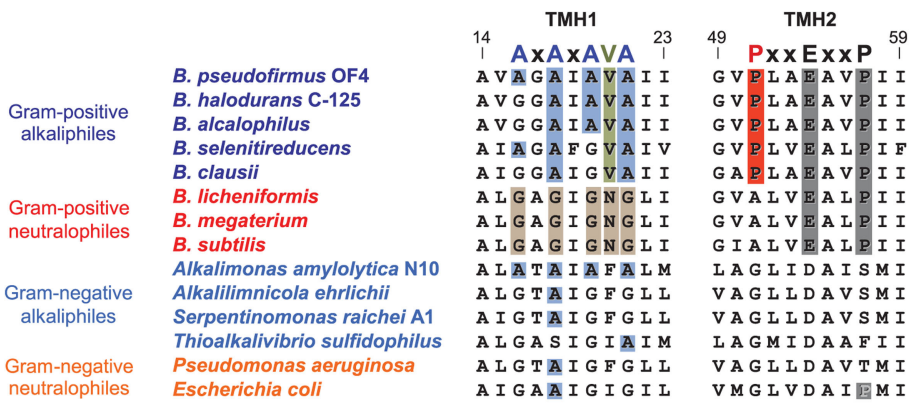

FIGURE 8 | Alignment of the key regions of TMH1 and TMH2 of different *c*-rings contrasting the features of the Gram-positive *Bacillus* alkaliphiles with the sequences of Gram-negative alkaliphiles. The names of Gram-positive alkaliphiles are shown in blue, while the Gram-negative alkaliphiles are in light blue. In addition, Gram-positive neutralophiles are in red and Gram-negative neutralophiles are in orange. The TMH1 alkaliphile motif AxAxAx(V)A at positions 16 through 22 (*B. pseudofirmus* OF4 numbering) is shown in blue, and V21 between the last two alanines is shown in green. These features are mostly absent in Gram-negative alkaliphiles, with the notable exception of *Alkalimonas amylolytica* N10, whose sequence is AxAxAxA, i.e., similar to *B. pseudofirmus* OF4, except for the absence of V21. None of the Gram-negative alkaliphiles has the motif of *Bacillus* alkaliphiles in TMH2, PxxExxP, where the proline (P51 in *B. pseudofirmus* OF4) unique to alkaliphiles is shown in red. Yet these Gram-negative alkaliphiles are expected to be proton-coupled, lacking the Na^+-binding residues of *I. tartarticus* (see **Figure 5**).

role in alkaliphilic *Bacillus* strains. It will be of interest to examine whether the *c*-ring of *A. amylolytica* N10 has a higher *c*-subunit stoichiometry than those of the other Gram-negative alkaliphiles shown, all of which have only a single N-terminal helix alanine. It is also notable that *Serpentinomonas raichei* A1 grows in an unusually high pH environment, even for alkaliphiles (pH 11.6),

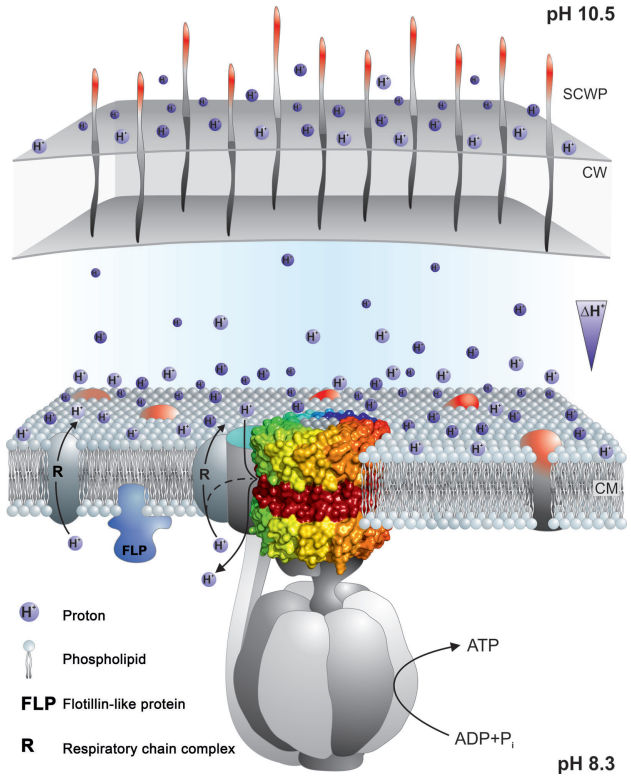

FIGURE 9 | Summary of properties that may contribute to a delayed loss of protons pumped by the respiratory chain to the bulk medium outside the cell. The F_1F_o-ATP synthase is shown embedded in the cytoplasmic membrane with a proton-pumping respiratory chain element near the synthase. Nearness might be supported by properties of the phospholipids that facilitate rapid movement of protons on or near the membrane surface and/or by an innate tendency of some respiratory complexes to form super-complexes to enhance electron transport and its attendant proton-pumping. Micro-domains in the coupling membrane, such as those attributed to the presence of flotillins, may contribute to compartmentalization. In addition, the cell wall (CW) and secondary cell wall layers (SCWP) may provide a significant barrier, especially in Gram-negative bacteria that have outer membranes as well as other SCWPs, but also in Gram-positive bacteria such as alkaliphiles with multiple, charged SCWPs that could form a significant barrier. For more detailed explanations, see the text. The observation of reduced capacity for alkaliphily in *Bacillus halodurans* C-125 and *Bacillus pseudofirmus* OF4 when negatively charged SCWPs are lost by mutation, is suggestive of some proton trapping on the outside surface of cell wall. This is indicated by the protons shown to be associated with that surface.

without features that are critical to alkaliphilic *Bacillus* strains (Suzuki et al., 2014).

The Gram-negative alkaliphiles are likely to be protected by the outer membrane that they possess, and perhaps the outer membrane of mitochondria should be considered for playing at least some role in delaying pumped proton equilibration with the bulk phase or cytoplasm. As shown in **Figure 9**, there are additional strategies that may contribute to delays in proton equilibration with the bulk phase. It has been suggested that particular phospholipids might play a role, and specifically the high cardiolipin level of *B. pseudofirmus* OF4 might delay proton equilibration (Haines and Dencher, 2002), but at least in *B. pseudofirmus* OF4, mutants lacking detectable cardiolipin were not impaired in non-fermentative growth at high pH (Liu et al., 2014).

Other delays in proton equilibration might involve the entire periplasmic space, which was shown in Gram-positive bacteria by Matias and Beveridge (2005) is surrounded in bacteria by cell wall layers and additional layers of various secondary cell wall polymers that are often highly charged (Takami, 2010). In *B. pseudofirmus* OF4, mutational loss of the S-layer gene *slp* results in a significant deficit in non-fermentative growth at the upper pH range and the S-layer itself is only one of several SLH-motif polymers that contribute to charges on the outside surfaces. Additional contributions are made by charged carbohydrate polymers and a poly-glutamic acid polymer (Gilmour et al., 2000; Janto et al., 2011). In alkaliphilic *B. halodurans* C-125, the polymers are different but also appear to be candidates for delaying proton equilibration. The polymers in the *B. halodurans* C-125 surface include teichuronopeptides, teichuronic acids, and poly-glutamate and poly-glucuronate that are proposed to impact very significantly on the actual pH that this alkaliphile can maintain in the periplasm (Aono, 1987; Tsujii, 2002).

Further elements, that are constituents of the membranes themselves, should also be considered in connection with retention of protons at near the membrane surface. Carotenoids have been found to lend the yellow color to many alkaliphile membranes and it is possible that carotenoids might impart properties to the cytoplasmic membrane that enhance closeness of proton pumps and synthases, in addition to their likely role in scavenging reactive oxygen species (Aono and Horikoshi, 1991; Steiger et al., 2015).

Finally, even stronger candidates for promoting micro-domains that might bring the proton pumps into greater proximity with the ATP synthase are membrane flotillins and their associated proteins (Lopez and Kolter, 2010; Bach and Bramkamp, 2013, 2015; Bramkamp and Lopez, 2015). *B. halodurans* C-125 has an alkali-inducible flotillin-T (Zhang et al., 2005) and *B. pseudofirmus* OF4 has a flotillin-A candidate as well as several NfeD protein candidates that are associated with flotillins. It will be of interest to see whether mutational loss of any of these diminishes the alkaliphilic capacity of these alkaliphiles.

Conclusion

Alkaliphilic bacteria contribute substantially to numerous technologies, some traditional and others at the cutting edge of new applications of alkaliphile products or their cellular capacities for decontamination of specific commercial settings. Alkaliphiles also are of ecological interest as they are part of serpentinizing sites. The finding that alkaliphilic aerobes that grow non-fermentatively, use energy derived from a proton-pumping respiratory chains and complete oxidative phosphorylation using proton-coupled ATP synthases has challenged a tenet of the formal Mitchellian chemiosmotic hypothesis. Rather than focusing only on narrow solutions to the thermodynamic problem that this re-consideration raises, it is worth considering the broader physiology of alkaliphiles, which may have evolved numerous adaptations that together contribute to their extremophilic capacities.

Author Contributions

All five authors participated in planning aspects of the manuscript, provided critical advice about the organization and content during the drafting, which was done by TK, and reviewed the submitted version. LP produced **Figures 6, 7**, and **9**, with input from TM and TK, SS contributed the images for **Figure 1** and critical advice and expertise on the serpentinization sections, and DH produced **Table 1** and **Figures 5** and **8**, and drafted **Figures 2** and **3** as well as the figure legends with TK.

Acknowledgments

This work was supported by NIGMS grant RO1 GM28454 to TK. TM would like to express our gratitude to Werner Kühlbrandt for support of TM's laboratory for the past 9 years. The work in TM's laboratory was supported by the Collaborative Research Center (SFB) 807 of the German research Foundation (DFG), the Cluster of Excellence "Macromolecular Complexes" (CEF-MC) at the Goethe University Frankfurt (Project EXC 115). NSF-EAR Grant No 1424646 supported the work of SS.

References

Aino, K., Narihiro, T., Minamida, K., Kamagata, Y., Yoshimune, K., and Yumoto, I. (2010). Bacterial community characterization and dynamics of indigo fermentation. *FEMS Microbiol. Ecol.* **74**, 174–183. doi:10.1111/j.1574-6941.2010.00946.x

Allegretti, M., Klusch, N., Mills, D. J., Vonck, J., Kühlbrandt, W., and Davies, K. M. (2015). Horizontal membrane-intrinsic alpha-helices in the stator a-subunit of an F-type ATP synthase. *Nature* **521**, 231–240. doi:10.1038/nature14185

Angevine, C. M., and Fillingame, R. H. (2003). Aqueous access channels in subunit a of rotary ATP synthase. *J. Biol. Chem.* **278**, 6066–6074. doi:10.1074/jbc.M210199200

Aono, R. (1987). Characterization of structural component of cell walls of alkalophilic strain of *Bacillus* sp. C-125. Preparation of poly(gamma-L-glutamate) from cell wall component. *Biochem. J.* **245**, 467–472.

Aono, R., and Horikoshi, K. (1991). Carotenes produced by alkaliphilic yellow-pigmented strains of *Bacillus*. *Agric. Biol. Chem.* **55**, 2643–2645. doi:10.1271/bbb1961.55.2643

Arechaga, I., and Jones, P. C. (2001). The rotor in the membrane of the ATP synthase and relatives. *FEBS Lett.* **494**, 1–5. doi:10.1016/S0014-5793(01)02300-6

Attie, O., Jayaprakash, A., Shah, H., Paulsen, I. T., Morino, M., Takahashi, Y., et al. (2014). Draft genome sequence of *Bacillus alcalophilus* AV1934, a classic alkaliphile isolated from human feces in 1934. *Genome Announc.* **2**, e1175–e1114. doi:10.1128/genomeA.01175-14

Bach, J. N., and Bramkamp, M. (2013). Flotillins functionally organize the bacterial membrane. *Mol. Microbiol.* **88**, 1205–1217. doi:10.1111/mmi.12252

Bach, J. N., and Bramkamp, M. (2015). Dissecting the molecular properties of prokaryotic flotillins. *PLoS ONE* **10**:e0116750. doi:10.1371/journal.pone.0116750

Borkar, S. (2015). "Alkaliphilic bacteria: diversity, physiology and industrial applications," in *Bioprospects of Coastal Eubacteria*, ed. S. Borkar (Springer International Publishing).

Bowers, K. J., Mesbah, N. M., and Wiegel, J. (2009). Biodiversity of poly-extremophilic bacteria: does combining the extremes of high salt, alkaline pH and elevated temperature approach a physico-chemical boundary for life? *Saline Syst.* **5**, 9. doi:10.1186/1746-1448-5-9

Boyer, P. D. (2002). A research journey with ATP synthase. *J. Biol. Chem.* **277**, 39045–39061. doi:10.1074/Jbc.X200001200

Bramkamp, M., and Lopez, D. (2015). Exploring the existence of lipid rafts in bacteria. *Microbiol. Mol. Biol. Rev.* **79**, 81–100. doi:10.1128/MMBR.00036-14

Brazelton, W. J., Morrill, P. L., Szponar, N., and Schrenk, M. O. (2013). Bacterial communities associated with subsurface geochemical processes in continental serpentinite springs. *Appl. Environ. Microbiol.* **79**, 3906–3916. doi:10.1128/AEM.00330-13

Cook, G. M., Keis, S., Morgan, H. W., Von Ballmoos, C., Matthey, U., Kaim, G., et al. (2003). Purification and biochemical characterization of the F_1F_o-ATP synthase from thermoalkaliphilic *Bacillus* sp. strain TA2.A1. *J. Bacteriol.* **185**, 4442–4449. doi:10.1128/JB.185.15.4442-4449.2003

Crespo-Medina, M., Twing, K. I., Kubo, M. D. Y., Hoehler, T. M., Cardace, D., McCollom, T., et al. (2014). Insights into environmental controls on microbial communities in a continental serpentinite aquifer using a microcosm-based approach. *Front. Microbiol.* **5**:604. doi:10.3389/Fmicb.2014.00604

De Stefani, D., Raffaello, A., Teardo, E., Szabo, I., and Rizzuto, R. (2011). A forty-kilodalton protein of the inner membrane is the mitochondrial calcium uniporter. *Nature* **476**, 336–340. doi:10.1038/nature10230

DeCaen, P. G., Takahashi, Y., Krulwich, T. A., Ito, M., and Clapham, D. E. (2014). Ionic selectivity and thermal adaptations within the voltage-gated sodium channel family of alkaliphilic *Bacillus*. *Elife* **3**, doi:10.7554/eLife.04387

Dimroth, P. (1997). Primary sodium ion translocating enzymes. *Biochim. Biophys. Acta* **1318**, 11–51. doi:10.1016/S0005-2728(96)00127-2

Dimroth, P., and Cook, G. M. (2004). Bacterial Na^+- or H^+-coupled ATP synthases operating at low electrochemical potential. *Adv. Microb. Physiol.* **49**, 175–218. doi:10.1016/S0065-2911(04)49004-3

Dong, H., and Fillingame, R. H. (2010). Chemical reactivities of cysteine substitutions in subunit *a* of ATP synthase define residues gating H^+ transport from each side of the membrane. *J. Biol. Chem.* **285**, 39811–39818. doi:10.1074/jbc.M110.175844

Durell, S. R., and Guy, H. R. (2001). A putative prokaryote voltage-gated Ca^{2+} channel with only one 6TM motif per subunit. *Biochem. Biophys. Res. Commun.* **281**, 741–748. doi:10.1006/bbrc.2001.4408

Dzioba-Winogrodzki, J., Winogrodzki, O., Krulwich, T. A., Boin, M. A., Hase, C. C., and Dibrov, P. (2009). The *Vibrio cholerae* Mrp system: cation/proton antiport properties and enhancement of bile salt resistance in a heterologous host. *J. Mol. Microbiol. Biotechnol.* **16**, 176–186. doi:10.1159/000119547

Frost, B. R., and Beard, J. S. (2007). On silica activity and serpentinization. *J. Petrol.* **48**, 1351–1368. doi:10.1093/petrology/egm021

Fujinami, S., and Fujisawa, M. (2010). Industrial application of alkaliphiles and their enzymes – past, present and future. *Environ. Technol.* **31**, 845–856. doi:10.1080/09593331003762807

Fujinami, S., Terahara, N., Krulwich, T. A., and Ito, M. (2009). Motility and chemotaxis in alkaliphilic *Bacillus* species. *Future Microbiol.* **4**, 1137–1149. doi:10.2217/fmb.09.76

Fujisawa, M., Fackelmayer, O. J., Liu, J., Krulwich, T. A., and Hicks, D. B. (2010). The ATP synthase *a*-subunit of extreme alkaliphiles is a distinct variant: mutations in the critical alkaliphile-specific residue Lys-180 and other residues that support alkaliphile oxidative phosphorylation. *J. Biol. Chem.* **285**, 32105–32115. doi:10.1074/jbc.M110.165084

Gaballo, A., Abbrescia, A., Palese, L. L., Micelli, L., Di Summa, R., Alifano, P., et al. (2006). Structure and expression of the atp operon coding for F_1F_o-ATP synthase from the antibiotic-producing actinomycete *Nonomuraea sp*. ATCC 39727. *Res. Microbiol.* **157**, 675–683. doi:10.1016/j.resmic.2006.02.005

Gessesse, A., Hatti-Kaul, R., Gashe, B. A., and Mattiasson, B. (2003). Novel alkaline proteases from alkaliphilic bacteria grown on chicken feather. *Enzyme Microb. Technol.* **32**, 519–524. doi:10.1016/S0141-0229(02)00324-1

Gilmour, R., Messner, P., Guffanti, A. A., Kent, R., Scheberl, A., Kendrick, N., et al. (2000). Two-dimensional gel electrophoresis analyses of pH-dependent protein expression in facultatively alkaliphilic *Bacillus pseudofirmus* OF4 lead to characterization of an S-layer protein with a role in alkaliphily. *J. Bacteriol.* **182**, 5969–5981. doi:10.1128/JB.182.21.5969-5981.2000

Goto, T., Matsuno, T., Hishinuma-Narisawa, M., Yamazaki, K., Matsuyama, H., Inoue, N., et al. (2005). Cytochrome *c* and bioenergetic hypothetical model for alkaliphilic *Bacillus* spp. *J. Biosci. Bioeng.* **100**, 365–379. doi:10.1263/jbb.100.365

Grant, S., Sorokin, D. Y., Grant, W. D., Jones, B. E., and Heaphy, S. (2004). A phylogenetic analysis of Wadi el Natrun soda lake cellulase enrichment cultures and identification of cellulase genes from these cultures. *Extremophiles* **8**, 421–429. doi:10.1007/s00792-004-0402-7

Grant, W. D. (2003). "Alkaline environments and biodiversity," in *Extremophiles (Life Under Extreme External Conditions)*, eds C. Gerday and N. Glansdorff (Oxford: Eolss Publishers). Available at: http://www.eolss.net

Guffanti, A. A., Finkelthal, O., Hicks, D. B., Falk, L., Sidhu, A., Garro, A., et al. (1986). Isolation and characterization of new facultatively alkalophilic strains of *Bacillus* species. *J. Bacteriol.* **167**, 766–773.

Haines, T. H., and Dencher, N. A. (2002). Cardiolipin: a proton trap for oxidative phosphorylation. *FEBS Lett.* **528**, 35–39. doi:10.1016/S0014-5793(02)03292-1

Hamamoto, T., Hashimoto, M., Hino, M., Kitada, M., Seto, Y., Kudo, T., et al. (1994). Characterization of a gene responsible for the Na^+/H^+ antiporter system of alkalophilic *Bacillus* species strain C-125. *Mol. Microbiol.* **14**, 939–946. doi:10.1111/j.1365-2958.1994.tb01329.x

Heberle, J. (2000). Proton transfer reactions across bacteriorhodopsin and along the membrane. *Biochim. Biophys. Acta* **1458**, 135–147. doi:10.1016/S0005-2728(00)00064-5

Heberle, J., Riesle, J., Thiedemann, G., Oesterhelt, D., and Dencher, N. A. (1994). Proton migration along the membrane surface and retarded surface to bulk transfer. *Nature* **370**, 379–382. doi:10.1038/370379a0

Herschy, B., Whicher, A., Camprubi, E., Watson, C., Dartnell, L., Ward, J., et al. (2014). An origin-of-life reactor to simulate alkaline hydrothermal vents. *J. Mol. Evol.* **79**, 213–227. doi:10.1007/s00239-014-9658-4

Hicks, D. B., and Krulwich, T. A. (1990). Purification and reconstitution of the F_1F_o-ATP synthase from alkaliphilic *Bacillus firmus* OF4. Evidence that the enzyme translocates H^+ but not Na^+. *J. Biol. Chem.* **265**, 20547–20554.

Hicks, D. B., Wang, Z., Wei, Y., Kent, R., Guffanti, A. A., Banciu, H., et al. (2003). A tenth *atp* gene and the conserved *atpI* gene of a *Bacillus atp* operon have a role in Mg^{2+} uptake. *Proc. Natl. Acad. Sci. U.S.A.* **100**, 10213–10218. doi:10.1073/pnas.1832982100

Hiramatsu, T., Kodama, K., Kuroda, T., Mizushima, T., and Tsuchiya, T. (1998). A putative multisubunit Na^+/H^+ antiporter from *Staphylococcus aureus*. *J. Bacteriol.* **180**, 6642–6648.

Hoffmann, A., and Dimroth, P. (1991). The ATPase of *Bacillus alcalophilus* reconstitution of energy-transducing functions. *Eur. J. Biochem.* **196**, 493–497. doi:10.1111/j.1432-1033.1991.tb15841.x

Horikoshi, K. (1999). Alkaliphiles: some applications of their products for biotechnology. *Microbiol. Mol. Biol. Rev.* **63**, 735–750.

Horikoshi, K. (2006). *Alkaliphiles, Genetic Properties and Applications of Enzymes*. Tokyo: Springer.

Horikoshi, K. (2011). "2.8 enzymes isolated from alkaliphiles," in *Extremophiles Handbook*, ed. K. Horikoshi (Tokyo: Springer), 162–177.

Humayoun, S. B., Bano, N., and Hollibaugh, J. T. (2003). Depth distribution of microbial diversity in Mono Lake, a meromictic Soda Lake in California. *Appl. Environ. Microbiol.* **69**, 1030–1042. doi:10.1128/AEM.69.2.1030-1042.2003

Ibrahim, A. S. A., Al-Salamah, A. A., El-Tayeb, A., El-Bdawi, M. A., El-Badawi, Y. B., and Antranikian, G. (2012). A novel cyclodextrin glycosyltransferase from alkaliphilic *Amphibacillus* sp. NPST-10: purification and properties. *Int. J. Mol. Sci.* **13**, 10505–10522. doi:10.3390/ijms130810505

Ito, M., Guffanti, A. A., Oudega, B., and Krulwich, T. A. (1999). *mrp*, a multigene, multifunctional locus in *Bacillus subtilis* with roles in resistance to cholate and to Na^+ and in pH homeostasis. *J. Bacteriol.* **181**, 2394–2402.

Ito, M., Hicks, D. B., Henkin, T. M., Guffanti, A. A., Powers, B. D., Zvi, L., et al. (2004a). MotPS is the stator-force generator for motility of alkaliphilic *Bacillus*, and its homologue is a second functional Mot in *Bacillus subtilis*. *Mol. Microbiol.* **53**, 1035–1049. doi:10.1111/j.1365-2958.2004.04173.x

Ito, M., Xu, H. X., Guffanti, A. A., Wei, Y., Zvi, L., Clapham, D. E., et al. (2004b). The voltage-gated Na^+ channel Na_vBP has a role in motility, chemotaxis, and pH homeostasis of an alkaliphilic *Bacillus*. *Proc. Natl. Acad. Sci. U.S.A.* **101**, 10566–10571. doi:10.1073/pnas.0402692101

Ito, S., Shikata, S., Ozaki, K., Kawai, S., Okamoto, K., Inoue, S., et al. (1989). Alkaline cellulase for laundry detergents – production by *Bacillus* Sp Ksm-635 and enzymatic-properties. *Agric. Biol. Chem.* **53**, 1275–1281. doi:10.1271/bbb1961.53.1275

Ivey, D. M., and Krulwich, T. A. (1991). Organization and nucleotide sequence of the *atp* genes encoding the ATP synthase from alkaliphilic *Bacillus firmus* OF4. *Mol. Gen. Genet.* **229**, 292–300. doi:10.1007/BF00272169

Ivey, D. M., and Krulwich, T. A. (1992). Two unrelated alkaliphilic *Bacillus* species possess identical deviations in sequence from those of other prokaryotes in regions of F_o proposed to be involved in proton translocation through the ATP synthase. *Res. Microbiol.* **143**, 467–470. doi:10.1016/0923-2508(92)90092-3

Janto, B., Ahmed, A., Ito, M., Liu, J., Hicks, D. B., Pagni, S., et al. (2011). Genome of alkaliphilic *Bacilluspseudofirmus* OF4 reveals adaptations that support the ability to grow in an external pH range from 7.5 to 11.4. *Environ. Microbiol.* **13**, 3289–3309. doi:10.1111/j.1462-2920.2011.02591.x

Jones, B. E., Grant, W. D., Duckworth, A. W., and Owenson, G. G. (1998). Microbial diversity of Soda Lakes. *Extremophiles* **2**, 191–200. doi:10.1007/s007920050060

Joshi, A.A., Kanekar, P.P., Kelkar, A.S., Shouche, Y.S., Vani, A.A., Borgave, S.B., et al. (2008). Cultivable bacterial diversity of alkaline Lonar lake. *Micro. Ecol.* **55**, 163–172.

Kelley, D. S., Karson, J. A., Fruh-Green, G. L., Yoerger, D. R., Shank, T. M., Butterfield, D. A., et al. (2005). A serpentinite-hosted ecosystem: the lost city hydrothermal field. *Science* **307**, 1428–1434. doi:10.1126/science.1102556

Kojima, M., Kanai, M., Tominaga, M., Kitazume, S., Inoue, A., and Horikoshi, K. (2006). Isolation and characterization of a feather-degrading enzyme from *Bacillus pseudofirmus* FA30-01. *Extremophiles* **10**, 229–235. doi:10.1007/s00792-005-0491-y

Kosono, S., Haga, K., Tomizawa, R., Kajiyama, Y., Hatano, K., Takeda, S., et al. (2005). Characterization of a multigene-encoded sodium/hydrogen antiporter (Sha) from *Pseudomonas aeruginosa*: its involvement in pathogenesis. *J. Bacteriol.* **187**, 5242–5248. doi:10.1128/JB.187.15.5242-5248.2005

Kosono, S., Morotomi, S., Kitada, M., and Kudo, T. (1999). Analyses of a *Bacillus subtilis* homologue of the Na^+/H^+ antiporter gene which is important for pH homeostasis of alkaliphilic *Bacillus* sp. C-125. *Biochim. Biophys. Acta* **1409**, 171–175. doi:10.1016/S0005-2728(98)00157-1

Krulwich, T. A. (1995). Alkaliphiles: 'basic' molecular problems of pH tolerance and bioenergetics. *Mol. Microbiol.* **15**, 403–410. doi:10.1111/j.1365-2958.1995.tb02253.x

Krulwich, T. A., Federbush, J. G., and Guffanti, A. A. (1985). Presence of a nonmetabolizable solute that is translocated with Na^+ enhances Na^+-dependent pH homeostasis in an alkalophilic *Bacillus*. *J. Biol. Chem.* **260**, 4055–4058.

Krulwich, T. A., and Ito, M. (2013). "Prokaryotic alkaliphiles," in *The Prokaryotes*, 4th Edn, eds E. Rosenberg, E. F. Delong, F. Thompson, S. Sory, and E. Stackbrandt (New York, NY: Springer), 441–469.

Krulwich, T. A., Sachs, G., and Padan, E. (2011). Molecular aspects of bacterial pH sensing and homeostasis. *Nat. Rev. Microbiol.* **9**, 330–343. doi:10.1038/nrmicro2549

Kumar, C. G., and Takagi, H. (1999). Microbial alkaline proteases: from a bioindustrial viewpoint. *Biotechnol. Adv.* **17**, 561–594. doi:10.1016/S0734-9750(99)00027-0

Lane, N., Allen, J. F., and Martin, W. (2010). How did LUCA make a living? Chemiosmosis in the origin of life. *Bioessays* **32**, 271–280. doi:10.1002/bies.200900131

Lane, N., and Martin, W. F. (2012). The origin of membrane bioenergetics. *Cell* **151**, 1406–1416. doi:10.1016/j.cell.2012.11.050

Lee, A., Vastermark, A., and Saier, M. H. Jr. (2014). Establishing homology between mitochondrial calcium uniporters, prokaryotic magnesium channels and chlamydial IncA proteins. *Microbiology* **160**, 1679–1689. doi:10.1099/mic.0.077776-0

Lee, J. W. (2012). Proton-electrostatics hypothesis for localized proton coupling bioenergetics. *Bioenergetics* **1**, 104. doi:10.4172/2167-7662.1000104

Liu, J., Fackelmayer, O. J., Hicks, D. B., Preiss, L., Meier, T., Sobie, E. A., et al. (2011). Mutations in a helix-1 motif of the ATP synthase *c*-subunit of *Bacillus pseudofirmus* OF4 cause functional deficits and changes in the *c*-ring stability and mobility on sodium dodecyl sulfate-polyacrylamide gel electrophoresis. *Biochemistry* **50**, 5497–5506. doi:10.1021/bi2005009

Liu, J., Fujisawa, M., Hicks, D. B., and Krulwich, T. A. (2009). Characterization of the functionally critical AXAXAXA and PXXEXXP motifs of the ATP synthase *c*-subunit from an alkaliphilic *Bacillus*. *J. Biol. Chem.* **284**, 8714–8725. doi:10.1074/Jbc.M808738200

Liu, J., Hicks, D. B., and Krulwich, T. A. (2013). Roles of AtpI and two YidC-type proteins from alkaliphilic *Bacillus pseudofirmus* OF4 in ATP synthase assembly and nonfermentative growth. *J. Bacteriol.* **195**, 220–230. doi:10.1128/JB.01493-12

Liu, J., Ryabichko, S., Bogdanov, M., Fackelmayer, O. J., Dowhan, W., and Krulwich, T. A. (2014). Cardiolipin is dispensable for oxidative phosphorylation and non-fermentative growth of alkaliphilic *Bacillus pseudofirmus* OF4. *J. Biol. Chem.* **289**, 2960–2971. doi:10.1074/jbc.M113.536193

Liu, M., Yuan, Y., Zhang, L. X., Zhuang, L., Zhou, S. G., and Ni, J. R. (2010). Bioelectricity generation by a Gram-positive *Corynebacterium* sp strain MFC03 under alkaline condition in microbial fuel cells. *Bioresour. Technol.* **101**, 1807–1811. doi:10.1016/j.biortech.2009.10.003

Liu, X., Gong, X., Hicks, D. B., Krulwich, T. A., Yu, L., and Yu, C. A. (2007). Interaction between cytochrome caa_3 and F_1F_o-ATP synthase of alkaliphilic *Bacillus pseudofirmus* OF4 is demonstrated by saturation transfer electron paramagnetic resonance and differential scanning calorimetry assays. *Biochemistry* **46**, 306–313. doi:10.1021/bi0619167

Logan, B. E., Hamelers, B., Rozendal, R. A., Schrorder, U., Keller, J., Freguia, S., et al. (2006). Microbial fuel cells: methodology and technology. *Environ. Sci. Technol.* **40**, 5181–5192. doi:10.1021/es0605016

Lopez, D., and Kolter, R. (2010). Functional microdomains in bacterial membranes. *Genes Dev.* **24**, 1893–1902. doi:10.1101/gad.1945010

Ma, Y., Xue, Y., Grant, W. D., Collins, N. C., Duckworth, A. W., Van Steenbergen, R. P., et al. (2004). *Alkalimonas amylolytica* gen. nov., sp. nov., and *Alkalimonas delamerensis* gen. nov., sp. nov., novel alkaliphilic bacteria from Soda Lakes in China and East Africa. *Extremophiles* **8**, 193–200. doi:10.1007/s00792-004-0377-4

Martin, W., Baross, J., Kelley, D., and Russell, M. J. (2008). Hydrothermal vents and the origin of life. *Nat. Rev. Microbiol.* **6**, 805–814. doi:10.1038/nrmicro1991

Martin, W., and Russell, M. J. (2007). On the origin of biochemistry at an alkaline hydrothermal vent. *Philos. Trans. R. Soc. Lond. B Biol. Sci.* **362**, 1887–1925. doi:10.1098/rstb.2006.1881

Matias, V. R. F., and Beveridge, T. J. (2005). Cryo-electron microscopy reveals native polymeric cell wall structure in *Bacillus subtilis* 168 and the existence of a periplasmic space. *Mol. Microbiol.* **56**, 240–251. doi:10.1111/j.1365-2958.2005.04535.x

Matthies, D., Preiss, L., Klyszejko, A. L., Muller, D. J., Cook, G. M., Vonck, J., et al. (2009). The c13 ring from a thermoalkaliphilic ATP synthase reveals an extended diameter due to a special structural region. *J. Mol. Biol.* **388**, 611–618. doi:10.1016/j.jmb.2009.03.052

McMillan, D. G., Keis, S., Berney, M., and Cook, G. M. (2009). Nonfermentative thermoalkaliphilic growth is restricted to alkaline environments. *Appl. Environ. Microbiol.* **75**, 7649–7654. doi:10.1128/AEM.01639-09

McMillan, D. G., Keis, S., Dimroth, P., and Cook, G. M. (2007). A specific adaptation in the a subunit of thermoalkaliphilic F_1F_O-ATP synthase enables ATP synthesis at high pH but not at neutral pH values. *J. Biol. Chem.* **282**, 17395–17404. doi:10.1074/jbc.M611709200

Meier, T., Faraldo-Gómez, J. D., and Börsch, M. (2011). "ATP synthase: a paradigmatic molecular machine," in *Molecular Machines in Biology*, ed. J. Frank (Cambridge: Cambridge University Press), 208–238.

Meier, T., Ferguson, S. A., Cook, G. M., Dimroth, P., and Vonck, J. (2006). Structural investigations of the membrane-embedded rotor ring of the F-ATPase from *Clostridium paradoxum*. *J. Bacteriol.* **188**, 7759–7764. doi:10.1128/JB.00934-06

Meier, T., Krah, A., Bond, P. J., Pogoryelov, D., Diederichs, K., and Faraldo-Gómez, J. D. (2009). Complete ion-coordination structure in the rotor ring of Na^+-dependent F-synthases. *J. Mol. Biol.* **391**, 498–507. doi:10.1016/j.jmb.2009.05.082

Meier, T., Morgner, N., Matthies, D., Pogoryelov, D., Keis, S., Cook, G. M., et al. (2007). A tridecameric c ring of the adenosine triphosphate (ATP) synthase from the thermoalkaliphilic *Bacillus* sp strain TA2.A1 facilitates ATP synthesis at low electrochemical proton potential. *Mol. Microbiol.* **65**, 1181–1192. doi:10.1111/j.1365-2958.2007.05857.x

Meier, T., Polzer, P., Diederichs, K., Welte, W., and Dimroth, P. (2005). Structure of the rotor ring of F-type Na^+-ATPase from *Ilyobacter tartaricus*. *Science* **308**, 659–662. doi:10.1126/science.1111199

Mesbah, N. M., Cook, G. M., and Wiegel, J. (2009). The halophilic alkalithermophile *Natranaerobius thermophilus* adapts to multiple environmental extremes using a large repertoire of Na^+ (K^+)/H^+ antiporters. *Mol. Microbiol.* **74**, 270–281. doi:10.1111/j.1365-2958.2009.06845.x

Mesbah, N. M., and Wiegel, J. (2012). Life under multiple extreme conditions: diversity and physiology of the halophilic alkalithermophiles. *Appl. Environ. Microbiol.* **78**, 4074–4082. doi:10.1128/AEM.00050-12

Meyer-Dombard, D. R., Woycheese, K. M., Yargicoglu, E. N., Cardace, D., Shock, E. L., Gulecal-Pektas, Y., et al. (2015). High pH microbial ecosystems in a newly discovered, ephemeral, serpentinizing fluid seep at Yanartas (Chimera), Turkey. *Front. Microbiol.* **5**:723. doi:10.3389/fmicb.2014.00723

Mitchell, P. (1961). Coupling of phosphorylation to electron and hydrogen transfer by a chemiosmotic type of mechanism. *Nature* **191**, 144–148. doi:10.1038/191144a0

Mulkidjanian, A. Y., Bychkov, A. Y., Dibrova, D. V., Galperin, M. Y., and Koonin, E. V. (2012). Origin of first cells at terrestrial, anoxic geothermal fields. *Proc. Natl. Acad. Sci. U.S.A.* **109**, E821–E830. doi:10.1073/pnas.1117774109

Mulkidjanian, A. Y., Dibrov, P., and Galperin, M. Y. (2008). The past and present of sodium energetics: may the sodium-motive force be with you. *Biochim. Biophys. Acta* **1777**, 985–992. doi:10.1016/J.Bbabio.2008.04.028

Mulkidjanian, A. Y., Heberle, J., and Cherepanov, D. A. (2006). Protons @ interfaces: implications for biological energy conversion. *Biochim. Biophys. Acta* **1757**, 913–930. doi:10.1016/j.bbabio.2006.02.015

Mulkidjanian, A. Y., Makarova, K. S., Galperin, M. Y., and Koonin, E. V. (2007). Inventing the dynamo machine: the evolution of the F-type and V-type ATPases. *Nat. Rev. Microbiol.* **5**, 892–899. doi:10.1038/nrmicro1767

Ojemyr, L. N., Lee, H. J., Gennis, R. B., and Brzezinski, P. (2010). Functional interactions between membrane-bound transporters and membranes. *Proc. Natl. Acad. Sci. U.S.A.* **107**, 15763–15767. doi:10.1073/pnas.1006109107

Paar, A., Costa, S., Tzanov, T., Gudelj, M., Robra, K. H., Cavaco-Paulo, A., et al. (2001). Thermo-alkali-stable catalases from newly isolated *Bacillus* sp for the treatment and recycling of textile bleaching effluents. *J. Biotechnol.* **89**, 147–153. doi:10.1016/S0168-1656(01)00305-4

Park, S., Ryu, J. Y., Seo, J., and Hur, H. G. (2012). Isolation and characterization of alkaliphilic and thermotolerant bacteria that reduce insoluble indigo to soluble leuco-indigo from indigo dye vat. *J. Korean Soc. Appl. Biol. Chem.* **55**, 83–88. doi:10.5012/bkcs.2012.33.1.83

Payandeh, J., Gamal El-Din, T. M., Scheuer, T., Zheng, N., and Catterall, W. A. (2012). Crystal structure of a voltage-gated sodium channel in two potentially inactivated states. *Nature* **485**, 135–139. doi:10.1038/nature11077

Pogoryelov, D., Klyszejko, A. L., Krasnoselska, G. O., Heller, E. M., Leone, V., Langerd, J. D., et al. (2012). Engineering rotor ring stoichiometries in the ATP synthase. *Proc. Natl. Acad. Sci. U.S.A.* **109**, E1599–E1608. doi:10.1073/pnas.1120027109

Preiss, L., Klyszejko, A. L., Hicks, D. B., Liu, J., Fackelmayer, O. J., Yildiz, O., et al. (2013). The *c*-ring stoichiometry of ATP synthase is adapted to cell physiological requirements of alkaliphilic *Bacillus pseudofirmus* OF4. *Proc. Natl. Acad. Sci. U.S.A.* **110**, 7874–7879. doi:10.1073/pnas.1303333110

Preiss, L., Langer, J. D., Hicks, D. B., Liu, J., Yildiz, O., Krulwich, T. A., et al. (2014). The c-ring ion binding site of the ATP synthase from *Bacillus pseudofirmus* OF4 is adapted to alkaliphilic lifestyle. *Mol. Microbiol.* **92**, 973–984. doi:10.1111/Mmi.12605

Preiss, L., Yildiz, O., Hicks, D. B., Krulwich, T. A., and Meier, T. (2010). A new type of proton coordination in an F_1F_o-ATP synthase rotor ring. *PLoS Biol.* **8**:e1000443. doi:10.1371/journal.pbio.1000443

Putnoky, P., Kereszt, A., Nakamura, T., Endre, G., Grosskopf, E., Kiss, P., et al. (1998). The *pha* gene cluster of *Rhizobium meliloti* involved in pH adaptation and symbiosis encodes a novel type of K^+ efflux system. *Mol. Microbiol.* **28**, 1091–1101. doi:10.1046/j.1365-2958.1998.00868.x

Qi, Q., and Zimmermann, W. (2005). Cyclodextrin glucanotransferase: from gene to applications. *Appl. Microbiol. Biotechnol.* **66**, 475–485. doi:10.1007/s00253-004-1781-5

Ren, D., Navarro, B., Xu, H., Yue, L., Shi, Q., and Clapham, D. E. (2001). A prokaryotic voltage-gated sodium channel. *Science* **294**, 2372–2375. doi:10.1126/science.1065635

Rieger, B., Junge, W., and Busch, K. B. (2014). Lateral pH gradient between OXPHOS complex IV and F_oF_1 ATP-synthase in folded mitochondrial membranes. *Nat. Commun.* **5**, 3103. doi:10.1038/ncomms4103

Roadcap, G. S., Sanford, R. A., Jin, Q. S., Pardinas, J. R., and Bethke, C. M. (2006). Extremely alkaline (pH > 12) ground water hosts diverse microbial community. *Ground Water* **44**, 511–517. doi:10.1111/j.1745-6584.2006.00199.x

Roh, Y., Chon, C. M., and Moon, J. W. (2007). Metal reduction and biomineralization by an alkaliphilic metal-reducing bacterium, *Alkaliphilus metalliredigens* (QYMF). *Geosci. J.* **11**, 415–423. doi:10.1007/BF02857056

Sandén, T., Salomonsson, L., Brzezinski, P., and Widengren, J. (2010). Surface-coupled proton exchange of a membrane-bound proton acceptor. *Proc. Natl. Acad. Sci. U.S.A.* **107**, 4129–4134. doi:10.1073/pnas.0908671107

Sarethy, I. P., Saxena, Y., Kapoor, A., Sharma, M., Sharma, S. K., Gupta, V., et al. (2011). Alkaliphilic bacteria: applications in industrial biotechnology. *J. Ind. Microbiol. Biotechnol.* **38**, 769–790. doi:10.1007/s10295-011-0968-x

Schrenk, M. O., Kelley, D. S., Bolton, S. A., and Baross, J. A. (2004). Low archaeal diversity linked to subseafloor geochemical processes at the lost city hydrothermal field, mid-Atlantic ridge. *Environ. Microbiol.* **6**, 1086–1095. doi:10.1111/j.1462-2920.2004.00650.x

Slater, E. C. (1987). The mechanism of the conservation of energy of biological oxidations. *Eur. J. Biochem.* **166**, 489–504. doi:10.1111/j.1432-1033.1987.tb13542.x

Sorokin, D. Y., Berben, T., Melton, E. D., Overmars, L., Vavourakis, C. D., and Muyzer, G. (2014). Microbial diversity and biogeochemical cycling in Soda Lakes. *Extremophiles* **18**, 791–809. doi:10.1007/s00792-014-0670-9

Sorokin, D. Y., Kuenen, J. G., and Muyzer, G. (2011). The microbial sulfur cycle at extremely haloalkaline conditions of Soda Lakes. *Front. Microbiol.* **2**:44. doi:10.3389/Fmicb.2011.00044

Sorokin, D. Y., Van Den Bosch, P. L. F., Abbas, B., Janssen, A. J. H., and Muyzer, G. (2008). Microbiological analysis of the population of extremely haloalkaliphilic sulfur-oxidizing bacteria dominating in lab-scale sulfide-removing bioreactors. *Appl. Microbiol. Biotechnol.* **80**, 965–975. doi:10.1007/s00253-008-1598-8

Spiess, F. N., Macdonald, K. C., Atwater, T., Ballard, R., Carranza, A., Cordoba, D., et al. (1980). East pacific rise – hot springs and geophysical experiments. *Science* **207**, 1421–1433. doi:10.1126/Science.207.4438.1421

Steed, P. R., and Fillingame, R. H. (2009). Aqueous accessibility to the transmembrane regions of subunit *c* of the *Escherichia coli* F_1F_o ATP synthase. *J. Biol. Chem.* **284**, 23243–23250. doi:10.1074/jbc.M109.002501

Steiger, S., Perez-Fons, L., Cutting, S. M., Fraser, P. D., and Sandmann, G. (2015). Annotation and functional assignment of the genes for the C30 carotenoid pathways from the genomes of two bacteria: *Bacillus indicus* and *Bacillus firmus*. *Microbiology* **161**, 194–202. doi:10.1099/mic.0.083519-0

Stock, D., Gibbons, C., Arechaga, I., Leslie, A. G. W., and Walker, J. E. (2000). The rotary mechanism of ATP synthase. *Curr. Opin. Struct. Biol.* **10**, 672–679. doi:10.1016/S0959-440X(00)00147-0

Sturr, M. G., Guffanti, A. A., and Krulwich, T. A. (1994). Growth and bioenergetics of alkaliphilic *Bacillus firmus* OF4 in continuous-culture at high pH. *J. Bacteriol.* **176**, 3111–3116.

Suzuki, S., Ishii, S., Wu, A., Cheung, A., Tenney, A., Wanger, G., et al. (2013). Microbial diversity in the Cedars, an ultrabasic, ultrareducing, and low salinity serpentinizing ecosystem. *Proc. Natl. Acad. Sci. U.S.A.* **110**, 15336–15341. doi:10.1073/pnas.1302426110

Suzuki, S., Kuenen, J. G., Schipper, K., Van Der Velde, S., Ishii, S., Wu, A., et al. (2014). Physiological and genomic features of highly alkaliphilic hydrogen-utilizing Betaproteobacteria from a continental serpentinizing site. *Nat. Commun.* **5**, 3900. doi:10.1038/Ncomms4900

Suzuki, T., Ozaki, Y., Sone, N., Feniouk, B. A., and Yoshida, M. (2007). The product of *uncI* gene in F_1F_o-ATP synthase operon plays a chaperone-like role to assist *c*-ring assembly. *Proc. Natl. Acad. Sci. U.S.A.* **104**, 20776–20781. doi:10.1073/pnas.0708075105

Swartz, T. H., Ikewada, S., Ishikawa, O., Ito, M., and Krulwich, T. A. (2005). The Mrp system: a giant among monovalent cation/proton antiporters? *Extremophiles* **9**, 345–354. doi:10.1007/s00792-005-0451-6

Takami, H. (2010). "Genomics and evolution of alkaliphilic *Bacillus*-related species," in *Part 2. Extremophiles: Alkaliphiles, 2.9. Extremophiles Handbook*, eds K. Horikoshi, G. Antranikian, A. Bull, F. Robb, and K. Stetter (New York, NY: Springer), 183–212.

Takami, H., Nakasone, K., Takaki, Y., Maeno, G., Sasaki, R., Masui, N., et al. (2000). Complete genome sequence of the alkaliphilic bacterium *Bacillus halodurans* and genomic sequence comparison with *Bacillus subtilis*. *Nucleic Acids Res.* **28**, 4317–4331. doi:10.1093/nar/28.21.4317

Thongaram, T., Hongoh, Y., Kosono, S., Ohkuma, M., Trakulnaleamsai, S., Noparatnaraporn, N., et al. (2005). Comparison of bacterial communities in the alkaline gut segment among various species of higher termites. *Extremophiles* **9**, 229–238. doi:10.1007/s00792-005-0440-9

Thongaram, T., Kosono, S., Ohkuma, M., Hongoh, Y., Kitada, M., Yoshinaka, T., et al. (2003). Gut of higher termites as a niche for alkaliphiles as shown by culture-based and culture-independent studies. *Microbes Environ.* **18**, 152–159. doi:10.1264/jsme2.18.152

Tsujii, K. (2002). Donnan equilibria in microbial cell walls: a pH-homeostatic mechanism in alkaliphiles. *Colloids Surf. B Biointerfaces* **24**, 247–251. doi:10.1016/S0927-7765(01)00244-2

Walker, J. E. (2013). The ATP synthase: the understood, the uncertain and the unknown. *Biochem. Soc. Trans.* **41**, 1–16. doi:10.1042/BST20110773

Wang, Z., Hicks, D. B., Guffanti, A. A., Baldwin, K., and Krulwich, T. A. (2004). Replacement of amino acid sequence features of *a*- and c-subunits of ATP synthases of alkaliphilic *Bacillus* with the *Bacillus* consensus sequence results in defective oxidative phosphorylation and non-fermentative growth at pH 10.5. *J. Biol. Chem.* **279**, 26546–26554. doi:10.1074/jbc.M401206200

Watt, I. N., Montgomery, M. G., Runswick, M. J., Leslie, A. G. W., and Walker, J. E. (2010). Bioenergetic cost of making an adenosine triphosphate molecule in animal mitochondria. *Proc. Natl. Acad. Sci. U.S.A.* **107**, 16823–16827. doi:10.1073/pnas.1011099107

Wilkens, V., Kohl, W., and Busch, K. (2013). Restricted diffusion of OXPHOS complexes in dynamic mitochondria delays their exchange between cristae and engenders a transitory mosaic distribution. *J. Cell. Sci.* **126**, 103–116. doi:10.1242/jcs.108852

Williams, R. J. (1978). The multifarious couplings of energy transduction. *Biochim. Biophys. Acta* **505**, 1–44. doi:10.1016/0304-4173(78)90007-1

Ye, Q., Roh, Y., Carroll, S. L., Blair, B., Zhou, J. Z., Zhang, C. L., et al. (2004). Alkaline anaerobic respiration: isolation and characterization of a novel alkaliphilic and metal-reducing bacterium. *Appl. Environ. Microbiol.* **70**, 5595–5602. doi:10.1128/AEM.70.9.5595-5602.2004

Yoshida, M., Muneyuki, E., and Hisabori, T. (2001). ATP synthase – a marvellous rotary engine of the cell. *Nat. Rev. Mol. Cell Biol.* **2**, 669–677. doi:10.1038/35089509

Yumoto, I. (2002). Bioenergetics of alkaliphilic *Bacillus* spp. *J. Biosci. Bioeng.* **93**, 342–353. doi:10.1016/S1389-1723(02)80066-4

Yumoto, I., Yamazaki, K., Hishinuma, M., Nodasaka, Y., Suemori, A., Nakajima, K., et al. (2001). *Pseudomonas alcaliphila* sp nov., a novel facultatively psychrophilic alkaliphile isolated from seawater. *Int. J. Syst. Evol. Microbiol.* **51**, 349–355. doi:10.1099/00207713-51-2-349

Zhang, H-M., Li, Z., Tsudome, M., Ito, S., Takami, H., and Horikoshi, K. (2005). An alkali-inducible flotillin-like protein from *Bacillus halodurans* C-125. *Protein J.* **24**, 125–131. doi:10.1007/s10930-004-1519-3

Zhang, T. T., Zhang, L. X., Su, W. T., Gao, P., Li, D. P., He, X. H., et al. (2011). The direct electrocatalysis of phenazine-1-carboxylic acid excreted by *Pseudomonas alcaliphila* under alkaline condition in microbial fuel cells. *Bioresour. Technol.* **102**, 7099–7102. doi:10.1016/j.biortech.2011.04.093

Zhang, X., Ren, W., DeCaen, P., Yan, C., Tao, X., Tang, L., et al. (2012). Crystal structure of an orthologue of the NaChBac voltage-gated sodium channel. *Nature* **486**, 130–134. doi:10.1038/nature11054

Conflict of Interest Statement: The authors declare that the research was conducted in the absence of any commercial or financial relationships that could be construed as a potential conflict of interest.

Advantages of publishing in Frontiers

OPEN ACCESS
Articles are free to read, for greatest visibility

COLLABORATIVE PEER-REVIEW
Designed to be rigorous – yet also collaborative, fair and constructive

FAST PUBLICATION
Average 85 days from submission to publication (across all journals)

COPYRIGHT TO AUTHORS
No limit to article distribution and re-use

TRANSPARENT
Editors and reviewers acknowledged by name on published articles

SUPPORT
By our Swiss-based editorial team

IMPACT METRICS
Advanced metrics track your article's impact

GLOBAL SPREAD
5'100'000+ monthly article views and downloads

LOOP RESEARCH NETWORK
Our network increases readership for your article

Frontiers
EPFL Innovation Park, Building I • 1015 Lausanne • Switzerland
Tel +41 21 510 17 00 • Fax +41 21 510 17 01 • info@frontiersin.org
www.frontiersin.org

Find us on